UNDERSTANDING AND IMPROVING HIGH CELL DENSITY FERMENTATIONS WITH CELL RECYCLE USING AFEX™ TREATED CORN STOVER FOR ETHANOL PRODUCTION

By

Cory James Sarks

A DISSERTATION

Submitted to
Michigan State University
in partial fulfillment of the requirements
for the degree of

Chemical Engineering—Doctor of Philosophy

2015

ABSTRACT

UNDERSTANDING AND IMPROVING HIGH CELL DENSITY FERMENTATIONS WITH CELL RECYCLE USING AFEX™ TREATED CORN STOVER FOR ETHANOL PRODUCTION

By

Cory James Sarks

The cellulosic ethanol industry in the U.S. just built its first large plants. However, cellulosic ethanol is not widely considered economical. Previously, the Biomass Conversion Research Laboratory at Michigan State University created the RaBIT (Rapid Bioconversion with Integrated recycling Technology) process to improve cellulosic ethanol economics. The RaBIT process was successful in reducing capital cost, enzyme loading, and processing time while also increasing xylose consumption and ethanol productivity. However, cell recycling, a key component of the process, was not sustainable as xylose consumption decreased after each recycling event. The work presented in this dissertation investigated the cause of this decrease and through process changes eliminated the decrease.

Four key variables were investigated for this work: strain suitability, nutrient deficiency, cell viability, and degradation product effects. Results showed that strains with sufficiently high specific xylose consumption rates were suitable for the RaBIT process. Studies of nutrient deficiency and cell viability showed that the specific xylose consumption rates were decreasing upon cell recycle and significant cell death was taking place during the xylose consumption phase. Degradation products were found to progressively accumulate within the cell. This accumulation was credited as the chief cause for decreasing cell performance upon recycle.

Three process changes were implemented to improve RaBIT process fermentations. The combination of shortening fermentation time from 24 to 11 h and continuous feeding of hydrolysate eliminated the xylose consumption rate decrease. The new RaBIT fermentation process was capable of 0.8 g/L improved xylose consumption over 10 cycles. Previously, xylose consumption decreased by 3.6 g/L over just 1 cycle. The third process change allowed for the separation of cells based on age. The capability to selectively remove older cells showed benefit over non-selective removal of cells. However, cell removal over ten cycles was not sustainable as xylose consumption and cell mass decreased.

Economic analysis was performed comparing the new RaBIT process to a traditional cellulosic ethanol process. The RaBIT process showed economic benefit over the traditional process, but was highly dependent on achieving an extended number of fermentation cycles. The RaBIT process does have clear benefits with regards to capital investment as initial investment and enzyme price sensitivity are low. Life cycle analysis showed that the RaBIT process was an improvement with regards to global climate change potential and acidification, but worse with regards to energy production and eutrophication when compared to the traditional cellulosic ethanol process.

This work is dedicated to Johnny Sarks.

ACKNOWLEDGMENTS

I would like to thank my committee members (Professors Bruce E. Dale, Venkatesh Balan, R. Mark Worden, and Eric Hegg) for spending their valuable time advising me. I specifically thank Dr. Dale and Dr. Balan for providing me this opportunity in the Biomass Conversion Research Laboratory (BCRL). I am very thankful for Dr. Mingjie Jin who was my biggest mentor during most of my time at Michigan State University.

There are many people who have helped with this work as part of the BCRL. I greatly thank Christa Gunawan for running an enormous number of HPLC samples and Pete Donald for producing kg upon kg of AFEX™ treated biomass. Other members I thank are Dr. Rebecca Ong, Margie Magyar, James Humpula, and anybody else who was a member during my time. I thank MBI for biomass production and resume padding opportunity in Chapter 3. I specifically thank Dr. Bryan Bals for the economic analysis presented in Chapter 3. Great Lakes Bioenergy Research Center Area 3 members are also thanked for their collaboration. I specifically thank Dr. Trey K. Sato, Dr. Jeff Piotrowski, and Alan Higbee of Area 3 for their contributions in my research.

I finally thank Samantha Chapman, Jon "Valdez" Brook, and Caitlin Kowalsky for tolerating my periodic research rants.

AFEX is a registered trademark of MBI (Lansing, MI)

TABLE OF CONTENTS

LIST OF TABLES

LIST OF FIGURES

KEY TO ABBREVIATIONS AND SYMBOLS

Abbreviations

AFEX – Ammonia Fiber Expansion

BCRL – Biomass Conversion Research Laboratory

CBP – Consolidated Bio-Processing

CSL – Corn Steep Liquor

DCW – Dry Cell Weight

EtOH – Ethanol

GLBRC – Great Lakes Bioenergy Research Center

HPLC – High Performance Liquid Chromatography

LCA – Life cycle analysis

MESP – Minimum Ethanol Selling Price

NREL – National Renewable Energy Laboratory

OD – Optical Density

RaBIT – Rapid Bioconversion with Integrated recycling Technology

RM – Rich Medium/Media

SHF – Separate Hydrolysis and Fermentation

SSCF – Simultaneous Saccharafication and Co-Fermentations

TCI – Total capital investment

U.S. – United States

Symbols

C_x – Xylose concentration

C_{wp} – Weisz-Prater Criterion

C_{xs} – Xylose surface concentration

C_{xmin} – Minimum xylose concentration

D_e – Effective diffusivity

D_{xw} – Diffusion of xylose in water

E_f – Effectiveness factor

k_x – Reaction constant

R – Radius

$r_a'(obs)$ – Observed reaction rate

X – Viable cell concentration

σ_c – Constriction factor

Φ_p – Porosity

CHAPTER 1: INTRODUCTION AND BACKGROUND

1.1 Introduction

Current industrial life styles on planet earth are not sustainable. Use of fossil energy to run our economy has created a period of great wealth that is currently being threatened. If fossil energy runs out before alternative energy sources are developed, the future will be drastically different from the past/present. Environmentally, the greenhouse gasses produced from our fossil fuel use are changing the climate (IPCC, 2007). While not completely proven, increasing greenhouse gas concentrations are likely to cause negative changes to our environment (Haines et al., 2006).

Transportation fuels account for 34% of our fossil energy dependence (LLNL, 2013). While many options are available for renewable transportation such as hydrogen and electricity produced by wind, solar power, or the burning of biomass, liquid fuels are the most practical. For some applications such as jet travel, ocean travel, long-haul trucking, and other high tonnage applications, electricity is not a viable option: only energy-dense liquid fuels will perform adequately. A liquid fuel is more easily inserted into the current infrastructure. One of the most promising liquid fuel replacements is ethanol. Ethanol is currently being produced biologically on a large scale here in the US using corn, and in Brazil using sugar cane (U.S. EIA, 2013; UNICA, 2014). Brazil is the prime example of ethanol as a transportation fuel working. Currently, ethanol equals 40% of Brazil's transportation fuel from both 100% pure ethanol and gasoline/ethanol blends (UNICA, 2014). However, the use of food crops to produce bioethanol, the current practice, is not considered sustainable for most of the world. To sustainably replace transportation fuels using bioethanol, non-food sources feedstocks are required. Use of cellulosic biomass to produce ethanol helps remove the food vs. fuel debate (Ajanovic, 2011).

Cellulosic biomass comes from sources such as agricultural residues, woody biomass, and native perennial grasses. Agricultural residues such as corn stover can be harvested with little or no impact on food production. Woody biomass and native perennial grasses can be planted on land not suitable for food production (Carroll and Somerville, 2009). By 2030, it is projected that over 1 billion dry tons of cellulosic biomass will be available for under $60/ton (U.S. DOE, 2011). One billion dry tons of biomass is capable of replacing around 30% of current fossil transportation fuels (U.S. DOE, 2011). With increases in efficiency and use of hybrid technology, this percentage could be higher by 2030.

1.2 Background

1.2.1 Biomass

Lignocellulosic biomass, or more simply cellulosic biomass, defines the dry material that makes up plants. In simplicity, cellulosic biomass is composed of three materials: cellulose, hemicellulose, and lignin. Cellulose is the most abundant organic polymer on earth (Pérez and Samain, 2010). Cellulose is a long chain of β(1-4) linked glucose molecules (Pérez and Samain, 2010). These long chains are bound together by hydrogen bonding to form micro-fibrils which provide the support in plant cell walls (Pérez and Samain, 2010). Hemicelluose is a complex branched polymer of various sugars such as glucose, xylose, arabinose, manose, and galactose (Saha, 2003). Furthermore, the sugars present in hemicellulose chains are frequently modified with chemical groups such as methyl and acetyl groups (Saha, 2003). Hemicellulose works to provide additional structure by forming many different linkages between cellulose, proteins, and lignin (Achyuthan et al., 2010; Saha, 2003). The final major component, lignin, then fills in space while creating crosslinkages with the cellulose, hemicellulose, and proteins (Achyuthan et al., 2010). Lignin is composed of three main compounds: p-coumaryl alcohol, coniferyl alcohol,

and sinapyl alcohol (Achyuthan et al., 2010). These three units have the same basic structure of phenylpropanoids but with varying degrees of methoxylation (Figure 1). The cell wall matrix formed by cellulose, hemicellulose, and lignin creates a material highly resistant to chemical or biological degradation.

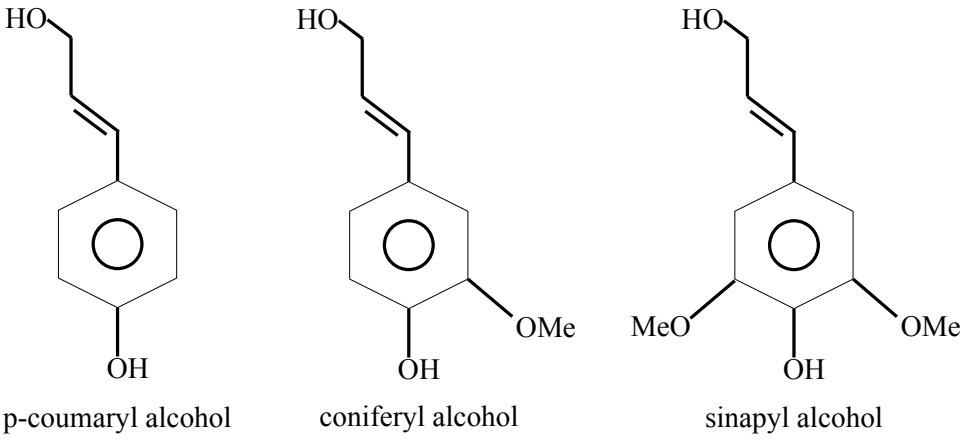

Figure 1 Lignin component structures

Cellulosic biomass for fuel production can come from many different sources. The most comprehensive listing of potential feedstocks can be found in the U.S. Billion Ton Update. The largest unutilized source of currently available cellulosic biomass is agricultural residues (U.S. DOE, 2011). The majority of agricultural residue is the non-edible plant fractions grown during food production (Nigam and Singh, 2011). Corn stover currently contributes 62% of total agricultural residues (U.S. DOE, 2011). Other sources of agricultural residues are wheat straw, rice field residues, and prunings (U.S. DOE, 2011). In the future, energy crops are projected to be the dominant feedstock available for fuel production (U.S. DOE, 2011). Common energy crops are grasses (switchgrass, miscanthus, etc.) and woody species (poplar, pine, etc.) (U.S.

DOE 2011). Energy crops are attractive due to their high yields on marginal lands (Varvel et al., 2008).

1.2.2 Pretreatment

Cellulosic biomass requires pretreatment for efficient conversion to monomeric sugars. Monomeric sugars can be converted by microbes into useful fuels and chemicals. The first step in pretreatment is normally particle size reduction (Vidal et al., 2011). This is typically necessary to increase the surface area available for chemical and biochemical attack. The general consensus is that the smaller the particle size the better overall conversion (Vidal et al., 2011). However, there are some conflicting reports for specific cases (Vidal et al., 2011). After particle size reduction, the biomass is treated by converting polysaccharides to monosaccharides or increasing accessibility for enzymatic degradation. There are many types of pretreatments such as the simple dilute acid pretreatment, steam explosion pretreatment, and the highly effective but expensive ionic liquid pretreatment (Alvira et al., 2010).

For this research, ammonia fiber expansion (AFEX) pretreatment will be used. AFEX is an alkaline pretreatment developed in Dr. Bruce E. Dale's lab at Michigan State University. A novelty of the AFEX pretreatment is the dry-to-dry processing (Balan et al., 2009). For pretreatment, biomass is adjusted to the correct moisture before being loaded into a reactor and charged with ammonia (Bals et al., 2010). The temperature inside the reactor is increased also resulting in a pressure increase (Chundawat et al., 2011). The combination of high temperature and pressure promotes the breaking of chemical bonds and the solubilization/melting of lignin (Chundawat et al., 2011; Chundawat et al., 2007; Krishnan et al., 2010). The pressure is then released causing the rapid vaporization of the ammonia and water (Bals et al., 2010). This causes the physical expansion of the biomass fiber and also the forced movement of solubilized

lignin towards the outside of the cell walls resulting in greater enzyme accessibility (Chundawat et al., 2011). A key benefit to the AFEX process is low sugar degradation during the pretreatment (Li et al., 2011). Many other pretreatments such as dilute acid degrade sugars resulting in higher levels of degradation products compared to AFEX pretreatment (Chundawat et al., 2010). Degradation products inhibit down stream enzymatic hydrolysis and microbial fermentation (Palmqvist et al., 1996).

1.2.3 Enzymatic Hydrolysis

After the AFEX pretreatment process, enzymes are required to hydrolyze the cellulose and hemicellulose into monomeric sugars that can be later metabolized by microorganisms during fermentation. The advantage of using enzymes for hydrolysis, when compared to chemical hydrolysis, is their specificity (Alonso et al., 2010). Chemical hydrolysis, while faster, forms other side products at the expense of yield (Alonso et al., 2010). The disadvantage of enzymes compared to chemical routes is their high cost and slow hydrolysis rates (Alonso et al., 2010). The hope is that techniques can be developed to create more efficient enzymes and lower their production cost. In order to enzymatically hydrolyze cellulosic biomass, a wide variety of enzymes are required. For cellulose, three main categories of enzymes are required for complete hydrolysis. The first enzyme is an endoglucanase (Pérez et al., 2002). The endoglucanase family of enzymes makes a cleavage in the middle of the cellulose chain (Pérez et al., 2002). This cleavage provides a reducing and non-reducing end for attack by cellobiohydrolases (Pérez et al., 2002). The cellobiohydrolases start at the end of a chain and progressively move down it, while breaking off shorter chains of glucose; most commonly, cellobiose, a glucose dimer, is released (Nidetzky et al., 1994). The last enzyme required is beta-glucosidase (Pérez et al., 2002). Beta-glucosidase works to split cellobiose into glucose monomers (Pérez et al., 2002).

The enzymatic hydrolysis of hemicellulose is more complicated than cellulose due to multiple sugar types and linkages requiring more individual and unique enzymes (Saha, 2003). The complete mechanism of hemicellulose hydrolysis and the enzymes required are still not completely understood or known (Yang et al., 2011). Xylan, a large component of hemicellulose, is degraded in much the same way as cellulose with very similar enzyme classes. Endoxylanase is required to create short oligosaccharides that are broken into monomers by xylosidase (Pérez et al., 2002). Other enzymes are also required to break linkages between different sugars or to break off modifications on the sugars (Pérez et al., 2002). Enzymatic hydrolysis is very dynamic and complicated because of these many different enzymes. The activity of an enzyme may be dependent on the product of a different enzyme. Access of one class of enzymes (eg, the cellulases to cellulose), may be enhanced by other enzymes, for example, the hemicellulases. Furthermore, many enzymes display feedback inhibition by their products (Gan et al., 2003). This makes creating synergy between different enzymes very important.

1.2.4 Fermentation

Once monomeric sugars are available, microorganisms can be used to convert the sugars into fuel. The use of microorganisms to produce valuable products from sugar has been around thousands of years. The most common, and one of the simplest, is the conversion of glucose to ethanol. Ethanol is already produced commercially from sucrose or starch (U.S. EIA, 2013; UNICA, 2014). This conversion process is traditionally done using the yeast strain *Saccharomyces cerevisiae. S. cerevisiae* naturally produces ethanol from glucose at concentrations greater than 100 g/L and at high rates (Çaylak and Sukan, 1998). On the bacteria side, *Zymomonas mobilis* also shows good ethanol production at high rates and concentrations

over 100 g/L (Rogers et al.,1979). Neither of these organisms, however, naturally consumes xylose. The consumption of xylose is necessary for the economical production of a biofuel from cellulosic biomass such as corn stover, which can contain approximately 20% xylan by weight (Jin et al., 2012a; Balan et al., 2009). However, xylose conversion genes from natural xylose consuming organisms such as *Scheffersomyces (Pichia) stipitis* have the capability of being engineering into organisms lacking the xylose consumption ability (Ho et al., 1999). This gene insertion allows microorganisms such as *S. cerevisiae* and *Z. mobilis* to produce high concentrations of ethanol using both glucose and xylose (Sarks et al., 2014). Unfortunately, the xylose consumption by these genetically modified organisms is slow and easily inhibited by degradation products produced during pretreatment (Jin et al., 2012b). The inhibition of xylose consumption substantially diminishes the economics of ethanol production.

Xylose consumption lags behind glucose consumption for multiple reasons. First, xylose fermentation is not as energetically favorable as glucose fermentation. Xylose fermentation yields 1.67 mol ATP/mol xylose, while glucose fermentation yields 2 mol ATP/mol glucose. Second, xylose transport into microbial cells is limited. Generally, glucose is preferentially transported into cells before xylose (Ren et al., 2009). This even occurs for the *Z. mobilis* Glf transporter, which can transport xylose into the cell twice as fast as glucose (Ren et al., 2009). Furthermore, *S. cerevisiae*, a strain largely seen as ideal for lignocellulosic fermentations, can not actively transport xylose into the cell and relies on facilitated diffusion (Kötter and Ciriacy, 1993). Facilitate diffusion is not limiting during high xylose concentrations, but does start to limit at low xylose concentrations (Kötter and Ciriacy, 1993). Finally, use of the xylose reductase-xylitol dehydrogenase pathway causes redox and cofactor imbalances in yeast and

fungi (McMillan, 1993). This problem does not occur in the bacterial xylose isomerase pathway (McMillan 1993).

1.2.5 Cellulosic Ethanol Economics

Currently, production of cellulosic ethanol is not economically attractive. Despite an estimate of $2.15/gal of ethanol ($3.27/gal of gasoline equivalent) by Humbird et al. (2011), few companies have invested in commercial cellulosic ethanol plants. This economic unattractiveness can be attributed to three major factors: high capital investment costs, high enzyme costs, and biomass supply chain risks (Kazi et al., 2010; Eranki et al., 2011; Hess et al., 2007). Part of the high capital investment costs are associated with the long residence time required for traditional cellulosic ethanol processes. Enzymatic hydrolysis can take 2 to 5 days for completion, while fermentation can also take 2 to 5 days for full xylose utilization (Kristensen et al., 2009; Sarks et al., 2014). Past economic modelings showed enzyme loadings were responsible for approximately 50% of the total manufacturing costs (Kazi et al., 2010). Finally, biomass supply chains are currently non-existent. This creates a scenario where the supply chain won't be set up until the biorefinery is built, but the biorefinery won't be built until there is a guaranteed biomass supply chain.

To improve cellulosic ethanol economics, researchers are focusing on three main areas: novel pretreatments, enzyme development, and microbial engineering/adaptation. Most new/novel pretreatments such as ionic liquids or gamma-valerolactone produce highly digestible biomass, but are not attractive economically mainly due to catalyst recycling requirements (Klein-Marcuschamer et al., 2011; Luterbacher et al., 2014). Enzyme research is performed to improve the activity of specific enzymes, find new activities, or improve enzyme combinations to enhance synergy. Enzymes have been improved significantly by companies such as

Novozymes (Novozymes 2014a; Novozymes 2014b). However, significant improvement is difficult due to the number of enzymes required for full biomass deconstruction (Gao et al., 2011). Finally, microbial engineering/adaption has produced many good ethanologens through the years. However, microbe evolution is slow and highly dependent on initial strain choice (Jin et al., 2013; Piotrowski et al., 2014; Schwalbach et al., 2012). Little work has been done to address the biomass supply chain concerns.

The Biomass Conversion Research Laboratory (BCRL) is attempting to solve all three issues using two approaches. The first is creating pretreatment depots to solve the biomass supply chain issues. Using AFEX pretreatment in a depot setting allows the creation of a biomass supply chain based primarily on animal feed production before the presence of cellulosic ethanol refineries (Bals and Dale, 2012). Upon startup of these refineries, biomass could be shifted from animal feed to bioethanol eliminating the supply chain risks. To reduce capital investment cost and enzyme loadings, process development was employed.

1.2.6 Historical Process Development

With the exception of different pretreatments, the cellulosic ethanol process has not changed much. The most significant change implemented in recent years was simultaneous saccharification and co-fermentation (SSCF) instead of separate hydrolysis and fermentation (SHF) (Taherzadeh and Karimi, 2007). This change was important in mitigating monomeric sugar inhibition on enzymes for high solid loadings. Other attempts at changing the process appear to be too complicated and expensive or not suitable for current technology. One example is consolidated bio-processing (CBP) where no microorganism can currently produce high enough concentration of enzymes and ethanol in a short enough time (Taherzadeh and Karimi, 2007). Other examples are the use of filters, and nanoparticles for recycling cells or enzymes,

which are expensive and add more processing issues such as membrane fouling (Qi et al., 2012; Ivanova et al., 2011).

1.2.7 RaBIT Process

Process development by the BCRL resulted in the Rapid Bioconversion with Integrated recycling Technology (RaBIT) process (Figure 2) (Jin et al, 2012a). While simple, the RaBIT process managed to address two of the major causes for poor economics associated with cellulosic ethanol: capital cost and enzymes. Enzymatic hydrolysis was shortened by taking advantage of the high enzymatic hydrolysis rate period during the first 24 h. To achieve the sugar levels required for >40 g/L ethanol, the solids loading and enzyme loading were increased to avoid the slow rate period. To make the catalyst increase economical, enzymes are recycled while not using costly membranes or immobilization supports. Enzymes are naturally bound to the unhydrolyzed solids and are recycled into the next enzymatic hydrolysis cycle. This simple process step easily recovers about 50% of the initial enzyme loading. Furthermore, this approach allows the more easily hydrolyzed biomass to be digested first, while the more recalcitrant biomass can be recycled increasing its residence time. A concern for this process was the possible creation of highly viscous slurries. However, high solids loading enzymatic hydrolysis (up to 40% initial dry matter) has been demonstrated using tumbling reactors (Jørgensen et al., 2007). To further reduce capital cost, fermentation time was shortened. By use of high cell loadings, slow xylose consumption rates are eliminated, thereby shortening the fermentation process from 5 days to 1 day and greatly reducing capital cost. The fermentation rate was enhanced by increasing the initial inoculum by about 10 fold. This is made economical by recycling the cells to the next fermentation cycle. Recycling of cells is performed in both the brewing and sugar cane ethanol industries (Zhao and Bai, 2009). The only major concerns are

efficient separation of the solids and liquid after enzymatic hydrolysis and the decrease in performance by the recycled yeast. The first demonstration of the RaBIT process by Jin et al. (2012a) showed a reduction of processing time by around 120 h and an enzyme savings of up to 50%. For the SHF set up, this saved 62% of the capital costs associated with enzymatic hydrolysis and fermentation tanks and 38% of the cost associated with enzyme production (Jin et al., 2012a).

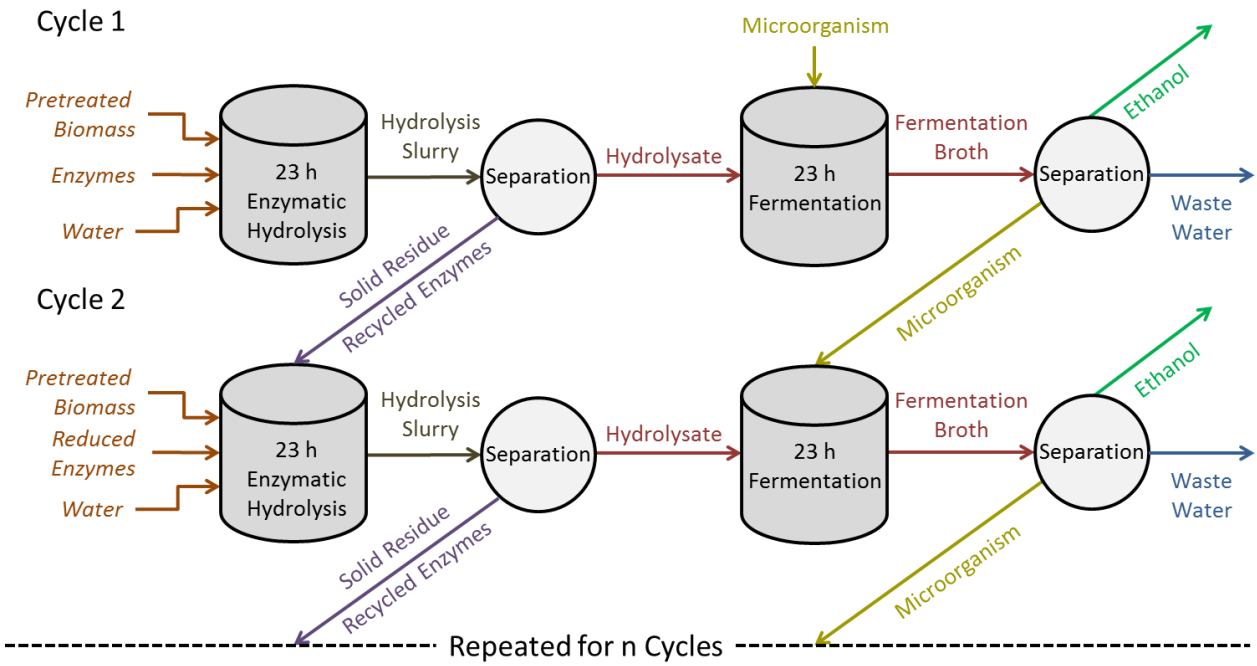

Figure 2 23 hour RaBIT process diagram.

One significant problem associated with the RaBIT process was the decrease in xylose consumption upon recycling of the cells as observed in work reported by Jin et al. (2012) using *Saccharomyces cerevisiae* 424A(LNH-ST). A similar process reported by Fan et al. (2013) using *Pichia guilliermondii* exhibited the same xylose consumption decrease upon cell recycle. This decrease in xylose consumption may limit the number of cell recycle events, thereby decreasing the potential cost savings of the process.

1.3 Research Objectives

The objective of the research reported in this dissertation was to investigate the cause for decreased xylose consumption upon cell recycle during the RaBIT process. To accomplish this primary objective, the following topics were investigated: strain testing (Chapter 2), nutrient supplementation (Chapter 4), cell population viability (Chapter 4), and pretreatment degradation product effects (Chapter 5). The information gained from the three investigative chapters was

used to implement process changes to improve cell population recycle (Chapter 6). Economic and life cycle analysis were then used to compare the latest RaBIT process to a traditional cellulosic ethanol process (Chapter 7). Studies on optimization of the traditional cellulosic ethanol process are reported in Chapter 3.

CHAPTER 2: STRAIN EVALUATION

Abstract

Strains were evaluated for their performance in traditional and RaBIT fermentations to determine the most suitable strain for future research in this dissertation. Evaluation was also performed to find correlations between RaBIT fermentation performance and traditional fermentation performance. The results identified *S. cerevisiae* GLBRCY128 and *Z. mobilis* 8b as the most suitable strains for RaBIT and traditional fermentations, respectively. Strains capable of performing RaBIT fermentations required specific xylose consumption rates above 0.075 g/g/h.

2.1 Introduction

Previously, high cell density fermentations with cell recycle using AFEX corn stover hydrolysate had only been performed in our lab using *S. cerevisiae* 424A(LNH-ST). As previously mentioned, the xylose consumption ability of this yeast decreased when the cell population was recycled. In other reported research, *Pichia guilliermondii* was used for high cell density fermentations using corn cob hydrolysate with the same observed xylose consumption decrease (Fan et al., 2013). Experiments were needed to determine if the xylose consumption decrease is present in all strains and whether or not other strains can effectively perform high cell density fermentations with cell recycle (RaBIT fermentations). To further our knowledge, strains were tested using RaBIT and traditional fermentations for comparison. In total, 9 strains were tested including four *S. cerevisiae* strains, three *S. stipitis* strains, a *Z. mobilis* strain, and an *Escherichia coli* strain. From all these tested strains, the best RaBIT fermenting strain was chosen and used for further RaBIT fermentation investigations presented in this dissertation

(Chapters 4-6). The best traditional fermenting strain was chosen and used to optimize a traditional cellulosic ethanol process (Chapter 3).

2.2 Materials and Methods

2.2.1 Biomass and pretreatment

Corn stover was provided by the Great Lakes Bioenergy Research Center (GLBRC). The corn (Pioneer 36H56) from which the stover was produced was planted in May of 2009 in field 570-N at the Arlington Agricultural Research Station in Columbia Country, WI and harvested in November of 2009. The biomass was pretreated by the Biomass Conversion Research Laboratory (BCRL) located at Michigan State University in East Lansing, MI using the AFEX pretreatment process as previously described in the literature (Balan et al., 2009). AFEX pretreatment conditions were: 1:1 ammonia to biomass ratio by mass, 60% moisture on dry weight basis, 100^{o}C, and 30 min. reaction time. Glucan, xylan, and acid insoluble lignin content plus ash were 38.0%, 23.8%, and 20.4% by dry mass, respectively. The corn stover was stored at 4 ^{o}C.

2.2.2 Microorganisms and seed culture preparation

Saccharomyces cerevisiae GLBRCY73 was genetically modified to contain xylose reductase, xylitol dehydrogenase, and xylulokinase genes (Sato et al., 2013). *S. cerevisiae strains* GLBRCY127 and GLBRCY128 were genetically modified to contain xylose isomerase and xululokinase genes (Parreiras et al., 2014). 424A(LNH-ST) was generously provided by Prof. Nancy W. H. Ho of Purdue University (West Lafayette, IN). *S. cerevisiae* 424A was genetically modified with multiple copies of xylose reductase and xylitol dehydrogenase genes

from *Scheffersomyces (Pichia) stipitis* and an endogenous xylulokinase gene incorporated in the chromosome (Ho et al., 1999).

Zymomonas mobilis 8b was provided by MBI, International (Lansing, MI) and was originally obtained from the National Renewable Energy Laboratory (Golden, CO) (Mohagheghi et al., 2004).

Scheffersomyces (Pichia) stipitis FPL-061 and FPL-DX26 strains were provided by Prof. Thomas W. Jeffries of the University of Wisconsin (Madison, WI) (Sreenath and Jeffries, 1999). NRRL Y-7124 was obtained from the Agricultural Research Service Culture Collection (National Center Agricultural Utilization Research, Peoria, IL) (Slininger et al., 1985).

Escherichia coli KO11 was obtained from the American Type Culture Collection having designated number 55124 (Ohta et al., 1991).

All strains were maintained in glycerol stocks at -80 °C. Seed cultures were prepared in medium containing 100 g/L dextrose, 25 g/L xylose, 10 g/L Yeast Extract, and 20 g/L Tryptone. Seed cultures were performed in 250 mL Erlenmeyer flasks using a 100 mL working volume. The initial OD_{600} of seed cultures was 0.1. Cultures were incubated at 30 °C and 150 RPM for 20 h. After 20 h, 1 mL of the culture was transferred to new media for an additional 20 h. The cultivation was made aerobic by use of a foam stopper for *S. stipitis* strains. All other seed cultures were cultured microaerobically using a rubber stopper pierced by a needle.

2.2.3 Enzymatic hydrolysis

Enzymatic hydrolysis at 6% (w/w) glucan loading was performed in 1 L baffled Erlenmeyer flasks with a total reaction mixture of 400 g (biomass, water, enzymes, and acid). Biomass was loaded in fed batch mode by adding half the biomass at t = 0 h and the other half at

t = 2 h. The enzyme cocktail consisted of 20 mg protein/g glucan Cellic CTec2 (Novozymes), 5 mg/g Cellic HTec2 (Novozymes), and 5 mg/g Multifect Pectinase (Genencor). Hydrolysis was performed for 48 h at 50 °C and 250 RPM using a pH of 4.8. Adjustments to pH were made using 10 M potassium hydroxide or 12.1 M hydrochloric acid. Hydrolysis slurry was centrifuged in 2 L bottles at 7500 RPM for 30 minutes and then sterile filtered. This hydrolysate was used for fermentation without external nutrient supplementation unless otherwise indicated.

2.2.4 Fermentations

Fermentations were performed in 125 mL Erlenmeyer flasks using 50 mL of hydrolysate. Cells for inoculation were harvested by centrifugation from the seed cultures. Inoculation size was determined by dry cell weight (DCW) concentration. Inoculations were performed at 0.1g/L for traditional fermentations, 4 g/L DCW for RaBIT fermentations using *Z. mobilis* and *E. coli,* and 7.5, 8.0, 9.0, 10, or 12.0 g/L DCW for RaBIT fermentations using *S. cerevisiae* and *S. stipitis*. The initial (starting) pH was adjusted using 10 M potassium hydroxide. Initial pH for *S. cerevisiae* and *S. stipitis* was 5.5. Initial pH values for *Z. mobilis* and *E. coli* were 6.0 and 7.0, respectively. The pH for the *E. coli* was buffered using 0.05 M MOPS and adjusted twice daily. The pH for all other strains was not adjusted during the fermentations. The fermentations were performed in a shaking incubator at 150 RPM. Temperature was set at 37 °C for *E. coli* and 30 °C for all other strains before temperature optimization. After optimization, the temperature was increased to 32 °C for *S. cerevisiae* GLBRCY128. The flasks were under microaerobic conditions. Traditional fermentations were incubated for 5 days. RaBIT fermentations were performed for 24 h. At the end of each RaBIT fermentation stage, the broth was centrifuged in 50 mL centrifuge tubes at 4000 RPM for 10 minutes. The corresponding cell pellets were then

inoculated into fresh hydrolysate to begin the next cycle. All fermentation experiments were performed with at least 2 biological replicates.

2.2.5 Measurements of cell population

The optical density at 600 nm was used to measure the cell concentration of the fermentation broths. The OD_{600} measurement was then correlated to the DCW by use of a calibration curve.

2.2.6 HPLC Analysis

Glucose, xylose, and ethanol concentrations were analyzed by HPLC using a Biorad Aminex HPX-87H column. Column temperature was maintained at 50 ^{o}C. Mobile phase (5 mM H_2SO_4) flow rate was 0.6 mL/min.

2.3 Results and Discussion

Nine different strains were tested for their suitability in high cell density fermentations with cell recycling. The four *Saccharomyces cerevisiae* strains, three *Scheffersomyces stipitis* strains, one *Escherichia coli* strain, and one *Zymomonas mobilis* strain were chosen to represent all major ethanologens publicly available for commercial use. The first goal of our study was to identify a suitable strain to further investigate high cell density fermentations with cell recycle for the RaBIT process. The second goal was to determine if the RaBIT process could be carried out by all ethanologens.

Strain evaluation was performed using 6% (w/w) glucan loading AFEX treated corn stover hydrolysate. Both traditional fermentations (Figure 3) and RaBIT fermentations (Figure 4) were performed using each strain. By performing both types of fermentations, we hoped to observe correlations between the two processes that would help identify strains suitable for the

RaBIT process. In the strain evaluation using traditional fermentation methods, *S. cerevisiae* 424A and *Z. mobilis* 8b showed the best performance, yielding over 40 g/L ethanol and consuming all but 5 g/L and 6.5 g/L xylose, respectively. Strain 8b was able to consume 75% of the xylose after 48 h, while 424A had only consumed 56% of the xylose by 48 h. *S. cerevisiae* GLBRCY128 (Y128) was the next highest performing strain yielding 39 g/L ethanol and consuming all but 13 g/L xylose. However, its fermentation rate was much slower than either 424A or 8b (Table 2). The results summarized in Figure 3 show that three of the nine strains were suitable for RaBIT fermentations: Y128, 424A, and 8b. These three strains were capable of consuming almost all of the glucose and xylose in the first fermentation cycle and produced more than 40 g/L of ethanol. Of the three strains, 424A showed the best potential for cell recycle due to greater xylose consumption in the second cycle coupled with less reduction in ethanol production during the second cycle. However, Y128 and 8b gave greater ethanol yields. Due to higher xylitol and glycerol production by 424A (Table 1), we hypothesized that use of the xylose isomerase pathway instead of the xylose reductase-xylitol dehydrogenase pathway was a factor for the higher ethanol production per gram of sugar consumed observed with Y128 and 8b. Using the xylose reductase-xylitol dehydrogenase pathway requires xylose to be converted to xylitol before conversion to xylulose leading to an equilibrium concentration of xylitol that is typically not converted to ethanol (Kuyper et al., 2004). The xylose isomerase pathway/enzyme directly converts xylose to xylulose eliminating the build up of xylitol (Kuyper et al., 2004). Glycerol is also produced to counteract the redox imbalance in the xylose reductase-xylitol dehydrogenase pathway (Kuyper et al., 2004). The xylose reductase enzyme requires the oxidation of NADPH to $NADP^+$, while the xylitol dehydrogenase reduces NAD^+ to NADH creating the imbalance (Kuyper et al., 2004). The xylose isomerase enzyme, by oxidizing and

then reducing either NADPH or NADH, does not create a redox imbalance (Kuyper et al., 2004). The higher cell mass concentration was seen as a benefit for the 424A and Y128 strains. Excess cell mass can perhaps become a biorefinery co-product, for example, as animal feed. For these reasons, Y128 was chosen over 424A as the most promising of these nine strains for further evaluation in the RaBIT process. A major goal of these further studies is to understand and then overcome the reduced cell performance that accompanies cell recycling.

E. coli KO11 performance was vastly improved in the RaBIT fermentation compared to the traditional fermentation. *E. coli* KO11 was able to consume almost 3 times as much xylose and produce over 7.5 g/L more ethanol in the 24 h RaBIT fermentation compared to the 120 h traditional fermentation. The benefit of increased cell loading appeared to help *E. coli* KO11 overcome poor inhibitor resistance and detoxification. Interestingly, Y128 also showed a large improvement by consuming 8 g/L more xylose, while producing 5 g/L more ethanol in the RaBIT fermentation compared to the traditional 120 h fermentation. In the case of Y128, increasing the cell loading appears to have resulted in a greater overall xylose consumption rate allowing for more complete xylose consumption. The seven other strains studied gave comparable or worse performance when comparing RaBIT fermentations to traditional fermentations.

Table 1 Final RaBIT fermentation concentrations

Experiment	Glucose, g/L	Xylose, g/L	Xylitol, g/L	Glycerol, g/L	Ethanol, g/L
S. cerevisiae 424A(LNH-ST)					
Cycle 1	1.53 ± 0.00	3.14 ± 0.03	0.99 ± 0.03	6.00 ± 0.01	40.78 ± 0.06
Cycle 2	1.77 ± 0.01	4.01 ± 0.05	1.52 ± 0.01	5.81 ± 0.01	40.54 ± 0.04
S. cerevisiae GLBRCY128					
Cycle 1	0.00 ± 0.00	3.28 ± 0.05	0.00 ± 0.00	2.89 ± 0.02	44.47 ± 0.04
Cycle 2	0.00 ± 0.00	6.92 ± 0.06	0.00 ± 0.00	2.73 ± 0.00	42.32 ± 0.04
Z. mobilis 8b					
Cycle 1	0.98 ± 0.02	4.90 ± 0.06	0.00 ± 0.00	0.67 ± 0.00	43.87 ± 0.06
Cycle 2	1.02 ± 0.01	6.71 ± 0.03	0.00 ± 0.00	0.77 ± 0.03	42.89 ± 0.11

Error values represent standard deviations

S. stipitis FPL-061 performed comparably to *S. cerevisiae* GLBRCY73 (Figure 3 & Figure 4). However, *S. stipitis* FPL-DX26 and Y-7124 were not capable of consuming most of the glucose during RaBIT fermentations (Figure 4). We hypothesize that the latter two strains require supplemental oxygen as typical for most *S. stipitis* strains (Laplace et al., 1991).

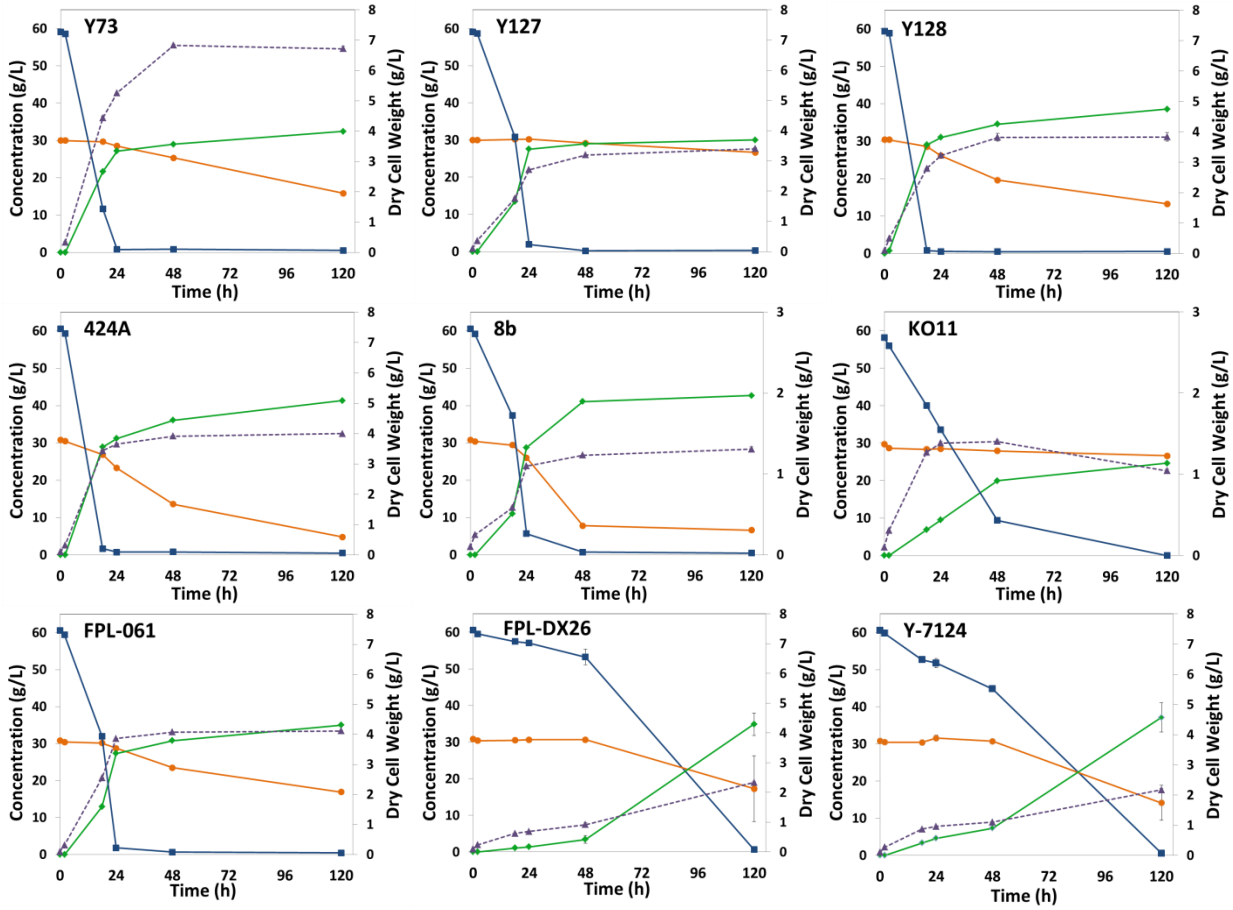

Figure 3 Strain evaluations during traditional fermentations using AFEX corn stover hydrolysate. Concentrations are shown for glucose (blue squares), xylose (orange circles), ethanol (green diamonds), and dry cell weight (purple triangles). Error bars represent standard deviations and are present for all data points but may be hidden by the symbol.

Comparing the results of the traditional and RaBIT fermentations, the performance of the RaBIT process seems to be tied to the specific xylose consumption rate. The three strains (424A,

8b, and Y128) with a specific xylose consumption rate greater than 0.075 g/g/h were capable of performing RaBIT process fermentations (Table 2). This high rate is necessary due to the nature of the RaBIT process. An assumption is that all strains have a cell population ceiling that depends on the availability of sugar and nutrients. The ceiling in the RaBIT fermentation system depends on cell maintenance needs, cell biomass yields on substrates, and cell growth/death rate. The cell population ceiling is the maximum cell density that could be sustainably maintained in RaBIT fermentation system. It would then be necessary for each strain to have a sufficient specific xylose consumption rate to consume the xylose in 24 h when near or below this ceiling. An initial cell density above the ceiling can result in improved performance during the first cycle, but poor performance after recycling of the cells (data not shown). For the typical *S. cerevisiae* strains, the required xylose consumption rate appears to be around 0.075 g/g/h.

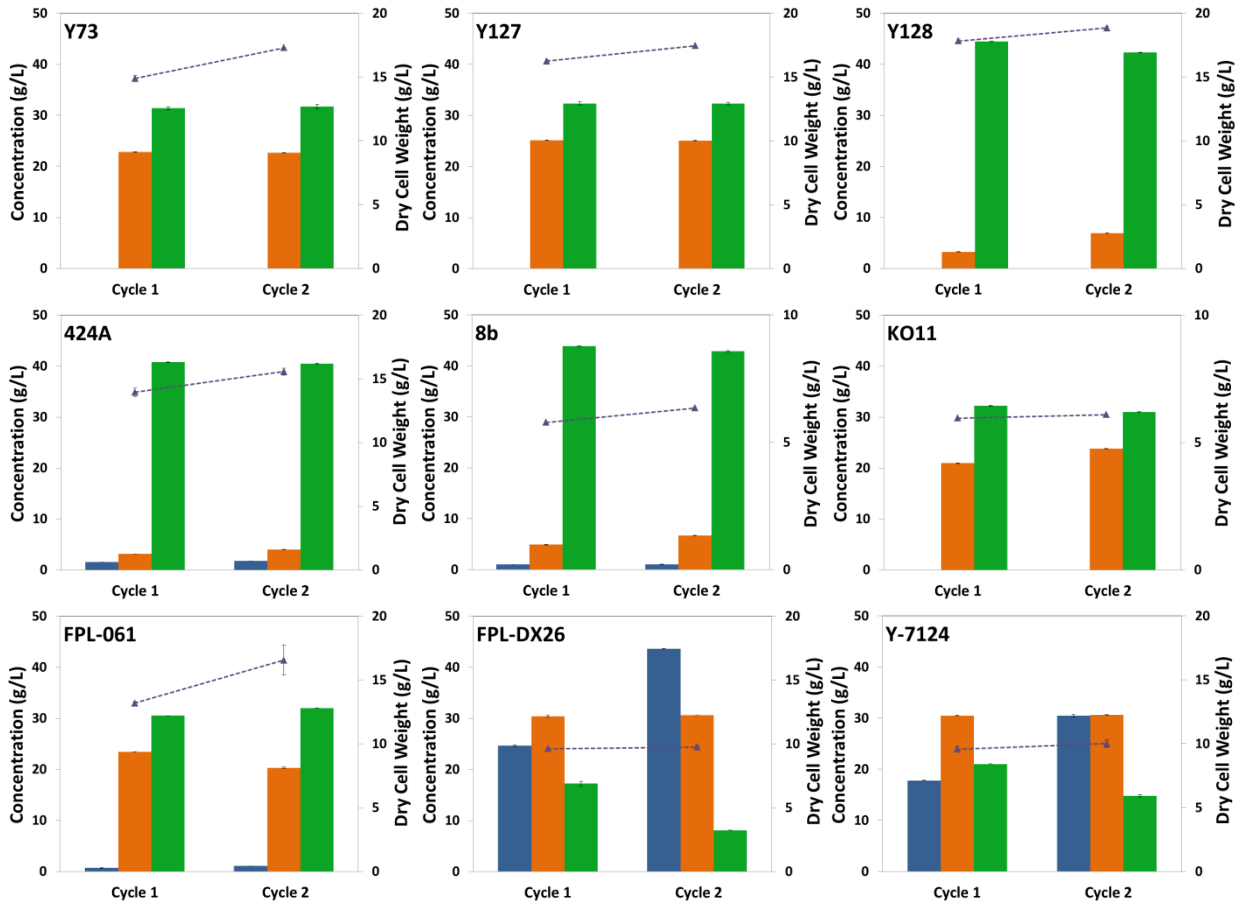

Figure 4 Strain evaluations during RaBIT fermentations using AFEX corn stover hydrolysate. The initial glucose and xylose concentrations were 62 g/L and 32 g/L respectively. Final concentrations are shown for glucose (blue), xylose (orange), ethanol (green), and dry cell weight (purple triangles). Error bars represent standard deviations and are present for all data points but may be hidden by the symbol.

The performance of *S. stipitis* FPL-061 shows there may be more required for a strain to be successful at RaBIT fermentations than just a high specific xylose consumption rate. FPL-061 exhibits 2.5 fold faster specific xylose consumption rate than *S. cerevisiae* Y73. Despite this, the RaBIT fermentation performance between the two strains is similar even with regards to cell concentration. FPL-061 does appear to have a longer lag phase compared to Y73 and other *S. cerevisiae* strain (see glucose consumption patterns in Figure 3). It is possible that FPL-061 more slowly detoxifies pretreatment degradation products than the yeast. A slow detoxification

rate also appears to be the reason why the other two *S. stipitis* strains (FPL-DX26 and Y-7124) performed poorly for both RaBIT and traditional fermentations.

Overall, this comparison also shows one of the key benefits of the RaBIT process, namely increased ethanol productivity (gram EtOH/fermentation volume/time) with the corresponding potential reductions in capital cost. The RaBIT fermentations increased ethanol productivity by more than two fold for the three suitable strains (Table 2). For Y128 specifically, the ethanol productivity increased by 2.5 fold for the RaBIT fermentation compared to a 48 h traditional fermentation.

Table 2 Traditional Fermentation and RaBIT Fermentation Comparison

	Specific Xylose Cons. Rate[+,a], g/g/hr	48 hr Traditional Fermentation EtOH Prod.[*,b], g/L/hr	120 hr Traditional Fermentation EtOH Prod.[*,c], g/L/hr	Avg. RaBIT Fermentation EtOH Prod.[*,d], g/L/hr	Traditional Fermentation EtOH Conc., g/L	Avg. RaBIT Fermentation EtOH Conc., g/L
Strain						
FPL-061	0.055 ± 0.001	0.642 ± 0.001	0.292 ± 0.002	1.304 ± 0.032	35.1 ± 0.2	31.3 ± 0.8
FPL-DX26	0.002 ± 0.008	0.071 ± 0.022	0.291 ± 0.026	0.529 ± 0.190	34.9 ± 3.1	12.7 ± 4.6
Y-7124	0.033 ± 0.031	0.152 ± 0.002	0.309 ± 0.033	0.747 ± 0.129	37.1 ± 4.0	17.9 ± 3.1
Y73	0.022 ± 0.001	0.604 ± 0.001	0.271 ± 0.001	1.315 ± 0.017	32.5 ± 0.1	31.6 ± 0.4
Y127	0.015 ± 0.003	0.603 ± 0.007	0.250 ± 0.001	1.346 ± 0.014	30.0 ± 0.2	32.3 ± 0.3
Y128	0.077 ± 0.003	0.720 ± 0.006	0.322 ± 0.001	1.808 ± 0.045	38.6 ± 0.1	43.4 ± 1.1
424A	0.107 ± 0.001	0.752 ± 0.002	0.345 ± 0.003	1.694 ± 0.005	41.3 ± 0.3	40.7 ± 0.1
8b	0.650 ± 0.011	0.856 ± 0.004	0.356 ± 0.001	1.808 ± 0.021	42.7 ± 0.1	43.4 ± 0.5
KO11	0.077 ± 0.003	0.416 ± 0.001	0.205 ± 0.000	1.319 ± 0.026	24.6 ± 0.0	31.6 ± 0.6

[+]Specific xylose consumption rate was calculated by dividing the xylose consumed by the time period and average dry cell weight concentration as correlated from OD measurements.

[*]Ethanol productivity was calculated by dividing the ethanol concentration by time of fermentation.

Calculated from (a) 24 to 48 hr, (b)0 to 48 hr, (c) 0 to 120 hr, or (d) 0 to 24 hr.

Average RaBIT fermentation calculations were performed by averaging the data from the two cycles.

Error values represent standard deviations

2.4 Conclusion

We found that not all ethanologens are suitable for RaBIT platform fermentations. Of the nine tested ethanologens, *Saccharomyces cerevisiae* 424A(LNH-ST), *Zymomonas mobilis* 8b, and *S. cerevisiae* GLBRCY128 showed good performance in the RaBIT fermentation process. Y128 was chosen for further optimization of process conditions. *Z. mobilis* 8b was chosen for optimization of a traditional fermentation process. Strains having a specific xylose consumption rate above 0.075 g/g/h showed acceptable RaBIT fermentation performance.

CHAPTER 3: TRADITIONAL PROCESS OPTIMIZATION AND EVALUATION USING ZYMOMONAS MOBILIS 8B

Abstract

Work reported in this chapter optimized process conditions and performed economic analysis for an industrially relevant cellulosic biomass to ethanol process. Corn stover was pretreated using the AFEX™ process before being pelletized. Novozymes' Cellic CTec3 and HTec3 were used to hydrolyze the biomass. *Zymomonas mobilis* 8b was used for fermentation. he optimizations performed were based on: seed culture media, fermentation temperature, nutrient addition, inoculum size, and process time. The economic analysis showed that changing the seed culture medium from a mixture of pure sugars, yeast extract, and potassium phosphate to AFEX corn stover hydrolysate and corn steep liquor provided the largest reduction in the minimum ethanol selling price (MESP) at $0.37/gal. In total, the optimizations reduced the baseline MESP by $0.44/gal. A 96 h combined enzymatic hydrolysis and fermentation process time yielded 0.211 g ethanol/g corn stover.

3.1 Introduction

The work in Chapter 3 benchmarked a traditional cellulosic ethanol process using commercially relevant reactants. Optimization information was later used for life cycle assessment and techno-economic analysis for comparison with the RaBIT process. The biomass used for Chapter 3 work was different from the biomass used in Chapter 2, 4, 5, and 6 with the exception of the mass balances performed in Chapter 6. The biomass was supplied by MBI and treated using either lab scale or pilot scale gaseous AFEX pretreatment. The gaseous AFEX process minimizes costs by condensing gaseous ammonia onto biomass and recovering that

gaseous ammonia onto subsequent beds of biomass by alternately condensing and evaporating the ammonia. The lab scale gaseous ammonia process showed slight improvements over the traditional AFEX process with regards to digestibility (Campbell et al., 2013). The biomass provided by MBI was also densified using a pellet mill. Pelletization does not affect digestibility (Bals et al., 2013). The work in this Chapter was an extension of previous research on AFEX pretreatment, pelletization, and enzymatic hydrolysis reported by Campbell et al. (2013) and Bals et al. (2013).

The biocatalysts used for this study represent some of the best available for AFEX-treated biomass. CTec3 and HTec3 are the latest commercial enzymes available through Novozymes. Their predecessors, CTec2 and HTec2 (used in Chapters 2 and 4), have been widely used in the literature for cellulosic biomass to sugar conversion with great success. According to Novozymes' website, CTec3 shows approximately 1.5 fold higher conversion efficiency compared to CTec2 due to addition of GH61 enzymes, improved beta-glucosidases, and new hemicellulases (Novozymes, 2014a). HTec3, with added endo-xylanase and beta-xylosidase activities, shows 600% improvement over the previous generation of enzymes (Novozymes, 2014b). *Zymomonas mobilis* 8b was chosen as the ethanologen for this research. *Z. mobilis* 8b was developed at the National Renewable Energy Lab (NREL) and engineered to consume xylose (Mohagheghi et al., 2004). *Z. mobilis* strains are attractive due to higher ethanol metabolic yields on average compared to the more traditionally-used *Saccharomyces cerevisiae* strains (Dien et al., 2003). Previous work using AFEX corn stover hydrolysate showed that *Z. mobilis* 8b completely consumes xylose within 48 h and outperformed the industrially-relevant *S. cerevisiae* 424A(LNH-ST) strain created by Dr. Nancy Ho of Purdue University (Chapter 2).

Important process conditions were optimized to improve ethanol yield and process economics (seed culture media, fermentation temperature, nutrient addition, and inoculum size). The optimal process time was determined in combination with mass balances on sugar and ethanol. An economic analysis was performed to estimate cost savings for each individual optimization and to determine the optimal processing time. Next, lab scale (10 L) and pilot scale (450 L) gaseous AFEX pretreatments were compared for their effects on digestability and fermentability of the pretreated corn stover. The seed culture method was also re-optimized.

3.2 Materials and Methods

3.2.1 Corn Stover

The corn stover was harvested from Hamilton County, Iowa, and baled by Iowa State University in October, 2011. The biomass was milled using a 1 inch screen and subsequently dried to less than 5% moisture. The composition was determined to be 34.8% glucan, 18.8% xylan, 3.2% arabinan, and 12.2% acid insoluble lignin. Further details on the corn stover used can be found in Campbell et al. (2013).

3.2.2 AFEX Lab scale Pretreatment

The biomass was pretreated using 10 L packed bed reactors as described by Campbell et al. (2013). In brief, the biomass was loaded at 25% moisture before heating to > 80 °C using low pressure steam. Gaseous ammonia was then added at a 1:1 ammonia to biomass ratio by mass. After ammonia loading, the biomass was soaked for 30 min before the ammonia was released. Steam was then used to strip out the remaining ammonia. The biomass was then dried in a convection oven maintained at 50 °C.

3.2.3 AFEX Pilot scale Pretreatment

The corn stover was pre-wetted to 18-20% moisture and packed into perforated stainless steel baskets at a density of ~80-100 kg dry weight/m3. Seven baskets were loaded into a 450 L vertical reactor ~45 cm diameter and 2.7 m tall and sealed shut. Steam was introduced to force out air and preheat the reactor to 90˚C. Ammonia vapor at 60˚C was added at the top of the reactor at an amount equal to 0.6 g/g dry biomass. The average temperature in the reactor after ammonia addition was 100˚C. The biomass was allowed to sit for 30-150 minutes with no external heating before ammonia release. Residual ammonia was removed by introducing low pressure steam at the top of the reactor and allowing ammonia vapor to escape from the bottom. The release ammonia was transferred to a second reactor for a subsequent batch of AFEX treatment. The baskets of treated biomass were then removed with the contents placed in burlap sacks. The sacks were then dried at 45˚C in a forced convection oven.

3.2.4 Densification

After pretreatment, the biomass was pelletized to increase bulk density. The pelleting process was performed as described in Bals et al. (2013) using a Buskirk Engineering PM810 flat die pellet mill. First, the mill was preheated to 70 °C by running distiller's dry grains and solubles through the pelletizer. AFEX treated biomass soaked in distilled water to 20% moisture was then run through the pellet mill. After pelleting, the biomass was dried in a convection oven at 50 °C. The pellets were stored at room temperature.

3.2.5 Enzymatic Hydrolysis

The enzymatic hydrolysis was performed in 250 mL baffled Erlenmeyer flasks. The biomass pellets were added at 20% solids loading using a total reaction mass of 100 grams. If biomass was autoclaved to prevent microbial contamination, the flasks were first covered with

foil and an aluminum culture cap with no added water before being autoclaved at 121 °C for 20 minutes. Autoclaved distilled water was added to reach the 100 gram final reaction mass minus the future enzyme, nutrient, and inoculum requirements. The pH was adjusted to 5.0 using 12.1 M hydrochloric acid. The commercial enzymes Cellic CTec3 and HTec3 (Novozymes, Franklinton, NC, USA) were added at a 10 mg protein/g glucan loading for each. The enzymes were diluted using distilled water due to their high viscosity and filtered through a 22 micron filter for sterility. The flasks were incubated in a shaker at 50 °C and 250 RPM. Hydrolysis time was 48 h except when testing optimal processing time during the mass balances when 12, 24, and 48 h hydrolysis times were used.

3.2.6 Microorganism and Seed Cultures

Zymomonas mobilis 8b was used for the fermentations. The strain was provided by the NREL and was previously engineering to utilize xylose (Mohagheghi et al., 2004).

The seed culture preparation involved stages. For optimization of lab scale pellet fermentations, the first stage containing a "rich media" composed of 100 g/L glucose, 20 g/L xylose, 10 g/L yeast extract, and 2 g/L potassium phosphate was inoculated using a glycerol stock. This stage was performed in 15 mL centrifuge tubes with a 10 mL reaction volume under anaerobic conditions. Future seed culture stages were performed in 125 mL Erlenmeyer flasks using a reaction volume of 50 mL and a 5% inoculum. The media for the second stage was identical to the first stage or a combination of corn stover hydrolysate and corn steep liquor (5, 10, 25, or 50 g/L). Seed cultures were incubated in a shaker at 32 °C and 100 RPM until late exponential phase (see Table 3 for incubation times).

For optimization of pilot scale pellet fermentations, the first stage containing a "rich media" composed of 100 g/L glucose, 20 g/L xylose, 10 g/L yeast extract, and 2 g/L potassium phosphate was inoculated using a glycerol stock. This stage was performed in 125 mL Erlenmeyer flasks with a 50 mL reaction volume. Future seed culture stages were performed in 250 mL Erlenmeyer flasks using a reaction volume of 100 mL. The media for the second stage was identical to the first stage or a combination of corn stover hydrolysate (10, 15, 20, 22% solids loading), dextrose (0, 25, or 50 g/L), and corn steep liquor (0, 5, 10, 25, or 50 g/L). At times, a third seed culture stage was utilized using variable media as optioned above. Seed cultures were incubated in a shaker at 32 °C and 100 RPM until late exponential phase (see Table 3 for incubation times). Inoculum sizes between stages and specific media composition are given in Table 9.

Table 3 Seed culture media incubation times

	Seed Culture Incubation Time (h)
Skid-Scale Experiments	
Rich Media	7.5
Hydrolysate	16.5
Pilot-Scale Experiments	
Rich Media	11
15% Solids Hydrolysate	11
15% Solids Hydrolysate + 25 g/L Dextrose	13
15% Solids Hydrolysate + 50 g/L Dextrose	18
22% Solids Hydrolysate	16

3.2.7 Fermentation

The fermentation was performed without separation of the hydrolysate from the unhydrolyzed solids and was conducted in the same flask as the enzymatic hydrolysis with the exception of the temperature test (see below). The pH was adjusted to 6.0 using 10 M potassium

hydroxide. Inoculation was performed by directly adding the *Z. mobilis* seed culture on a percent weight basis assuming a density of 1 g/mL. Inoculum sizes of 2.5%, 5%, and 10% of the total reaction mass (biomass, water, enzyme, corn steep liquor, acid, and inoculum) were used for this paper. Corn steep liquor (CSL) was added to the fermentation as a nutrient source. The CSL was weighed onto plastic dishes to the nearest 0.01 g and washed into the fermentation using the inoculum broth. The fermentations were conducted at 150 RPM using a shaking incubator. Fermentations were performed at 30, 32, 35, 37, or 40 °C depending on the experiment.

For temperature testing, fermentations were performed using a synthetic media (70 g/L glucose, 40 g/L xylose, and 10 g/L yeast). Fermentations were performed in 125 mL Erlenmeyer flask. Synthetic media was added to a volume of 49 mL. Inoculum size was 1 mL providing an initial OD of ~0.1. The flasks were shaken in an incubator at 150 RPM. All fermentation experiments were performed with at least 2 biological replicates.

3.2.8 Cell Population Measurement

OD was measured 600_{nm} using a Beckman Coulter DU 720 spectrophotometer. Samples were diluted to stay within a raw reading of 0.1-1. OD measurements were initially taken for each medium before inoculation and subtracted from later readings as a "blank."

Cell viability was measured by plating. The fermentation slurry was serially diluted and 20 µL of each dilution was plated onto agar plates (25 g/L glucose, 5 g/L yeast extract, 10 g/L tryptone, and 2% agar). Plates were placed in a stationary incubator at 30 °C for two days. After two days, the plates were removed and individual colonies counted.

3.2.9 Composition and Oligomeric Sugar Analysis

Compositional analysis of biomass and unhydrolyzed solids was performed using the NREL's standard analytical method as described in Sluiter et al. (2010). The samples were milled before composition analysis using a Cyclotec^{TM} 1093 mill (Foss, Denmark) equipped with a 2 mm screen. Oligomeric and polymeric sugars were determined as also described in Sluiter et al. (2010).

3.2.10 HPLC Analysis

Samples taken during experiments were frozen at -20 °C for storage purposes until they were ready to be analyzed. Before analysis, the samples were centrifuged and the supernatant was diluted 10x before being run through the HPLC. Glucose, xylose, lactate and ethanol concentrations were analyzed through a Biorad Aminex HPX-87H column. Column temperature was maintained at 50 ^{o}C. The 5 mM H_2SO_4 mobile phase flow rate was 0.6 mL/min.

3.2.11 Mass Balance

A mass balance was performed by first accounting for all sugars initially present in the biomass before enzymatic hydrolysis using the compositional analysis as mentioned above. After fermentation, the solids and liquids were separated by centrifugation at 5300 RPM for 30 min. The oligomeric sugars, monomeric sugars, and ethanol were analyzed for the liquid stream as described above. The mass and volume of the liquid stream was recorded. The water content of the wet solids was determined by addition of a known volume of water. Change in monomeric sugars and ethanol was used to determine the initial water content using the following equation:

$$Volume_{initial} * Concentration_{initial} = (Volume_{initial} + Volume_{addition}) * Concentration.$$

The solids were then washed with distilled water three times at a ratio of 2:1 by mass.

3.2.12 Economic Analysis

For economic analysis, a model based heavily on the 2011 NREL Technical Report (Humbird et al., 2011) was built in Microsoft Excel. This report combines a rigorous mass and energy balance of a simulated cellulosic ethanol plant with industry estimates of capital and operating costs. The model was modified as required based on the results obtained from this study. Equipment was resized using the scaling factors provided in the NREL report as needed, and energy costs were estimated as proportional to the material flows in each operation. Multiple changes were made to the model to adapt it to AFEX pellets and the fermentation changes. The size of the plant was not changed from 2,205 dry ton/day. These changes are as follows (the areas mentioned are labeled as such in the NREL report and represent major processes in the refinery):

- Areas 100 and 200 (feedstock handling and pretreatment) were eliminated. For feedstock handling, an installed cost of $4.5 million was estimated based on corn grain handling (Kwiatkowski et al., 2006). Pellets are expected to be handled similarly to corn grain. Pretreatment is performed in the depot setting and thus is not needed at the refinery.
- Area 300 (hydrolysis and fermentation) was redesigned in Excel to account for the differing residence times, inputs, and conversions. A sugar and ethanol mass balance was performed, which was used to size all equipment and estimate energy requirements. The vertical plug flow liquefaction tank in the NREL report was eliminated, as liquefaction can occur in conventional reactors with AFEX pellets.
- Area 400 (enzyme production) was eliminated, as Novozymes enzymes were used in this experiment. Instead, the cost of enzymes was estimated at $3.60/kg protein. This

represents the enzyme production costs associated from the original NREL report (Humbird et al., 2011).

- Area 500 (distillation) was similar to the NREL report. The distillation column energy required was estimated based on the ethanol concentration using values provided by Katzen International (Madson, n.d.).
- Area 600 (wastewater treatment) was replaced with the wastewater treatment approach in the 2002 NREL technical report (Aden et al., 2002). This approach is less expensive than the 2011 approach, but was replaced due to the high salt content in acid pretreated biomass. AFEX pretreatment does not generate enough salts to require the 2011 approach.
- Area 700 and 900 (storage and utilities) were identical to the NREL report, with various pieces of equipment resized as needed.
- Area 800 (power and steam cogeneration) was sized according to the hydrolysis and fermentation mass balance. The boiler was sized based on total solids entering, and the energy generated based on the relative energy content of each major component of the biomass. Total energy requirements throughout the refinery determined the excess electricity produced.

3.3 Results and Discussion

3.3.1 Enzymatic hydrolysis on autoclaved and non-autoclaved AFEX skid-scale pellets

Enzymatic hydrolysis was performed using the same method outlined by Bals et al. (2013) with an increased solids loading. The previous work by Bals was performed to optimize enzymatic hydrolysis conditions. Initial experiments in the work reported here indicated a bacterial contamination was present associated with lactate production (Figure 5). Lactate levels

varied between hydrolysis experiments resulting in varied fermentation performance (data not shown). To eliminate the contamination, the pellets were autoclaved before enzymatic hydrolysis. The autoclaving process was performed without added water. A dry autoclaving process would limit the formation of degradation products. Figure 5 shows that lactate was not found during enzymatic hydrolysis after the pellets were autoclaved for 20 minutes at 121 °C.

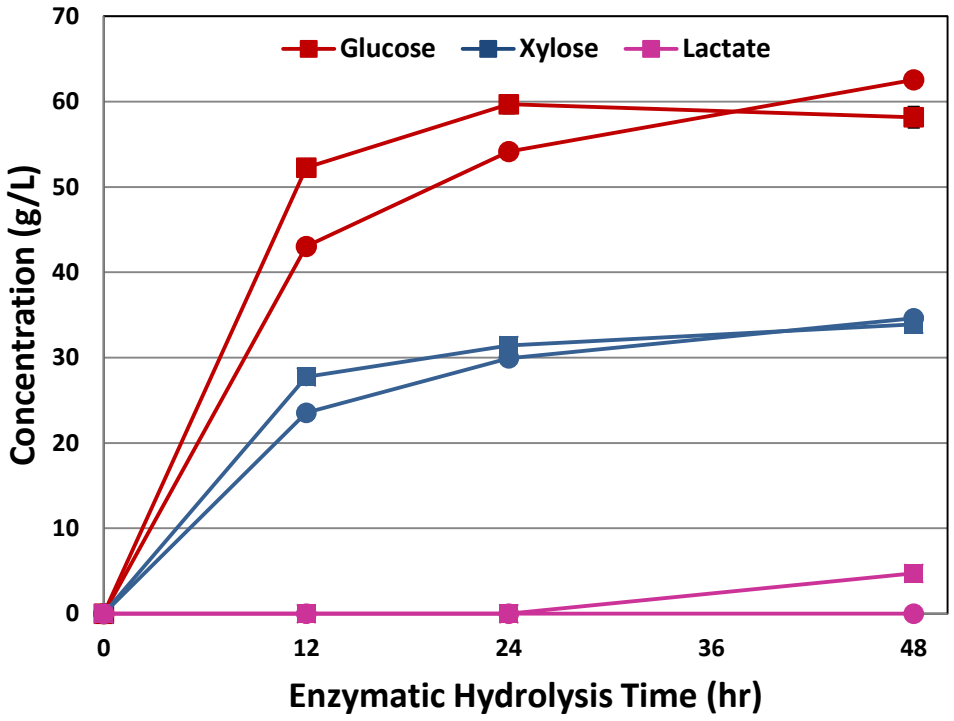

Figure 5 Sugar release profiles comparing no autoclaving (squares) and autoclaving (circles) prior to enzymatic hydrolysis. Error bars represent standard deviations and are present for all data points but may be hidden by the symbol.

One drawback to heating biomass is sugar degradation. However due to AFEX pretreatment not hydrolyzing polymeric sugar chains, degradation product formation was assumed minimal. The composition of autoclaved and non-autoclaved pellets, summarized in Table 4, confirmed that no significant degradation of sugars occurred. Heating may have slightly affected the pellet structure without affecting total hydrolysis yield. The glass transition

temperature of corn stover is reported as approximately 75 °C, while lignin has a potentially higher reported glass transition temperature of 100 °C to 170 °C (Kaliyan and Morey, 2009; Irvine, 1985). The pelleting process was performed at around 70 °C to 75 °C or greater (Bals et al., 2013; Campbell et al., 2013). The autoclave temperature was at 121 °C. Thus a change in the distribution or physical structure of the lignin may have been possible. This could explain the lower initial hydrolysis rate when autoclaved pellets were used despite a similar sugar yield at 48 h when accounting for the lactate production (Figure 5). It may be possible to eliminate sterilization entirely for the commercial process. Similar large scale fermentations using the same AFEX corn stover pellets and *Z. mobilis* 8b have been performed by MBI with no observable performance loss due to the contamination (data not shown).

Table 4 Biomass composition based on dry weight

Process	% Glucan	% Xylan	% Arabinan	% Acid Insoluble Lignin	% Ash
AFEX Skid-scale Treated Pellets	34.4% ± 0.9%	20.6% ± 0.7%	3.2% ± 0.1%	15.4% ± 0.1%	14.5% ± 0.1%
Autoclaved AFEX Treated Pellets	34.2% ± 1.5%	20.5% ± 0.9%	3.2% ± 0.2%	16.7% ± 0.6%	14.8% ± 0.1%

Errors values represent standard deviations

3.3.2 Optimization of seed culture media for skid-scale pellets

The effect of different seed culture media on hydrolysate fermentations was investigated for *Z. mobilis* 8b. The following rich media recipe was used for culturing the strain: 10 g/L yeast extract, 2 g/L potassium phosphate monobasic, 100 g/L glucose, and 20 g/L xylose. This rich media would be expensive and create added complexity in an industrial situation. For these reasons, we chose to use hydrolysate produced from the enzymatic hydrolysis of pelleted AFEX treated corn stover. The hydrolysate was prepared in the same fashion as above, but without autoclaving and added preparation of centrifugation to remove solids and filtration through a 22 micron filter for sterility. Corn steep liquor (CSL), a less expensive nutrient source relative to yeast extract, was added to the hydrolysate at various concentrations. For all cases, rich media was used during the first stage seed culture lasting 7.5 h. After the first stage, a second stage seed culture was inoculated using the first stage. The 16.5 h second stage seed culture used varying media. The fermentation conditions for this experiment can be found in Table 5.

Final ethanol concentration after 48 h of fermentation on solids-containing enzymatic hydrolysis was used to evaluate seed culture media effectiveness. The results in Figure 6 showed that hydrolysate + CSL seed cultures performed as well as the rich media seed cultures. Interestingly, the xylose consumption was reduced as the CSL concentration in the seed culture media increased. This likely indicates that CSL contains inhibitors as well as beneficial nutrients. In the end, a hydrolysate + CSL media was the superior seed culture media due to a lower projected cost. A CSL concentration of 10 g/L was chosen to supplement the hydrolysate due to the increased ethanol produced during the culturing phase (data not shown). Overall, the CSL concentration during the seed culture stage may be deemed unimportant due to similar results when varying the concentration. Furthermore, choosing a higher CSL concentration than

necessary during the seed culture stage would likely reduce the CSL requirement during fermentation, leading to a similar overall CSL loading per ton biomass. The CSL requirement during fermentation was optimized later.

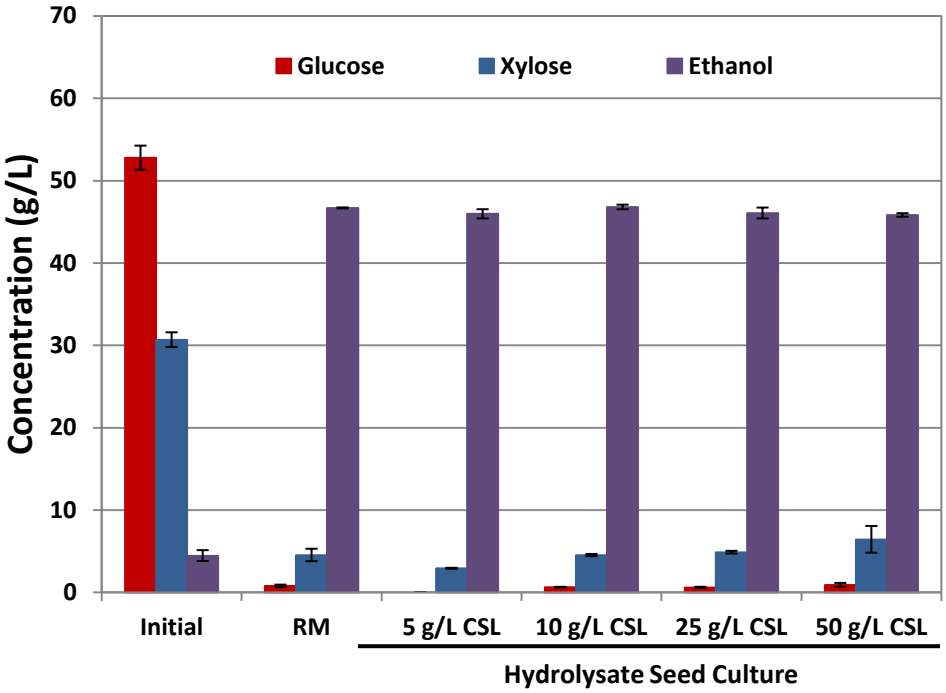

Figure 6 Fermentation performance comparisons using different seed culture media: rich medium (RM) and hydrolysate with varying concentration of added corn steep liquor (CSL). Fermentations were conducted at 30 °C for 48 h using 48 h hydrolysate, 10% inoculum, and 1% CSL. Initial sugar and ethanol concentrations after inoculation and prior to fermentation are on the left. Error bars represent standard deviations.

Table 5 Process conditions summary

Parameter	Seed Culture Optimization	Temperature Optimization	CSL Addition Optimization	Inoculum Optimization	Time Course Study
Culture Media	Variable	Hydrolysate + CSL	Hydrolysate + CSL	Hydrolysate + CSL	Hydrolysate + CSL
Temperature (°C)	30	30, 32, 35, 37, 40	35	35	35
CSL Addition	1%	1%	0%, 0.25%, 0.5%, 1%	0.25%	0.25%
Inoculum Size	10%	10%	10%	2.5%, 5%, 10%	5%
Figure	Fig. 2	Fig. 3a	Fig. 3b	Fig. 4	Fig. 5

3.3.3 Optimization of fermentation conditions for skid-scale pellets

Three fermentation conditions were optimized: temperature, nutrient addition, and inoculum size. A summary of fermentation conditions can be found in Table 5. The fermentation temperature is especially important in a simultaneous saccharification and co-fermentation (SSCF) process. The hydrolysis rate of lignocellulose-degrading enzymes typically increases with increasing temperature up to around 50 °C. Therefore, a higher fermentation temperature is desirable to achieve greater hydrolysis during the primarily fermentation stage after inoculation. Initially, *Z. mobilis* 8b was tested for its ethanol production at five different temperatures (30, 32, 35, 37, and 40 °C) using a synthetic media composed of 70 g/L glucose, 40 g/L xylose, and 10 g/L yeast extract. The fermentations were started with a 2% (v/v) inoculum. The results showed that *Z. mobilis* 8b fermentation performance increased as the temperature increased to 3 7°C (Figure 7b). At 40 °C, growth was inhibited and fermentation performance decreased (Figure 7). The SSCF process (48 h enzymatic hydrolysis followed by 48 h fermentation) was then tested using a fermentation temperature of 37 °C compared to the base case of 30 °C. Unlike the case when using synthetic media, *Z. mobilis* 8b was unable to ferment effectively at 37 °C, likely due to the presence of pretreatment degradation products (Figure 8a). Next, the fermentation was attempted at 35 °C. At this temperature, the results were comparable to the results in the previous seed culture media optimization experiments (Figure 6). It was then decided to proceed with 35 °C fermentations without further testing of temperatures.

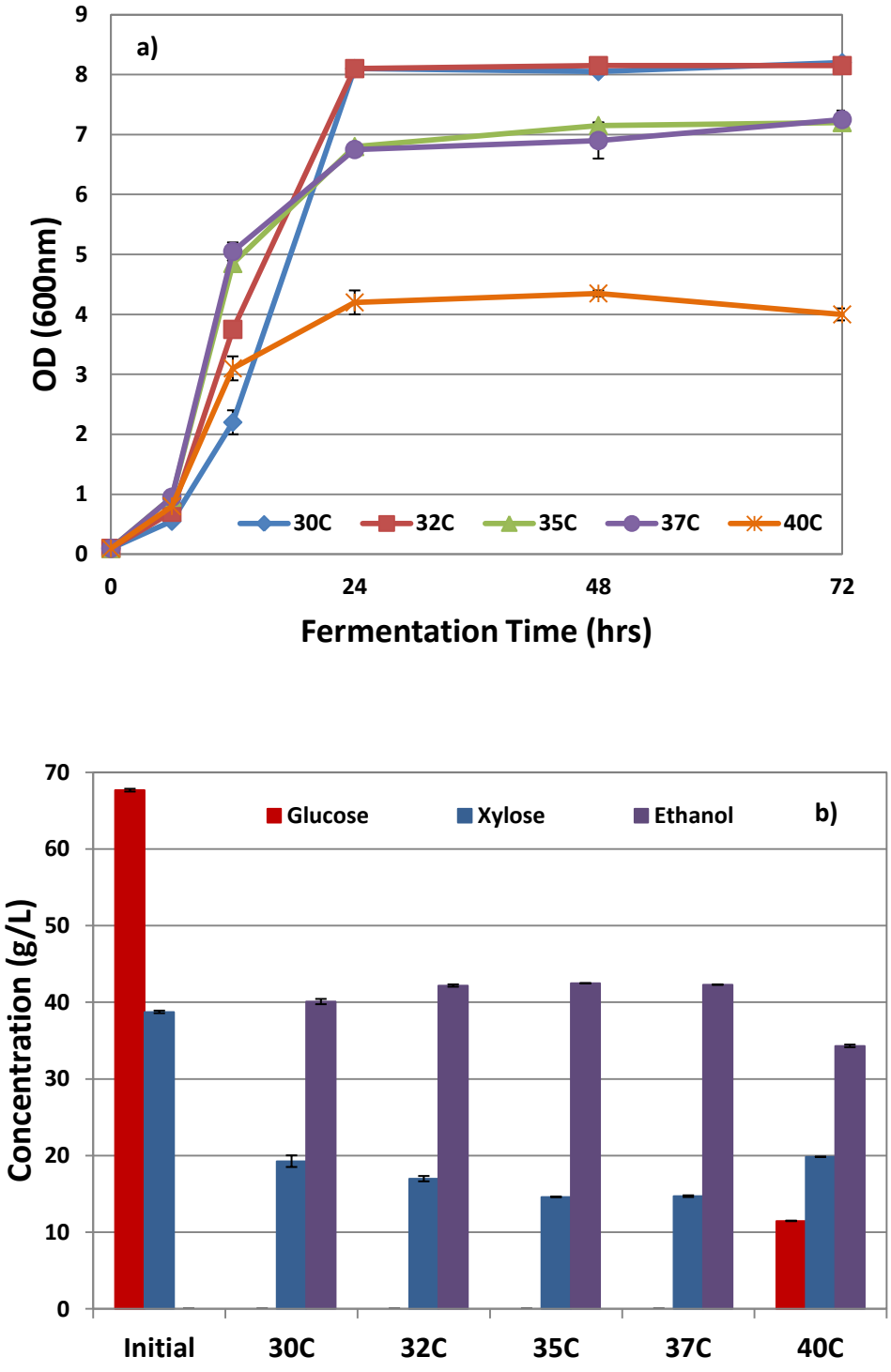

Figure 7 *Z. mobilis* 8b temperature test using synthetic media showing a) OD measurements and b) final 72 h concentrations. Error bars represent standard deviations.

After the optimal temperature was determined, nutrient addition was investigated (Figure 8b). Literature supports the use of corn steep liquor (CSL) as a cheap nutrient for fermentations using *Z. mobilis* (Lawford and Rousseau, 1997; Lawford and Rousseau, 2002). Additions of 0%, 0.25%, 0.5%, and 1% CSL were tested. In the previous experiments, 1% CSL was added. CSL addition improved fermentation performance over the 0% CSL case. Surprisingly, 0.25% CSL addition provided the most benefit, generating 3.3 g/L more ethanol compared to the 0% CSL control. Less ethanol was produced when 0.5% or 1% CSL were used. Generally when adding a nutrient source, fermentation performance through growth and increased sugar consumption is expected to improve. It is possible that increasing CSL promoted cell growth and diverted sugar conversion away from ethanol production. Additionally, higher concentrations of CSL could create more inhibition through increased inhibitor concentration, while increased nutrient concentration showed less benefit. All cases showed similar sugar consumption.

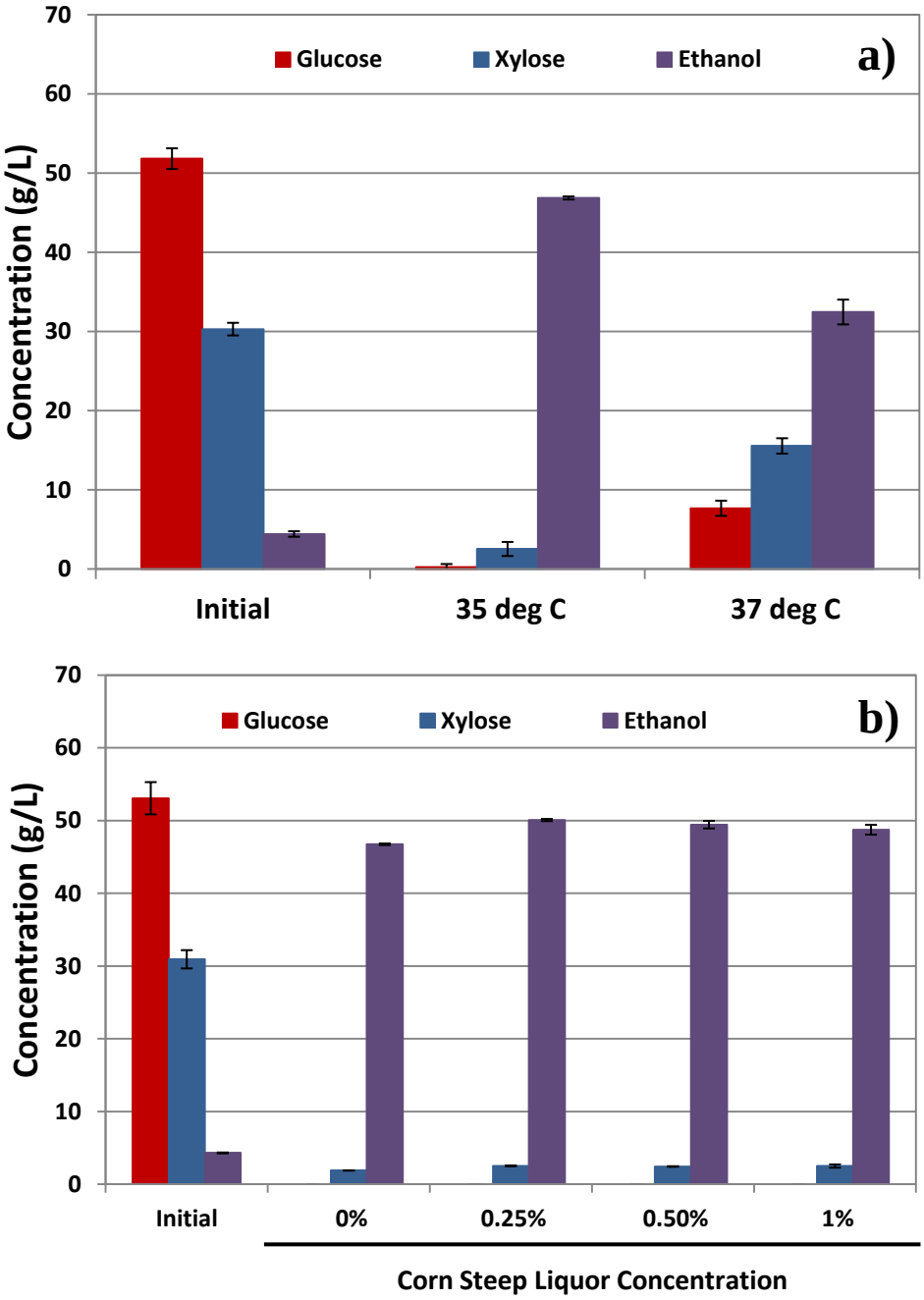

Figure 8 Effect of a) temperature and b) corn steep liquor (CSL) addition on fermentation performance. Fermentation was conducted for 48 h using 48 h enzymatic hydrolysate. Final fermentation results are shown in the figure. Both experiments used hydrolysate + 10 g/L CSL seed cultures and 10% inoculums. Temperature optimization experiments used 1% CSL addition during fermentation and CSL optimization experiments used 35 °C. Error bars represent standard deviations.

The final fermentation condition optimized was the inoculum size. Reducing the inoculum size saves costs associated with media preparation, tank size, and operational costs.

Inocula of 2.5%, 5%, and 10% (total slurry mass basis) were tested (Figure 9). Previously, 10% inoculums had been used. The difference in inoculum sizes caused a significant difference in glucose consumption rates and ethanol production rates. The viable cell counts and xylose consumption were less affected. When removing the ethanol added due to the inoculum difference, 5% and 10% inocula showed equal performance, and were both superior to a 2.5% inoculum. Overall, a 5% inoculum was chosen as optimal due to the equal ethanol production and the same xylose consumption at 48 h.

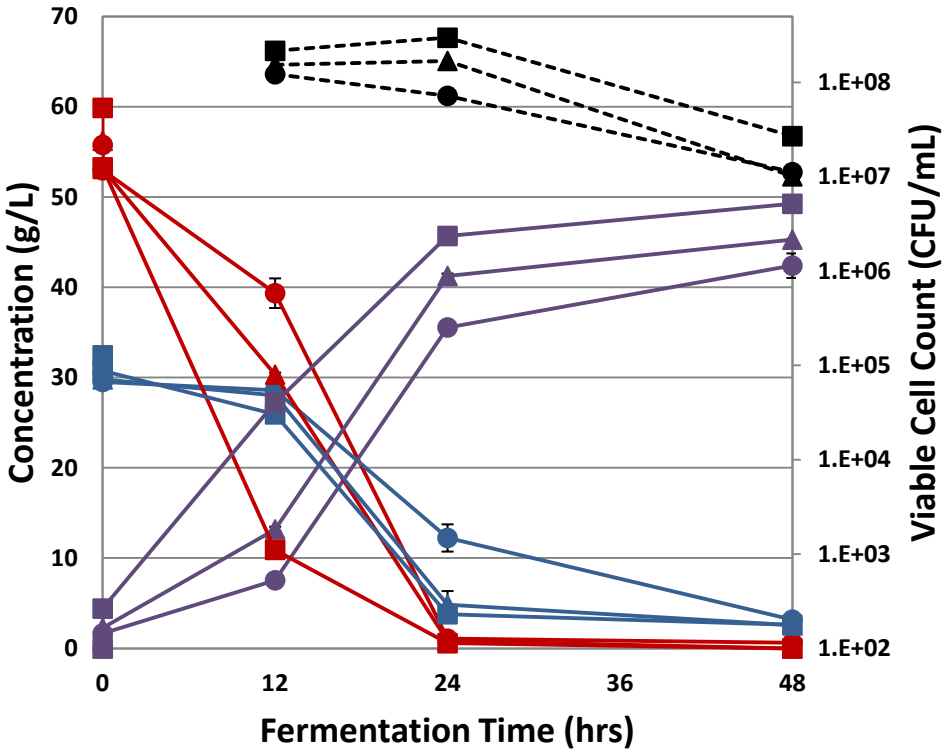

Figure 9 Effect of inoculation size on fermentation in AFEX hydrolysate. Inoculum sizes included 2.5% (circles), 5.0% (triangles), and 10% (squares) inoculums. Concentrations (solid lines) during fermentation for glucose (red), xylose (blue), and ethanol (purple) are shown along with viable cell counts (black dotted line). Seed culture media was hydrolysate + 10 g/L CSL. Fermentation was performed at 35 °C using 0.25% CSL. Error bars represent standard deviations.

3.3.4 Time course study

A time course of the process was performed to examine the fermentation reaction kinetics. Increasing the fermentation temperature from 30 °C to 35 °C might have facilitated shorter processing times due to an increased enzymatic hydrolysis rate. Shortening the processing time could reduce costs if the ethanol yield was not greatly impacted. The results in Figure 10 indicated a potential for shortening the process. Approximately 86% of the sugar was released after 24 h of enzymatic hydrolysis compared to sugar release after 48 h. At 48 h, the enzymatic hydrolysis was inoculated. The fermentation results were similar with 91% of the ethanol production complete after 24 h of fermentation (72 h total) compared to the 48 h results (96 h total). The fermentation was extended for another 48 h (144 h total). The added fermentation time resulted in approximately 1.5 g/L additional ethanol production.

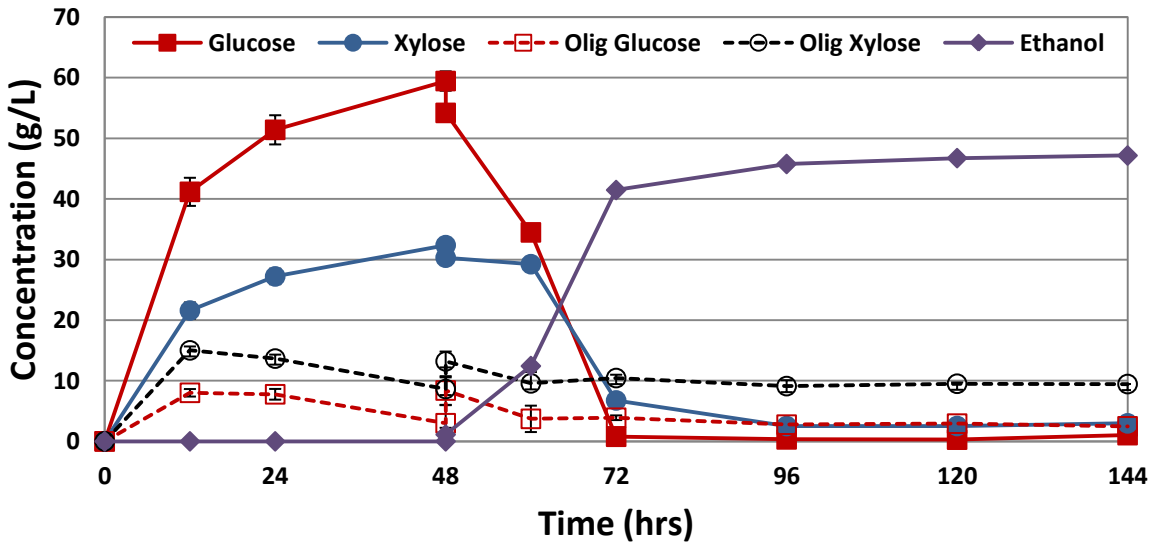

Figure 10 Time-course of enzymatic hydrolysis and ethanol fermentation on AFEX corn stover pellets. Monomeric (closed symbols) and oligomeric (open symbols) sugar concentrations for glucose (red squares) and xylose (blue circles) along with ethanol (purple diamonds) are shown in the figure. Enzymatic hydrolysis was performed at 50 °C for 48 h followed by adding 0.25% of CSL and inoculation of *Z. mobilis* seed culture prepared in hydrolysate + 10 g/L CSL. Fermentation was performed at 35 °C using 0.25% CSL and a 5% inoculum. Error bars represent standard deviations.

3.3.5 Mass balances

Mass balances were performed for three different process scenarios. The 48 h process scenario consisted of 12 h enzymatic hydrolysis followed by 36 h fermentation. The 72 h process scenario used 24 h enzymatic hydrolysis and 48 h fermentation. The 96 h process scenario was the same as earlier experiments in this work using both 48 h enzymatic hydrolysis and fermentation. The results of the mass balances for all three process scenarios can be seen in Table 6 along with conversions and yields in Table 7. For all three processes, the final sugar concentrations were similar. The remaining total monomeric sugar concentrations were 4.9, 4.2, and 2.2 g/L for the 48, 72, and 96 h processes, respectively. However, the final ethanol concentrations were 37.5, 44.4, and 47.4 g/L for the same processes, respectively. Overall, the 96 h process gave the highest ethanol yield (48 h enzymatic hydrolysis followed by 48 h fermentation). The full 96 h were crucial for further hydrolyzing the biomass into monomeric sugars that the microbe can consume. For the 96 h process, a total of 0.211 g ethanol was produced from 1 g of corn stover with monomeric glucose and monomeric xylose conversions of 74.1% and 65.5%, respectively. Both the process time and ethanol yield are large improvements over previous work using AFEX corn stover and different enzymes and microbe (Table 8).

Table 6 Process Mass Balances

Process	Final Monomeric Glucose, gm	Final Monomeric Xylose, gm	Final Oligomeric Glucose, gm	Final Oligomeric Xylose, gm	Final Polymeric Glucose, gm	Final Polymeric Xylose, gm	Final Ethanol, gm
48 h†	0.05 ± 0.00	0.35 ± 0.03	0.31 ± 0.01	1.08 ± 0.00	2.44 ± 0.06	1.05 ± 0.03	3.13 ± 0.01
72 h‡	0.04 ± 0.00	0.31 ± 0.00	0.27 ± 0.01	0.90 ± 0.02	1.80 ± 0.01	0.80 ± 0.02	3.73 ± 0.00
96 h‼	0.00 ± 0.00	0.19 ± 0.00	0.24 ± 0.01	0.83 ± 0.06	1.73 ± 0.06	0.78 ± 0.04	4.22 ± 0.02

Based on initial dry biomass loading of 20 gm (7.604 gm Initial Glucose; 4.655 gm Initial Xylose)

†12 h enzymatic hydrolysis followed by 36 h fermentation

‡24 h enzymatic hydrolysis followed by 48 h fermentation

‼48 h enzymatic hydrolysis followed by 48 h fermentation

Error values represent standard deviations

Table 7 Process Metrics

Process	Ethanol Metabolic Yield*, g/g	Glucan Conv.+, %	Xylan Conv.+, %	Glucose Ferm. Conv.#, %	Xylose Ferm. Conv.#, %	Biomass to EtOH Conv. Efficiency^, g/g
48 h†	0.449 ± 0.007	63.9 ± 0.9	54.3 ± 0.7	99.0 ± 0.1	86.0 ± 1.2	0.156 ± 0.000
72 h‡	0.439 ± 0.002	72.8 ± 0.0	63.5 ± 0.9	99.3 ± 0.0	89.6 ± 0.0	0.187 ± 0.000
96 h‼	0.466 ± 0.001	74.1 ± 0.6	65.5 ± 0.3	100.0 ± 0.0	93.7 ± 0.0	0.211 ± 0.001

* Calculated from total ethanol produced divided by total sugars consumed

+ Calculated from total monomeric sugar produced divided by theoretical sugar available in initial biomass

Calculated from total monomeric sugar consumed divided by total monomeric sugar available for consumption

^ Calculated from total ethanol produced divided by initial biomass

†12 h enzymatic hydrolysis followed by 36 h fermentation

‡24 h enzymatic hydrolysis followed by 48 h fermentation

‼48 h enzymatic hydrolysis followed by 48 h fermentation

Error values represent standard deviations

Table 8 Comparison of ethanol production using AFEX corn stover

Glucan Loading, %	Enzymes*	Total Enzyme Loading, mg/g glucan	Microbe	Total Processing Time, h	Ethanol Titer, (g/L)	Ethanol Yield, g EtOH/g corn stover	Reference
7.0	CTec3, Htec 3	20	*Z. mobilis* 8b	96	47.4	0.211	This study
6.0	A1500, AXY, MP	36	*S. cerevisiae* 424A(LNH-ST)	192	38.4	0.195	(Jin et al., 2013)
6.0	A1500, AXY, MP	36	*S. cerevisiae* 424A(LNH-ST)	144	36	0.185	(Jin et al., 2013)
6.0	SCP, N188, MX, MP	45	*S. cerevisiae* 424A(LNH-ST)	264	40	0.192	(Lau and Dale, 2009a)

*A1500: Accelerase 1500; AXY: Accelerase XY; MX: Multifect Xylanase; MP: Multifect Pectinase; SCP: Spezyme CP; N188: Novozymes 188

3.3.6 Economic analysis

Economic analysis was performed to understand the impact of the process changes studied in this chapter. The first analysis estimated the savings provided by the process optimizations performed (Figure 11a). Economic estimates are reported as a minimum ethanol selling price (MESP). The MESP was calculated as a breakeven price for a 10 year loan at 8% interest. The ability to effectively use a hydrolysate + CSL seed culture media saved $0.37/gal due to eliminating non-cellulosic sugar and yeast extract. Increasing the fermentation temperature did not provide any significant savings. Decreasing the CSL supplementation during fermentation and the inoculum size saved a further $0.05/gal and $0.02/gal, respectively. In total, all of the process optimizations reduced the MESP by $0.44/gal. A further $0.05/gal savings occurs if autoclaving is not performed. This analysis did not include changes in sugar or ethanol yields and may be understated.

The same economic analysis was performed comparing the three processing periods (48 h, 72 h, and 96 h). The results in Figure 11b show that the 96 h process provided superior economics. The 13% increase in ethanol production compared to the 72 h overall process more than offset the 33% increase in processing time.

While the current MESP of $2.90/gal is not economically attractive with respect to gasoline, there are many opportunities to further reduce the cost of cellulosic ethanol. Enzyme improvement has been steadily reducing enzyme loading and process time. While less potential may exist for microbe improvement, genetically engineering microbes for consumption of oligomeric sugars could further reduce enzyme loadings and increase yield. Transporting oligomeric sugars inside of the cell could reduce transporter energy requirements, potentially reduce enzyme loadings, allow for energy saving by using phosphorolysis instead of hydrolysis,

and help with osmotic regulation. Improvements in processing, such as the Rapid Bioconversion with Integrated recycling technology (RaBIT) process, is another way to reduce capital and enzyme costs (Jin, 2012a). Increasing the size of the biorefineries to something closer to oil refineries (~30,000 tons per day) using pellets shipped long distances could also significantly reduce costs. Finally, processing of lignin into valuable co-products instead of simple combustion could increase revenue. All of these potential changes could add up to a substantial decrease in MESP creating a more economically attractive process in the future.

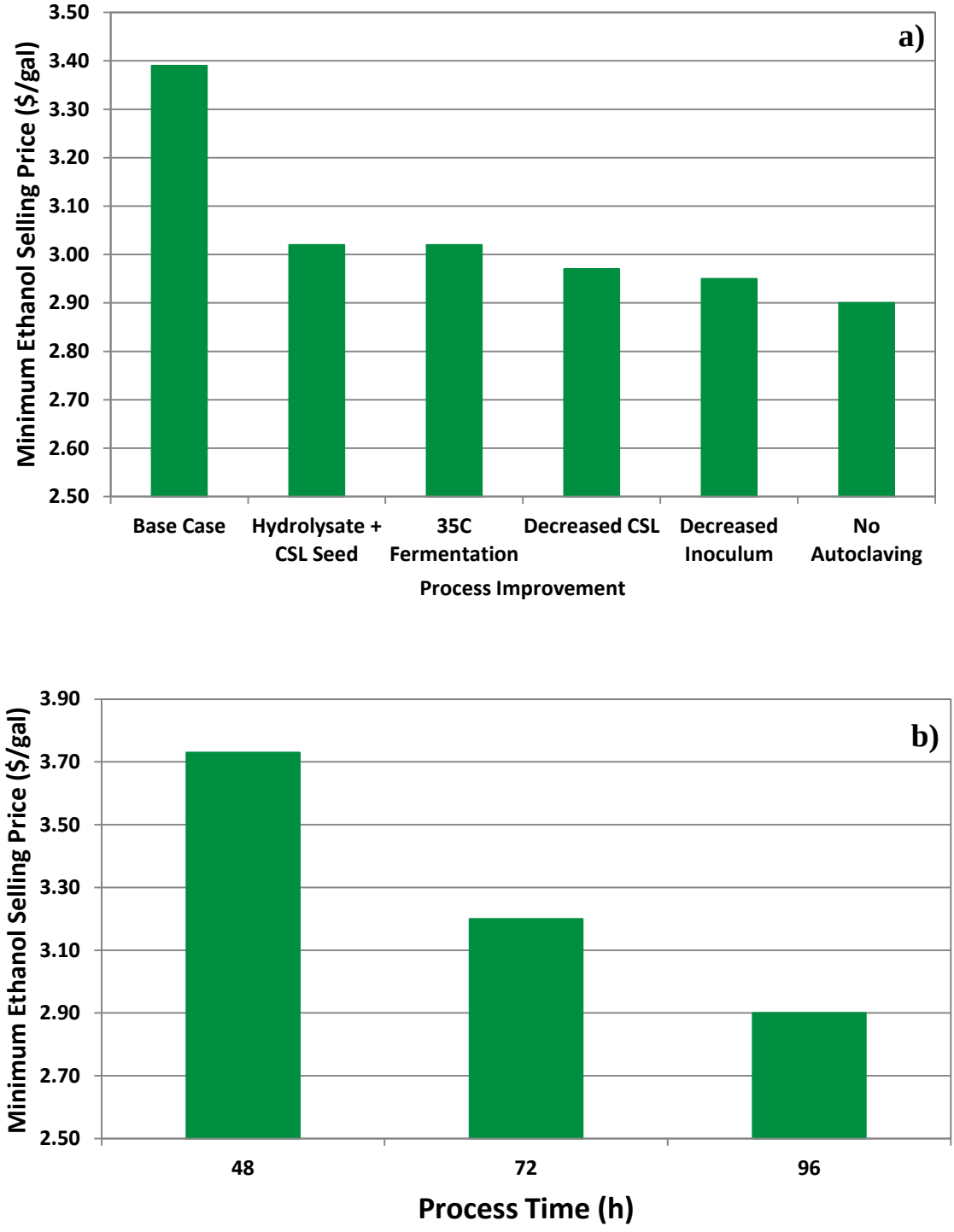

Figure 11 Minimum ethanol selling process a) after each sequential process optimization and b) for different process times.

3.3.7 Comparing skid scale (10 L) and pilot scale (450 L) AFEX

AFEX pretreated corn stover prepared at the pilot scale was supplied for comparison to lab scale AFEX pretreated corn stover. When scaling up the AFEX process, significant gains were experienced in both carbohydrate conversion and ethanol yield. Figure 12a and b show the difference between autoclaved AFEX pellets produced from the skid scale (10 L) and pilot scale (450 L). The enzymatic hydrolysis results for the skid scale material were similar to data published by Bals et al. (2013), which used a similar procedure. When comparing skid scale versus pilot scale, pilot scale pretreatment showed a 19% and 15% increase in monomeric sugar release after 48 h for glucose and xylose, respectively. Sugar consumption after fermentation was near complete for both pilot and lab scale biomass with pilot scale showing a 15% increase in ethanol production compared to skid scale.

The reason for improved conversion is unknown at this point. Both reported and internal data show no difference between AFEX corn stover before and after pelletization (Bals et al., 2013). Previous scale-up of the AFEX process from a stirred batch reactor to the 10 L packed bed reactor showed an approximate 5% increase in glucan hydrolysis yield (Campbell et al., 2013). It is possible that scale up increased ammonia residence time. Furthermore, the biomass near the inlets and outlets experience greater quantities of ammonia and/or steam possibly resulting in more severe pretreatment for parts of the bed. It may also be that the larger bed simply provides better contact between the ammonia and the biomass, with fewer portions of the bed that are not contacted uniformly.

Dry autoclaving (no added water) was performed to guarantee results were not affected by contamination. As before, contamination levels in the lab scale pellets were high enough to produce variation in fermentation results (data not shown). Significant contamination was not

present in the pilot scale pellets as autoclaving did not produce any significant change in final conversion and yield (Figure 12b and c). This is expected as AFEX pretreatment does not hydrolyze polymeric sugar chains to monomeric sugars which can more easily form degradation products under high temperatures (Teymouri et al., 2005).

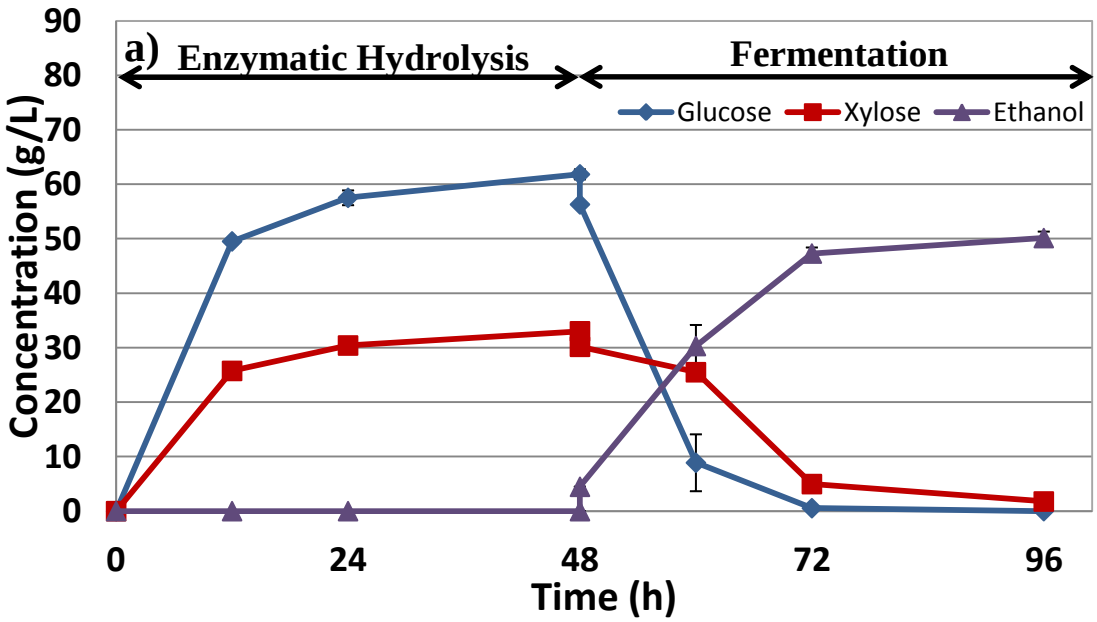

Figure 12 Comparison of a) autoclaved lab scale b) autoclaved pilot scale c) non-autoclaved pilot scale enzymatic hydrolysis and fermentation at 100 g scale. Enzymatic hydrolysis was performed using 20% solids loading and 10 mg protein/g glucan for both CTec3 and HTec3 at 50 °C. Fermentation was performed at 32 °C using a 10% inoculum of *Z. mobilis* 8b and 0.5% added CSL. Error bars represent standard deviations and are present for all data points but may be hidden by the symbol.

Figure 12 (cont'd)

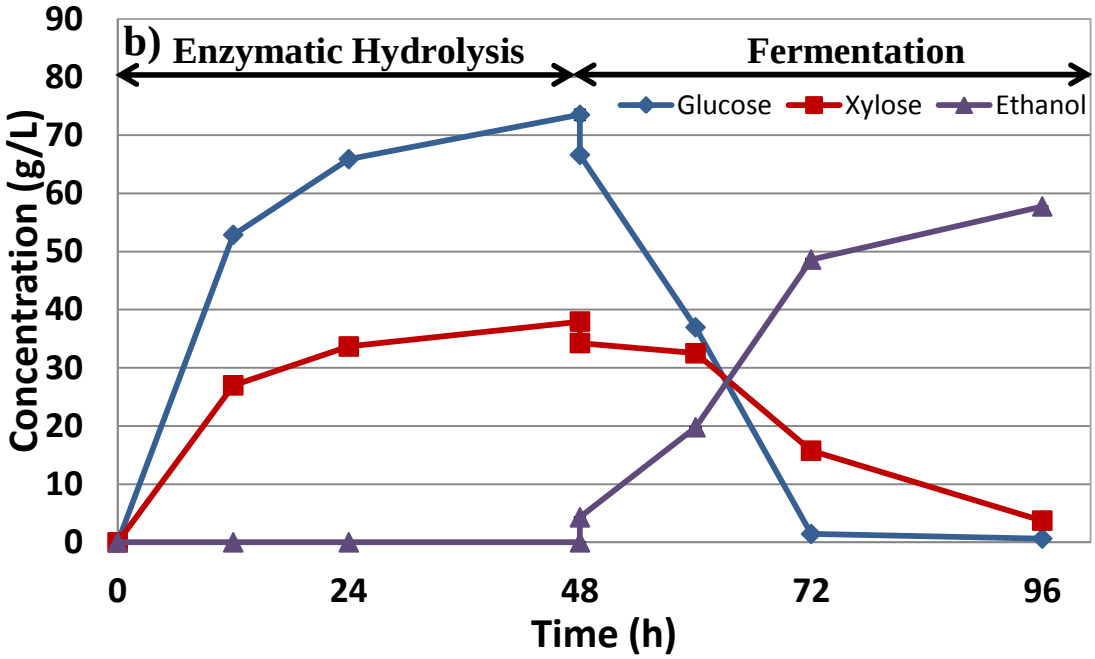

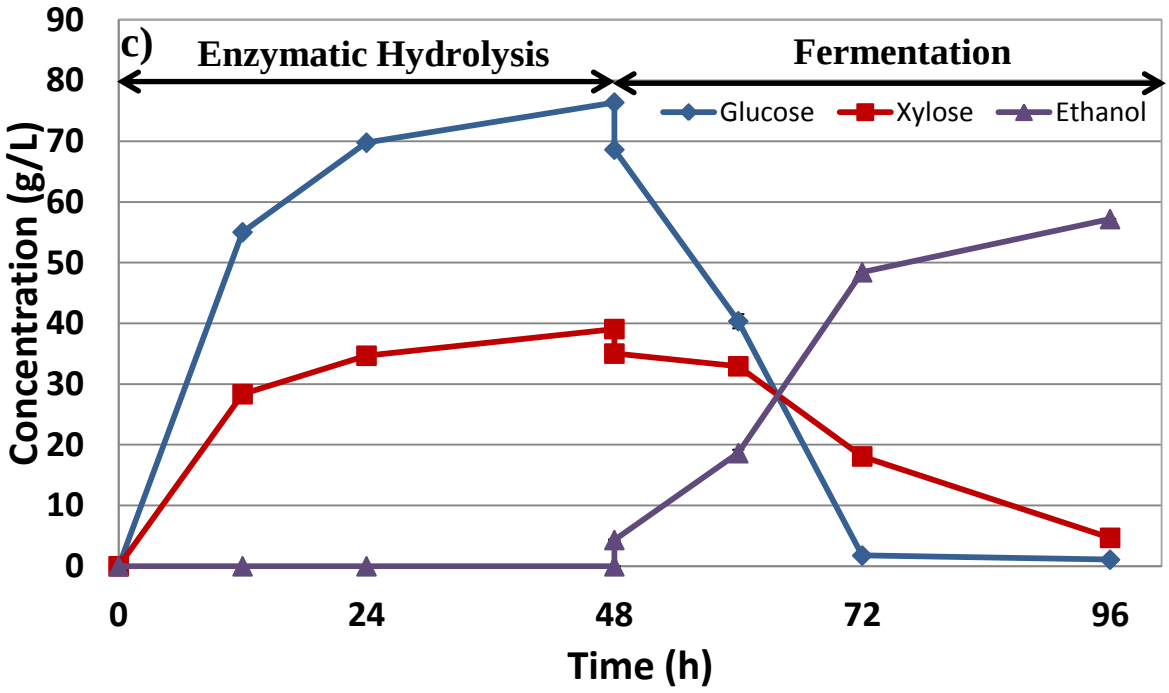

3.3.8 Optimization of seed culture media for pilot-scale pellets

After switching to the pilot-scale pellets, the previously used seed culture method did not produce enough cell mass for complete utilization of xylose (data not shown). For this reason,

the seed culture approach was re-investigeated. Table 9 shows the final ODs for different hydrolysates and different experiments. Initial ODs of the media prior to inoculation were taken as blanks. Rich media was used as the first seed culture stage using a frozen glycerol stock. The second stage tested the different concentrated hydrolysates and compared them to a second stage using rich media. The rich media seed culture was incubated for 10 h while the hydrolysate seed cultures were incubated for 11-18 h. Five of the seven initially tested hydrolysates were capable of growing to an OD >50% compared to the rich media seed culture. For simplicity, the 22% solids loading hydrolysate (same as initial process loading) with 10% inoculum was chosen for further investigation. The second experiment investigated the effect of CSL on the hydrolysate using 22% solids loading hydrolysate. The addition of CSL did not significantly improve the OD. However, it was decided to use 0.25% CSL for future tests to stay consistent with the SSCF procedure.

Table 9 Seed culture optical density measurements

Media	Inoculum	CSL (g/L)	Added Dextrose (g/L)	OD (600nm)
Experiment 1				
Rich Media	5%	0	0	6.62 ± 0.11
10% Solids Hydrolysate	5%	0	0	2.72 ± 0.00
10% Solids Hydrolysate	10%	0	0	2.90 ± 0.02
15% Solids Hydrolysate	5%	0	0	3.35 ± 0.04
15% Solids Hydrolysate	10%	0	0	3.43 ± 0.03
20% Solids Hydrolysate	5%	0	0	3.30 ± 0.02
20% Solids Hydrolysate	10%	0	0	3.60 ± 0.05
22% Solids Hydrolysate	5%	0	0	2.83 ± 0.05
22% Solids Hydrolysate	10%	0	0	3.39 ± 0.05
Experiment 2				
22% Solids Hydrolysate	10%	0	0	3.36 ± 0.04
22% Solids Hydrolysate	10%	5	0	3.44 ± 0.04
22% Solids Hydrolysate	10%	10	0	3.36 ± 0.05
22% Solids Hydrolysate	10%	25	0	3.05 ± 0.15
22% Solids Hydrolysate	10%	50	0	2.32 ± 0.06
Experiment 3				
15% Solids Hydrolysate	10%	5	50	4.22 ± 0.10

Error values represent standard deviations

The next step compared the use of the 22% solids hydrolysate final seed culture media to the rich media seed culture. Figure 13a shows that the final ethanol concentrations after 72 h of fermentation were comparable. Using the 22% solids hydrolysate, however, did cause the fermentation to lag behind when compared to rich media. This was expected due to the difference in final ODs for the seed cultures. Figure 13b shows that the 44% higher viable cell concentration for the rich media seed culture fermentation at 24 h was the likely cause for the sugar consumption lag.

Adding a second hydrolysate seed culture stage would further reduce cost by approximately 10%. The low ODs generated previously did cause concern. To improve the OD, sugar was added to 15% solids loading hydrolysate. Calculations showed that 15% solids loading hydrolysate with a 10% inoculum had a comparable OD yield per gram of sugar consumed when compared to the rich media seed culture (data not shown). Approximately 50 g/L of glucose was added to bring the glucose concentration up to 100 g/L. Adding 50 g/L of sugar to 15% solids loading hydrolysate resulted in ODs of 123% and 64% compared to 22% solids loading hydrolysate seed culture and rich media seed culture, respectively (Table 9: Experiment 3).

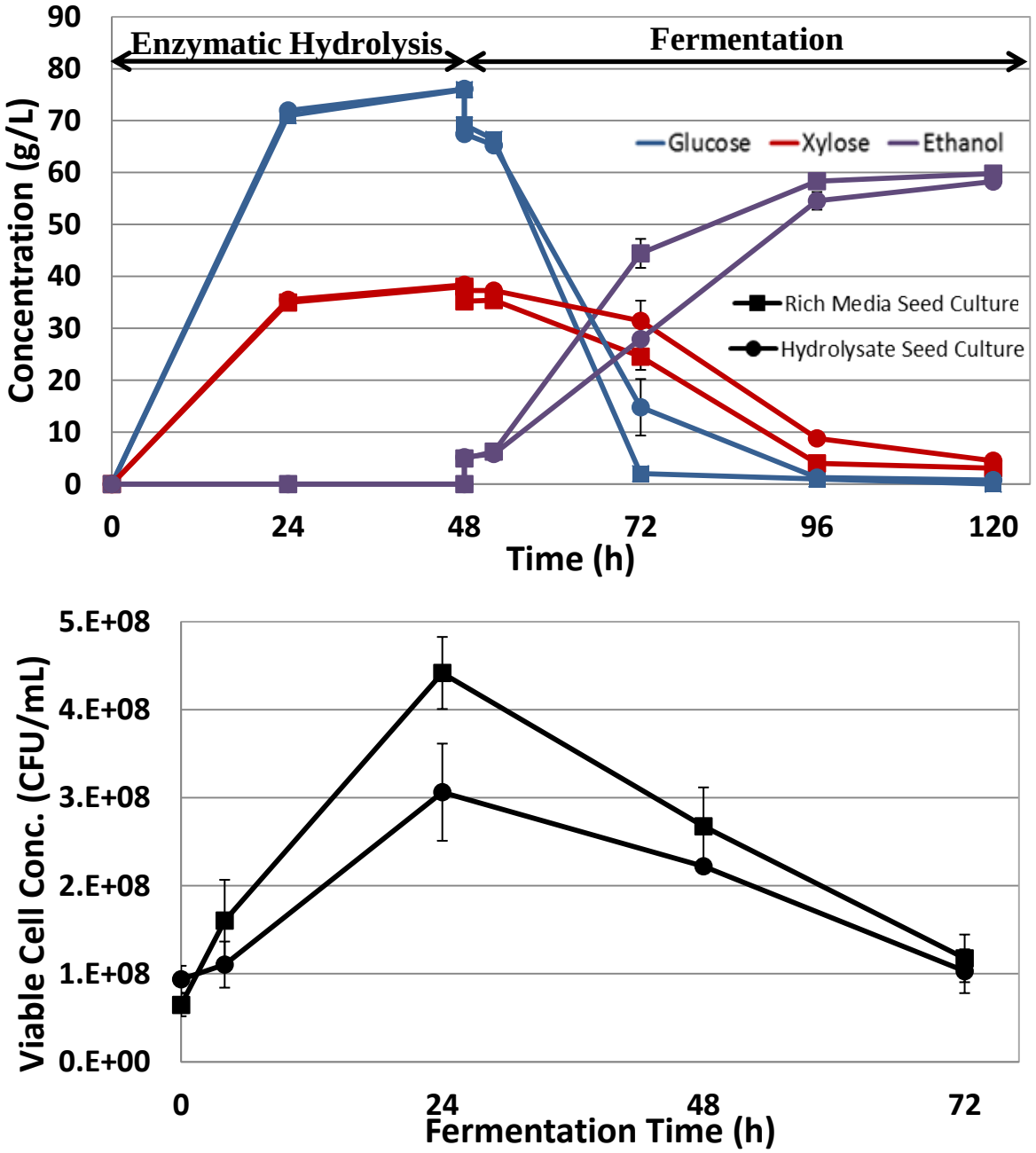

Figure 13 Comparing rich media (squares) and hydrolysate (circles) seed cultures at 100 g scale. Concentrations for a) glucose (blue), xylose (red), ethanol (violet), and b) viable cells (black) are shown. Enzymatic hydrolysis was performed using 20% solids loading and 10 mg protein/g glucan for both CTec3 and HTec3 at 50 °C. Fermentation was performed at 32 °C using a 10% inoculum of *Z. mobilis* 8b and 0.5% added CSL. Error bars represent standard deviations and are present for all data points but may be hidden by the symbol.

Figure 14 shows the results for comparing three different seed cultures prepared in three distinct stages. The first train uses 3 rich media stages. The second has one rich media stage,

one 15% solids loading hydrolysate stage with 50 g/L added glucose, and 5 g/L CSL, and a final stage of 22% solids loading hydrolysate with 5 g/L CSL. The third train used one rich media stage, and two 22% solids loading hydrolysate with 5 g/L CSL stages. Easy reference is shown in Table 10. Seed train 2 was successful in reducing the lag associated with using a hydrolysate seed culture as seen in Figure 13. After 72 h of fermentation, the ethanol concentration, when using seed train 2, was only 0.28 g/L lower than seed train 1.

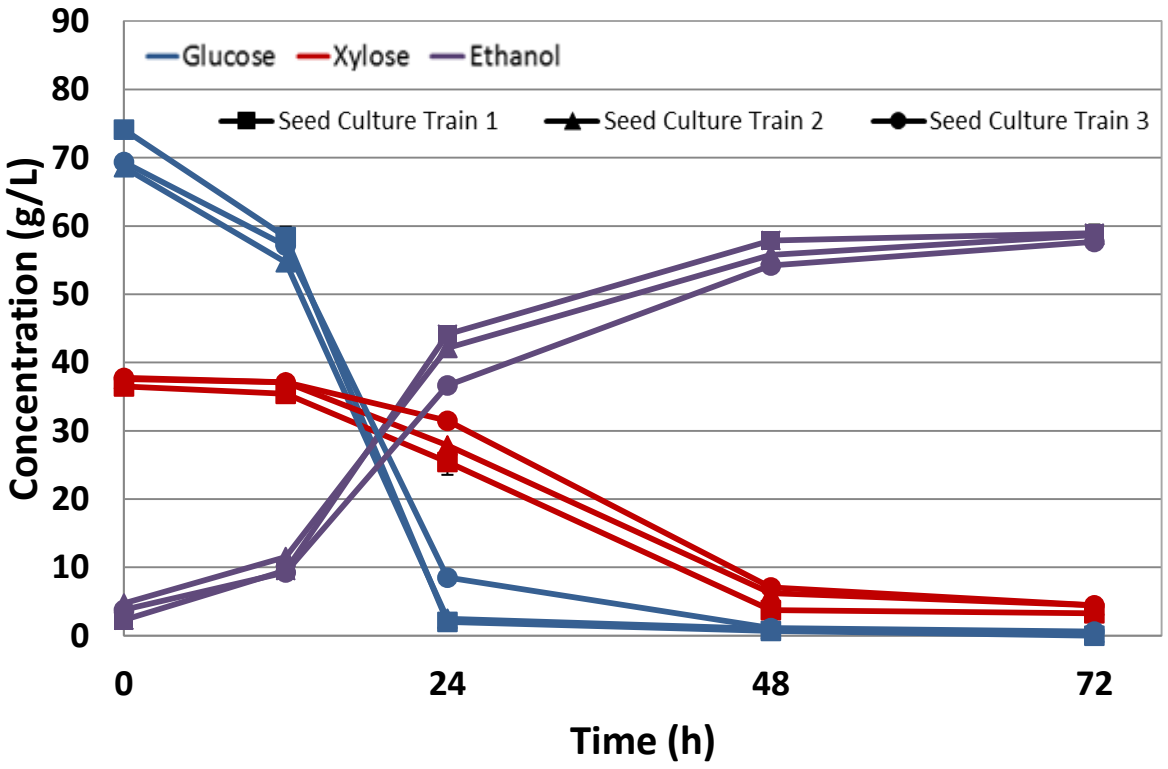

Figure 14 Comparing fermentation results for seed culture trains 1 (squares), 2 (triangles), and 3 (cirles) at 100 g scale (see Table 3). Concentrations for glucose (blue), xylose (red), and ethanol (violet) are shown. Enzymatic hydrolysis was performed using 20% solids loading and 10 mg protein/g glucan for both CTec3 and HTec3 at 50 °C. Fermentation was performed at 32 °C using a 10% inoculum of *Z. mobilis* 8b and 0.5% added CSL. Error bars represent standard deviations and are present for all data points but may be hidden by the symbol.

Table 10 Seed culture train details

	Culture Media		
Seed Train	**First Stage**	**Second Stage**	**Third Stage**
1	Rich Media	Rich Media	Rich Media
2	Rich Media	15% Solids Hydrolysate	22% Solids Hydrolysate
3	Rich Media	22% Solids Hydrolysate	22% Solids Hydrolysate

Inoculum Size: 5% for rich media, 10% for hydrolysates

Addition: 0.5% CSL added to 15% and 22% solids hydrolysates, 50 g/L added to 15% solids hydrolysate

Incubation Time: 11 h for first stage rich media, 10 h for second and third stage rich media, 18 h for 15% solids hydrolysate, 16 h for 22% solids hydrolysate

3.4 Conclusions

This chapter shows the current state of industrially relevant technology for the conversion of pelleted AFEX corn stover to ethanol along with a comparison of lab-scale and pilot-scale pretreatment. Novozymes Cellic CTec3 and HTec3 industrial enzyme cocktails and *Z. mobilis* 8b were used for production of sugars and ethanol, respectively. Selected fermentation conditions were optimized: seed culture media (hydrolysate + 10 g/L CSL), fermentation temperature (35 °C), corn steep liquor as a nutrient source (0.25%), and inoculum size(5%). These optimizations reduced the minimum ethanol selling price (MESP) by $0.44/gal. The optimized MESP was $2.90/gal, assuming autoclaving was not necessary. When testing shorter process times, the economic analysis showed that a 12% ethanol yield loss incurred more cost than a 25% processing time decrease could save. Scaling up from lab-scale to pilot-scale improved ethanol production by 15%.

CHAPTER 4: EFFECT OF NUTRIENT ADDITION ON RABIT FERMENTATIONS

Abstract

Fermentation conditions were optimized for *S. cerevisiae* GLBRCY128. Three different nutrient sources (corn steep liquor, yeast extract, and wheat germ) were evaluated for their potential to improve xylose consumption by recycled cells. Corn steep liquor was found to reduce the deleterious impacts of cell recycle, and improved specific xylose consumption rates. Capacitance readings were used to accurately measure viable cell mass. These measurements showed that the specific xylose consumption rate of the yeast cell population was decreasing during the RaBIT process.

4.1 Introduction

Three key factors have been identified as potential causes for xylose consumption decrease upon cell recycle: lack of nutrients, degradation product effects, and cell aging. Nutrient deficiency could limit growth or prevent proper cell maintenance. Degradation products could be accumulating during RaBIT enzymatic hydrolysis cycles or inside the cell. Cell population aging could be limit growth or overall population stability. The first factor, lack of nutrients, was investigated in this Chapter. AFEX hydrolysate has been proven capable of supporting microbial growth without nutrient supplementation (Lau et al., 2008). However, most previous work has been performed using low cell densities and not the high cell densities associated with the RaBIT process. The nutrient level in AFEX hydrolysate may not be sufficient to support high cell densities. Three different nutrient supplements were used to test this theory: yeast extract, wheat germ, and corn steep liquor.

Also investigated was the viability of the cell population during RaBIT fermentations. Traditionally, techniques such as optical density measurements, staining, or plating are used to measure cell population and viability. Optical density (OD) measurements, while simple and commonly used, can provide misleading results and don't directly measure cell viability. OD measurements are performed by measuring the scattering of light. Measuring light scatter is not capable of differentiating between live and dead cells. After exponential growth phase, OD measurements will often overestimate the amount of live cells due to dead cells not having time to dissolve into solution. Results in Jin et al. 2012 showed that during RaBIT fermentations the OD increased over each cycle. It is questionable whether the amount of viable cells was increasing as the final xylose consumption decreased.

A possible solution would be staining to determine which cells are viable. Stains such as methylene blue are oxidized to colorless in cells with intact membranes. Non-viable cells are not be able to oxidize methylene blue and are easily distinguished by their blue color. Another solution would be to utilize the cell plating method. Plating cells involves diluting the cell solution, then dotting a known volume and dilution of the cell solution onto agar plates made using an utilizable carbon source and nutrients. When diluted to the right concentration, cell colonies from single cells can be counted to determine the viable cell concentration. While the last two methods are adequate for determining cell viability, they are not guaranteed to be accurate for *Saccharomyces cerevisiae* GLBRCY128 (Y128), the strain in this study, due to its flocculating nature. Attempts were made to deflocculate Y128 by traditional means using acid and chelating agents without success. To accurately measure the viable cells a Biomass Monitor 200 made by Aber Instruments was used. The biomass monitor measures the capacitance of the solution. The physical makeup of cells allows their bio-volume to be estimated by capacitance

due to cell membranes having low electrical permittivity (Harris et al., 1986). This is especially true at low frequencies. As measurement frequency increases, electrical permittivity will also increase (Harris et al., 1986). To measure capacitance, a capacitance reading between two electrodes is measured. The background capacitance of the liquid solution is then subtracted from the overall reading to provide the capacitance from biovolume. Once a cell's membrane loses integrity it will no longer provide a capacitance reading. Capacitance has been shown to be an accurate estimate of viable dry cell weight (Austin et al., 1994).

For this chapter, RaBIT fermentation conditions were optimized for *S. cerevisiae* GLBRCY128; the optimal RaBIT fermentation strain as determined in Chapter 2. Nutrient addition was then tested as a way to eliminate the decrease in xylose consumption upon recycle. Next, the viable cell profile was determined by measuring capacitance for both a control and optimal nutrient loading.

4.2 Materials and Methods

4.2.1 Biomass and pretreatment

Corn stover was provided by the Great Lakes Bioenergy Research Center (GLBRC). The corn (Pioneer 36H56) from which the stover was produced was planted in May of 2009 in field 570-N at the Arlington Agricultural Research Station in Columbia Country, WI and harvested in November of 2009. The biomass was pretreated by the Biomass Conversion Research Laboratory (BCRL) located at Michigan State University in East Lansing, MI using the AFEX pretreatment process as previously described in the literature (Balan et al., 2009). AFEX pretreatment conditions were: 1:1 ammonia to biomass ratio, 60% moisture on dry weight basis,

100 ^{o}C, and 30 min. reaction time. Glucan, xylan, and acid insoluble lignin content plus ash were 38.0%, 23.8%, and 20.4% by dry mass, respectively. The corn stover was stored at 4 ^{o}C.

4.2.2 Microorganisms and seed culture preparation

Saccharomyces cerevisiae GLBRCY128 was genetically modified to contain xylose isomerase and xululokinase genes and was kindly provided by Dr. Trey K. Sato (Parreiras et al., 2014). The strain was maintained in glycerol stocks at -80 °C. Seed cultures were prepared in medium containing 100 g/L dextrose, 25 g/L xylose, 10 g/L Yeast Extract, and 20 g/L Tryptone. Seed cultures were performed in 250 mL Erlenmeyer flasks using a 100 mL working volume. The initial OD_{600} of seed cultures was 0.1. Cultures were incubated at 30 °C and 150 RPM for 20 h. After 20 h, 1 mL of the culture was transferred to new media for an additional 20 h. The culture was made microaerobic by using a rubber stopper pierced by a needle.

4.2.3 Enzymatic hydrolysis

Enzymatic hydrolysis at 6% (w/w) glucan loading was performed in 1 L baffled Erlenmeyer flasks with a reaction mixture (biomass, water, enzymes, and acid) of 400 g. Biomass was loaded in fed batch mode by adding half the biomass at t = 0 h and the other half at t = 2 h. The enzyme cocktail consisted of 20 mg enzyme protein/g glucan of Cellic CTec2 (Novozymes), 5 mg/g of Cellic HTec2 (Novozymes), and 5 mg/g of Multifect Pectinase (Genencor). Hydrolysis was performed for 48 h at 50 °C and 250 RPM using a pH of 4.8. Adjustments to pH were made using 10 M potassium hydroxide or 12.1 M hydrochloric acid. Hydrolysis slurry was centrifuged in 2 L bottles at 7500 RPM for 30 minutes and then sterile filtered. Hydrolysate was used for fermentation without external nutrient supplementation unless otherwise indicated.

4.2.4 Shake flask fermentations

Fermentations were performed in 125 mL Erlenmeyer flasks using 50 mL of hydrolysate. Cells for inoculation were harvested by centrifugation from the seed cultures. Inoculation size was determined by dry cell weight (DCW) concentration. Inoculations were performed at 7.5, 8.0, 9.0, 10, or 12.0 g/L DCW. The pH was initially adjusted using 10 M potassium hydroxide. Initial pH for *S. cerevisiae* was 5.5 during strain testing before pH optimization and 6.0 after. The pH was not adjusted during the fermentations. The fermentations were performed in a shaking incubator at 150 RPM. Temperature was set 30 °C for all other strains before temperature optimization. After optimization, the temperature was increased to 32 °C for *S. cerevisiae* GLBRCY128. The flasks were under microaerobic conditions. Fermentations were performed for 24 h. At the end of each RaBIT fermentation stage, the broth was centrifuged in 50 mL centrifuge tubes at 4000 RPM for 10 minutes. The corresponding cell pellets were then inoculated into fresh hydrolysate to begin the next cycle. All fermentation experiments were performed with at least 2 biological replicates.

4.2.5 Five cycle fermentation in bioreactor

Five cycle RaBIT fermentations (five fermentations with 4 recycle events) were performed in a 0.5 L bioreactor with a 60% working volume. Temperature and stirring rate were set at 32 °C and 300 RPM, respectively. A 6% glucan loading hydrolysate (60 g/L glucose and 30 g/L xylose) with an initial pH of 6.0 and 10 g/L DCW inoculum were used, as described above. A capacitance probe was utilized to monitor viable cell density. The recycle process was carried out the same as shake flask fermentations and described above. All fermentation experiments were performed with at least 2 biological replicates.

4.2.6 Nutrient additions

Yeast extract (Becton Dickinson), corn steep liquor (Sigma Aldrich) and Wheat germ (MP Biomedicals) were added at concentrations of 1.0, 2.5, or 5.0 g/L. Yeast extract and corn steep liquor were weighed out and added to the hydrolysate before fermentation. Wheat germ was added to the enzymatic hydrolysis mixture at the beginning of the hydrolysis (the final mixture density was assumed as1 g/L).

4.2.7 Measurements of cell population

The optical density at 600 nm was used to measure the cell concentration of the fermentation broths. The OD_{600} measurement was then correlated to the DCW by use of a calibration curve.

Viable cell mass was measured by correlating capacitance readings from an Aber Instruments Ltd. Biomass Monitor 200. The capacitance versus viable dry cell mass correlation was created by taking samples during exponential phase seed cultures. The samples were centrifuged and dried before being compared to the capacitance readings to produce a linear correlation between capacitance and viable cell concentrations.

4.2.8 HPLC Analysis

Glucose, xylose and ethanol concentrations were analyzed by HPLC using a Biorad Aminex HPX-87H column. Column temperature was maintained at 50 ^{o}C. Mobile phase (5 mM H_2SO_4) flow rate was 0.6 mL/min.

4.3 Results and Discussion

4.3.1 Process optimizations

The initial cell loading, initial pH, and temperature for RaBIT fermentations (24 h) using *S. cerevisiae* GLBRCY128 (Y128) were optimized. Initial cell loading is the key to rapid fermentation and was examined in 6.0% glucan loading hydrolysate. Cell loadings of 10 g/L, 9 g/L, 8 g/L, and 7.5 g/L (DCW) were tested at 30 ^{o}C and an initial pH of 5.5 (Figure 15). An initial cell loading of 10 g/L DCW was required to achieve the goal of consuming all but <5 g/L xylose.

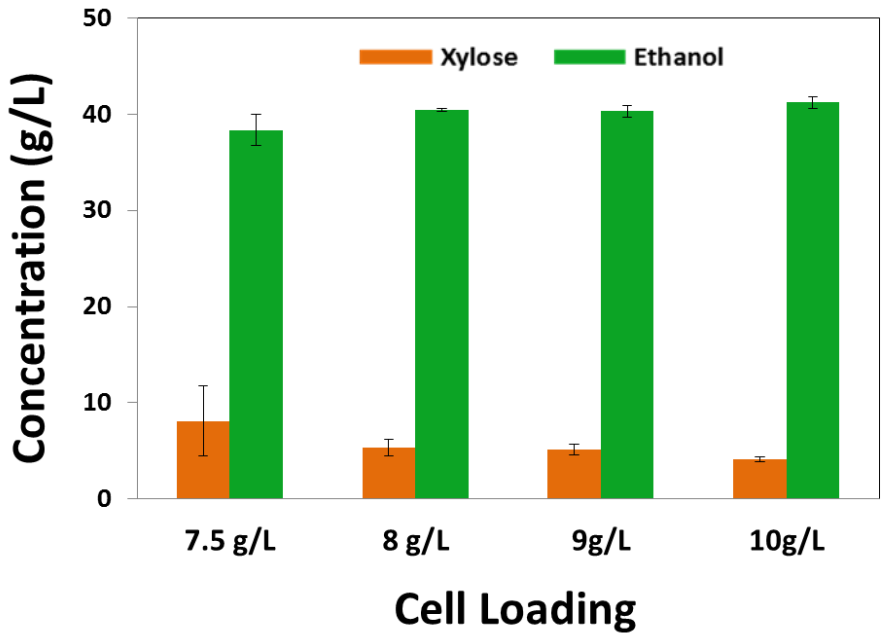

Figure 15 Effect of different initial cell loadings during RaBIT fermentation. Final concentrations are shown for xylose (orange) and ethanol (green). Cell loadings are reported as dry cell weight concentration. Error bars represent standard deviations.

To investigate the effects of temperature and initial pH on the RaBIT fermentation, an initial cell loading of 7.5 g/L DCW was used and 3-cycle RaBIT fermentations were performed. Using a cell loading of 7.5 g/L DCW would not be sufficient for complete xylose consumption

and would thereby enable better discrimination of changes in xylose consumption due to changing temperatures and pH. The optimum temperature was determined using an initial pH of 5.5. The results (Figure 16a) showed that increasing temperature from 30 °C to 32 °C did not significantly affect the fermentation, with only 1 g/L more ethanol produced on average at 32 °C compared to 30 °C. Performance decreased at 35 °C with 2.5 g/L less ethanol produced on average compared to 32 °C. At 35 °C, the ethanol metabolic yield was possibly reduced due to cell maintenance requirements. The fermentations performed at 37 °C greatly affected the cell population. The 70% drop in ethanol production during cycle 2 was likely due to significant cell death at the elevated temperature. At the end of the first cycle at 37 °C, no viable colonies were found when plating at 6,250,000 (50^4) dilution ratio. Viable colonies were found for all other temperatures and cycles. Also, OD measurements indicated that the cell mass at the end of cycles 1 and 2 was less than the initial inoculum when fermenting at 37 °C unlike other temperatures.

The final optimization test determining the optimal initial pH is shown in Figure 16b. At 32 °C and 7.5 g/L DCW initial loading, the optimal pH was 6.0. At this pH, the highest ethanol titers were reached. Furthermore for the first time during this work, ethanol production increased after both recycling events. An initial pH of 6.5 was also attempted, but produced unstable cell behavior as manifested by large variability in results (data not shown). Another experiment was performed to determine if the higher pH was beneficial due to the physiological state of the cell or due to precipitation of inhibiting compounds (Appendix A). Hydrolysates prepared by raising the pH from 4.8 (enzymatic hydrolysis pH) to 5.0, 5.5, or 6.0 were compared based on their effects on fermentation to hydrolysates that were raised to pH 6, sterile filtered, and then acidified back down to 5.0, 5.5, or 6.0. This study was necessary since raising pH can cause the

removal/precipitation of degradation products as is commonly practiced in overliming (Mohagheghi et al., 2006). The results showed no significant difference in fermentability of the two sets of hydrolysates indicating that pH was affecting cellular physiological state rather than precipitating inhibitors.

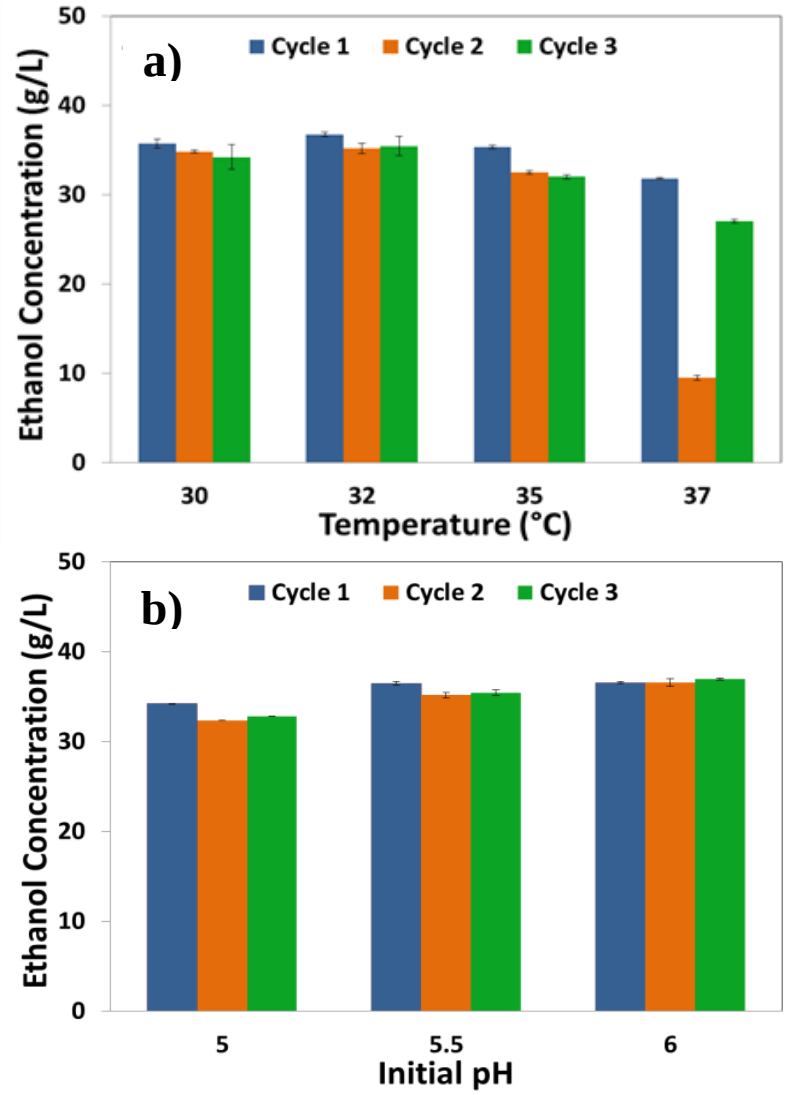

Figure 16 Optimization of temperature and pH for 3-cycle RaBIT fermentation process. Temperature optimization (a) was performed at an initial pH of 5.5 and initial cell loading of 7.5 g/L DCW. pH optimization (b) was performed at a temperature of 32 °C and initial cell loading of 7.5 g/L DCW. Final ethanol concentrations are shown. Error bars represent standard deviations.

4.3.2 Nutrient testing

As shown in Figure 15, xylose consumption decreases when recycling Y128. Decreasing xylose consumption was also experienced during the optimization studies (data not shown). Lack of sufficient nutrients may be one reason for decreasing xylose consumption upon cell recycling. AFEX treated corn stover supports cell growth to high concentrations (Lau et al., 2009). However, there may not be enough nutrients present to fully support the high cell populations in the demanding RaBIT process conditions. Three different nutrient sources were tested: yeast extract, wheat germ, and corn steep liquor. Yeast extract, the product of autolysed yeast cells, was used as an ideal nutrient source. However, yeast extract would not be feasible industrially due to its high price. Corn steep liquor (CSL) and wheat germ were chosen as cheaper and more practical options. CSL is the cheaper of the two and is produced as a by-product of corn wet-milling (Liggett and Koffler, 1948). CSL provides a reasonable amount of nutrients, but also contains inhibitors such as lactic acid (Liggett and Koffler, 1948). Furthermore, CSL is well established as a nutrient source for industrial fermentations (Lawford and Rousseau, 1997). Wheat germ is a by-product of flour milling (de Vasconcelos et al., 2013). It contains high levels of metals such as zinc and magnesium (Table 11), which have been shown to help yeast resist ethanol stress (Zhu et al., 2006; Zhao and Bai, 2012).

The addition of yeast extract (Figure 17b) did not benefit the fermentation greatly. Compared to control experiments (Figure 17a), the addition of up to 5 g/L yeast extract improved the xylose consumption by about 2 g/L and showed up to 2 g/L higher ethanol production. However, yeast extract addition did not prevent the decrease in xylose consumption upon cell recycle.

Table 11 Nutrient Additive Compositions

	Corn Steep Liquor(Liggett and Koffler 1948)	Yeast Extract(Anon. 2006)	Wheat Germ(Agricultural Research Service 2013)
Water	45-50%	3.10%	11.12%
Total N	2.7-4.5%	10.90%	-
Amino N	1-1.8%	6%	-
Ash	9-10%	11.20%	-
Ca	0.5-1.5 pdm	130ug/g	39ug/g
Cu	0-0.001 pdm	-	0.79ug/g
Fe	0.01-0.05 pdm	55.3ug/g	6.26ug/g
Mg	0.5-1.0 pdm	750ug/g	239ug/g
Mn	0.004-0.0125 pdm	-	13.30ug/g
K	1-25 pdm	31950ug/g	842ug/g
Na	-	4900ug/g	12ug/g
P	2.0-3.0 pdm	-	892ug/g
Phosphate	-	3.27%	-
S	0.34 pdm	-	-
Sulfate	-	0.09%	-
Zn	0.0005-0.005 pdm	-	12.29ug/g

pdm = percent dry matter

Wheat germ was added before enzymatic hydrolysis so that hydrolysis could help release the nutrients (Figure 17c). The addition of 5.0 g/L wheat germ improved the overall xylose consumption by up to 3.5 g/L and ethanol production by up to 4.5 g/L for the third cycle. These results concur with our initial hypothesis that wheat germ would allow the yeast to resist the higher ethanol concentrations by consuming more xylose and lowering the cell maintenance energy requirements. The xylose consumption, however, still decreased during subsequent cycles.

Adding CSL to the fermentation broth provided the best results (Figure 17d). CSL promoted increased xylose consumption in subsequent cycles. This was observed at CSL concentrations of 1, 2.5, and 5 g/L. The best results were at 2.5 g/L. At the higher CSL concentration of 5 g/L, ethanol production decreases, likely due to excess cell growth or inhibition from the CSL. In the third cycle, the addition of CSL caused 3.5 g/L more xylose consumption and 2.5 g/L more ethanol production compared to the control. Additionally, the improvement between the first and third cycle showed 2 g/L more consumed xylose and 1.25 g/L more ethanol. This may indicate an increase in cell viability across cycles.

Wheat germ and CSL were also added in combination (Figure 18). Improved ethanol production and increased xylose consumption after each cycle were expected. The results, however, were similar to those for yeast extract addition. There was an initial benefit to the fermentation but still caused a significant decrease in xylose consumption and ethanol production as the cycles progressed. It is possible that high nutrient concentrations promote excess growth but deplete nutrients that are vital for cell maintenance later in the fermentation. This explanation would also account for the similar results seen when adding yeast extract.

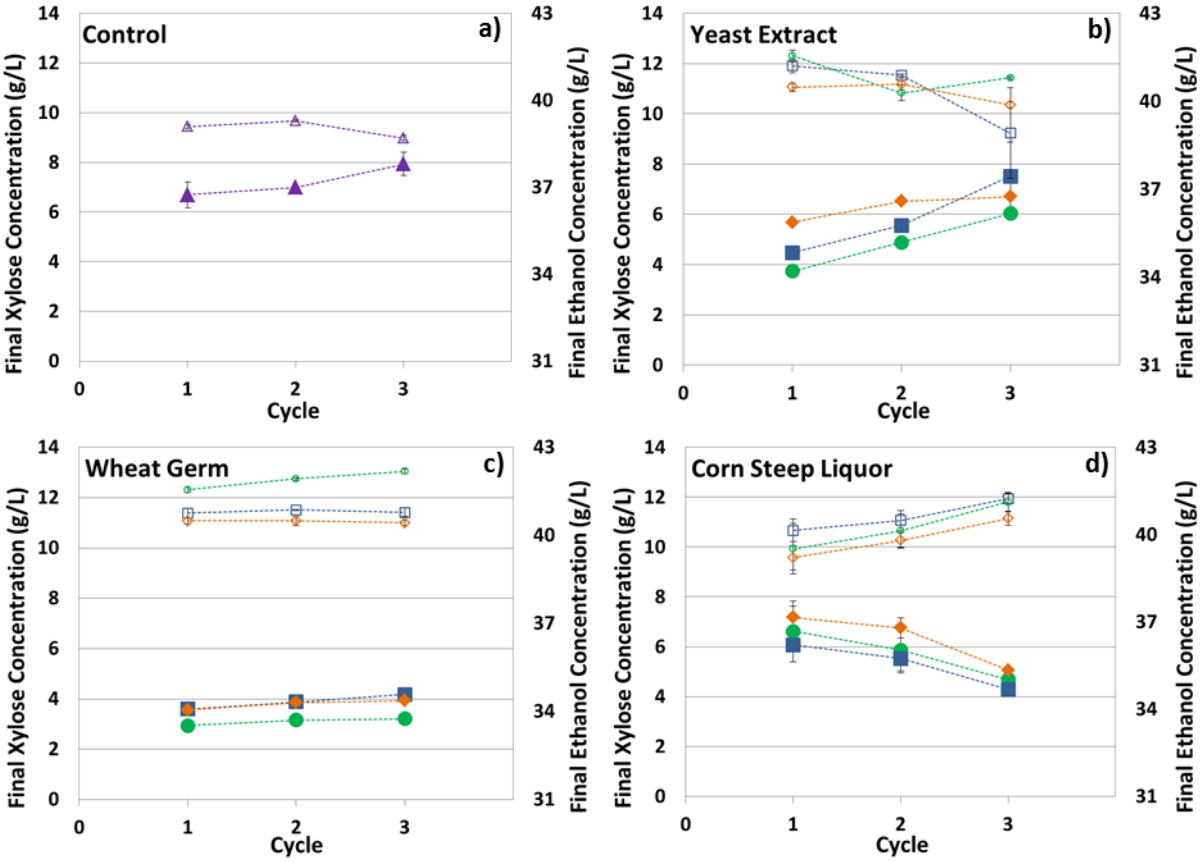

Figure 17 Effect of nutrient addition on RaBIT fermentation process. Fermentation conditions consisted of 6% glucan loading hydrolysate, 32 °C, initial pH of 6.0, and initial cell loading of 7.5 g/L DCW. Closed symbols represent xylose concentration while open symbols represent ethanol concentration. Nutrient concentrations of 1 g/L (orange diamonds), 2.5 g/L (blue squares), and 5.0 g/L (green circles) were tested for each nutrient source. Initial glucose and xylose concentrations were approximately 58 g/L and 29 g/L respectively. Error bars represent standard deviations and are present for all data points but may be hidden by the symbol.

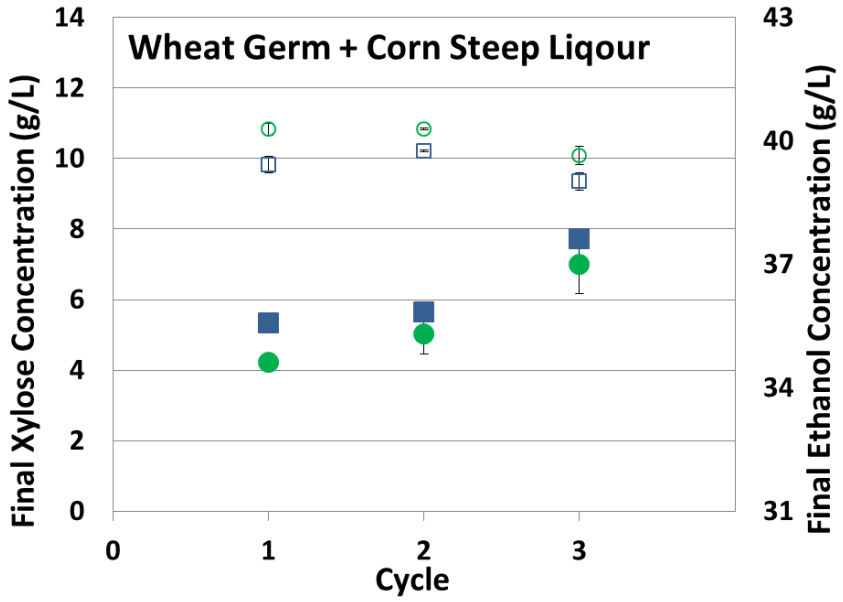

Figure 18 Combination of corn steep liquor and wheat germ at a 50% ratio as a nutrient source. Closed symbols represent xylose concentration while open symbols represent ethanol concentration. Total concentrations of 1 g/L (blue squares) and 2 g/L (green circles) were tested. Error bars represent standard deviations and are present for all data points but may be hidden by the symbol.

The final nutrient test was performed by adding CSL (2.5 g/L) during the xylose consumption phase (at 6 h) rather than at the beginning of the fermentation (Figure 19). The addition of the CSL at the beginning was more beneficial to both xylose consumption and ethanol production. This indicates that nutrient addition is more important during the high growth phase than during high stress xylose consumption phase. However, the xylose consumption still improved over each cycle regardless of when the CSL was added.

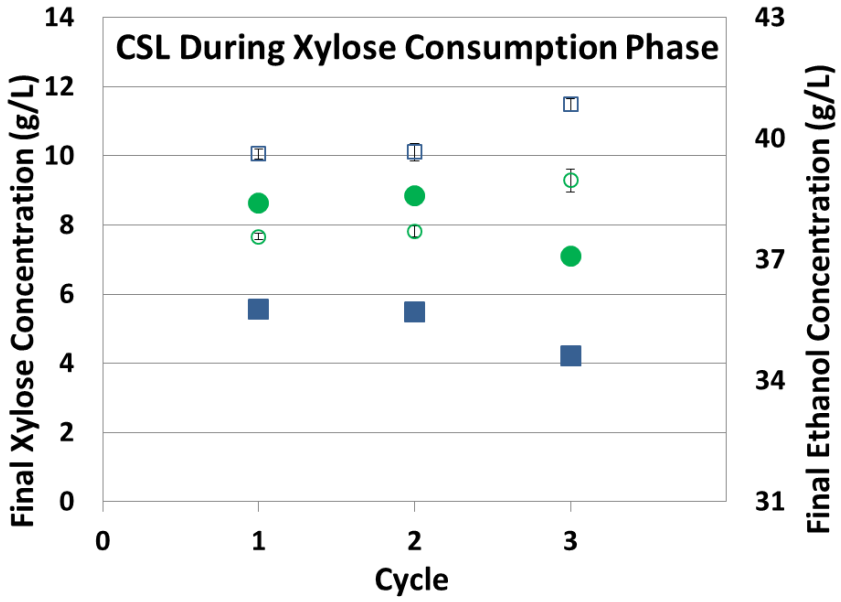

Figure 19 2.5 g/L Corn steep liquor addition time testing. Closed symbols represent xylose concentration while open symbols represent ethanol concentration. Addition were made at t=0 h (blue squares) and t=6 h (green circles). Error bars represent standard deviations and are present for all data points but may be hidden by the symbol.

When analyzing all the results taken together, a possible explanation emerges for the difference in results observed between the three nutrient sources. Yeast extract may contain adequate nutrients that benefit growth, but may be low in nutrients that maintain the cell population through the xylose consumption phase. Wheat germ may primarily contain nutrients that benefit cell maintenance and ethanol tolerance, but may lack nutrients that promote growth. Most nutrients in CSL may benefit cell maintenance and ethanol tolerance, but have enough nutrients to promote growth, while not depleting the important cell maintenance and ethanol tolerance nutrients.

4.3.3 Five cycle viable cell profiling

Comparisons over five fermentation cycles were performed in a bioreactor to better imitate industrial conditions. The experimental goal was to profile the viable cell mass through

five cycles by use of a capacitance probe. A no nutrient addition case was compared to the optimal nutrient addition case (2.5 g/L CSL) as determined previously. The five cycle comparison used the optimal initial inoculum of 10 g/L DCW, initial pH of 6.0, and fermentation temperature of 32 °C. Previously, cell population was measured using the OD method. OD measurement does not accurately measure the viable cell population. This problem was solved using a capacitance probe. Cells with intact membranes give a capacitance reading when an electrical current is passed around them. When the membrane is compromised, the current can pass through the cells and this capacitance is lost. Thus capacitance readings can measure cell biomass with intact membranes, while not including cells with disrupted membranes (Ferreira et al., 2005; Austin et al., 1994). Capacitance readings were taken every 10 seconds and averaged over 10 readings. An accurate viable cell profile was necessary for determining the cause of reduced xylose consumption as the number of recycle events increased. From previous OD measurements, there appeared to be little or no growth after the first cycle. A lack of cell growth or cell death could create a cell population that is accumulating biomass degradation products inside the cell causing reduced metabolic activity. Furthermore, OD measurements may not have accurately measured cell death. The outer membranes of some cells may have been disrupted enough to stop metabolic activity, but still have enough integrity to scatter the light associated with an OD measurement. Accurate viable cell measurements would also help determine if CSL addition benefited cell growth or cell metabolism.

The sugar, ethanol, and OD measurements are shown in Figure 20. Overall, 2.5 g/L added CSL slightly improved the performance compared to no CSL addition with regards to xylose consumption. With CSL addition, final xylose concentrations were 3.5 ± 0.25 for the first 4 cycles. Without the CSL addition, final xylose concentrations were 3.5 g/L, 4.7 g/L, 3.8 g/L,

and 6.1 g/L for cycles 1-4, respectively. Cycle 5 xylose concentrations and cycle 1-5 ethanol concentrations were comparable between the two cases. Fermentation performance was improved when using bioreactors instead of shake flasks as indicated by improved xylose consumption. The only significant difference between the two experimental environments was mixing. Mixing has been shown to affect cell growth rates (Yerushalmi and Volesky, 1985). It is also possible that mixing in the bioreactors reduced the size of cell flocs, thus reducing or eliminating potential sugar diffusion limitations in the flocs, and improving cell access to adequate sugars (Stratford & Keenan, 1988).

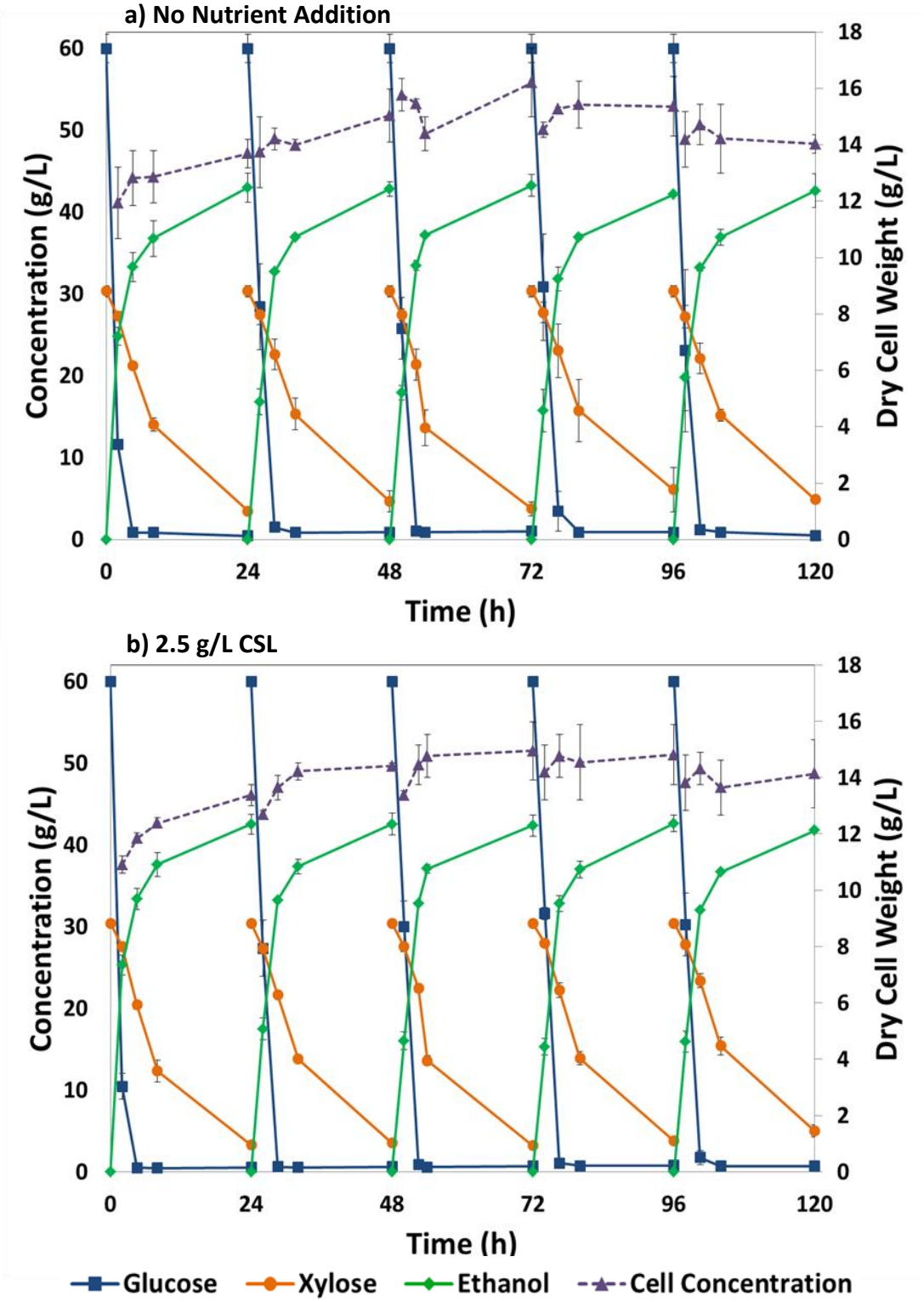

Figure 20 RaBIT fermentation process comparison in the presence and absence of nutrient supplementation. Here, a) no nutrient addition and b) 2.5 g/L CSL addition. Concentrations are shown for glucose (blue squares), xylose (orange circles), ethanol (green diamonds), and dry cell weight correlated from OD (purple triangles). Error bars represent standard deviations and are present for all data points but may be hidden by the symbol.

Figure 21 shows the viable cell density profile for both no nutrient addition and 2.5 g/L added CSL through five cycles. For all cycles, the viable cell density increases during the first 5 to 7 h. The growth phase appears to end shortly after all the glucose is consumed. After a brief stationary phase, the viable cell density then decreases rapidly during the rest of the xylose consumption phase. This general trend was observed during all cycles and for both no nutrients and 2.5 g/L added CSL. Cell death during yxlose consumption phase is not exclusive to high cell density fermentations. Figure 13 in Chapter 3 shows the same decrease for a low cell density fermentation.

Fermentation kinetics varied significantly between the case of no CSL addition and the CSL addition experiment (Table 12). Overall, when CSL was added, cells showed faster growth rates and faster death rates. Interestingly, when no nutrients were added the death rate increased in later cycles; possibly due to cell aging. When CSL was added, the death rates were similar between all five cycles. Differences were also present in the specific xylose consumption rates (gram xylose consumed/gram viable cell mass/hour). When no nutrients were added the specific xylose consumption rate was lower during the last 4 cycles compared to the first cycle. When CSL was added the specific xylose consumption rate was higher during cycles 2-4 compared to cycle 1. This indicated that cell populations were more metabolically active with the addition of CSL.

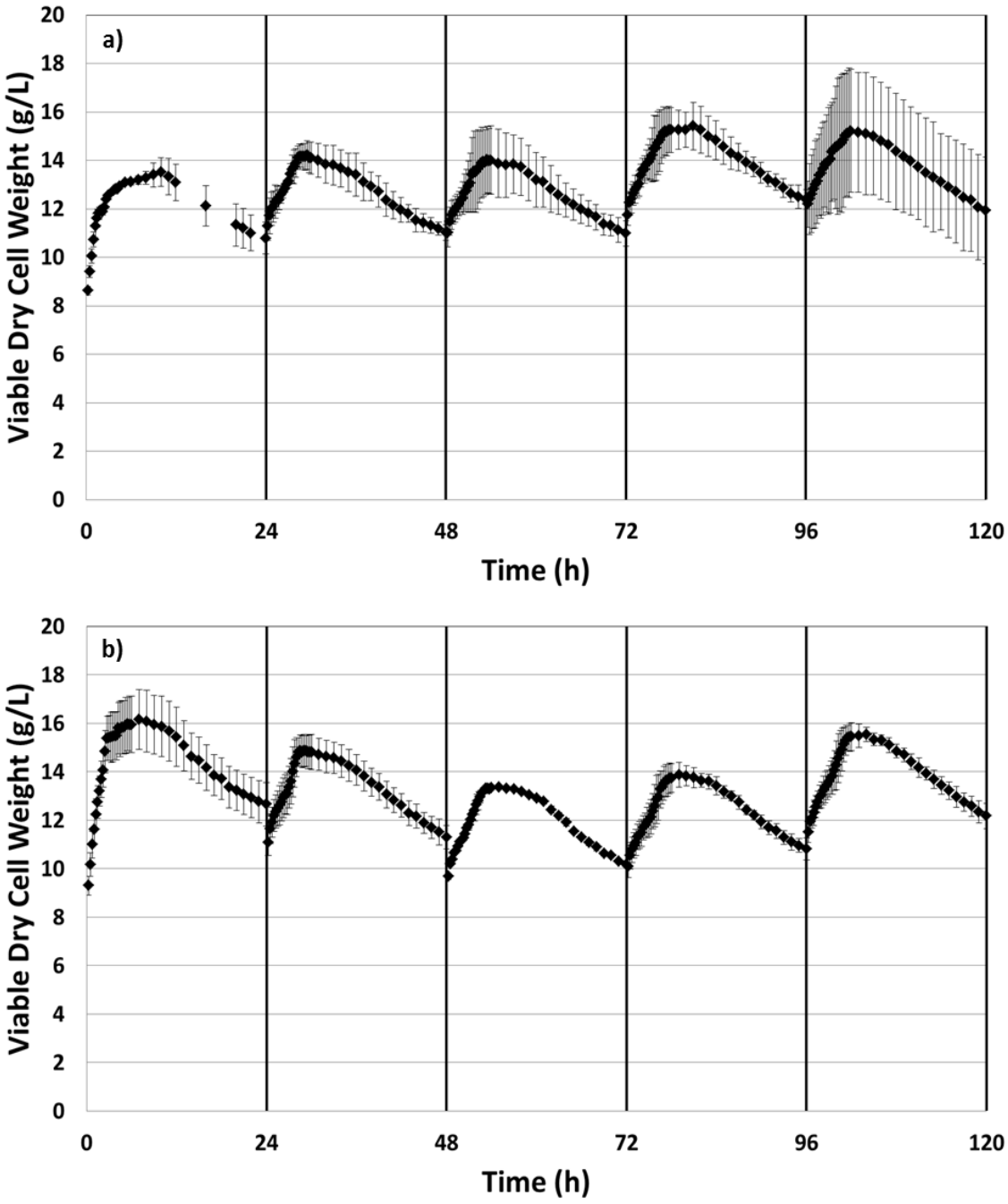

Figure 21 Measure of viable dry cell weight. Viable DCW was correlated from capacitance reading for 5 cycle RaBIT fermentations with a) no added nutrients and b) 2.5 g/L added corn steep liquor. Error bars represent standard deviations.

Table 12 RaBIT Fermentation Cellular Rates

	Specific Xylose Cons. Rate[+,a], g/g/h	Avg. Viable Cell Density[a], g/L DCW	Growth Rate[b], g/L/h	Death Rate[c], g/L/h
No Nutrients				
Cycle 1	0.092 ± 0.005	12.3 ± 0.5	0.401 ± 0.113	-0.156 ± 0.024
Cycle 2	0.084 ± 0.001	12.8 ± 0.5	0.624 ± 0.356	-0.176 ± 0.028
Cycle 3	0.088 ± 0.006	12.7 ± 0.9	0.547 ± 0.383	-0.176 ± 0.050
Cycle 4	0.072 ± 0.003	14.0 ± 0.7	0.579 ± 0.326	-0.180 ± 0.020
Cycle 5	0.079 ± 0.014	13.8 ± 2.0	0.478 ± 0.315	-0.197 ± 0.019
2.5 g/L CSL				
Cycle 1	0.079 ± 0.003	14.4 ± 1.0	0.831 ± 0.158	-0.214 ± 0.024
Cycle 2	0.084 ± 0.006	13.3 ± 0.6	0.841 ± 0.056	-0.208 ± 0.012
Cycle 3	0.094 ± 0.001	12.0 ± 0.0	0.728 ± 0.070	-0.196 ± 0.005
Cycle 4	0.089 ± 0.003	12.5 ± 0.4	0.718 ± 0.009	-0.189 ± 0.002
Cycle 5	0.076 ± 0.001	14.0 ± 0.4	0.688 ± 0.162	-0.210 ± 0.015

[+]Specific xylose consumption rate was calculated by dividing the xylose consumed by the time period and average viable dry cell weight concentration as correlated from capacitance readings.

Calculated from ([a]) 0 to 24 h, ([b]) 2 to 4.5 h, or ([c]) 8 to 24 h.

Average cell viable cell concentration was calculated using the integral method.

Error values represent standard deviations

The new insights gained from an accurate viable cell profile disprove the previous conjecture on how CSL, and likely yeast extract and wheat germ, affected RaBIT fermentation performance. The fact that CSL simultaneously promotes both growth and cell death does appear to agree with earlier evidence that CSL contains both beneficial nutrients and also inhibitors. The results also indicate that increasing cell turnover has the potential to eliminate the xylose consumption decrease upon recycle. Increasing cell turnover rates might be possible with process changes instead of costly nutrients.

4.4 Conclusion

RaBIT fermentation conditions using *S. cerevisiae* GLBRCY128 were optimized. Different nutrient supplementation protocols were evaluated to ascertain whether xylose

consumption could be improved during subsequent cycles of the RaBIT process. It was found that adding 2.5 g/L corn steep liquor (CSL) improved xylose consumption for the three cycles tested when 7.5 g/L initial dry cell weight (DCW) inoculum was used. However, the xylose consumption problems still existed when 10 g/L DCW inoculum was utilized for optimal ethanol production for five fermentation cycles. Capacitance monitoring indicated that there is both dynamic cell growth and death during each RaBIT cycle. Furthermore, the main cause of reduced xylose consumption with subsequent cycles is decreased specific xylose consumption rate rather than decreased viable cell mass.

CHAPTER 5: EFFECT OF PRETREATMENT DEGRADATION PRODUCTS ON RABIT FERMENTATIONS

Abstract

This chapter studied the effects of degradation products (low molecular weight compounds produced by pretreatment) on the microbes used in the RaBIT (Rapid Bioconversion with Integrated recycling Technology) process. Chemical genomic profiling was performed, showing no differences in hydrolysates produced during RaBIT enzymatic hydrolysis. Concentrations of degradation products were measured after different enzymatic hydrolysis cycles and fermentation cycles. Intracellular degradation product concentrations were also measured following fermentation. Degradation product concentrations did not change between RaBIT enzymatic hydrolysis cycles; the cell population retained their ability to oxidize/reduce (detoxify) aldehydes over five RaBIT fermentation cycles; and degradation products were accumulating within the cells as RaBIT fermentation cycles increased. Synthetic hydrolysate was used to confirm that pretreatment degradation products are the sole cause for xylose consumption decrease during RaBIT fermentations.

5.1 Introduction

Yeast recycling is a common practice in ethanol fermentations. The Brazilian sugar cane industry uses an initial yeast pitch and recycles the yeast population for the rest of the season (Wheals et al., 1999). Different species of yeast are also introduced naturally during the sugar cane process and may end up dominating the fermentations (da Silva-Filho et al., 2005). The beer industry recycles its yeast for a shorter period of time to eliminate any drift in the beer flavor due to mutation or adaptation (Huuskonen et al., 2010). If yeast recycling is performed

with no problems in other industries, what is different about our lignocellulosic RaBIT process? The three main differences are reduced nutrient levels, xylose fermentation, and the presence of pretreatment degradation products. The work in Chapter 2 showed that additional nutrients did not eliminate the trend toward decreasing xylose consumption and that significant cell death was occurring during the xylose consumption phase. Death during the xylose consumption phase was addressed in Chapter 6. Pretreatment degradation product effects are investigated in this Chapter.

Pretreatment of lignocellulosic biomass is necessary for its efficient conversion to monomeric sugars (Balan, 2014). Pretreatment processes are commonly performed at high temperature, high pressure, caustic, and/or acidic conditions, which generate compounds inhibitory to microorganisms (Balan, 2014; Du et al., 2010). Under acidic conditions, carbohydrates present in the biomass degrade into furfural or hydroxymethylfurfural and the lignin degrades into a variety of phenolic compounds (Du et al., 2010; Klinke et al., 2004). The AFEX process, compared to other pretreatment processes, produces many ammoniated compounds. A previous comparison of AFEX and dilute acid treated corn stover showed that dilute acid pretreatment produces 316% more acidic compounds, 142% more aromatics, 3555% more furans, but no nitrogenous compounds (Chundawat et al., 2010). Nitrogenous compounds are significantly less inhibitory than their acid counterparts (Tang et al., 2015).

Pretreatment degradation products inhibit microbes in lignocellulosic hydrolysates. Inhibition occurs for both cell growth and sugar consumption (Tang et al., 2015). Previous research has mostly been focused on the effect of degradation compounds during single batch fermentations. Our literature review has found no research looking into the effects of

degradation compounds on fermentations with cell recycling. The biggest concern, in the context of cell recycling, is that pretreatment degradation products accumulate within the cell.

Work reported in this chapterork investigated the effect of pretreatment degradation products on the performance of recycled cells. A yeast gene deletion study was performed to determine whether hydrolysate composition significantly changed across RaBIT enzymatic hydrolysis cycles. RaBIT fermentations were performed at different concentrations of pretreatment degradation products. Pretreatment degradation product concentrations were quantified before fermentation, after fermentation, and within the yeast cells. Finally, degradation product effects were investigated further using synthetic hydrolysate.

5.2 Materials and Methods

5.2 1 Biomass and Pretreatment

Great Lakes Bioenergy Research Center (GLBRC) corn stover was used for this study. The corn (Pioneer 36H56) was planted and harvested during 2010 at the Arlington Agricultural Research Station (Columbia County, WI). The biomass was pretreated using the AFEX process as previously described in the literature using a 5 gallon reactor (Balan et al., 2009). AFEX pretreatment conditions were as follows: 1:1 ammonia to biomass ratio, 60% moisture, 100 ^{o}C, and 30 min. reaction time. Composition analysis, following the method of Sluiter et al., 2010 showed the glucan, xylan, acid insoluble lignin, and ash contents were 31.4%, 18.6%, 13.08%, and 13.39%, respectively. The pretreated corn stover was stored at 4 ^{o}C.

5.2.2 Microorganism and Seed Culture Preparation

Saccharomyces cerevisiae GLBRCY128 was used for this study having previously been genetically modified and adapted by Dr. Trey K. Sato of the University of Wisconsin-Madison. Xylose isomerase and xululokinase genes were introduced to facilitate xylose utilization.

Seed cultures were prepared from glycerol stocks stored at -80 °C. Seed culture media contained 100 g/L dextrose, 25 g/L xylose, 20 g/L tryptone, and 10 g/L yeast extract. Erlenmeyer flasks (250 mL) containing 100 mL of seed culture media were inoculated with 0.1 OD_{600}. The cultures were incubated at 30 °C and 150 RPM in shaker incubators under microaerobic conditions for 22 h. After 22 h, fresh seed culture media was inoculated with 1% of the first seed culture medium and incubated under the same conditions for another 22 h.

5.2.3 RaBIT Enzymatic Hydrolysis

Enzymatic hydrolysis at 7% (w/w) glucan loading was performed using the RaBIT process in 250 mL baffled Erlenmeyer flasks using a 100 gm reaction mass (biomass, water, enzymes, and acid). The first cycle enzyme cocktail was 14.7 mg protein/g glucan Cellic CTec3 and 14.9 mg protein/g glucan Cellic HTec3 (Novozymes). Enzyme cocktail protein contents were provided by Novozymes. Hydrolysis was performed for 24 h at 50 °C and 250 RPM in a shaking incubator. The pH was maintained at 5.0 using 12.1 M hydrochloric acid. After 24 h, the hydrolysate slurry was centrifuged at 6200 RCF. The hydrolysate supernatant was poured off and the solids were recycled back into the next enzymatic hydrolysis cycle. Enzyme loadings were reduced to 60% and 50% of the original for cycle 2 and cycles 3+, respectively.

5.2.4 RaBIT Fermentations

Fermentations were performed in 125 mL Erlenmeyer flasks using 50 mL of hydrolysate. Cell pellets prepared by centrifugation of seed cultures were used to inoculate first cycle fermentations. The inoculum size was 10 g/L dry cell weight (DCW) concentration determined from an OD_{600} vs. DCW concentration plot. Initial pH was adjusted to 6.0 using 10 M potassium hydroxide. Fermentations were conducted for 24 h at 32 °C and 150 RPM in shaking incubators under microaerobic conditions. After 24 h, the fermentation broth was centrifuged at 3250 RCF and the resulting cell pellet was used to inoculate the next fermentation cycle. All fermentation experiments were performed with at least 2 biological replicates.

OD was measured 600_{nm} using a Beckman Coulter DU 720 spectrophotometer. Samples were diluted to stay within a raw reading of 0.1-1.

5.2.5 Chemical Genomics

Chemical genomic analysis of these hydrolysates was performed, as described previously, using a collection of ~4000 yeast deletion mutants (Piotrowski et al., 2015a; Piotrowski et al., 2015b). 200 µL cultures with the pooled collection of *S. cerevisiae* deletion mutants were grown in the different RABIT cycles of hydrolysates or Yeast Peptone glucose (YPD) medium in triplicate for 48 h at 30 °C under aerobic conditions. Genomic DNA was extracted from the cells and mutant-specific molecular barcodes were amplified using specially designed multiplex primers as described previously (Piotrowski et al., 2015b). The barcodes were sequenced using an Illumina HiSeq2500 in rapid run mode (Illumina, Inc, San Diego, CA). The average barcode counts for each yeast deletion mutant in the replicate hydrolysates were normalized against the YPD control in order to define sensitivity or resistance of individual

strains (chemical genetic interaction score). A resistant mutant has a positive interaction score, whereas a negative score indicates a sensitive mutant. The pattern of genetic interaction scores for all mutant strains represents the chemical genomic profile or "biological fingerprint" of a sample (Piotrowski et al., 2015a; Piotrowski et al., 2015b). Correlations of the chemical genomic profiles across cycles were calculated using Spotfire 5.5.0 (Tibco, Boston, MA, USA). The clustergram of the chemical genomic profiles were created in Cluster 3.0 (de Hoon et al., 2004), and visualized in Treeview (v1.1.6r4) (Page, 1996).

5.2.6 Degradation Product Analysis

To determine intracellular degradation product concentrations, cells were harvested by centrifugation at 3250 RCF. The cell pellet was then washed using PBS buffer (8 g/L sodium chloride, 0.2 g/L potassium chloride, 1.44 g/L sodium phosphate dibasic, and 0.24 g/L potassium phosphate monobasic). After a second centrifugation and removal of supernatant, the cell pellet was flash frozen using a dry ice in an ethanol bath. The cell pellet was then dissolved in a 40:40:20 (v/v/v) mixture of acetonitrile, methanol, and water along with 0.1% formic acid.

Quantification of degradation products was performed by HPLC high resolution/accurate mass spectrometry (RP-HPLC-HRAM MS) and headspace solid-phase microextraction gas chromatography-isotope dilution mass spectrometry (HS-SPME/IDMS). Specific methods are described in Keating et al., 2014.

5.2.7 Synthetic Hydrolysate

Synthetic hydrolysate was produced using a modified Great Lakes Bioenergy Research Center (GLBRC) synthetic hydrolysate recipe (Tang et al., 2015). Sugar and nutrient concentrations in the original synthetic hydrolysate were based on 6% glucan loading AFEX

corn stover hydrolysate. These concentrations were multiplied by 7/6ths to mimic the 7% glucan loading AFEX corn stover hydrolysate used in this Chapter. Degradation product concentrations were taken from the analysis presented in this work. The complete recipe is given in Appendix B.

5.2.8 HPLC Analysis

Glucose, xylose and ethanol concentrations were analyzed by HPLC using a Biorad Aminex HPX-87H column. Column temperature was maintained at 50 ^{o}C. Mobile phase (5 mM H_2SO_4) flow rate was 0.6 mL/min.

5.3 Results and Discussion

5.3.1 Glucan Loading Variation

The effect of degradation products on RaBIT fermentations was tested. To do this, hydrolysate was prepared using different glucan loadings (4.5%, 6.0%, 7.5%, and 9.0%). This created hydrolysates varying in degradation product, sugar, and nutrient concentrations. To minimize any sugar concentration difference, glucose and xylose were added based on initial HPLC data to final concentrations of ~60 g/L glucose and ~30 g/L xylose (data not shown). No nutrients were added to address varying nutrient concentrations.

The results in Figure 22 show that degradation products strongly affected xylose consumption both before and after cell recycle during RaBIT fermentations. Quantitative results can be seen in Table 13. Xylose consumption during specific cycles all show a linear correlation (R^2>0.96) between glucan loading and percent xylose consumption (Figure 23a). This was not the case for glucan loading and xylose consumption change between cycles (Figure 23b). This suggests that the potential xylose consumption within a cycle depends on degradation product

concentrations, while the observed decrease in xylose consumption decrease between cycles is the product of a different mechanism, possibly degradation product accumulation within cells. These conclusions assume that glucan loading was directly correlated to degradation production concentration and varying nutrient level did not significantly affect the results.

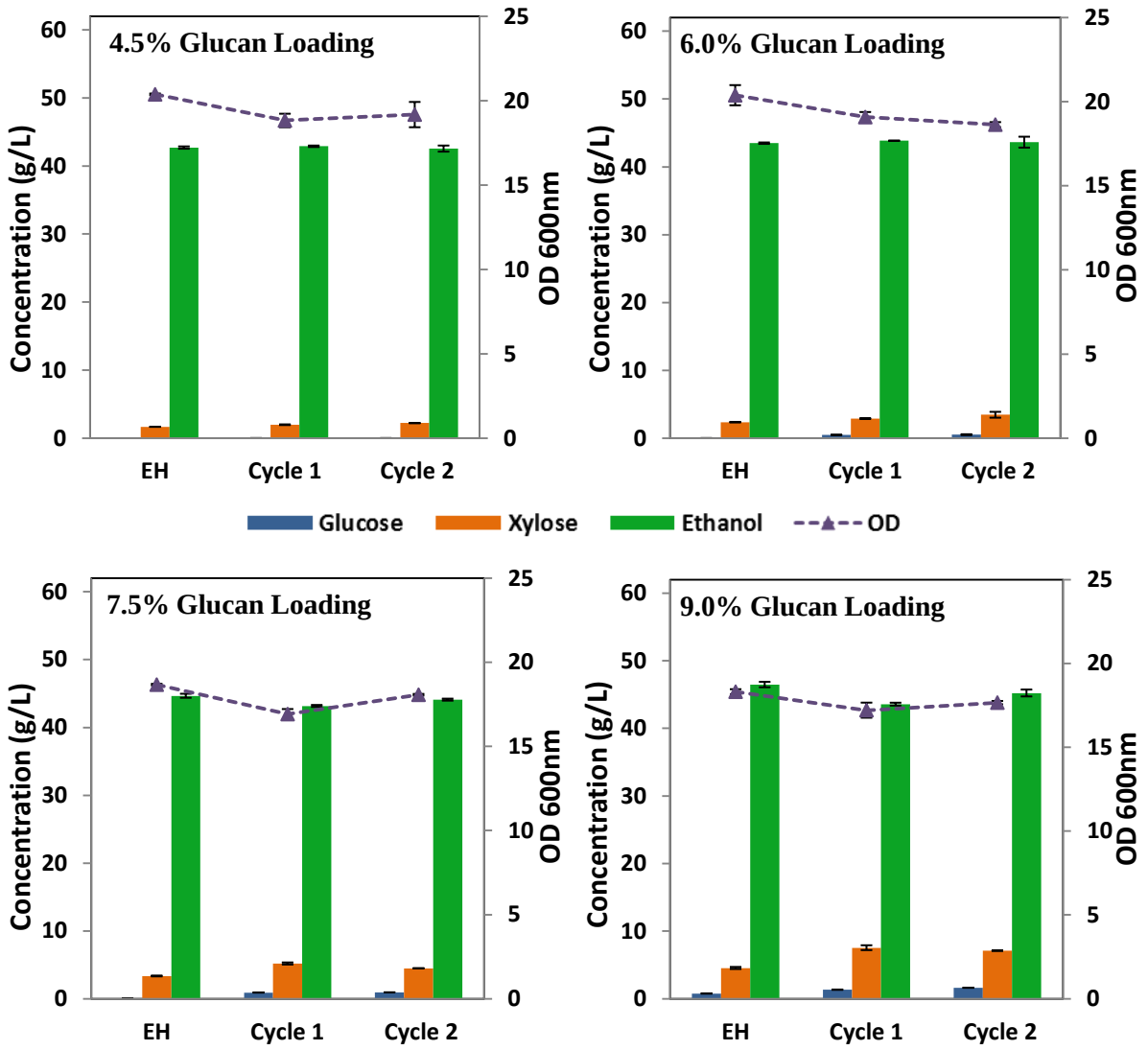

Figure 22 Glucan loading effect on RaBIT fermentations. Initial glucose and xylose concentrations were 59.2 ± 1.2 g/L and 30.5 ± 1.0 g/L, respectively. Final concentrations for glucose (blue), xylose (orange), and ethanol (green) are shown after 24 h fermentation along with OD (purple triangles). Error bars represent standard deviations.

Table 13 Increased glucan loading effect

Glucan Loading	Xylose Consumption		
	Cycle 1	Cycle 2	Cycle 3
4.5%	94%	93%	92%
6.0%	92%	91%	89%
7.5%	89%	83%	85%
9.0%	86%	76%	78%

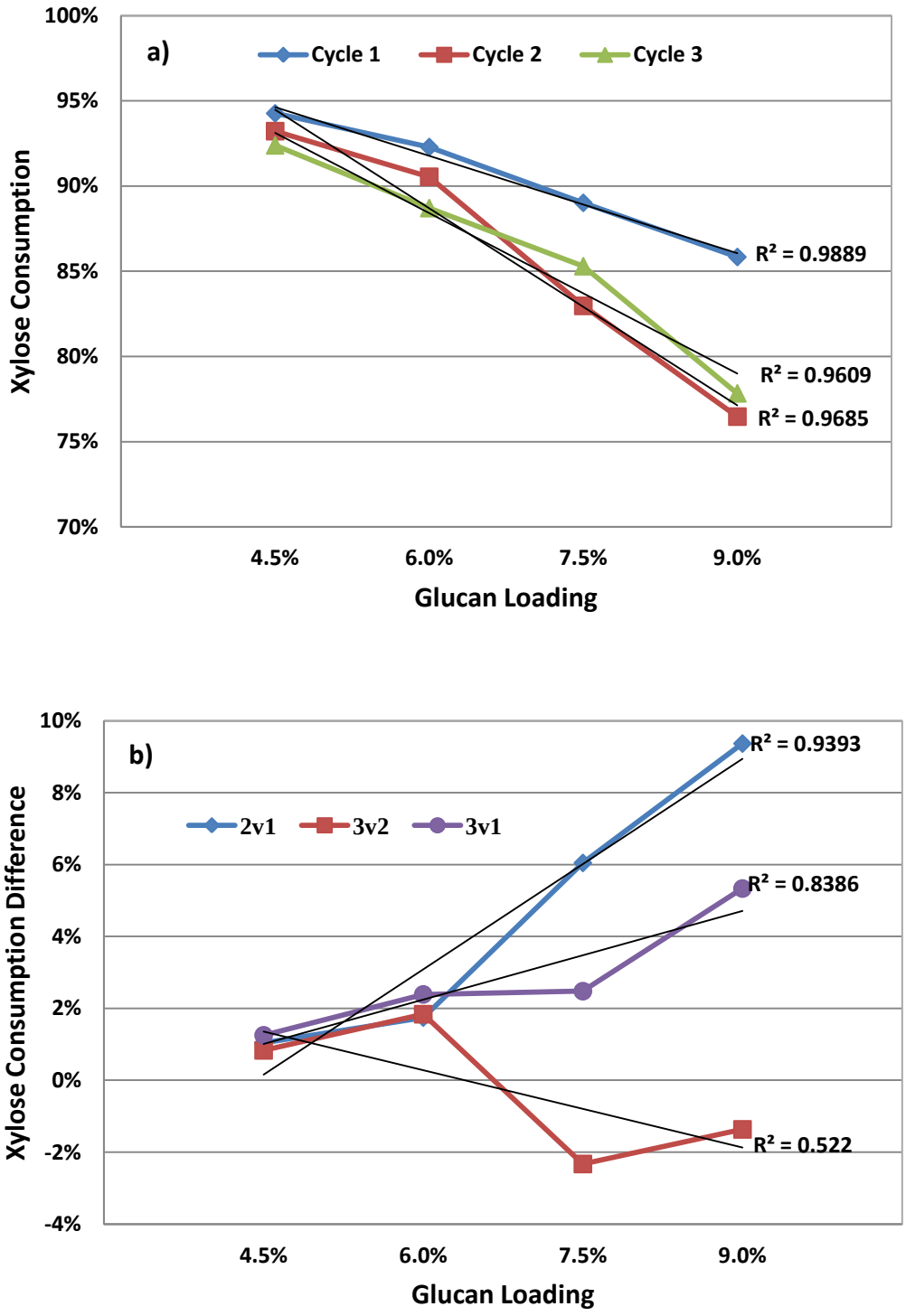

Figure 23 Glucan loading effect correlations for a) xylose consumption comparing different glucan loadings within RaBIT cycles and b) xylose consumption decrease between cycles.

5.3.2 Chemical-genomics Study

To further understand the RaBIT enzymatic hydrolysis process, hydrolysate variability between cycles was tested. Variation in hydrolysate was a potential cause for the decrease in xylose consumption upon cell recycle during RaBIT fermentations. Comparison between the work by Jin et al. (2012a) and results reported in Chapter 4 show that hydrolysate variation is not the sole reason for the decrease in xylose consumption, but it could not be ruled out as a contributing cause. To answer whether hydrolysate variation between cycles was present, chemical-genomic profiling was performed using a genome-wide deletion mutant collection of *S. cerevisiae*. Chemical-genomics is the study of chemical compound interactions with specific genes within an organism. This approach determined whether hydrolysate variability existed in RaBIT enzymatic hydrolysis using a biological "sensor" (individual genes).

Enzymatic hydrolysis was performed for 5 cycles using the RaBIT process. Ampicillin was added to eliminate any contamination effects. A clustergram of gene deletion response is shown in Figure 24. Quantitative analysis of the clustergram is shown in Figure 25. Overall, there appears to be no significant difference between hydrolysis cycles. When comparing all hydrolysate cycles to each other, the average correlation value (R) was 0.90 (Figure 25b). Figure 25a shows an example (comparison of cycles 1 and 5) of how correlation between cycles was performed. This eliminates hydrolysate variability as a cause for reduced xylose consumption upon cell recycle.

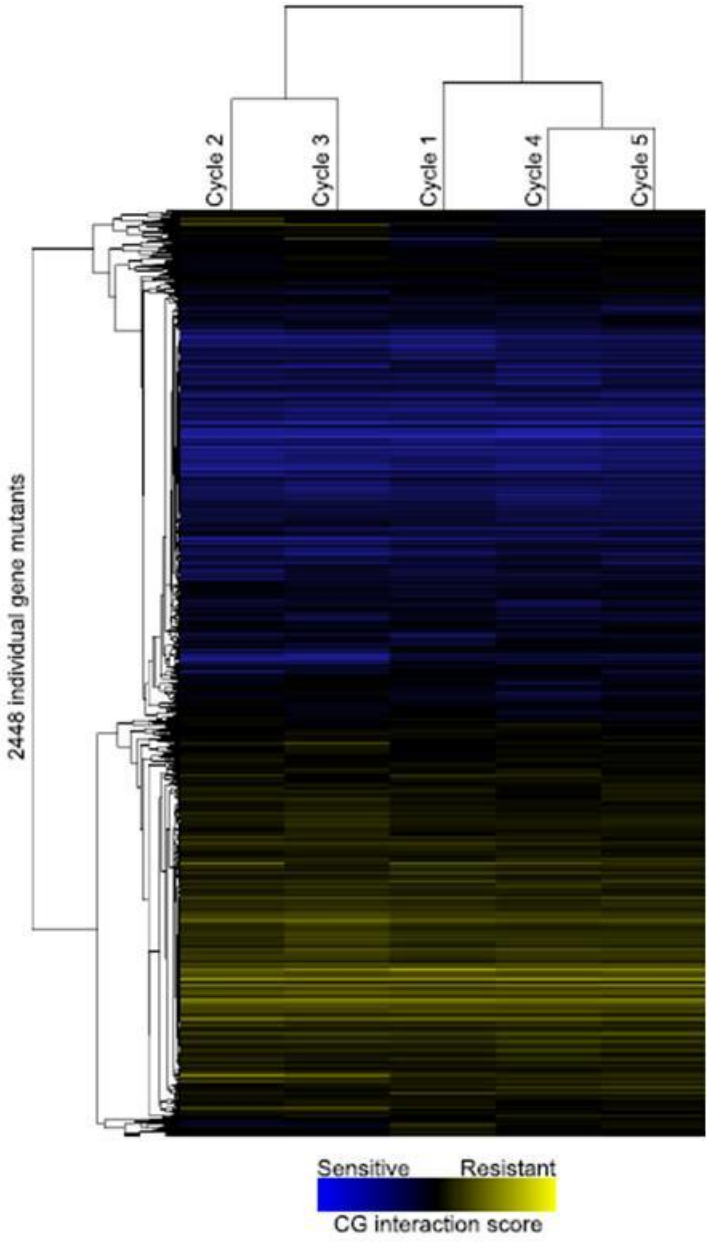

Figure 24 Clustergram showing the entire chemical genomic profile of sensitive (blue) and resistant (yellow) yeast mutants for all five cycle hydrolysates.

A

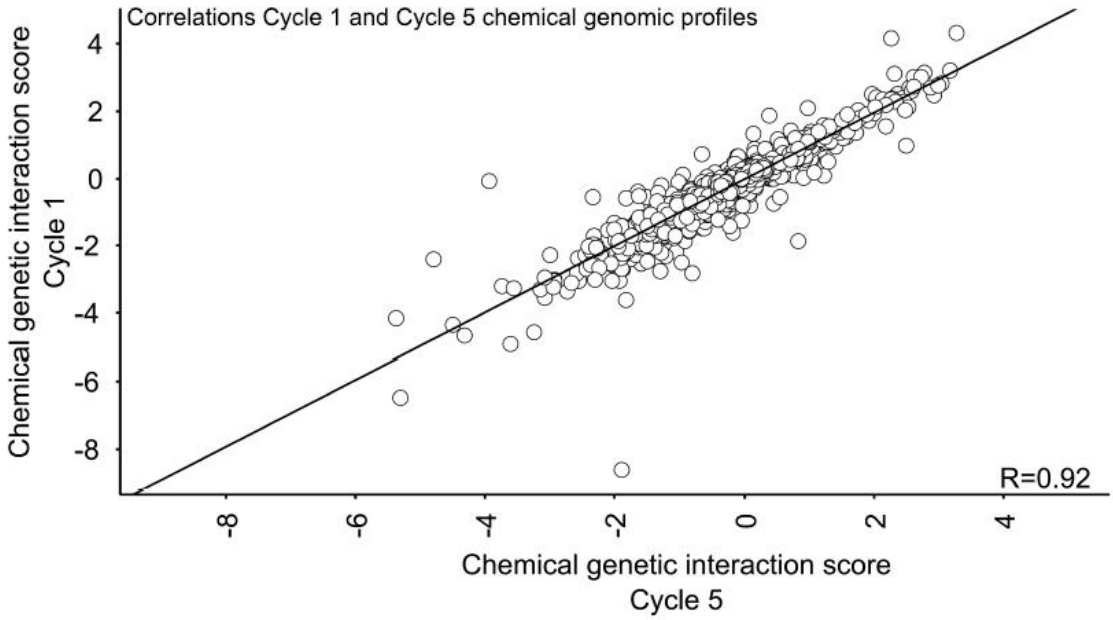

B

Correlations (R) of all chemical genomic profiles

	Cycle 5	Cycle 4	Cycle 3	Cycle 2	Cycle 1
Cycle 5	1				
Cycle 4	0.95	1			
Cycle 3	0.90	0.88	1		
Cycle 2	0.91	0.88	0.94	1	
Cycle 1	0.92	0.93	0.85	0.88	1

Figure 25 Quanitative analysis of chemical genomic profiling of RaBIT hydrolysates using a) chemical genetic interaction scores between cycle 1 and 5 and b) correlation coefficients comparing all 5 cycle hydrolysates.

5.3.3 Hydrolysate Degradation Products Quantification

Degradation product concentrations both before and after fermentation were quantified next. Results from the chemical-genomic study suggested that degradation product concentrations do not change between cycles. Quantifying the degradation compounds would

confirm this result, and also give insight into the dynamics of degradation products concentrations during the RaBIT process. Figure 26 shows that an increase in glucan loading, and therefore degradation product concentration, reduced the ability of the yeast cells to consume xylose. The subsequent decrease in xylose consumption by the recycled yeast populations could be caused by reduced cellular detoxification capability or by accumulation of degradation products within the cells.

The results of this study are shown in Table 14. In general, there is no significant difference in degradation product concentrations when comparing hydrolysate produced during different RaBIT enzymatic hydrolysis cycles (Figure 26; Table 14); the same is true when comparing hydrolysate after different RaBIT fermentation cycles (Table 14). These results are significant for two reasons. First, they eliminate the variation of degradation products between hydrolysis cycles as a possible cause for fermentation performance decrease in recycled cells. Second, they show that the yeast population retains the potential to detoxify hydrolysate when recycled (Figure 26). Detoxification potential was correlated to aldehyde oxidation/reduction; *S. cerevisiae* strains can reduce aldehydes into alcohols or oxidize them into acids, thereby decreasing inhibition. The results did not show whether detoxification rates decreased during successive cycles, which could be significant to RaBIT fermentation performance.

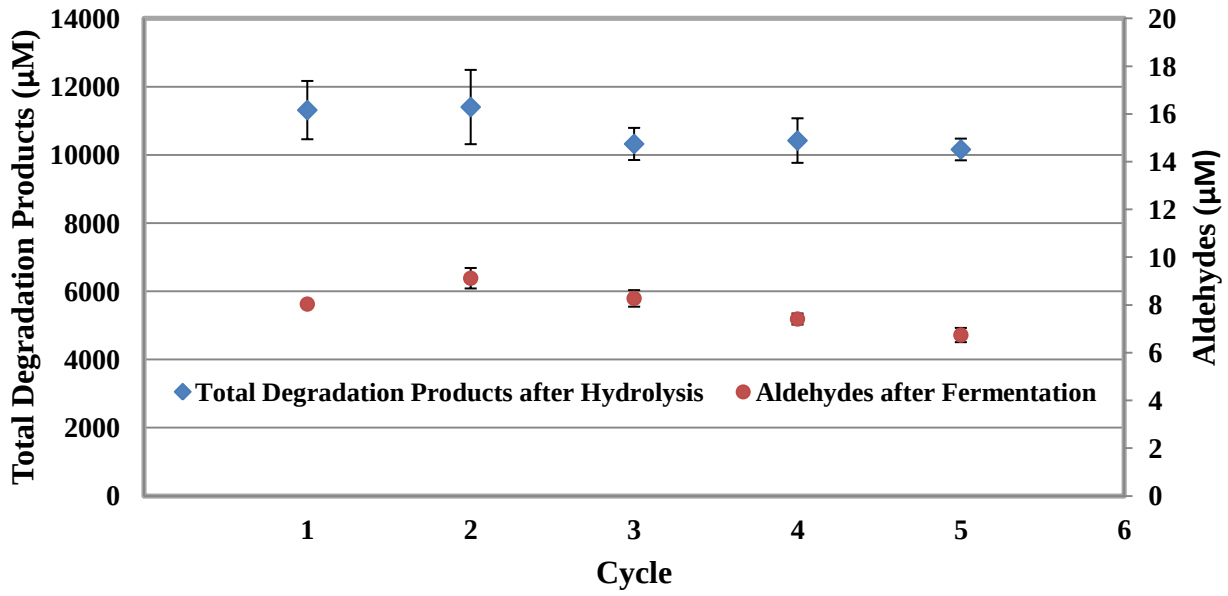

Figure 26 Key degradation product levels in hydrolysate before and after RaBIT fermentation. Error bars represent standard deviations and are present for all data points but may be hidden by the symbol.

This study was also performed to determine if any degradation products were disappearing from the medium or accumulating within the cell. Vanillin was the only compound significantly disappearing that could not be accounted for in a reduced or oxidized form due to detoxification. *S. cerevisiae* strains are not known to metabolize vanillin. However, they are capable of vanillin anabolism following genetic engineering (Brochado et al. 2010). Other fungi such as *Coniochaeta ligniaria* (Nichols et al. 2008) are capable of metabolizing vanillin. Degradation products could be accumulating within the cells but not be apparent due to measurement error.

Table 14 Degradation product levels in hydrolysate before and after fermentation

	Pre-fermentation (µmols/L)					Post-fermentation (µmols/L)				
	Cycle 1	Cycle 2	Cycle 3	Cycle 4	Cycle 5	Cycle 1	Cycle 2	Cycle 3	Cycle 4	Cycle 5
Phenolic Acids										
4-Hydroxybenzoic Acid	50.65 ± 5.99	53.96 ± 2.49	51.02 ± 1.64	40.89 ± 10.67	50.56 ± 4.39	72.21 ± 2.78	104.39 ± 4.16	107.50 ± 6.17	100.56 ± 5.08	99.50 ± 3.51
3-Hydroxybenzoic Acid	0.41 ± 0.04	0.45 ± 0.01	0.44 ± 0.03	0.43 ± 0.01	0.44 ± 0.05	0.39 ± 0.03	0.45 ± 0.01	0.45 ± 0.03	0.48 ± 0.02	0.53 ± 0.05
3,4-Dihydroxybenzoic Acid	3.03 ± 0.44	3.36 ± 0.15	3.31 ± 0.10	3.35 ± 0.19	3.62 ± 0.44	3.14 ± 0.05	3.72 ± 0.24	3.63 ± 0.15	3.75 ± 0.18	4.11 ± 0.26
2,3-Dihydroxybenzoic Acid			Not Detected					Not Detected		
Syringic Acid	7.73 ± 0.56	8.08 ± 0.30	7.76 ± 0.30	7.35 ± 0.17	7.75 ± 0.64	7.51 ± 0.39	8.08 ± 0.35	7.82 ± 0.48	7.62 ± 0.25	7.67 ± 0.44
Coumaric Acid	1768.72 ± 144.38	1810.45 ± 199.76	1552.14 ± 78.03	1509.55 ± 119.36	1389.91 ± 8.54	1634.03 ± 297.75	1765.65 ± 228.50	1452.29 ± 76.26	1534.41 ± 32.17	1421.67 ± 96.63
Ferulic Acid	48.24 ± 1.23	53.27 ± 2.97	49.14 ± 2.03	43.00 ± 1.43	44.21 ± 3.96	47.17 ± 3.70	53.41 ± 2.94	50.23 ± 3.60	59.68 ± 20.12	45.97 ± 2.19
Sinapic Acid	0.70 ± 0.19	0.54 ± 0.02	0.45 ± 0.03	0.41 ± 0.00	0.40 ± 0.02	1.45 ± 0.11	1.09 ± 0.12	1.07 ± 0.08	1.04 ± 0.14	1.05 ± 0.03
Vanillic Acid	33.44 ± 3.47	34.49 ± 0.31	32.73 ± 1.29	31.21 ± 1.05	32.81 ± 2.48	33.95 ± 1.44	44.19 ± 1.19	43.21 ± 2.01	39.69 ± 1.65	38.99 ± 1.57
DiFA 8-5-O	0.13 ± 0.01	0.13 ± 0.01	0.12 ± 0.01	0.11 ± 0.01	0.11 ± 0.01	0.13 ± 0.01	0.12 ± 0.04	0.15 ± 0.01	0.12 ± 0.01	0.12 ± 0.01
DiFA 8-8-C	0.16 ± 0.01	0.18 ± 0.00	0.18 ± 0.00	0.16 ± 0.00	0.15 ± 0.01	0.19 ± 0.00	0.22 ± 0.01	0.20 ± 0.01	0.18 ± 0.01	0.18 ± 0.01
DiFA 8-O-4	0.59 ± 0.02	0.64 ± 0.02	0.60 ± 0.01	0.55 ± 0.03	0.56 ± 0.02	0.58 ± 0.02	0.70 ± 0.02	0.66 ± 0.03	0.60 ± 0.04	0.59 ± 0.03
DiFA 8-8-O	0.64 ± 0.02	0.71 ± 0.02	0.76 ± 0.03	0.76 ± 0.04	0.82 ± 0.04	1.00 ± 0.02	1.11 0.07	1.04 ± 0.04	1.01 ± 0.04	1.06 ± 0.07
DiFA 8-8-THF			<0.1					<0.1		
DiFA 5-5			<0.1					<0.1		
DiFA 8-5-C			<0.1					<0.1		
DiFA 8-5-DC			<0.1					<0.1		
Phenolic Amides										
4-Hydroxybenzamide	27.54 ± 3.26	30.90 ± 1.68	28.71 ± 1.99	27.43 ± 1.17	28.34 ± 3.38	27.01 ± 2.37	31.82 ± 1.86	30.66 ± 2.23	28.71 ± 2.25	30.16 ± 1.70
Vanillamide	121.36 ± 5.72	138.95 ± 4.09	128.59 ± 5.99	122.29 ± 3.42	127.89 ± 11.19	121.51 ± 6.41	136.49 ± 6.90	132.16 ± 9.41	127.81 ± 8.06	130.11 ± 7.47
Coumaroyl Amide	6167.75 ± 500.83	6145.77 ± 570.72	5596.44 ± 236.19	5697.35 ± 472.44	5637.09 ± 222.62	5772.61 ± 980.13	5974.08 ± 534.08	5448.49 ± 154.40	5441.64 ± 133.66	5354.84 ± 213.54
Feruloyl Amide	2617.75 ± 171.48	2698.47 ± 293.46	2456.97 ± 124.99	2525.05 ± 29.90	2416.35 ± 32.45	2540.59 ± 414.23	2649.23 ± 206.50	2281.34 ± 214.45	2388.26 ± 89.53	2385.31 ± 34.96
Syringamide	34.74 ± 3.73	37.40 ± 1.28	33.52 ± 2.14	32.58 ± 1.26	33.93 ± 3.50	38.72 ± 3.30	41.19 ± 2.82	37.52 ± 3.16	35.29 ± 2.70	35.84 ± 2.35
Benzamide			Not Detected					Not Detected		
Phenolic Alcohols										
4-Hydroxybenzyl Alcohol	6.62 ± 1.66	5.86 ± 1.36	8.56 ± 0.00	6.23 ± 0.92	4.90 ± 0.14	94.92 ± 5.35	84.56 ± 8.18	81.43 ± 5.57	84.96 ± 3.69	97.89 ± 6.40
Vanillyl Alcohol			Not Detected			89.60 ± 8.29	97.04 ± 5.58	91.71 ± 7.54	93.96 ± 11.16	91.55 ± 5.69
Phenolic Aldehydes										
Coniferaldehyde			<0.25					<0.25		
Syringaldehyde	4.52 ± 0.58	5.98 ± 0.37	5.61 ± 0.25	5.51 ± 0.12	5.80 ± 0.67	0.93 ± 0.08	0.96 ± 0.02	0.87 ± 0.02	0.70 ± 0.03	0.63 ± 0.02
4-Hydroxybenzaldehyde	104.04 ± 6.18	128.98 ± 3.38	122.21 ± 7.08	122.76 ± 5.05	128.80 ± 16.54			Not Detected		
Vanillin	198.92 ± 1.61	198.32 ± 5.43	196.71 ± 7.74	199.92 ± 4.93	200.90 ± 4.28	7.11 ± 0.03	8.16 ± 0.40	7.40 ± 0.32	6.71 ± 0.20	6.11 ± 0.28
Phenolics										
4-Hydroxyacetophenone	2.27 ± 0.21	2.51 ± 0.08	2.38 ± 0.10	2.30 ± 0.10	2.40 ± 0.24	2.13 ± 0.11	2.46 ± 0.08	2.36 ± 0.14	2.26 ± 0.08	2.37 ± 0.11
Acetovanillone	4.19 ± 0.29	4.34 ± 0.19	4.08 ± 0.27	3.91 ± 0.07	4.11 ± 0.49	3.81 ± 0.24	4.35 ± 0.11	4.21 ± 0.23	3.94 ± 0.17	4.15 ± 0.26
Acetosyringone	5.72 ± 0.61	6.07 ± 0.41	5.20 ± 0.16	5.29 ± 0.43	5.31 ± 0.42	5.35 ± 0.43	6.31 ± 0.16	5.62 ± 0.95	5.15 ± 0.46	5.74 ± 0.29
Other										
5-Hydroxymethylfurfural	0.63 ± 0.02	0.72 ± 0.04	0.73 ± 0.08	0.66 ± 0.09	0.84 ± 0.10	0.41 ± 0.04	0.44 ± 0.03	0.44 ± 0.04	0.43 ± 0.02	0.43 ± 0.05
Azelaic Acid	30.66 ± 1.92	32.16 ± 0.54	32.16 ± 0.56	30.29 ± 0.65	30.85 ± 1.65	27.55 ± 1.31	31.44 ± 0.85	31.42 ± 1.02	29.25 ± 0.68	30.21 ± 0.95

Error values represent standard deviations

5.3.4 Degradation Product Accumulation in Cell

Whether or not degradation products accumulate inside cells during RaBIT fermentations was determined by solubilizing the whole cell mass. The results in Table 15 show that some specific degradation products accumulated within the cell mass and some did not. This experiment could not elucidate whether accumulation was occurring in the cytosol, membranes, mitochondria, etc. No specific molecular features were apparently required for accumulation. Different acids, alcohols, and amides were found to either accumulate or not accumulate. To attempt to explain the results, acid dissociation constants were compared for each accumulating compound. If a compound has an acid dissociation constant between 5.0-6.0 (fermentation pH) and 7.0 (intracellular pH), a compound could diffuse into the cell, protonate, and then not be able to diffuse back out. No correlation of the acid dissociation constant with intracellular accumulation was found (data not shown). Without knowledge of the accumulation location, speculation on possible mechanisms for accumulation is not very useful.

Table 15 Degradation product concentrations in post-fermentation cell pellet

	Cycle 1	Cycle 3	Cycle 5
	mmol/gm DCW		
Non-accumulating degradation products			
Vanillin	2.36 ± 0.06	2.00 ± 0.13	2.37 ± 0.07
4-Hydroxyacetophenone	1.49 ± 0.04	2.60 ± 0.43	1.72 ± 0.23
Acetovanillone	3.64 ± 0.18	4.98 ± 0.64	2.89 ± 0.37
Hydroxymethylfurfural	0.00 ± 0.00	0.00 ± 0.00	0.00 ± 0.00
Gamma-Valerolactone	0.05 ± 0.05	0.03 ± 0.04	0.00 ± 0.00
Benzoic Acid	52.42 ± 7.48	69.04 ± 10.52	49.70 ± 7.54
Ferulic Acid	65.12 ± 0.92	68.59 ± 10.90	45.03 ± 1.88
Vanillic Acid	57.53 ± 1.32	58.69 ± 7.43	38.32 ± 1.56
3-Hydroxybenzoic Acid	0.55 ± 0.02	0.65 ± 0.10	0.41 ± 0.06
4-Hydroxybenzoic Acid	91.85 ± 2.02	118.15 ± 15.47	113.32 ± 2.51
Sinapic Acid	2.43 ± 0.07	2.30 ± 0.66	1.74 ± 0.12
Syringic Acid	8.49 ± 0.44	8.06 ± 1.30	6.71 ± 0.32
Azeliac Acid	73.74 ± 0.79	59.81 ± 7.96	43.71 ± 1.22
4-Hydroxybenzaldehyde	0.61 ± 0.00	0.46 ± 0.05	0.29 ± 0.03
Syringaldehyde	0.54 ± 0.01	0.39 ± 0.02	0.18 ± 0.00
4-Hydroxybenzamide	21.03 ± 0.92	21.8 ± 2.77	20.70 ± 0.69
Accumulating degradation products			
Vanillyl Alcohol	22.77 ± 0.49	41.54 ± 10.27	66.01 ± 12.76
4-Hydroxybenzyl Alcohol	23.46 ± 1.25	25.59 ± 6.63	54.33 ± 8.41
3,4-Dihydroxybenzoic Acid	4.16 ± 0.42	4.81 ± 1.13	8.26 ± 0.32
Benzamide	0.13 ± 0.02	0.48 ± 0.22	0.71 ± 0.13
Syringamide	21.02 ± 1.74	26.63 ± 5.93	30.41 ± 3.49
Vanillamide	68.32 ± 3.76	80.37 ± 17.22	101.72 ± 0.59
Ferulamide	787.27 ± 62.84	846.97 ± 194.85	Over Limit

Error values represent standard deviations

Figure 27 shows a potential correlation between increasing intracellular degradation product concentrations and the final xylose concentration. These results, while strongly suggestive of this relationship, do not prove conclusively that accumulation of degradation products causes decreasing xylose consumption upon cell recycle. To better understand this potential relationship, experiments using synthetic hydrolysate were performed.

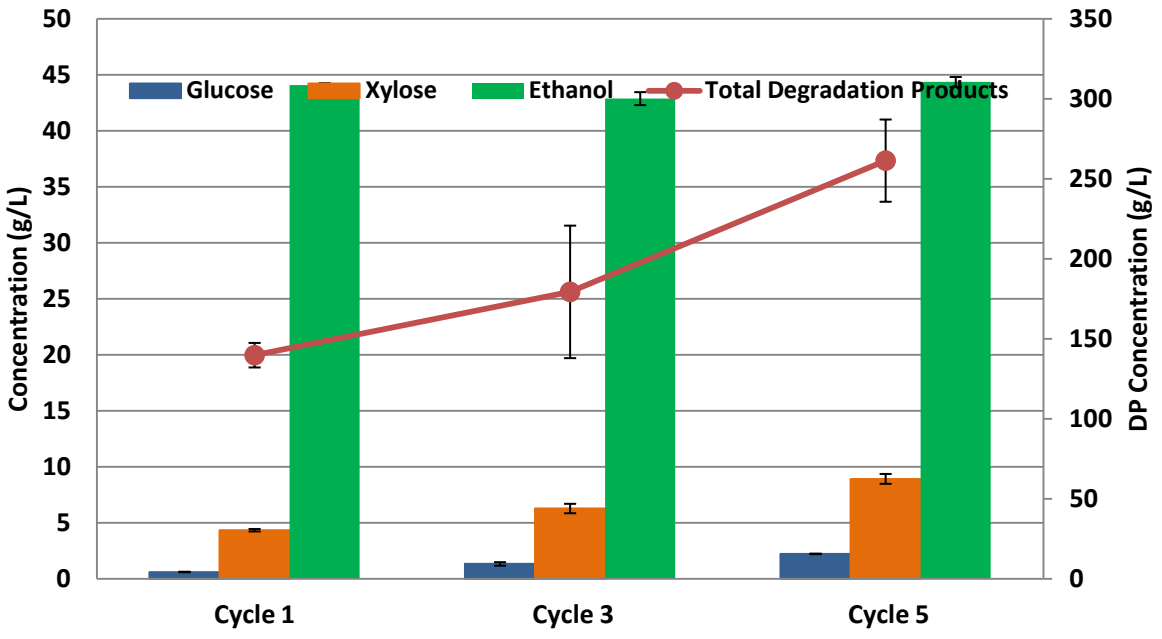

Figure 27 Degradation product accumulation and fermentation results for multiple RaBIT cycles. Final glucose (blue), xylose (orange), and ethanol (green) concentrations are shown after three 23 h RaBIT fermentations. Concentration of accumulating degradation products in the cell pellet are also shown (red circles). Error bars represent standard deviations.

5.3.5 Synthetic Hydrolysate Experiments

Synthetic hydrolysate was used to further investigate the effect of degradation products on RaBIT fermentations. The original synthetic hydrolysate recipe was developed for AFEX corn stover as outlined in Tang et al. (2015). On going work on synthetic hydrolysate yielded the recipe used for these experiments and is outlined in Table 27 in Appendix B. Not all degradation products were added. The degradation product concentrations found in 7% glucan loading AFEX corn stover hydrolysate are listed in Table 27 in Appendix B and were used to formulate synthetic hydrolysate at various degradation product concentrations (0x, 0.5x, 1x, and 2x). The concentration of degradation products normally found in 7% glucan loading AFEX corn stover hydrolysate was designated as 1x degradation products. Synthetic hydrolysate designated with 0x contained no degradation products. Synthetic hydrolysate designated with

0.5x and 2x degradation products contained half and double the normal concentration of degradation products, respectively.

The first synthetic hydrolysate experiment compared different degradation product concentrations. For this experiment, degradation production concentrations of 0x, 0.5x, 1x, and 2x in relation to 7% glucan loading AFEX hydrolysate concentrations were added to the synthetic hydrolysate. The results in Figure 28 showed that eliminating degradation products (0x) in hydrolysate allowed for complete xylose consumption and no cell performance decrease during RaBIT fermentations. When degradation product concentrations were increased to half the normal concentration (0.5x), residual xylose doubled from ~0.6 g/L to ~ 1.2 g/L. With the normal level of degradation products (1x), xylose consumption began to decrease upon cell recycle. The results for synthetic hydrolysate with 1x degradation products (Figure 28) were also very comparable to RaBIT fermentations in AFEX hydrolysate (Figure 29). The 1x degradation products synthetic hydrolysate did show better initial xylose consumption when compared to AFEX hydrolysate (2.71 g/L residual xylose vs 5.31 g/L residual xylose, respectively). However, the performance decrease after 5 fermentation cycles was more pronounced with 1x degradation product synthetic hydrolysate compared to AFEX hydrolysate (9.47 g/L residual xylose vs 8.28 g/L residual xylose, respectively). Increasing degradation product concentrations to 2x in synthetic hydrolysate, caused poor performance.

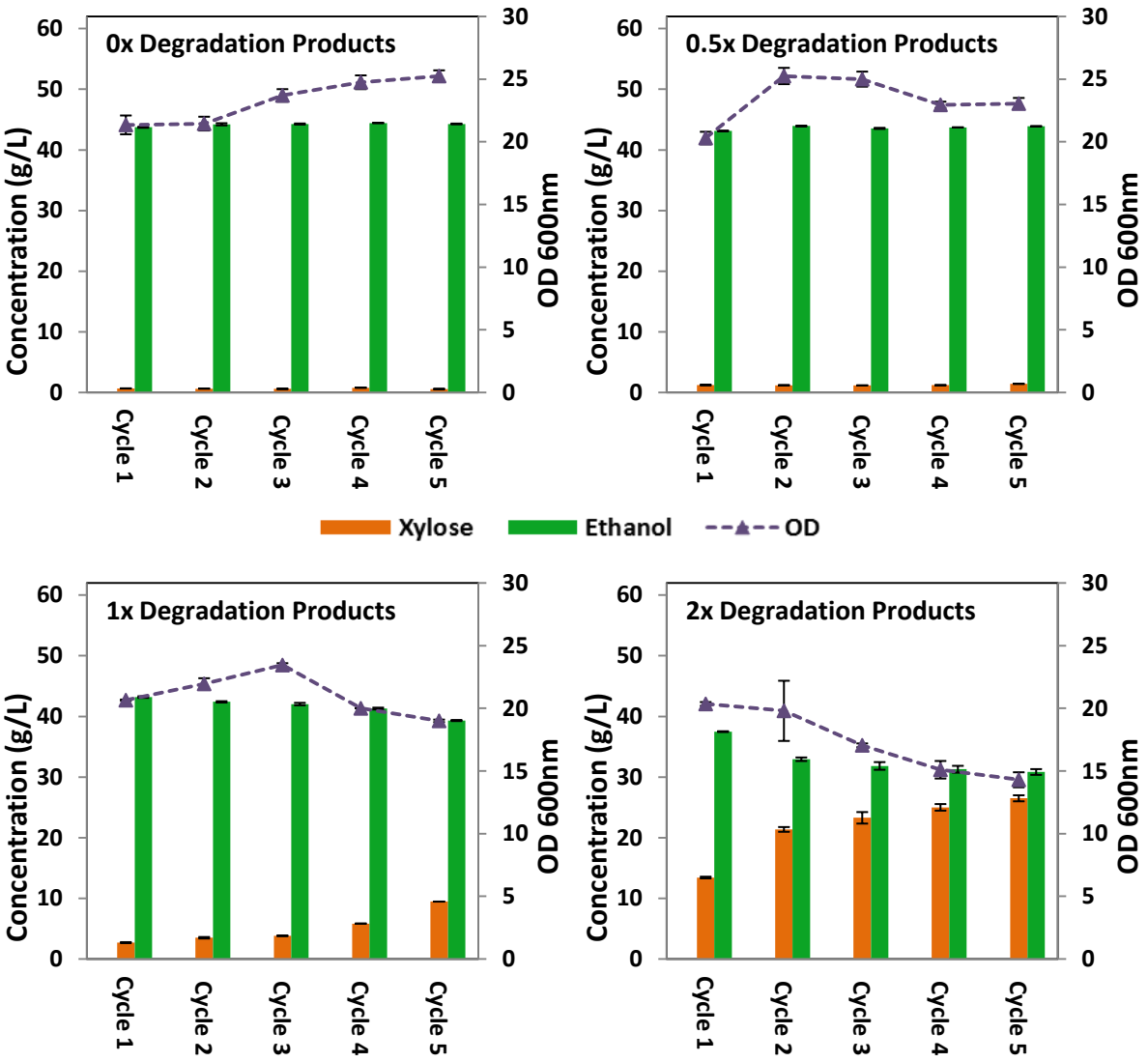

Figure 28 Synthetic hydrolysate experiments for varying concentration of degradation products. Concentration multipliers are relative to degradation product concentrations in 7% glucan loading AFEX hydrolysate. Concentrations for xylose (orange) and ethanol (green) along with OD (purple triangles) are reported. Original glucose and xylose concentrations were 60 g/L and 34 g/L, respectively. All glucose was consumed during each cycle. Error bars represent standard deviations.

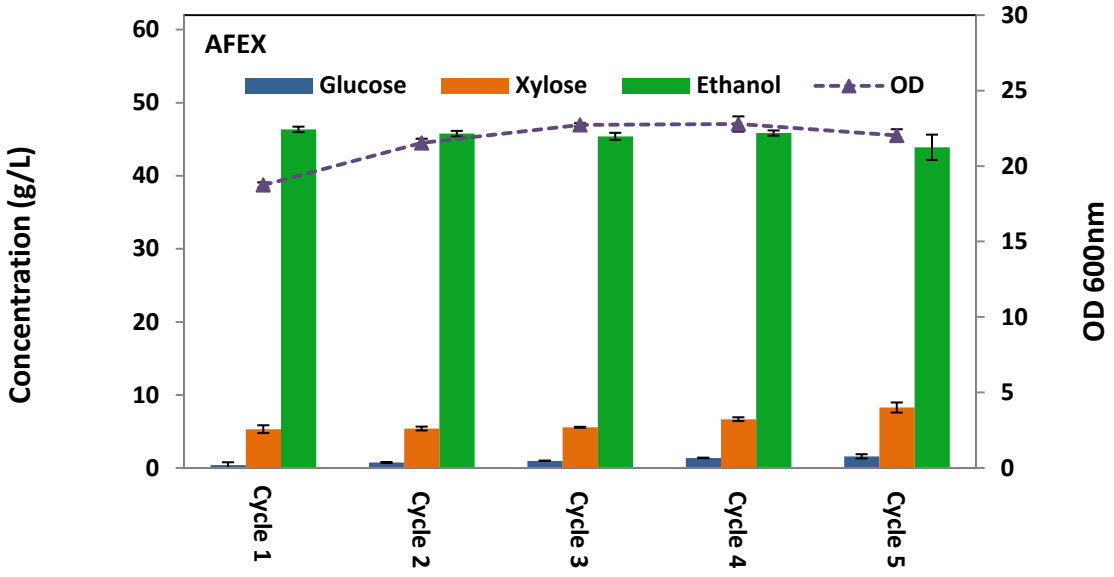

Figure 29 RaBIT fermentation using 7% glucan loading AFEX hydrolysate. Concentrations for glucose (blue), xylose (orange) and ethanol (green) along with OD (purple triangles) are reported. Original glucose and xylose concentrations were 59 g/L and 32 g/L, respectively. Error bars represent standard deviations

Accumulating degradation products and non-accumulating degradation products were also compared (Figure 30). The results showed that the accumulating degradation products were responsible for the decrease in xylose consumption. However, this was expected as accumulating degradation products represent over 95% of the total degradation product concentration.

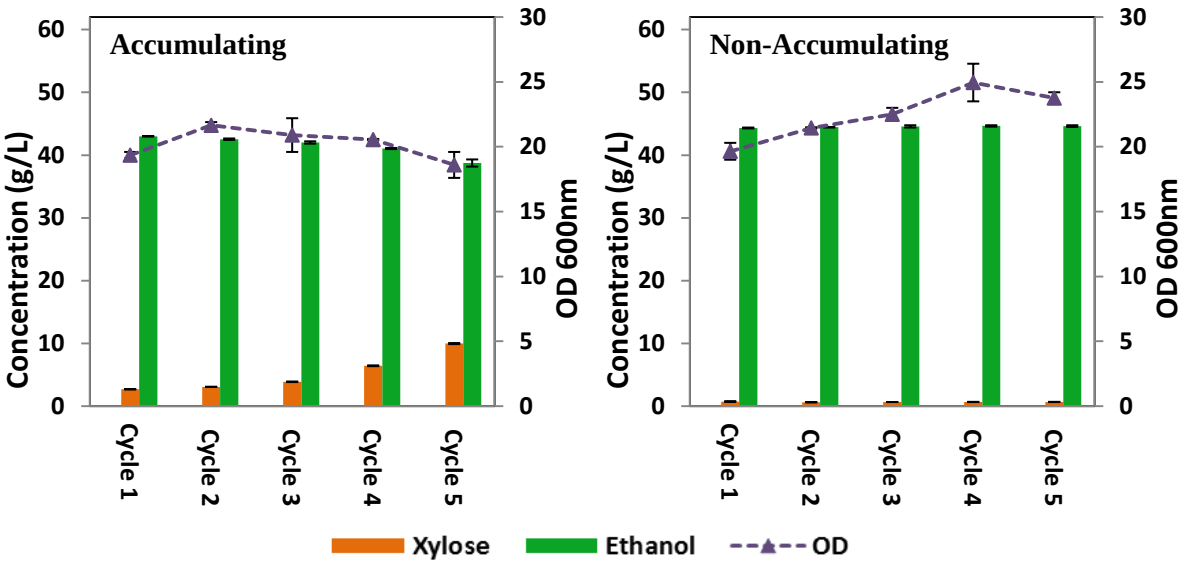

Figure 30 Synthetic hydrolysate experiments for accumulating vs non-accumulating degradation products (DPs). Concentrations for xylose (orange) and ethanol (green) along with OD (purple triangles) are reported. Original glucose and xylose concentrations were 60 g/L and 34 g/L, respectively. All glucose was consumed during each cycle. Error bars represent standard deviations.

Further experiments are needed to completely elucidate the effects of degradation products in RaBIT fermentations. It does appear likely that degradation production accumulation within cells is the cause of decreased xylose consumption upon cell recycle. Determining the how and how much each major degradation product accumulates is important and should be pursued. Fluorescent tagging of degradation products could help determine the location of accumulation within the cell.

5.4 Conclusions

Effect of degradation products was investigated in this chapter. Degrdation product concentrations between RaBIT cycles do not vary between RaBIT enzymatic hydrolysis cycles; thus enzymatic hydrolysis is not releasing different amounts of degradation products with different hydrolysis cycles. Chemical genomics was used to verify that the biological fingerprint between cycles was also unchanged. Quantification of degradation products after fermentation

showed that aldehyde detoxification by the cell population did not decrease over RaBIT fermentation cycles. Further work showed that certain degradation products accumulate within the cell during RaBIT fermentation cycles. Synthetic hydrolysate experiments showed that the presence of degradation products is the primary cause of decreased xylose consumption during RaBIT fermentations. The work was not able to conclusively link the accumulating degradation products to the decrease in xylose consumption between cycles, but this relationship is likely.

CHAPTER 6: PROCESS CHANGE INVESTIGATION

Abstract

Significant cell death during xylose consumption (Chapter 4) and accumulation of degradation products within the cell (Chapter 5) were previously identified as reasons for the decrease in xylose consumption capability of recycled cell populations within the RaBIT process. To overcome these issues, the following process changes were implemented: shortening fermentation time from 23 h to 11 h, fed-batch hydrolysate addition, and separation of cells based on age. These process changes allowed us to investigate the benefits of producing excess cell mass that could be sold as a biorefinery co-product. As a result, the first RaBIT process was created where no decrease in xylose consumption was observed over a total of 10 cycles. It was also discovered that generation of excess cell mass does not provide economic benefit.

6.1 Introduction

This chapter reports studies of process changes to improve cell recyclability and performance in RaBIT process fermentations. Chapter 4 showed that cell death occurs during the xylose consumption phase during RaBIT fermentations. Chapter 5 showed that accumulation of pretreatment degradation products within the cells was potentially the major cause for decrease in xylose consumption after recycling. Three process changes were implemented to solve these issues. Fermentation times were shortened from 23 h to 11 h to reduce cell death during the xylose consumption phase and to reduce degradation product accumulation within the cells. Fed-batch hydrolysate addition was implemented to introduce sugar during the fermentation phase when previously only xylose was consumed. Finally, cell settling was used to facilitate cell separation by age.

6.2 Materials and Methods

6.2.1 Lab Scale Biomass and Pretreatment

Great Lakes Bioenergy Research Center (GLBRC) corn stover was used for lab scale pretreatment. The corn (Pioneer 36H56) was planted and harvested during 2010 at Arlington Agricultural Research Station in Columbia County, WI. The biomass was pretreated using the AFEX process. AFEX pretreatment was performed as previously described in the literature using a 5 gallon reactor (Balan et al., 2009). AFEX pretreatment conditions were as follows: 1:1 ammonia to biomass ratio, 60% moisture, 100 ^{o}C, and 30 min. reaction time. Composition analysis following the method published by Sluiter et al. (2010) showed the glucan, xylan, acid insoluble lignin, and ash contents as 31.4%, 18.6%, 13.08%, and 13.39%, respectively. The pretreated corn stover was stored at 4 ^{o}C. Lab scale biomass was used for all experiments except for experiments in the Ten Cycle Mass Balances section.

6.2.2 Pilot Scale Biomass and Pretreatment

The corn stover was harvested from Hamilton County, Iowa, and baled by Iowa State University in October, 2011. Further details on the corn stover used can be found in Campbell et al. (2013). AFEX was performed in a pair of 450 L packed-bed reactors. The complete process description for the packed-bed reactors is given in Chapter 3. In brief, ammonia vapor was added at a 0.6 g/g biomass ratio to bed previously heated to 100˚C by steam injection. The biomass was allowed to sit for 30-150 minutes with no external heating before releasing the ammonia. Residual ammonia was removed by introducing low pressure steam at the top of the reactor allowing ammonia vapor to escape from the bottom. After pretreatment, the biomass was pelletized to increase bulk density. The pelleting process was performed as described in Bals et al. (2013) using a Buskirk Engineering PM810 flat die pellet mill. After pelleting, the biomass

was dried in a convection oven at 50 °C. The composition was determined as 34.8% glucan, 18.8% xylan, 3.2% arabinan, and 12.2% acid insoluble lignin. The pellets were stored at room temperature. Pilot scale pellets were used for the experiments performed for the Ten Cycle Mass Balances section.

6.2.3 Microorganism and Seed Culture Preparation

Saccharomyces cerevisiae GLBRCY128 was used for this study having previously been genetically modified and adapted by Dr. Trey K. Sato at the University of Wisconsin-Madison. Xylose isomerase and xululokinase genes were introduced to facilitate xylose utilization.

Seed cultures were prepared from glycerol stocks stored at -80 °C. Seed culture media contained 100 g/L dextrose, 25 g/L xylose, 20 g/L tryptone, and 10 g/L yeast extract. Erlenmeyer flasks (250 mL) containing 100 mL of seed culture media were inoculated with 0.1 OD_{600}. The cultures were incubated at 30 °C and 150 RPM in shaker incubators under microaerobic conditions for 22 h. After 22 h, fresh seed culture media was inoculated with 1% of the first seed culture medium and incubated under the same conditions for another 22 h.

6.2.4 RaBIT Enzymatic Hydrolysis

RaBIT enzymatic hydrolysis at 7% (w/w) glucan loading was performed in 4 L Chemglass glass jacketed reactors using a cycle 1 total reaction mass of 2000 gm (biomass, water, enzymes, and acid). The first cycle enzyme cocktail was 14.7 mg protein/g glucan Cellic CTec3 and 14.9 mg protein/g glucan Cellic Htec3 (Novozymes). Enzyme cocktail protein concentrations were provided by Novozymes. Jacket temperature was set at 50 °C and the impellor was maintained on the lowest setting (~200 RPM). The pH was maintained at 5.0 using 12.1 M hydrochloric acid. After 23 h, the hydrolysate slurry was centrifuged at 6200 RCF. The

hydrolysate supernatant was poured off and the solids were recycled back into the next enzymatic hydrolysis cycle. Enzyme loadings were reduced to 60% and 50% of the original loading for cycle 2 and cycles 3+, respectively. Starting at the end of Cycle 4, 25% of the solids were removed. These solids were discarded or used for the RaBIT SSCF when performing the mass balance.

6.2.5 RaBIT SSCF

Wet solids were removed from the RaBIT enzymatic hydrolysis process to prevent accumulation, and were used in a SSCF process to perform mass balance experiments. Solids removed were assumed to contain 60% moisture based on previous testing (40% solids). Water was added to dilute the slurry to 30% solids. Enzymes were then added on a solids basis of 0.540 mg protein/g solids and 0.547 mg protein/g solids for CTec3 and HTec3, respectively. The slurry was incubated for 6 h at 50 °C. After 6 h, the pH was adjusted to 6.0 and the slurry cooled to 32 °C. An inoculum of 0.1 g/L DCW was added using a cell pellet and assumed slurry density of 1 g/mL. Fermentation was then conducted for 66 h. The process was performed in the 4L Chemglass reactors using the lowest RPM setting.

6.2.6 RaBIT Fermentations

Fermentations were performed in either 0.5 L Sartorius bioreactors using a 400 mL final hydrolysate or 125 mL Erlenmeyer flasks using a 50 mL final hydrolysate volume. The reaction vessel used is noted in figure legends. Cell pellets after centrifugation of seed cultures were used to inoculate first cycle fermentations. Inoculation size was 10 g/L dry cell weight (DCW) concentration for 23 h RaBIT fermentations and 17.5 g/L DCW concentration for 11 h RaBIT fermentations determined from OD_{600} vs. DCW concentration plots. Initial pH was adjusted to

6.0 using 10 M potassium hydroxide. Fermentation cycles were conducted for 23 h or 11 h at 32 °C. Bioreactor fermentations were mixed at 300 RPM using a turbine impeller, while shake flask fermentations were mixed at 150 RPM using a shaking incubator. After each cycle, the fermentation broth was centrifuged at 3250 RCF and the cell pellet was recycled to the next fermentation cycle.

When settling cells using a separatory funnel, the whole fermentation broth was transferred to 60 mL (for shake flask) or 500 mL (for bioreactor) separatory funnels and allowed to settle for 20 minutes. Fractions were removed from the bottom and collected in centrifuge tubes based on volume graduations marked on the side. All fermentation experiments were performed with at least 2 biological replicates.

6.2.7 Fed-Batch Methods

When using glucose as the feed media, fed-batch addition was performed using a syringe and 500 g/L glucose solution. Hydrolysate fed-batch additions were made using an Ismatect peristaltic pump (C.P. 78017-10). The pump had four channels that used 1.3 mm internal diameter Tygon tubing purchased from Cole Parmer. Feed rate, volume, pump time, and pause time could be controlled. For standard fed-batch feeds, the volume was dispensed over time intervals. For continuous fed-batch feeds, a specific feed rate was applied for the feeding period.

6.2.8 HPLC Analysis

Glucose, xylose and ethanol concentrations were analyzed by HPLC using a Biorad Aminex HPX-87H column. Column temperature was maintained at 50^{o}C. Mobile phase (5 mM H_2SO_4) flow rate was 0.6 mL/min.

6.2.9 Cell Population Analysis

OD was measured 600_{nm} using a Beckman Coulter DU 720 spectrophotometer. Samples were diluted to stay within a raw reading of 0.1-1. OD measurements were initially taken for each medium before inoculation and subtracted from later readings as a "blank."

Cell viability was measured by methylene blue staining at 0.5% concentration. After staining, images of microscope slides were taken using a Motic B3 Professional Series microscope utilizing a 100x oil immersion lens and stored on a computer. The cells were counted using the digital images. Cell size was determined using the same images utilizing Motic Images Plus to measure the area of viable cells. The software allowed for calibration using a calibration slide.

6.2.10 Mass Balance

Mass balances were performed using pilot scale AFEX treated corn stover. The RaBIT enzymatic hydrolysis was performed over 5 cycles. The hydrolysate produced was stored at 4 °C in preparation for fermentation. Ampicillin was added during enzymatic hydrolysis at 50 mg/L in preparation for the long storage period.

The excess solids generated during cycles 4 and 5 of the RaBIT enzymatic hydrolysis were used in a one step SSCF experiment. A mass balance was then completed on the product slurry. The mass balance procedure quantified monomeric glucose, xylose, and ethanol in the

liquid by HPLC. Oligomeric glucose and xylose were quantified using acid hydrolysis as decribed in Sluiter et al. (2010). Glucan, xylan, lignin, and ash were quantified in the solids using composition analysis as described above. Liquid retained in the solids were accounted for by dilution and subsequent concentration change. Solids were washed 3 times with distilled water before drying to remove residual sugars. The solids were dried in a 90^{o}C oven until the mass was constant.

RaBIT fermentation mass balances were performed using 11 h fermentation cycles with fed-bath hydrolysate addition. Initial hydrolysate was 70% of the final volume with the other 30% fed consistently between 2 and 10 h. After each cycle, the cell population was recycled back at 100% or 90% with the bottom 10% removed after settling using a separatory funnel, depending on the experiment. The fermentation broth produced was weighed and its density recorded. Monomeric and oligomeric glucose and xylose along with ethanol were quantified for the resulting broth. Any removed cells were dried in 90^{o}C oven before being weighed.

6.3 Results and Discussion

6.3.1 High Resolution Sampling

A high resolution sampling experiment was conducted to elucidate important time points or kinetics within RaBIT process fermentations. Previous work detailed in Chapter 4 showed a similar comparison between sugar concentrations, ethanol concentration, and cell viability measured by capacitance. A major conclusion from this previous work was that the viable cell population decreased during the xylose consumption phase. Furthermore, the peak cell viability after the growth phase steadily increased over the first 4 cycles, while the 5th cycle peak cell viability stayed similar to the 4th cycle.

The results in Figure 31 show that exponential phase, stationary phase, and death phase are highly dependent on sugar concentrations. Exponential phase (cell growth period) exists only when glucose is present in each cycle. A stationary phase generally exists during the initial and relatively fast xylose consumption phase. Finally during the slow xylose consumption phase, the viable cell concentration drops rapidly. Time points were also established for glucose or hydrolysate feeding for future experiments detailed in this chapter.

The decrease in overall cell performance (and not just xylose consumption) upon recycle is readily apparent from this experiment. While 5 cycles was not enough to show a drastic difference in final xylose consumption, consumption and product rates showed a steady decrease. This was most apparent for glucose consumption rates. Surpisingly, 6 h was required for complete glucose utilization during the fifth cycle, while only 3.5 h was required for complete glucose utilization during the first cycle. Glucose consumption was previously assumed to be unaffected after cell recycling during the RaBIT fermentation process.

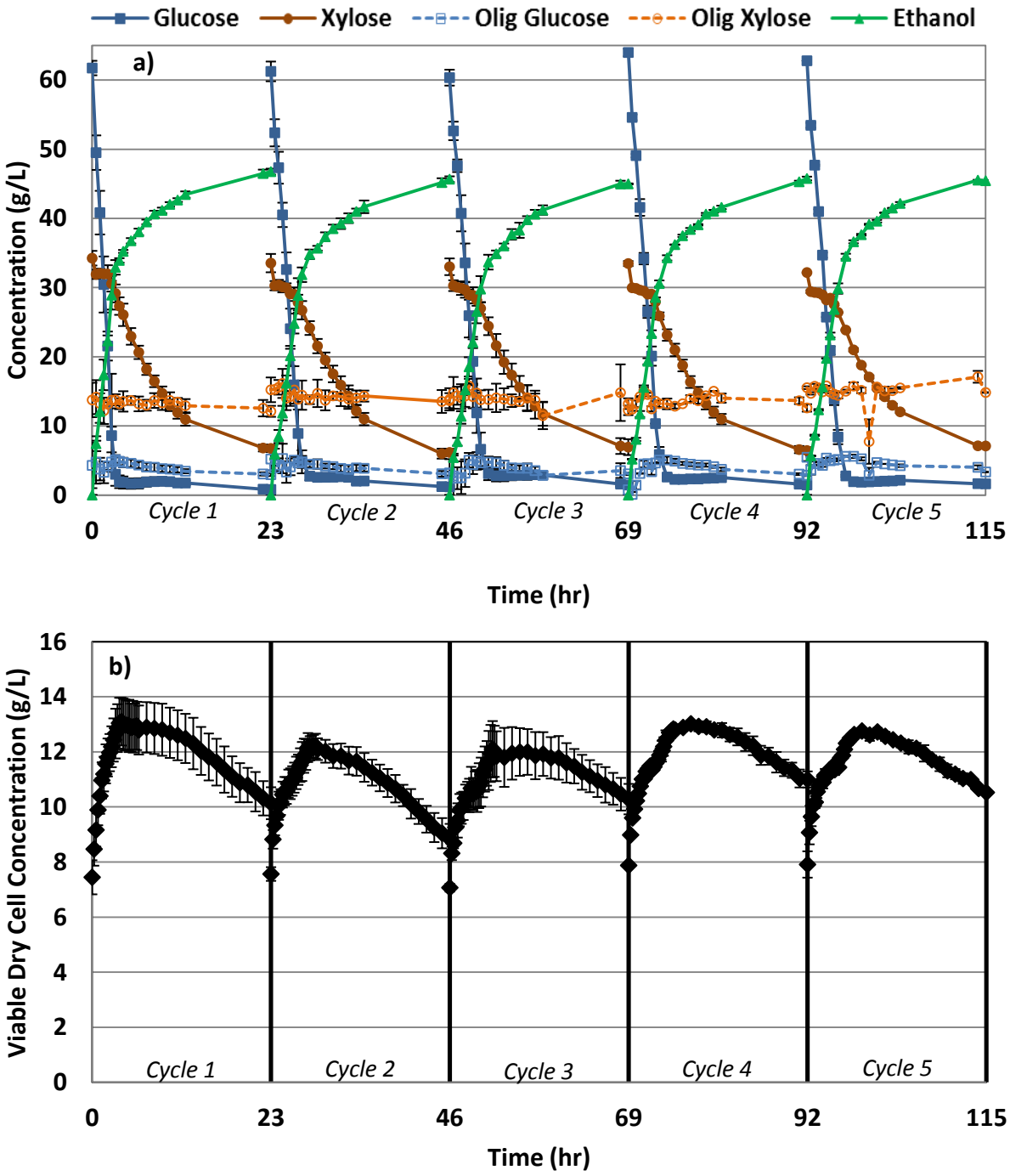

Figure 31 High resolution RaBIT fermentation sampling performed in bioreactors. Final concentrations are shown for glucose (dark blue closed squares), xylose (dark orange closed circles), ethanol (green closed triangles), oligomeric glucose (light blue open squares), and oligomeric xylose (light orange open circles) in a). Viable dry cell concentration measured by capacitance is shown b). Error bars represent standard deviations.

6.3.2 Mass Transfer Analysis

Cell death during the xylose consumption phase could be the result of two different mechanisms: not enough sugar/energy to sustain the population and/or mass transfer limitations due to cell flocculation. Mass transfer analysis for xylose diffusion and consumption was performed on the cycle 1 fermentation results seen in Figure 31 to determine if mass transfer limitations were present. The first step was determining if mass transfer or the reaction rate was the limiting factor during the xylose consumption phase. The Weisz-Prater Criterion was used to identify which factor was limiting (Equation 1). The Weisz-Prater Criterion states that for C_{wp} <<1 no diffusion limitations are present, while for C_{wp}>>1 diffusion limits dominate the system. The calculation uses the observed reaction rate per catalyst mass ($-r_a'(obs)$ [=] mol/g catalyst/s), and was obtained from specific xylose consumption rates taken from the high resolution sampling experiment. For this work, the catalyst is represented by the dry cell rate. During initial xylose constumption (~2 h), the observed reaction rate was -6.0x10^{-7} mol/g DCW/s. The cell density (ρ_c) was assumed as 1135 g/L (Bryan et al., 2009). The average cell radius (R [=] μm) was estimated as 37.6 μm using microscopic images of Y128 flocs. Initial surface concentration (C_{xs} [=] g/L) was taken from the HPLC results in Figure 31a. Effective diffusivity (D_e [=] μm^2/s, Equation 2) was calculated based on the following assumptions from the literature and microscopic images obtained from Y128 flocs. Diffusion of xylose in water (D_{xw} [=] μm^2/s) was found to be 0.073 μm^2/s (Ueadaira and Ueadaira, 1969). The porosity of a yeast floc (φ_p) was assumed as 0.5 (Teixeira and Mota, 1990). The constriction factor (σ_c) was assumed as 0.8. Tortuosity was calculated as 1.285 using estimations from microscopic images. After calculation, the effective diffusivity was found to be 0.0375 μm^2/s.

$$C_{wp} = \frac{-r_a'(obs)\rho_c R^2}{D_e C_{As}} \qquad (1)$$

$$D_e = \frac{D_{AB}\varphi_p \sigma_c}{\tau} \qquad (2)$$

The initial C_{wp} at the beginning of the xylose consumption phase was calculated as 0.80 mol/g catalyst. This value is neither much greater nor much less than 1. It was therefore assumed that some mass transfer limitations are present during RaBIT fermentation. Sensitivity analysis was then performed based on floc radius (Table 16). Measurements of the assume yeast floc radius were based on microscope images performed using non-mixed samples as in-situ measurement was not possible due to the equipment available so the true C_{wp} value may be much different from the assumed value. The sensitivity analysis showed that even up to a floc size of 1000 μm (2660% compared to estimated value [37.6 μm]) diffusion limitations are likely present but don't dominate the fermentation.

Table 16 Weisz-Prater Criterion calculations for various radii

	Theoretical Floc Radius (μm)							
	10	**25**	**37.6**	**50**	**100**	**250**	**500**	**1000**
C_{wp}	0.06	0.35	0.80	1.41	5.63	35.18	140.70	562.92

With diffusion limitation a concern, effectiveness factors were derived from the experimental data. Effectiveness factors (E_f) are normally calculated for solid, porous chemical catalysts and not on microbial catalysts. Ideally, a non-flocculating relative of the Y128 yeast strain would be used as a comparison. Data from a non-flocculating relative was not available. Therefore, values were derived from the data presented in Figure 31. The initial xylose consumption rate was assumed as non-diffusion limiting because of the constant xylose consumption rate observed from approximately 2 to 4 h. Ethanol inhibition was assumed

constant through out the xylose consumption phase. The difference in ethanol concentration, before and after xylose consumption, was about 10 g/L. Furthermore, ethanol tolerance in *Saccharomyces cerevisiae* is around 120 g/L, or approximately 3 fold higher than the levels experienced in the RaBIT process. Equation 3 tracks xylose concentration (C_x [=] g/L) over time represented in hours. The reaction constant (k_x [=] L/g cell/h) was approximated at -0.0105 using data from Figure 31. Viable cell concentration (X[=] g/L) was modelled using Equation 4. To calculate estimated effectiveness factors, the percent maximum rate was compared to various effectiveness factor models. The effectiveness factor model was fit by minimizing the sum of the square of the errors. The chosen model is shown in Equation 5. The minimum xylose concentration (C_{xmin} [=] g/L) was required as xylose consumption limits are present with varying levels of degradation products as previously shown in Chapter 5. For cycle 1, the C_{xmin} was estimated at 5 g/L. Coefficients a and b were determined to be 1 and -0.202, respectively.

$$\frac{d(C_x)}{d(t)} = -k_x C_x X E_f \qquad (3)$$

$$\frac{d(X)}{d(t)} = -0.1 \qquad (4)$$

$$E_f = a(1 - exp^{(b - C_{xmin})}) \qquad (5)$$

Results of the effectiveness factor PolyMath simulation are shown in Figure 32. The modeled xylose profile compares well to the experimental profile (Figure 32a). The effectiveness factor decreased as the xylose concentration decreased. At the end of the cycle, the effectiveness factor was about 0.7. It is possible then that up to 30% of the cells in the cell floc were not consuming xylose due to diffusion limitations. These results showed that cell death may be related to diffusion limitations in the cell flocs.

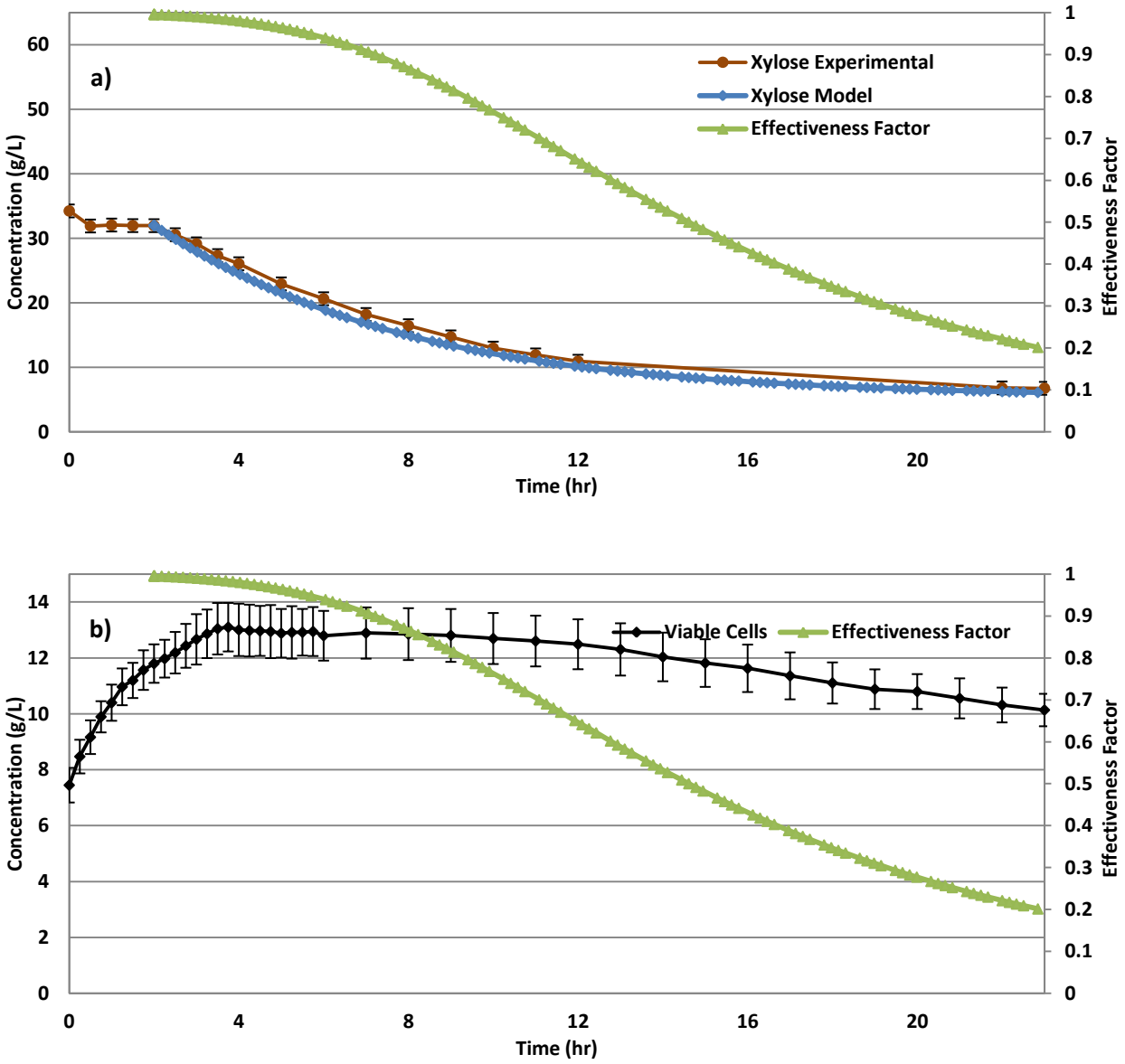

Figure 32 PolyMath xylose consumption modelling. a) Experimental and modelled xylose profiles compared with effectiveness factor. b) Viable cell concentration profile compared to effectiveness factor. Error bars represent standard deviations.

To help confirm these results, a Weisz-Prater criterion profile was calculated again using the effectiveness factor PolyMath modeling for the entire xylose consumption phase. The new equation is shown in Equation 5, which replace the observed reaction rate with the reaction rate model from Equation 3. The results are shown in Figure 33. Unexpectedly, the Weisz-Prater criterion decreased over time. This is due to the reaction rate decreasing faster than the

concentration. This result decreases the likelihood that diffusion limitation is an issue instead suggesting that other factors such as cell health concerns, cell age concerns, or the accumulation of degradation products over time are causing cell death.

$$C_{wp} = \frac{-k_x C_x X E_f \rho_c R^2}{D_e C_{xs}} \qquad (5)$$

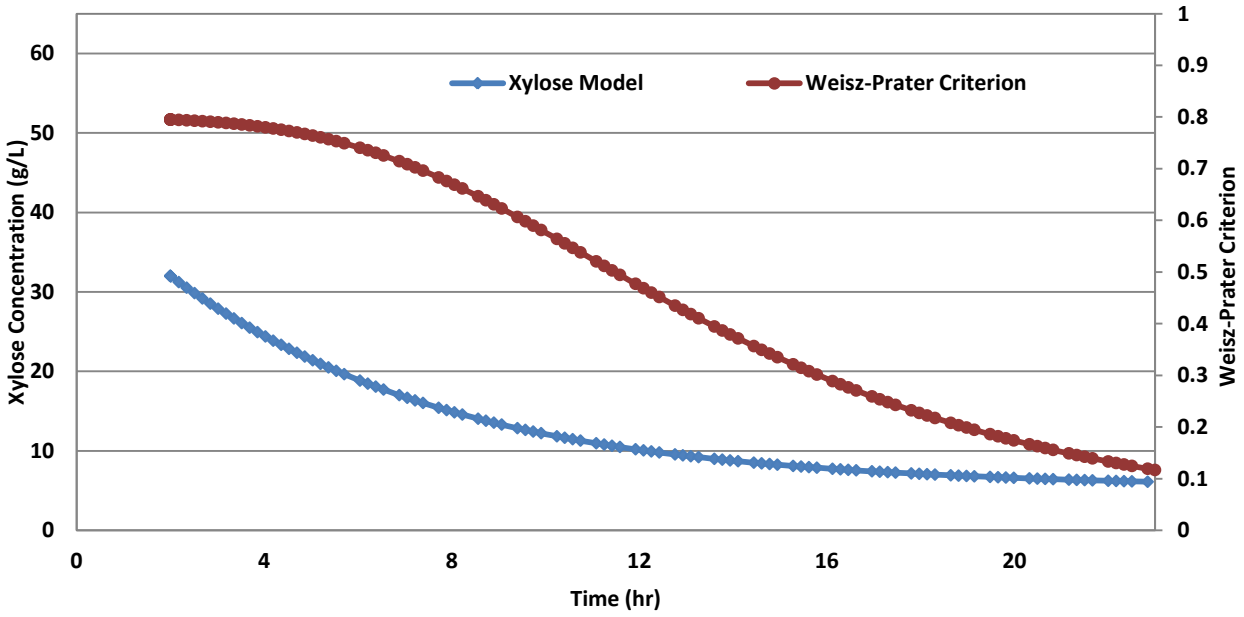

Figure 33 Weisz-Prater Criterion time profile with modelled xylose profile.

6.3.3 Shortening the Fermentation Process

Shortening fermentation cycle time from 23 h to 11 h was the first process change tested. Shortening the yeast cell residence time had the potential to correct two issues. The first was reducing cell death by shortening the xylose consumption phase. The second was reducing the time available for pretreatment degradation products to accumulate inside the cell.

First, appropriate initial cell loadings for an 11 h RaBIT fermentation were investigated. Results of this investigation are shown in Figure 34. As expected, increasing the inoculum size resulted in increased xylose consumption and ethanol production. Increasing the inoculum from

17.5 to 20 g/L DCW resulted in no significant difference in xylose consumption and ethanol production. For this reason, 17.5 g/L DCW concentration was chosen as the optimum for investigating an 11 h RaBIT fermentation process.

Three cycles were performed to see if the initial inoculum could be decreased. Results showed that it may be possible to lower the initial cell loading and allow the cell population to build up over RaBIT cycles to a level comparable to a higher initial cell loading. Reducing the inoculum to 10 g/L DCW only decreased ethanol yield by ~1% over 10 cycles if ethanol production between the two cases was assumed the same for cycles 4 – 10.

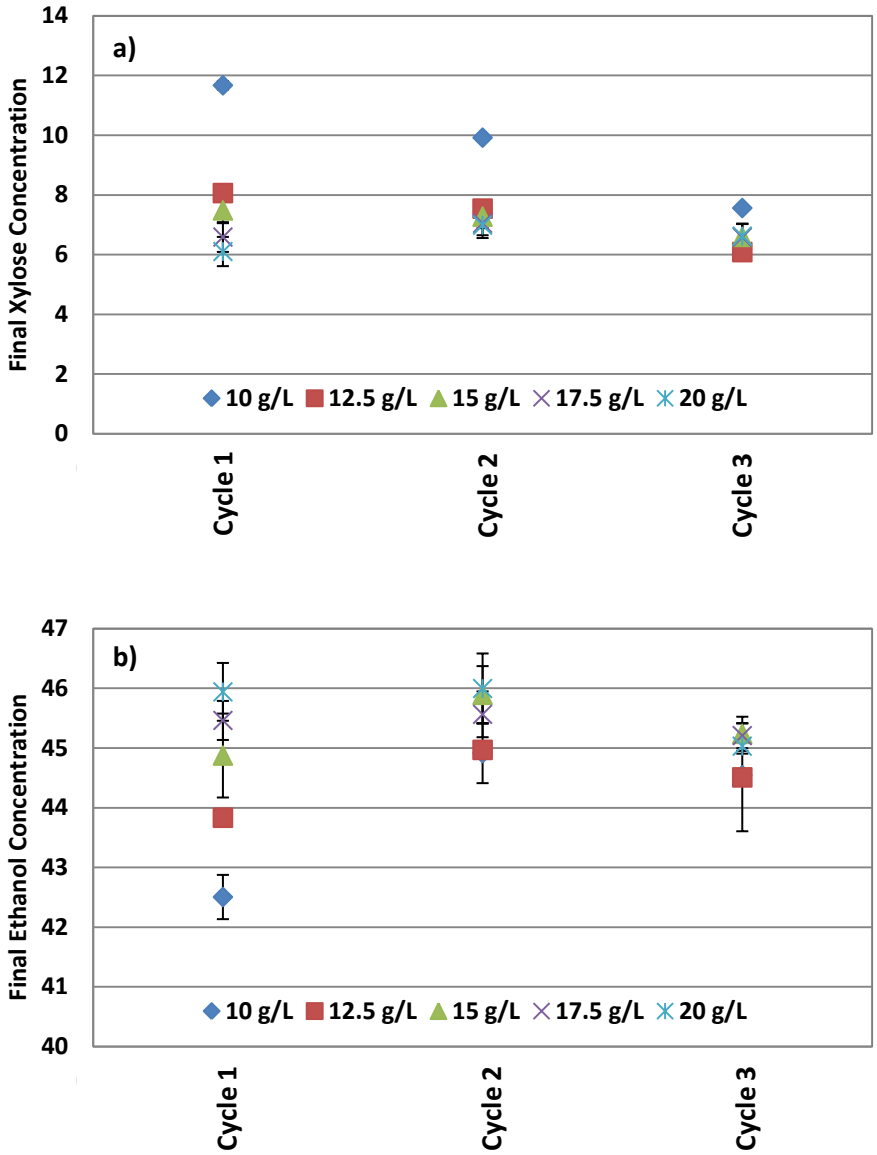

Figure 34 Fermentation results for different initial cell concentrations for 11 h RaBIT fermentation cycles performed in shake flasks. Results for a) xylose and b) ethanol are shown. Error bars represent standard deviations and are present for all data points but may be hidden by the symbol.

A comparison was performed between 23 h and 11 h fermentation cycle shake flask experiments. Results in Figure 35 show that shortening the fermentation cycles reduced the decrease in xylose consumption upon recycle. The difference between the fifth and first cycle xylose consumption were 6.2 g/L and 0.7 g/L for the 23 h and 11 h processes, respectively. The

final cycle xylose concentrations were 11.2 g/L and 7.6 g/L for the 23 h (5 cycles) and 11 h (10 cycles) respectively.

Improvement was also observed when comparing bioreactor data although the difference was less significant (Figure 31 and Figure 36). The differences between the fifth and first cycle xylose consumption were 1.2 g/L and -0.9 g/L for the 23 h and 11 h processes, respectively. However, the average xylose consumption was 1.34 g/L lower in the 11 h process compared to the 23 h process resulting in a 1.28 g/L lower average ethanol production for the 11 h process. The viable cell concentration profile for the 11 h process (Figure 36b) shows improvement over the 23 h process (Figure 31b). For the 11 h process, the peak viable cell concentration for every subsequent cycle was higher than the peak viable cell concentration for cycle 1. For the 23 h process, the opposite was true as the peak viable cell concentration for every subsequent recycle was lower than the peak viable cell concentration for cycle 1.

In conclusion, the 11 h process performed as designed by reducing both the decrease in cell performance after recycle and reducing cell death during the xylose consumption phase. Shortening the fermentation did, however, negatively affect the overall xylose consumption and ethanol production when performed in bio-reactors.

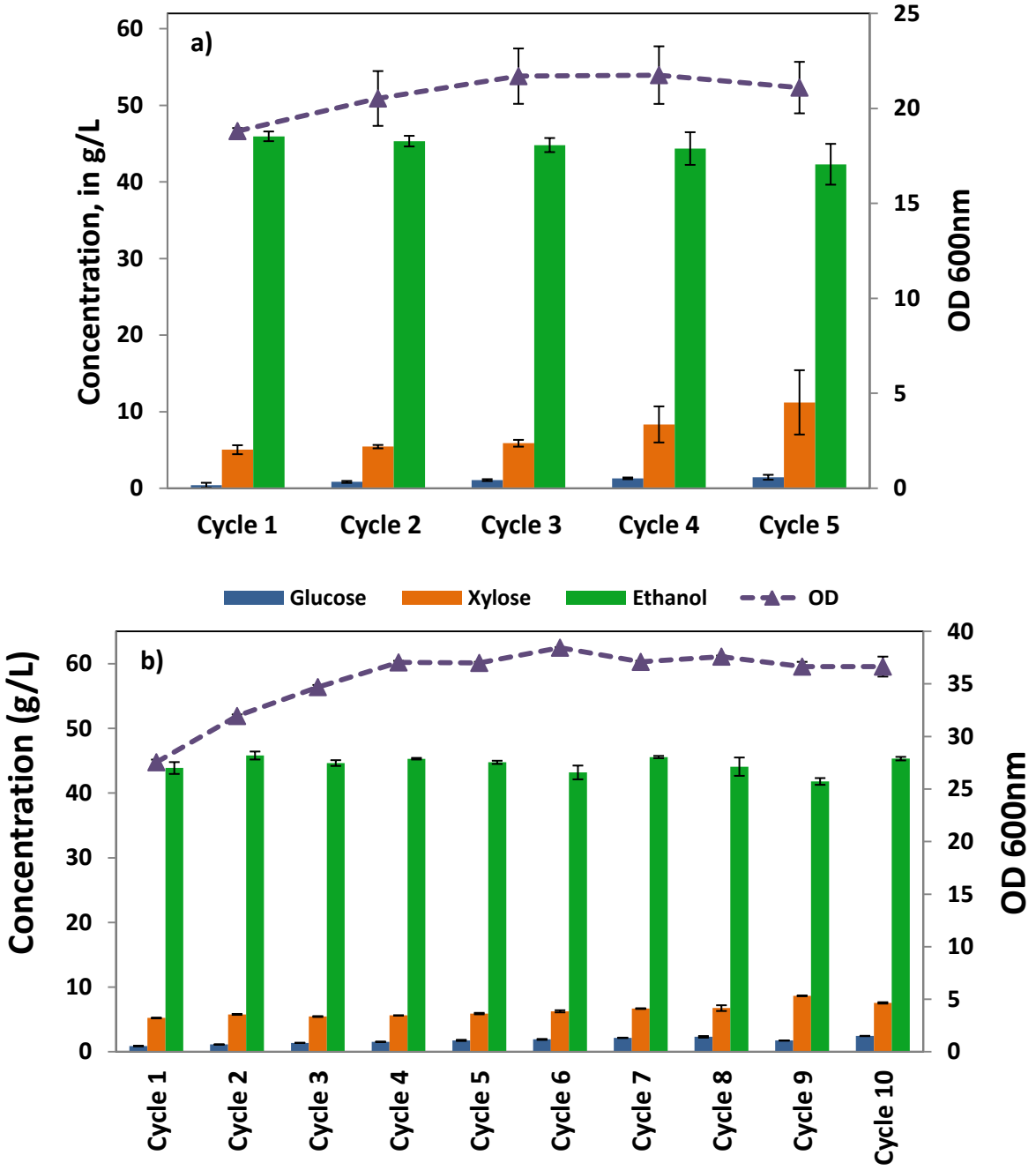

Figure 35 Shake flask comparison of a) 23 h and b) 11 h RaBIT fermentations. Final concentration are shown for glucose (blue), xylose (orange), and ethanol (green). OD measurements (purple triangles) are also shown. Average initial glucose and xylose concentrations were 59.5 ± 1.6 g/L and 32.0 ± 0.7 g/L, respectively. Error bars represent standard deviations.

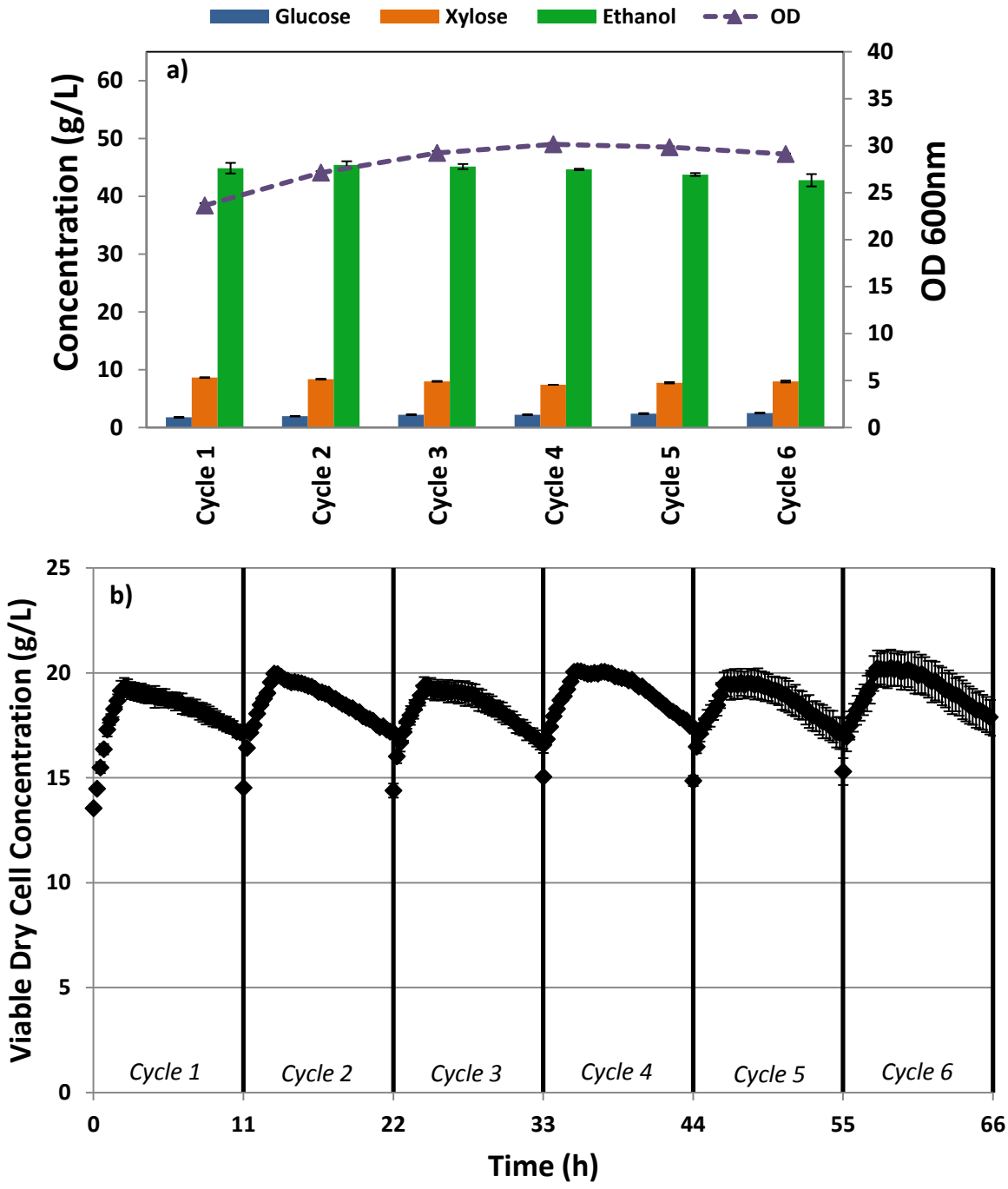

Figure 36 11 h RaBIT fermentation results using 0.5 L bioreactor. Final concentration are shown for glucose (blue), xylose (orange), and ethanol (green) in the top chart. OD measurements (purple triangles) are also shown. Average initial glucose and xylose concentrations were 59.4 ± 1.4 g/L and 32.0 ± 1.2 g/L, respectively. Viable dry cell concentration is shown in the bottom chart. Error bars represent standard deviations.

6.3.4 Fed-batch Addition of Sugar

To further improve the RaBIT process, fed-batch addition of sugar was investigated. Addition of sugar could eliminate the possible cellular energy deficit during the xylose consumption phase. To test the fed-batch concept, both pure glucose and hydrolysate containing both glucose and xylose were tested as the supplementation media.

Initially, fed-batch addition of glucose was tested using 23 h RaBIT fermentation cycles. 5 g/L of glucose was fed to the bioreactor at 11 h, 15 h, and 19 h during a RaBIT cycle. The added glucose promoted growth but could not eliminate the death phase (Figure 37). However, glucose addition did increase the final viable cell mass by 5%. Next, fed-batch addition using hydrolysate was tested. Shake flask experiments showed that the optimal initial volume of hydrolysate was 80% of the final hydrolysate volume with the other 20% added in 4 additions during the fermentation at 11, 14, 17, and 20 h (data not shown). The same process (80% hydrolysate initially added with 5% added at 11 h, 14 h, 17 h, and 20 h) was duplicated in bioreactors (Figure 38). Surprisingly, using hydrolysate improved performance more than adding just glucose leading to a 13% increase in final viable cell mass compared to the batch process. This was despite the glucose addition process providing 20 g/L additional sugar to the process compared to 0 g/L for the hydrolysate addition process (hydrolysate concentrations were ~60 g/L glucose and ~32 g/L xylose for reference). Addition of nutrients along with sugar when adding hydrolysate and not pure glucose may explain the increase in viable cell mass. Next, feeding the same 20% hydrolysate continuously between 11 h to 22 h was tested (Figure 39). Continuously feeding the hydrolysate only showed an 8% increase in final viable cell mass compared to the batch process. However, continuously feeding the hydrolysate could produce

increased cell turnover also creating benefit as generally after exponential phase a stationary phase is due to equal growth and death rates.

The benefit of fed-batch hydrolysate addition was also tested using the 11 h RaBIT fermentation process using the continuous addition method (Figure 40). Optimization experiments showed the optimal initial hydrolysate volume was 70% of the final hydrolysate volume (data not shown). The remaining 30% of the total hydrolysate volume was continuously added from 2 h to 10 h. The results in Figure 40 show that the final viable cell mass increased by 16% compared to the batch process. When including both process improvements of shortening the fermentation cycle time to 11 h and continuous fed-batch hydrolysate addition, viable cell mass production increased by 102% when comparing the difference between the final cell mass and initial cell mass.

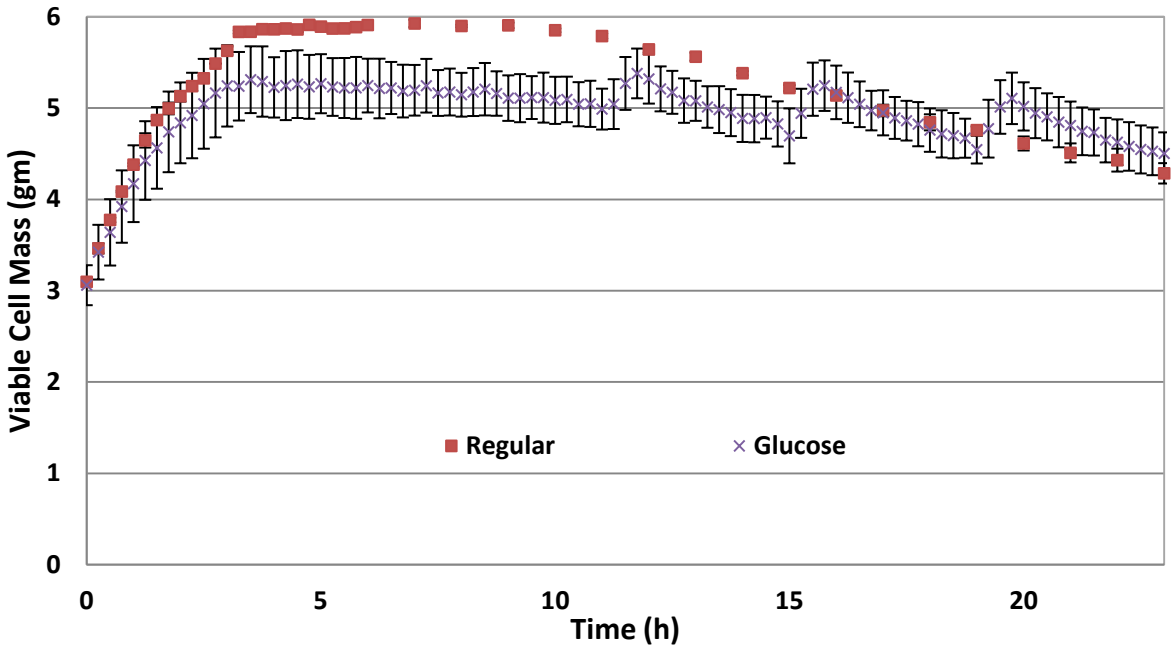

Figure 37 Viability comparison of regular 23 h RaBIT fermentation and 23 h RaBIT fermentation performed in bioreactors with periodic glucose feed. Error bars represent standard deviations.

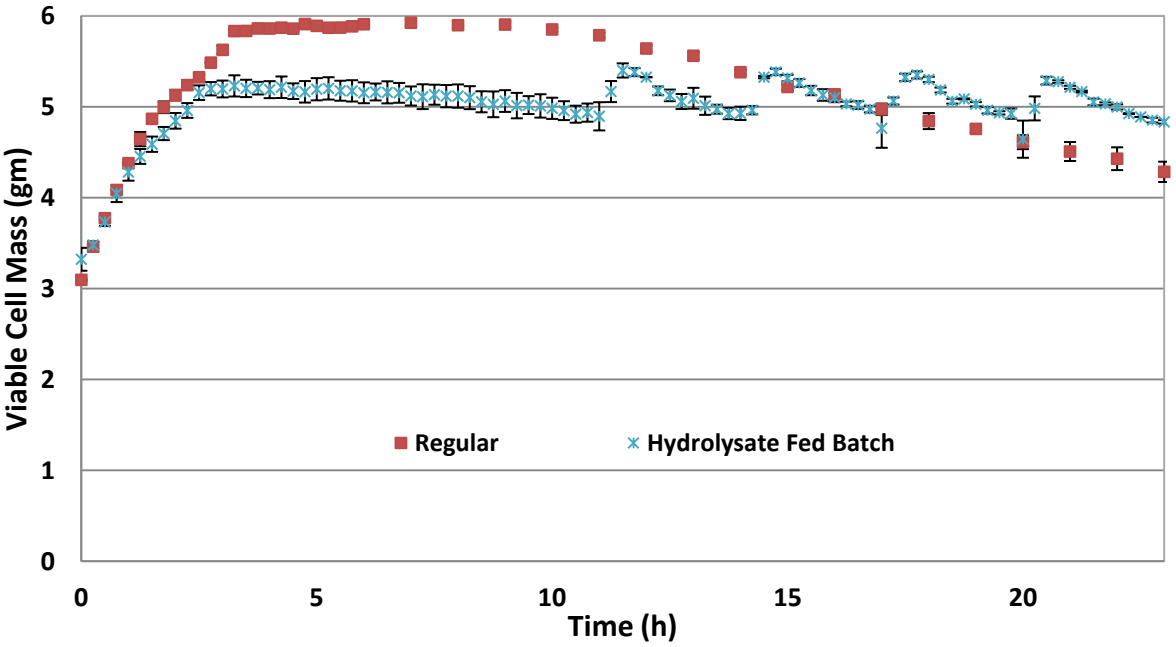

Figure 38 Viability comparison of regular 23 h RaBIT fermentation and 23 h RaBIT fermentation performed in bioreactors with fed-batch hydrolysate feed. Error bars represent standard deviations.

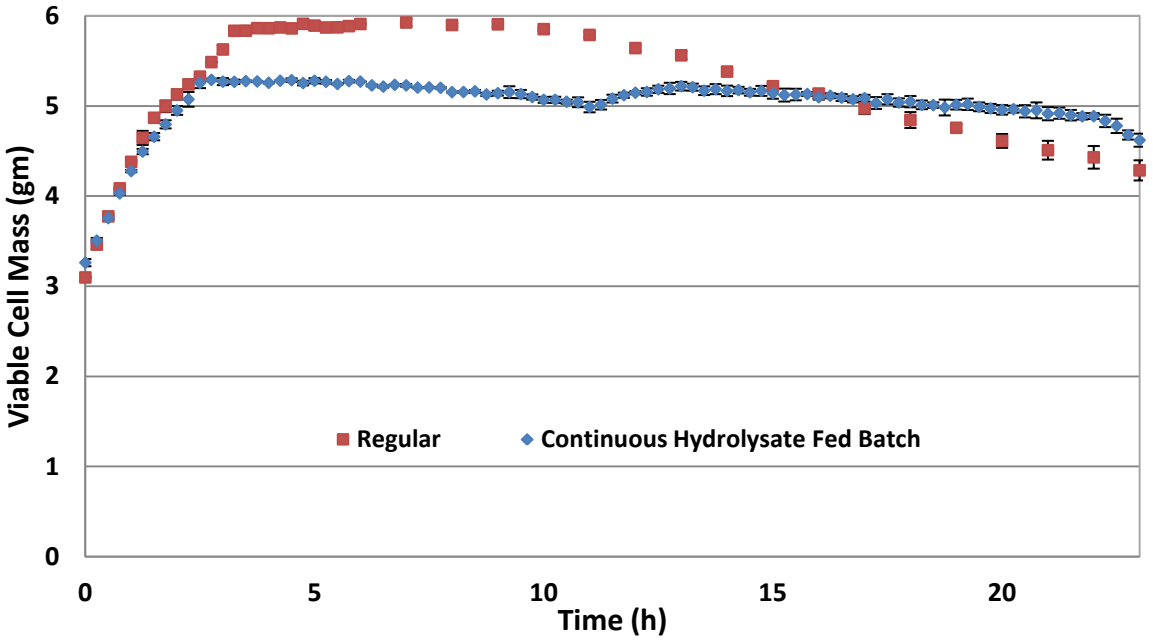

Figure 39 Viability comparison of regular 23 h RaBIT fermentation and 23 h RaBIT fermentation performed in bioreactors with continuous fed-batch hydrolysate feed. Error bars represent standard deviations.

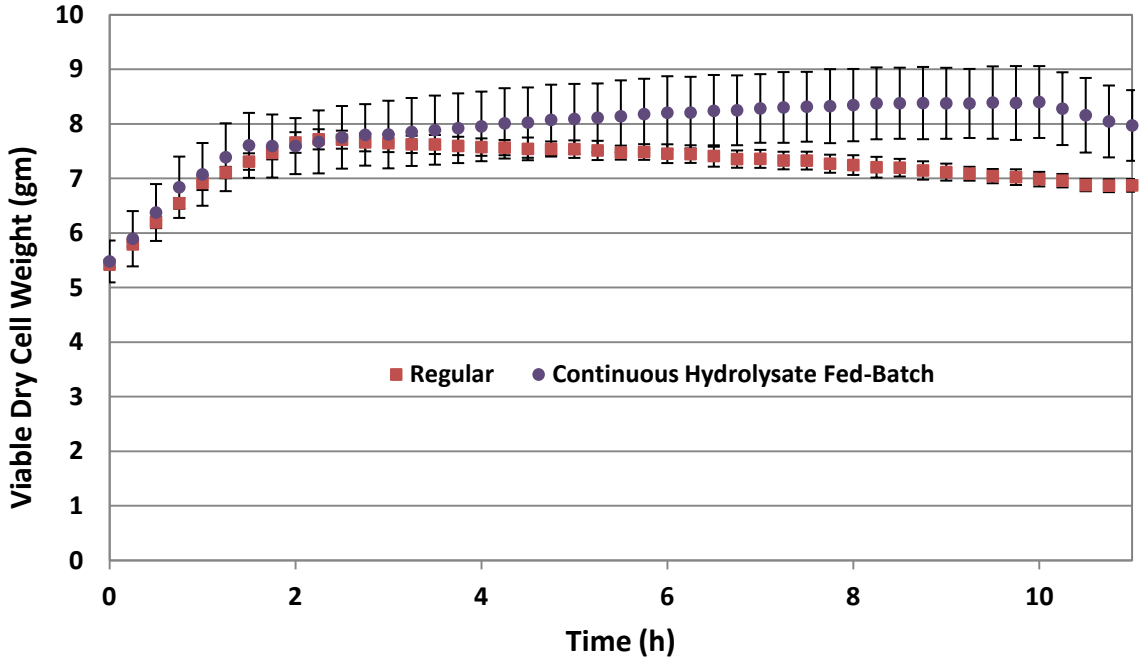

Figure 40 Viability comparison of regular 11 h RaBIT fermentation and 11 h RaBIT fermentation performed in bioreactors with continuous fed-batch hydrolysate feed. Error bars represent standard deviations.

6.3.5 Cell Separation

The cell population viability profiles show that cell death occurs during RaBIT fermentations. Fermentation performance could be potentially improved if cells could be separated based on viability (remove dead cells), activity (remove slower fermenting cells), or age (remove old cells). Removing dead, slow fermenting, or old cells could improve fermentation performance and potentially increase the mass of cells available for sale as an animal feed co-product. To separate cells, the flocculating nature of *S. cerevisiae* GLBRCY128 was utilized. Powell et al. (2003b) reported that flocculating yeast cells will settle based on size. Another publication by Powell et al. (2003a) showed that older cells are larger in size than young cells. A concern with the RaBIT process was the cell population average age may be increasing. Generally, cells grow and replicate faster when they are younger. Recycling the younger cells and removing the older cells may stimulate more cell mass production. However, Powell et al. (2003b) showed that older cells ferment better than young cells. For this work, cells were settled in a separatory funnel and the viable cell percentage, fermentation activity, and visible two dimensional cell area were measured after 23 h RaBIT fermentation cycles for different vertical fractions (layers in the funnel). Cells were settled for 20 minutes before the fractions were separated.

The first test determined the viable cell percentage of different fractions. After a RaBIT fermentation cycle, the cells were settled and different fractions based on their vertical locations were collected. Samples from the fractions were aliquoted and stained with methylene blue. Microscope images were taken and the viable cell counts were determined later when viewing the images on a computer. The results in Figure 41 show that there was no difference in viable cell percentage between the different fractions. It was noted that non-viable cells were

significantly smaller than viable cells potentially aiding in separation. However, cell flocs were made up of both viable and non-viable cells likely preventing any major separation based on size. This knowledge could be helpful for future separation techniques for non-flocculating cells or for a strain where flocculation could be controlled by use of pH or chemical addition

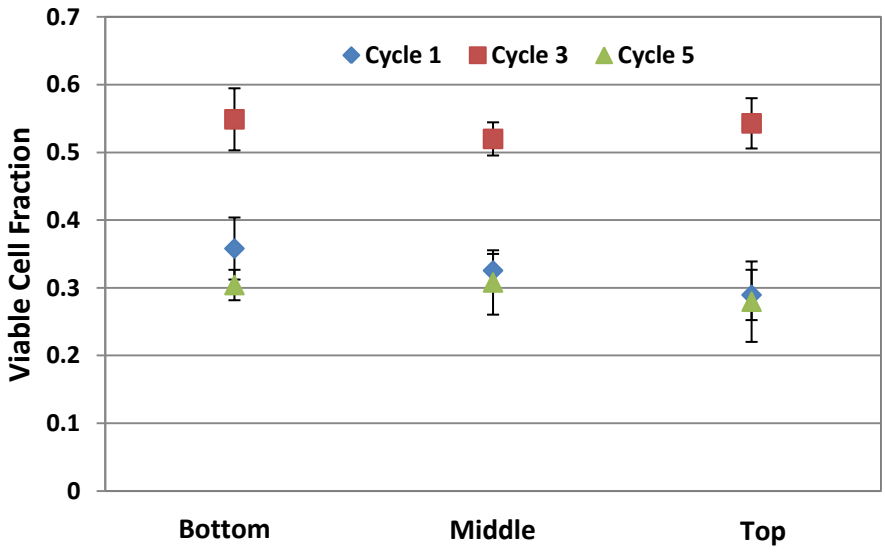

Figure 41 Fraction of viable cells after RaBIT Cycles 1, 3, & 5 performed in shake flasks and separated using a separatory funnel. Error bars represent standard deviations.

The next test monitored the fermentation performance of different settled fractions. Six equal fractions were taken and used to inoculate low cell density fermentations (1 g/L DCW inoculum) using AFEX hydrolysate. The results in Table 17 showed that cell activities did not significantly vary between fractions. Fermentation performance was very similar with regards to sugar consumption, ethanol production, and growth. This experiment did show the level of performance decrease occurring due to the recycling process. Glucose consumption, xylose consumption, and growth were decreased by 60%, 100%, and 85%, respectively, when using fifth cycle cells in traditional fermentations compared to first cycle cells (Figure 42). The same test was performed using hydrolysate previously fermented by a non-xylose utilizing

Saccharomyces cerevisiae strain to remove all glucose. No significant xylose consumption was observed when attempting to ferment hydrolysate containing only xylose (data not shown).

Table 17 Traditional shake flask fermentation performance after 24 h using RaBIT cycle separatory funnel settled cell fractions

Fraction*	Glucose (g/L)	Xylose (g/L)	Ethanol (g/L)	OD600
		Cycle 1		
1	1.78 ± 0.18	23.07 ± 1.28	37.37 ± 0.30	3.68 ± 0.10
2	1.88 ± 0.15	24.14 ± 0.92	36.88 ± 0.19	3.63 ± 0.19
3	1.97 ± 0.16	24.07 ± 1.15	36.49 ± 1.23	3.51 ± 0.10
4	2.04 ± 0.15	24.00 ± 0.95	36.79 ± 0.22	3.61 ± 0.12
5	1.99 ± 0.07	24.08 ± 1.16	37.04 ± 0.25	3.71 ± 0.07
6	1.98 ± 0.10	25.12 ± 0.83	36.39 ± 0.52	3.89 ± 0.15
		Cycle 3		
1	1.81 ± 0.35	26.70 ± 0.78	31.50 ± 1.75	2.80 ± 0.11
2	1.76 ± 0.36	26.44 ± 1.17	32.12 ± 1.08	2.72 ± 0.03
3	1.55 ± 0.12	27.27 ± 1.36	33.06 ± 0.73	2.86 ± 0.21
4	1.58 ± 0.12	26.82 ± 0.44	32.55 ± 0.59	2.89 ± 0.09
5	1.59 ± 0.06	26.57 ± 0.38	33.04 ± 0.65	2.75 ± 0.00
6	1.56 ± 0.07	27.01 ± 1.01	33.25 ± 0.49	2.79 ± 0.22
		Cycle 5		
1	33.91 ± 7.01	32.50 ± 0.82	12.11 ± 3.73	1.00 ± 0.03
2	35.18 ± 5.01	32.38 ± 0.77	11.29 ± 2.70	0.87 ± 0.03
3	34.44 ± 5.81	32.45 ± 0.66	11.16 ± 2.83	0.92 ± 0.04
4	32.22 ± 7.65	32.40 ± 0.93	12.79 ± 4.03	0.97 ± 0.05
5	32.87 ± 5.85	32.48 ± 0.84	12.43 ± 2.86	0.92 ± 0.03
6	38.80 ± 5.06	32.53 ± 0.73	9.20 ± 2.55	0.89 ± 0.08

* Fractions were ordered from bottom (1) to top (6)
Error values represent standard deviations

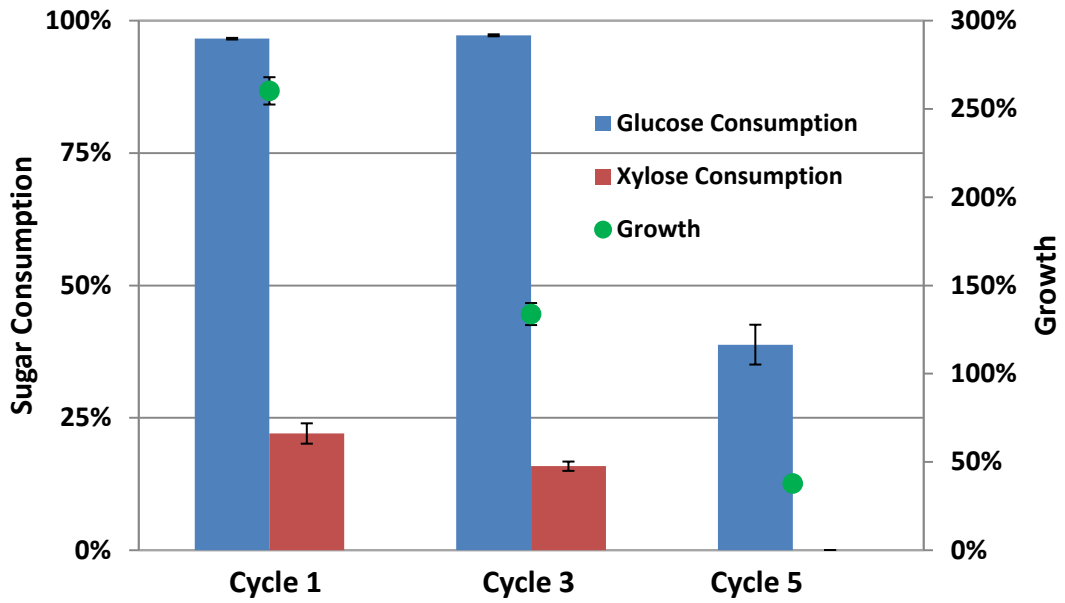

Figure 42 RaBIT cycle performance comparison using end of cycle cells for 23 h traditional fermentations (1 g/L DCW inoculum) using shake flasks. Error bars represent standard deviations and are present for all data points but may be hidden by the symbol.

Cell size was also measured for top and bottom separatory funnel settled cell fractions after RaBIT fermentation cycles. Only the viable cells were measured. Plates were made from methylene blue stained cells taken from the bottom and top mL in the separatory funnel. Pictures were taken using the microscope. Visible cell area was then measured using Motic Images Plus. The results indicated that the bottom cell fractions were in general larger than the top fractions (Table 18). Student t-tests were used to confirm the results were significant.

Table 18 Average viable cell area of 23 h shake flask RaBIT fermentation cycles after separatory funnel settling

	Cycle 1	**Cycle 3**	**Cycle 5**
Top*	21.0 ± 5.2	24.9 ± 5.8	26.9 ± 7.8
Bottom*	23.0 ± 5.9	26.1 ± 5.8	28.5 ± 8.0
Significance Level~	$p<0.001$	$p<0.001$	$p<0.001$

*Units are in μm^2
~Student t-test
Error values represent standard deviations

6.3.6 Cell Co-Production

The process changes to eliminate the decrease in xylose consumption targeted cell production. Shortening the fermentation time reduced cell death; fed-batch hydrolysate addition increased cell turnover; and removing older cells through settling had the potential to generate cell biomass while promoting growth of younger cells. These benefits could not only improve fermentation performance, but also generate a yeast co-product stream that could be sold as animal feed. Removing cells as a co-product could also promote more growth generating a younger and healthier cell population. For this set of experiments, 100% cell recycle was compared to 80% and 90% cell recycle. These tests were performed both by removing the bottom fraction of cells after settling using a separatory funnel and mixed cells. The 11 h continuous hydrolysate fed-batch (2 to 10 h) RaBIT process was used.

Fermentation results comparing 100%, 90%, and 80% cell recycle without using a separatory funnel are shown in

Figure 43(a-c). Removing 10% of the cells (90% recycle) showed the best fermentation performance with only a 0.45 g/L difference in xylose consumption when comparing cycles 1 and 3, while 100% cell recycle had a difference of 1.29 g/L. This confirms the hypothesis that removing cells could improve fermentation performance likely due to increased growth and cell turnover. When 80% of the cells were recycled, the xylose consumption decreased of 1.14 g/L xylose between cycles 1 and 2 was 317% and 518% higher than for 90% and 100% cell recycle, respectively. The xylose consumption decrease between cycles 1 and 3 for 80% cell recycle (1.14 g/L) was similar to the 100% cell recycle process (1.29 g/L) but larger than the 90% cell recycle process (0.45 g/L). When looking at OD measurements, 100% cell recycle was capable of accumulating cell mass, 90% cell recycle kept cell mass stable, and 80% cell recycle saw a

decrease in cell mass. It was concluded that 10% cell removal (90% cell recycle) appeared to be the approximate limit for cell removal, while improving fermentation performance and not decreasing cell concentration.

The next step tested whether cell removal after settling using a separatory funnel could improve the process. From the previous section, settling cells using a separatory funnel allowed for separation based on cell size. Smaller cells are generally younger (Powell et al., 2003a). Our goal was to recycle younger cells to limit any potential impact of cell aging and promote growth during RaBIT fermentations. This test was performed by removing the bottom 10% of separatory funnel settled cells. A density calibration was performed in order to remove an accurate percentage. The results are shown in

Figure 43d; 90% cell recycle along with Cell removal of 10% separatory funnel settled cells limited the xylose consumption decrease between cycles 1 and 3 to 0.31 g/L xylose compared to 0.45 g/L xylose for 10% removal of cells without settling. This difference was found to be significant using a student-t test (p value <0.05).

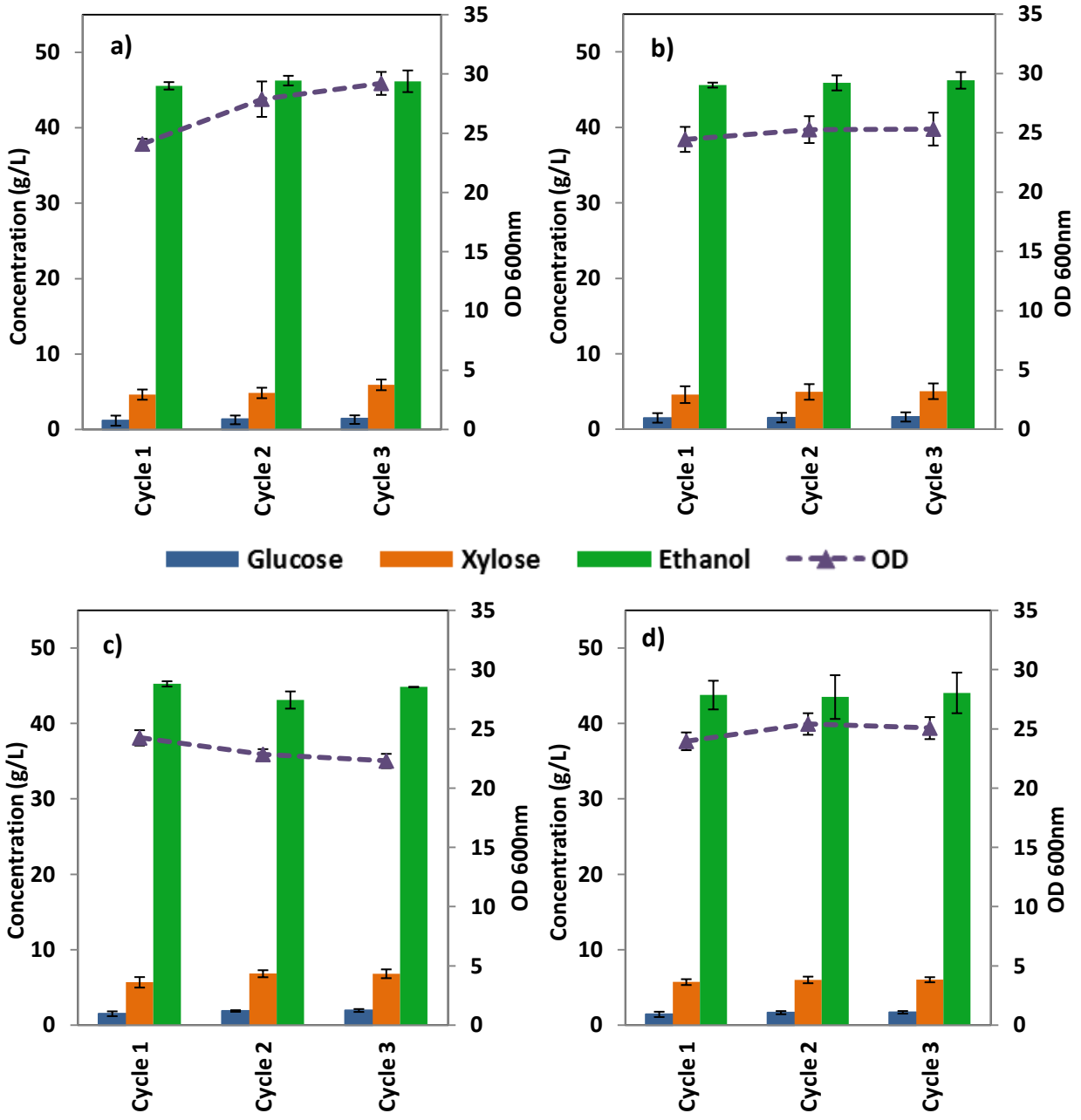

Figure 43 11 h fed-batch RaBIT fermentations performed in bioreactors with a) 100% b) 90% c) 80% or d) top 90% of separatory funnel cell recycle. Final concentration are shown for glucose (blue), xylose (orange), and ethanol (green) in the top chart. OD measurements (purple triangles) are also shown. Initial glucose and xylose concentrations were 57.2 ± 1.4 g/L and 32.5 ± 0.5 g/L, respectively. Error bars represent standard deviations.

6.3.7 Ten Cycle Mass Balances

Ten cycle RaBIT fermentations were performed testing 0% cell removal upon recycle and 10% separatory funnel bottoms cell removal upon recycle. The procedure included 11 h fermentation cycles and continuous fed-batch hydrolysate addition. Biomass was also switched from GLBRC 2010 corn stover pretreated in a 5 gallon reactor to MBI corn stover pellets treated in 450L pilot scale packed bed reactors using the gaseous AFEX process. This change was made to provide more industrially-relevant results. Results for 0% cell recycle are shown in Figure 44a. Over ten cycles, the xylose consumption decrease was eliminated. When removing 10% of the cells using the separatory funnel, the xylose consumption decrease was present (Figure 44b). However, the decrease of 3.58 g/L xylose over ten cycles was smaller than the 3.64 g/L xylose decrease exhibited in Figure 4 over a singular cycle. Worryingly, the OD decreased after cycle 2. This brings into question the long term sustainability of removing 10% of the cells. Figure 44a showed that with no cell removal, OD kept increasing over the 10 cycles. This suggests that some cell removal may still be possible, but at a lower percentage than 10%.

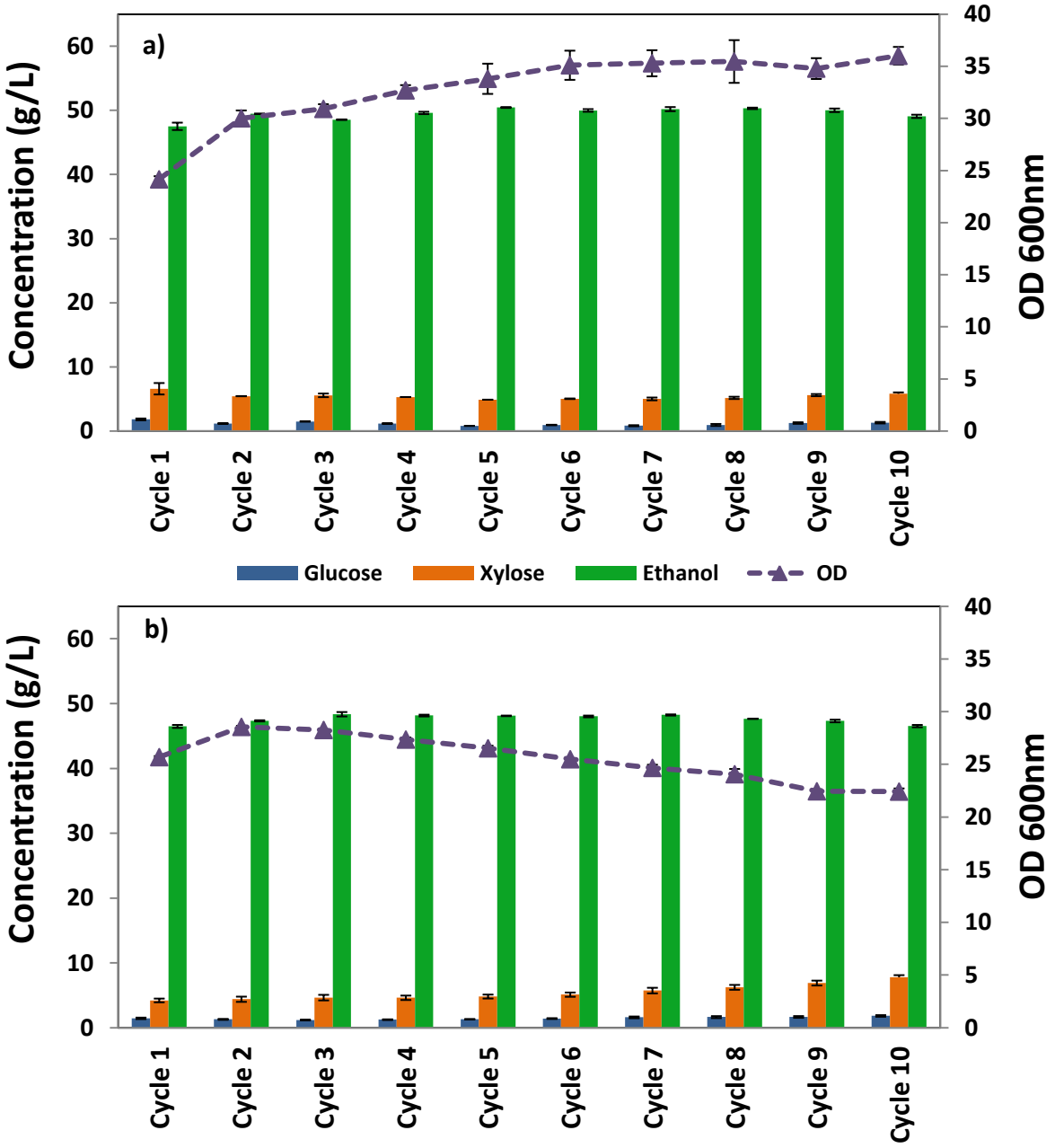

Figure 44 RaBIT fermentations using bioreactors comparing a) 0% cell removal during recycle and b) 10% cell removal from the bottom of a separtory funnel settled cell population. Final concentrations are shown for glucose (blue), xylose (orange), and ethanol (green) in the top chart. OD measurements (purple triangles) are also shown. Initial glucose and xylose concentrations were 63.0 ± 0.8 g/L and 31.2 ± 0.6 g/L, respectively. Error bars represent standard deviations and are present for all data points but may be hidden by the symbol.

Mass balances were performed to determine the economic benefit/detriment of cell removal in the RaBIT process. The mass balances included addition of an SSCF step as

previously reported by Jin et al. to increase ethanol yield (*In preparation).* The resulting mass balances are shown in Figure 45. When recycling 90% of the cells, ethanol yield dropped by 4% when compared to 100% cell recycling. However, yeast production increased by 16%. When comparing product generation, 100% cell recycle is the economic choice. Assuming yeast can sell for $400/tonne (approximate soy meal price) and ethanol sells for $2.50/gal, the 100% cell recycle process has 3.7% higher revenue. Ethanol prices would need to be as low $0.23/gal for the 90% cell recycle process to break even with the 100% cell recycle process. This assumes that process costs don't increase when performing the 90% cell recycle process. It is possible that a recycle percentage between 90% and 100% would be capable of maintaining a similar ethanol yield as 100% recycle and create an economic benefit for partial cell recycling.

Cells are not expected to be used forever in the RaBIT process. The process changes implemented were devised to extend the life of the cells as long as reasonably possible. Some form of cell removal will need to be used. This could be performed by removing a portion of the cells and replacing them with cells from new seed cultures, as performed in unpublished work by Jin et al. (In submission). Separation techniques may be capable of selectively removing old or dead cells. Further research will need to be performed in this area.

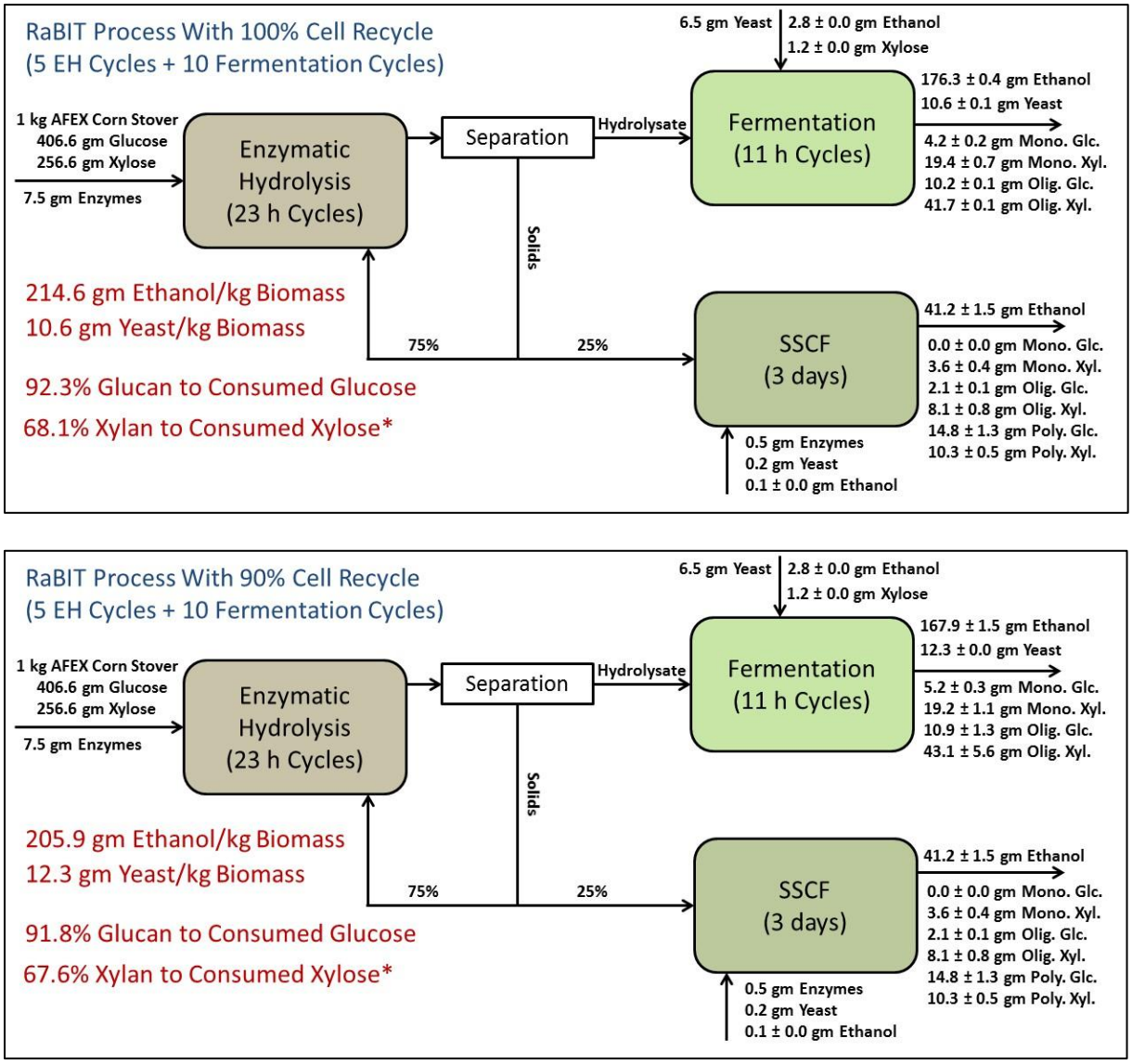

Figure 45 Mass balances for overall RaBIT processes using RaBIT bioreactor continuous hydrolysate fed-batch fermentations with 100% cell recycle or 90% cell recycle with the 10% cell removal from the bottom of separatory funnel settled cell populations (*) Xylan to consumed xylose was calculated by subtracting seed culture xylose from final residual xylose.

6.4 Conclusions

Process changes were investigated and implemented to improve RaBIT fermentation performance. Previously, RaBIT fermentation exhibited a decrease in xylose consumption upon cell recycle. RaBIT fermentation cycles were shortened to 11 h, thereby reducing the xylose consumption decrease. Furthermore, hydrolysate was added in a fed-batch manner improving

overall xylose consumption and increasing viable cell mass by 16%. Next, cell separation by settling using a separatory funnel was investigated. Cells could be settled by age allowing for older cells to be removed instead of recycled back into the process. Removing 10% of the cell population by this method resulted in improved performance over 0% cell removal, when testing for 2 recycle events. Testing cell removal over 10 cycles showed that 10% cell removal was unfavorable compared to 0% cell recycling. Overall however, improvements to the RaBIT process were capable of eliminating the decrease in xylose consumption over 10 cycles.

CHAPTER 7: LIFE CYCLE ASSESSMENT AND TECHNO-ECONOMIC STUDY

Abstract

The RaBIT (Rapid Bioconversion with Integrated recycling Technology) process has been previously described as an economically beneficial alternative to the SHF (Separate Hydrolysis and Fermentation) cellulosic ethanol process. In this chapter, the current RaBIT process was compared to a SSCF (Simultaneous Saccharafication and Co-Fermentation) process by the use of economic and life cycle analysis. Both the RaBIT and SSCF processes were performed experimentally using pilot scale AFEX corn stover pellets and industrially-relevant CTec3 and HTec3 enzymes. Both processes used their respective optimal strains as previously determined in Chapter 2. The results showed that the RaBIT process MESP (minimum ethanol selling price) was 9% lower compared to the traditional SSCF process. Life cycle analysis showed the RaBIT process had less impact for global climate change potential and acidification potential, while the SSCF process produced more energy and had less impact for eutrophication. Both processes were shown to be carbon negative

7.1 Introduction

Life cycle analysis (LCA) is a tool for determining the environmental sustainability for a process or product (Curran, 2006). Accuracy of an LCA as an absolute number can be questioned. However when used as a comparative tool, an LCA provides valuable knowledge on whether a process is more sustainable or better for the environment than a competing process and also serves as a benchmark to evaluate process changes for their effects on sustainability.

Techno-economic analysis can be used, in the same manner as an LCA, to estimate general costs and revenue for a process. In general, techno-economic analysis provides a rough estimate for product cost with accuracy depending on the quality of data available and the validity of the assumptions made. Using techno-economic analysis as a comparative tool can provide strong evidence as to whether one process is more economical than another.

Combining both of these tools to evaluate a new process is necessary when making an informed decision on whether to continue with process development or implementation. While preliminary economic analysis has been performed comparing previous iterations of RaBIT processes to other cellulosic ethanol processes, no LCA had been performed up to this time (Jin et al., 2012a). Furthermore, improvements in AFEX, enzymes, and microbes require constant updating of models. The work in this chapter will combine both analysis tools to look at two different processes: the RaBIT process with 100% cell recycle using *S. cerevisiae* GLBRCY128, and a SSCF (simultaneous saccharification and co-fermentation) process using *Z. mobilis* 8b.

7.2 Goal and Scope

The goal of this work was to compare a traditional cellulosic ethanol processes to the RaBIT process at a 20,000 ton/day scale using both life cycle and economic analysis. The life cycle analysis scope includeed all energy generation, energy consumption, and environmental impacts within the boundaries of cultivation, harvesting, transportation, chemical processing, biological processing, and combustion of the ethanol product as a fuel. Energy and global climate change potential associated with fertilizer, ammonia, and enzyme production were also included. Figure 46 represents a pictoral description of the scope of the analysis. In total, four different environmental impact categories were studied: energy usage, global climate change potential, acidification, and eutrophication.

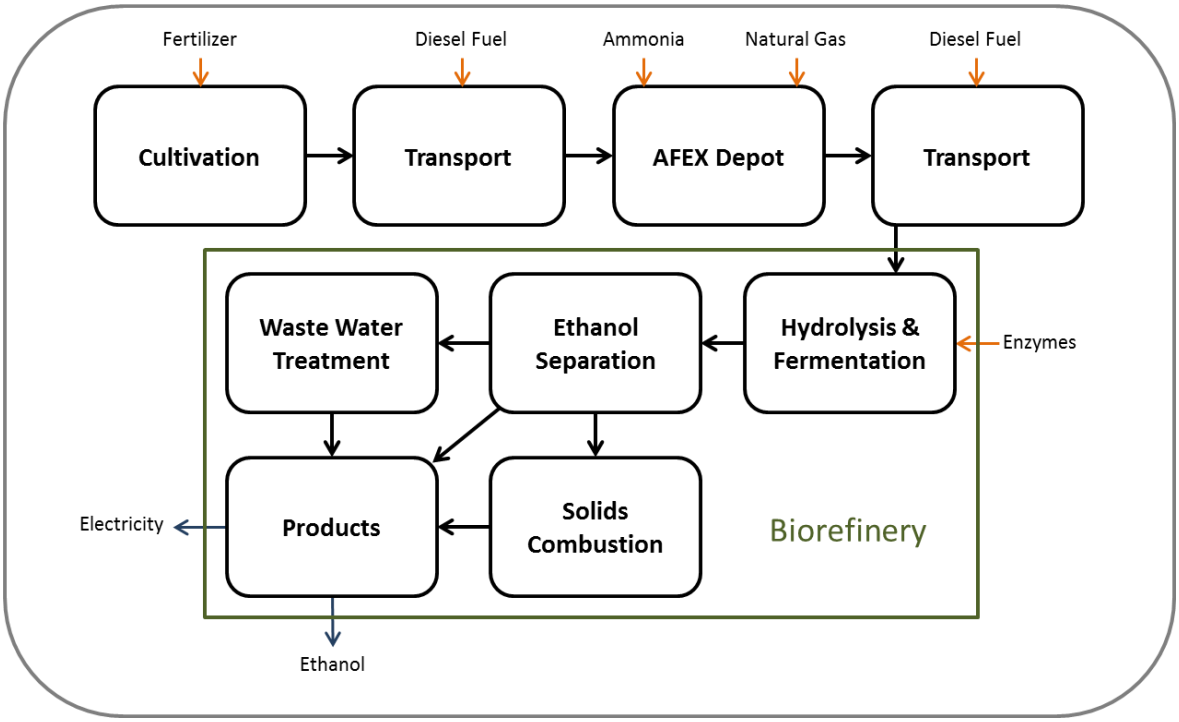

Figure 46 Analysis scope

7.3 Method

7.3.1 Cultivation and Harvesting Modeling

Corn stover production costs were based on compensating the farmer for costs not associated with grain production. For this study, an assumed 2 tons/acre of corn stover was removed after harvesting (Graham et al., 2007). For cultivation, only the cost of fertilizer allocated to the corn stover was considered. Total fertilizer inputs were 144 kg/ha/yr nitrogen, 56 kg/ha/yr phosphorus, and 70 kg/ha/yr as supplied by ammonia, phosphorus oxide, and potash, respectively (Sheehan et al., 2004). The percent biomass removed for corn stover was used to calculate the percentage of fertilizer for which the farmer is compensated. The compensated fertilizer percentage (3%) was based off of the carbon balance reported by Follett et al. (2012)

for total biomass generated per acre during corn cultivation, which included both above ground and below ground carbon.

Harvesting the corn stover was modeled as a single pass using an ear-snap combine, shredder, and round baler. Corn stover was harvested from two thirds of the total land (other third represented non-corn producing land or non-participation in the biorefining system). The farmer was compensated for capital, maintenance, fuel, and time for shredding, baling, and transporting the corn stover. Bale wrapping and storage costs of $25/ton were also included. The farmer was further compensated with a 10% profit based on total cost.

7.3.2 Transportation Modeling

The pretreatment depot concept was applied to this model. Depots can be used to pretreat low density biomass near the harvesting location. After harvesting, the low density material is AFEX-pretreated before being densified and shipped to the biorefinery. Densification allows for savings in transportation. In turn, the pelleted biomass can be shipped greater distance economically. Greater shipping distances allow for larger biorefineries that cost less due to economies of scale.

Bulk density of loose corn stover was assumed as 60kg/m^3. Pelletized corn stover leaving the depot was assumed a density of 400kg/m^3. Depots were sized at 100 MT/day. Transportation distances were estimated by creating a scaled map in Excel as seen in the scaled down figure in Figure 47. This determined a 3 mile average transport radius from field to depot and a 40.3 mile average transport radius from depot to biorefinery (61.3 mile total radius). Average transport radius for field to depot and depot to biorefinery were 3 miles and 40.3 miles, respectively. Fuel, wages, and truck rentals were included in the transportation cost.

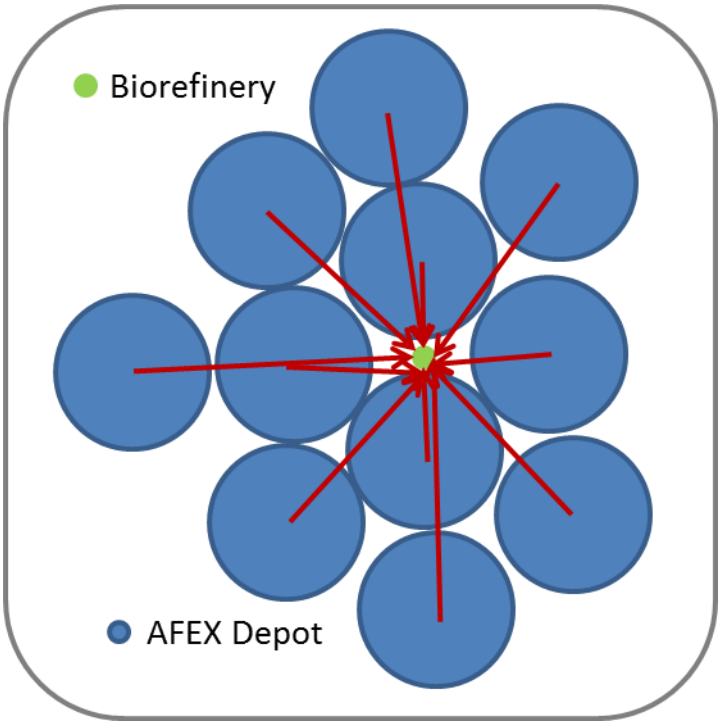

Figure 47 AFEX depot model concept

7.3.3 AFEX Depot Design

The AFEX depot was sized at 100 MT/day. The major inputs were corn stover, ammonia, and natural gas for steam production. Corn stover was priced based on the previous harvesting and cultivation modeling. Ammonia recycle was assumed to be 97% of the 0.6 ammonia to biomass mass ratio. Energy input from steam and compressor duty were estimated from process packed bed data acquired from MBI (Lansing, MI). The pellet mill design was based off a 10.2 MT/hr mill sold industrially (Alaska Pellet Mill, 2010). Major capital investments included a compressor, four pressure vessels (316 SS), a pellet mill, a boiler, and a steam generator. All but the pellet mill were priced using Peters, Timmerhaus, and West (2003).

7.3.4 Biorefinery Design

The biorefinery was sized at 20,000 tons/day. The size was chosen to take advantage of the AFEX depot concept. The RaBIT process and a traditional SSCF process were compared.

The mass balance for the RaBIT process was taken from Chapter 6, while the mass balance for the traditional SSCF process is reported below.

7.3.4.1 RaBIT Process

The RaBIT process flow diagram is shown in Figure 48. The mass balance data was previously presented in Chapter 6 (Figure 45). The 100% cell recycle process was used.

RaBIT enzymatic hydrolysis used pelleted pilot scale AFEX corn stover along with CTec3 and HTec3 enzymes. The process was modeled as consisting of ten 23 h cycles. After ten cycles, the yeast was discarded/sold as animal feed and the process was assumed to start over. The average enzyme loading for 10 cycles was 16.6 mg protein/g glucan. Solids were recycled at 100% for the first 3 cycles and 75% for subsequent cycles. The remaining 25% solids were used in the SSCF process. Enzymes used for the SSCF process were 7% of the original loading resulting in a total RaBIT process enzyme loading of 17.8 mg protein/g glucan. The SSCF process was inoculated with 0.1 g/L DCW cell pellet, after the 6 h pre-hydrolysis period, using *Saccharomyces cerevisiae* GLBRCY128 and fermented for 66 h. The separation for the solids and enzyme recycling step was modeled as performed by both centrifugation and filter pressing in separate cases. See Figure 48 for pictoral representation of details.

The RaBIT fermentation was modelled for both ten and twenty 11 h cycles while assuming the 10 cycle mass balance yield did not change when increasing to 20 cycles. After the 10 or 20 cycles, the process was assumed to start over. Different inoculum sizes were also modelled with the original mass balance using 17.5 g/L DCW cell pellets of *S. cerevisie* GLBRCY128. Hydrolysate was fed using the fed-batch method where 70% of the initial hydrolysate was added initially and the remaining 30% was fed continuously between 2 and 10

h. Separation for the yeast recycle step was modeled using centrifugation and assumed only 25% of the total broth required separation due to yeast flocculation and settling. See Figure 48 for pictoral representation of details.

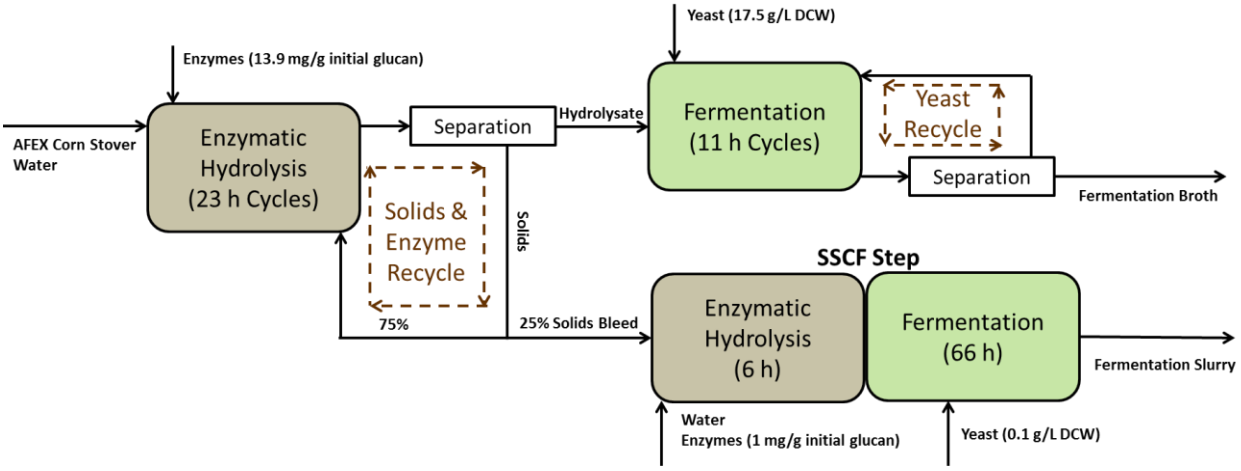

Figure 48 RaBIT process diagram

7.3.4.2 Traditional SSCF Process

The traditional SSCF process flow diagram is shown in Figure 49. The mass balance used is shown in Figure 50. The materials and method are detailed in Appendix C. The biomass was the same pelleted pilot scale AFEX corn stover as used for the RaBIT process. CTec3 and HTec3 were used at a 24.0 mg protein/g glucan loading. After 48 h of enzymatic hydrolysis, the SSCF was inoculated with 10% seed culture broth containing *Zymomonas mobilis* 8b. Unlike the RaBIT process, a cell pellet was not used and the whole broth was added. Corn steep liquor was added at 0.25%.

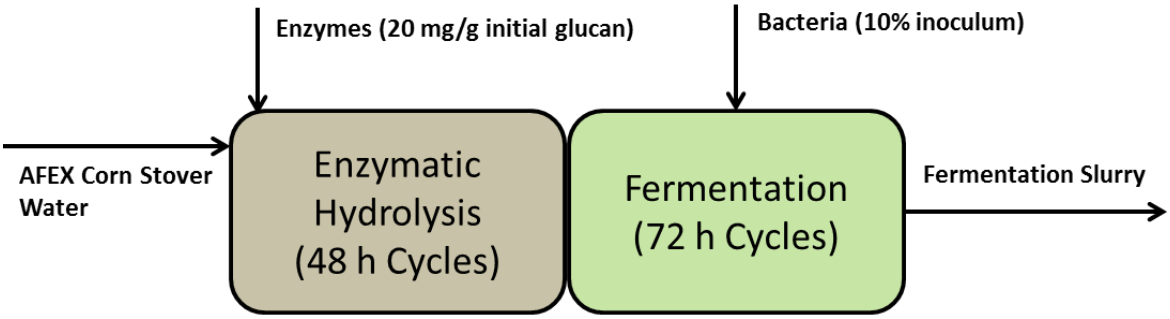

Figure 49 Traditional SSCF process diagram

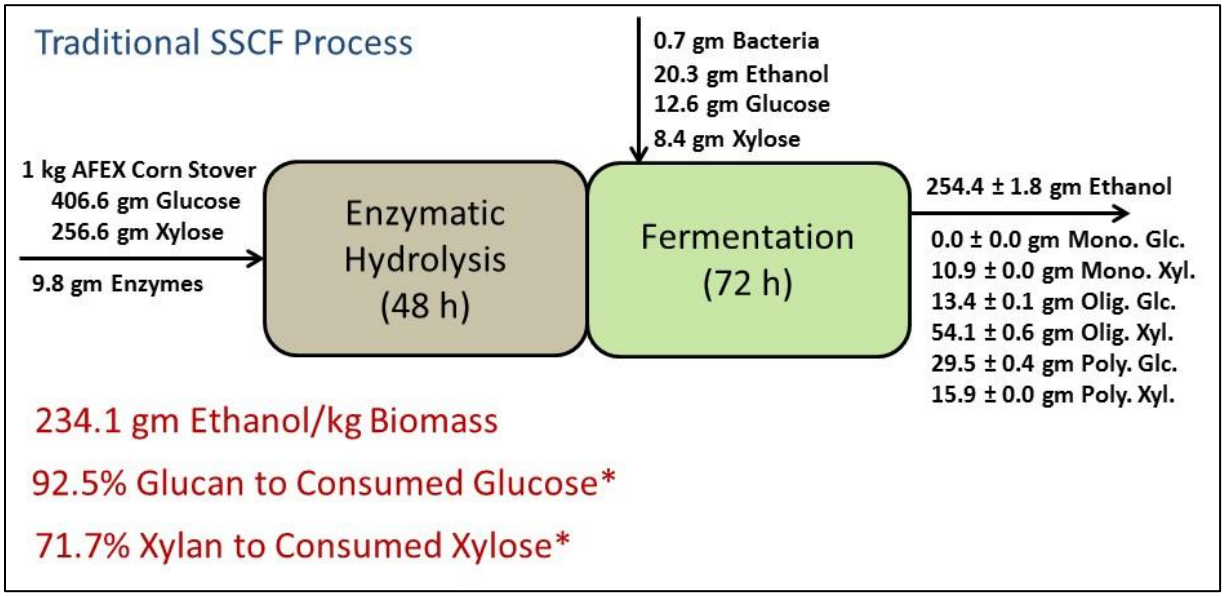

Figure 50 Traditional SSCF mass balance

7.3.4.3 Enzymatic Hydrolysis and Fermentation

All inputs and products were determined from the bioreactor mass balances. Mixing requirements were based on calculations using Perry's Chemical Engineers' Handbook for energy calculations and Stickel et al. 2009 for biomass slurry viscosity. Energy for heating the slurry up to 50 °C for enzymatic hydrolysis, cooling the slurry down to 32 °C for fermentation, and cooling for microbial metabolic heat generation were accounted for. Due to size, the reactors were assumed adiabatic and did not require inputs for maintaining temperature.

7.3.4.4 Seed Culture Trains

Seed culture trains were modeled for both *S. cerevisiae* GLBRCY128 and *Z. mobilis* 8b as described in Chapter 6 and Appendix C, respectively. The seed culture train for GLBRCY128 consisted of 5 stages with 1% inoculums, and 24 h culturing time per stage. The media consisted of 75 g/L glucose, 25 g/L xylose, 10 g/L yeast extract, and 20 g/L tryptone. The seed train was also modeled using 2 g/L potassium phosphate monobasic to replace 20 g/L tryptone as similar to the *Z. mobilis* seed train media. Elimination of tryptone decreased OD by 15%.

The seed culture train for 8b consisted of 6 stages with 5% inoculua, and 12 h culturing time per stage. The media consisted of 100 g/L glucose, 20 g/L xylose, 10 g/L yeast extract, and 2 g/L potassium phosphate monobasic.

7.3.4.5 Ethanol Separation

The distillation process used three different columns. The slurry was sent to the beer column with a 0.2 ethanol mol fraction distillate. All ethanol was assumed present in the distillate. The rectifying column received inputs from the beer column and stripping column. The distillate ethanol mol fraction for the rectifying column was 0.88 and the bottoms ethanol mol fraction was 0.03. The bottoms were sent to the stripping column to remove all ethanol with the distillate returned to the rectifying column at 0.2 ethanol mol fraction. The columns were designed using the McCabe-Thiele method in Excel. Rough optimization of the reflux ratio was performed to minimize energy use. Column pricing was determined from Peters, Timmerhaus, & West (2003).

After distillation, the 88% ethanol stream was sent to a molecular sieving unit. The sieve unit was designed as similar to an autoclave for economics due to the steam pressures required

for regenerating the zeolite. Zeolite performance data was taken from Patil and Patil (2012). After the molecular sieve unit, the ethanol had been purified to 99.8% by mass (molecular sieve limit).

7.3.4.6 Solids

Solids separation was performed by a continuous centrifuge designed using Perry's Chemical Engineer's Handbook. The centrifuge separated the bottom stream coming out of the beer column. The final separation was assumed similar to the lab centrifuge. For simplicity, no solids were assumed present in the liquid fraction.

The solids were burned while taking into account information from all three NREL Technical Reports (Aden et al., 2002; Kazi et al., 2010; Humbird et al., 2011). All capital costs were calculated from Peters, Timmerhaus, and West (2003). Electricity was generated after subtracting the steam required for other processes. No stripping of the flue gas was performed to to create a worst case scenario for the LCA.

7.3.4.7 Waste Water Treatment

Waste water treatment was designed according to the 2002 NREL Report. The treatment included anaerobic digestion producing methane and aerobic digestion. The treatment plant was priced in Peters, Timmerhaus, and West (2003). Electricity requirements for the waste water treatment facility were estimated at 1250 kWh/million gallons as reported by Moore (2012). Electricity required for air compression to 150 psia for aerobic digestion was also included.

7.3.4.8 Heating and Cooling

Heat exchangers were required for many parts of the process. Heating was provided by the condensation of steam and cooling was providing through cooling water produced by cooling

water towers. Heat exchangers were designed using approximate overall heat-transfer coefficients between steam, water, and light organic fluid (Peters, Timmerhaus, and West 2003). Pricing was generated from Peters, Timmerhaus, & West (2003).

Cooling water towers were designed around maximum wet bulb temperatures in the Midwest. Perry's Chemical Engineers' Handbook was then used for sizing. Cost estimates were performed using Peters, Timmerhaus, & West (2003).

7.3.4.9 Economics

Purchased costs for all major process equipment was summed and then multiplied by a Lang factor of 5 to get the total capital investment (TCI). Variable costs were calculated for the following: biomass, enzymes, corn steep liquor, potassium hydroxide, sulfuric acid, dextrose, xylose, yeast extract, tryptone, and potassium phosphate. Prices were taken from commodity pricing websites. Enzyme cost ($3.6/kg) was taken from the Humbird et al. (2011). Revenue was generated from ethanol and electricity. Electricity was sold for $0.14/kWh and represents a current average price for the U. S. (U.S. DOL, 2015). The tax rate was assumed 30% percent, with a loan rate of 10%. Net present values of zero were calculated for the four different/separate economic scenarios resulting in minimum selling prices: cultivation, harvesting, and transportation to depot; pretreatment at AFEX depot; transportation from depot to biorefinery; and bioprocessing at the biorefinery.

7.3.5 Life Cycle Categories

7.3.5.1 Eutrophication

Eutrophication potential was calculated based on field runoff from the nitrogen and phosphorus fertilizers. Runoff was estimated at 5.5% of the fertilizer applied according to Wu et

al. (1996). Phosphate equivalence conversions factors were taken from a report compiled by GHK (2006).

7.3.5.2 Acidification

Acidification potential was calculated from nitrogen volatilization during fertilizer application and nitrite and sulfate emissions from fuel and lignin burning. Nitrogen volatilization was estimated at 10% by Cherubini and Jungmeier (2010). Natural gas emissions were taken from the EPA. Diesel emissions were taken from Ergudenler et al. Solids burning emissions were estimated using elemental analysis. Hydrogen ion equivalence factors were taken from the TRACI model (U.S. EPA, 2012).

7.3.5.3 Global Climate Change

Global climate change potential included carbon sequestration by the corn plant, diesel combustion, natural gas combustion, ethanol combustion, biorefinery solids combustion, fertilizer emissions, ammonia production, enzyme production, and electricity production credits. Carbon sequestration data was taken from Follett et al. (2012). Soil organic carbon sequestration was allocated to corn stover based on the corn stover fraction removed divided by the total above ground carbon and then multiplied by the total carbon (both above and below ground). Emissions from fertilizer and ammonia production were estimated from Wood and Cowie (2004). Enzyme production carbon emissions were estimated by the GREET 2014 model. Average emissions for electricity use/generation were taken from the EPA (2015).

7.4 Results and Discussion

7.4.1 Biomass Production Economics

Biomass cost took into account fertilizer makeup, harvesting, storage, transportation to AFEX depots, AFEX processing, pelletization at the depot, and transportation from the depot to the biorefinery. The total cost of pretreated biomass delivered to the biorefinery was $170/MT. An individual breakdown of the costs can be seen in Table 19. If raw biomass was transported from the field to the biorefinery, transport costs would increase to $12.60/MT compared to $5.94/MT for the depot concept.

Table 19 Biomass production costs

Category	$/MT
Fertilizer	2.19
Harvesting	44.61
Storage	23.85
Transport to Depot	1.77
AFEX Depot Processing	93.07
Transport to Biorefinery	4.17

7.4.2 Process Economic Comparison

The economic comparison was performed using the traditional SSCF as a static model, while comparing multiple RaBIT process models. The model scenarios were compared based on the minimum ethanol selling price (MESP) in 2014 U.S. dollars.

Results for the economic comparison are shown in Table 20. In total, 6 different processes were compared. Both the traditional SSCF and RaBIT Process A used laboratory mass balance data as collected and modeled centrifugation for all solid/liquid separations. Using this comparison, the RaBIT process showed a 72% higher MESP compared to the SSCF process.

The price discrepancy was related to the separation costs and seed culture media costs resulting in 17% electricity revenue for RaBIT Process A compared to the SSCF Process and 81% higher manufacturing costs for RaBIT process A.

While initial economics for RaBIT process A were poor, potential for changes exists within the RaBIT process. The economics showed that enzymatic hydrolysis separation costs and seed culture cost were largely responsible for RaBIT Process A's poor economics. These costs could be lowered by using process changes. The simpler SSCF process would not benefit greatly from any process modifications.

The first RaBIT process modeling change lowered enzymatic hydrolysis separation costs. RaBIT Process B eliminated centrifugation from the EH recycling step to reduce electricity requirements and replaced it with plate and frame filter pressing operated with steam. Centrifugation was still used for fermentation/seed train separations and separating the solids from the beer column bottoms fraction. The switch to filter pressing saw a $200 million dollar decrease in TCI and 218% increase in electricity revenue. The electricity revenue was still 48% below the SSCF process mainly due to higher mixing costs associated with higher solids present in both the RaBIT EH and RaBIT SSCF steps. MESP for RaBIT Process B was reduced to $6.91/gal

The following three RaBIT process changes involved reductions in seed culture use. In RaBIT Process A and B, total seed culture mass was 2.5x higher than in the SSCF process and used a high concentration of tryptone. RaBIT Process C removed the 20 g/L tryptone ($5/kg) and replaced it with 2 g/L potassium phosphate monobasic ($1.5/kg) achieving the same nutrient concentrations as in the SSCF process. Experiments determined that this nutrient change

resulted in a 15% lower OD (data not shown). This was expressed in the model resulting in a $20 million increase in TCI due to increased seed culture reactor requirements. Higher mixing and centrifuge requirements resulted in a 5% decrease in electricity revenue, but was offset with the 15% reduction in manufacturing costs. MESP was further reduced to $5.74/gal

RaBIT Process D investigated reducing the initial inoculum from 17.5 to 10 g/L DCW. Previous results in Figure 34 (Chapter 6) showed that using a 10 g/L DCW inoculum caused a 2 cycle lag in performance likely causing a 1% ethanol yield decrease over 10 cycles. RaBIT Process E increased fermentation cycles by 10 up to 20. This change reduced the RaBIT seed culture requirements to 87% (by mass) of that required by the SSCF process. The ethanol yield was assumed to not change. This process change ended up decreasing RaBIT Process E's MESP enough to show a 7% savings compared to the SSCF process ($3.81/gal). TCI was reduced cumulatively by 30% compared to the SSCF process allowing for less capital investment risk.

Table 20 Traditional SSCF and RaBIT Process comparisons

	Traditional SSCF	RaBIT Process A	RaBIT Process B	RaBIT Process C	RaBIT Process D	RaBIT Process E
MESP ($/gal)	4.10	7.04	6.91	5.74	4.68	3.81
TCI ($)	1.78E+09	1.51E+09	1.31E+09	1.33E+09	1.28E+09	1.25E+09
Ethanol Revenue ($/yr)	2.08E+09	3.86E+09	3.72E+09	3.19E+09	2.35E+09	1.78E+09
Electricity Revenue ($/yr)	2.86E+08	4.72E+07	1.50E+08	1.43E+08	1.65E+08	1.77E+08
Yeast Revenue ($/yr)	-	2.29E+07	2.29E+07	2.29E+07	2.29E+07	2.29E+07
Manufacturing Costs ($/yr)	2.01E+09	3.63E+09	3.63E+09	3.10E+09	2.28E+09	1.74E+09

MESP: Minimum Ethanol Selling Price; TCI: Total Capital Investment; RaBIT Process A: Baseline process; RaBIT Process B: Replace centrifuge with filter press in EH recycle step; RaBIT Process C: Replace tryptone in seed culture to 2 g/L potassium phosphate; RaBIT Process D: Reduce inoculum from 17.5 g/L DCW to 10 g/L DCW; RaBIT Process E: Increase fermentation cycles to 20 from 10

Sensitivity analysis was performed to emphasize differences between the two processes. Sensitivity analysis was performed by changing three factors: enzyme cost, electricity selling price, and the Lang factor associated with the TCI calculation. The traditional SSCF Process and RaBIT process E were used for this study.

Results for the sensitivity analysis are shown in Figure 51. Overall, the results highlight the stability of the RaBIT process results. First for all cases, the RaBIT process MESP was lower than for the SSCF process. Secondly, the slope for the RaBIT process sensitivity lines was lower than for the SSCF process indicating less risk due to enzyme and electricity price fluctuations. Assuming RaBIT Process E can be industrially implemented, the RaBIT process appears to be a safer investment.

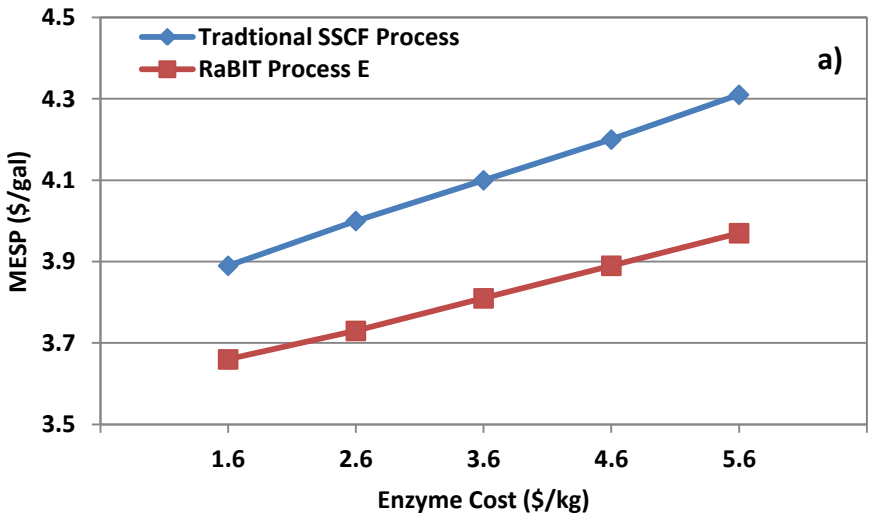

Figure 51 Sensitivity analysis for the Traditional SSCF Process and RaBIT Process E by altering a) enzyme cost, b) electricity selling price, and c) Lang factor

Figure 51 (cont'd)

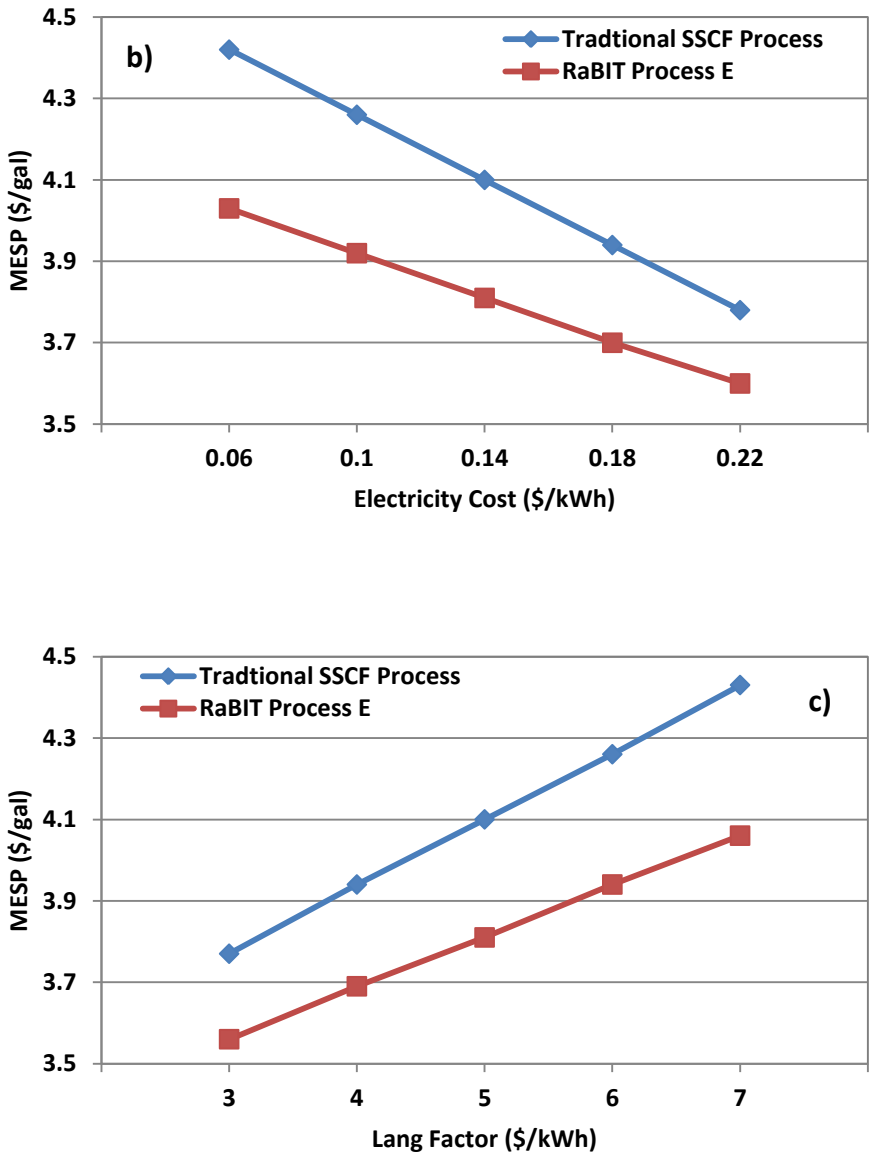

7.4.3 LCA Comparison

The LCA presented deviates slightly from the norm. Standard LCAs use a functional unit to compare two different processes. For this work, data was presented based on both a

20,000 ton/day plant and a more traditional per gallon of ethanol. For the rest of this chapter, RaBIT Process E will be referred to as the RaBIT Process.

Energy balances for the SSCF Process (Table 21) and RaBIT Process (Table 22) are shown below based on the 20,000 ton/day plant. As expected, the SSCF Process generates 25% more energy than the RaBIT Process due to greater ethanol yield and electricity generation. When based on the functional unit, the SSCF and RaBIT processes generate 58.2 MJ/gallon and 50.4 MJ/gallon, respectively. As a reference, a gallon of pure ethanol contains 80.5 MJ of energy.

Table 21 SSCF process energy balance (20,000 ton/day basis)

	Cultivation and Harvesting (MJ/yr)	Transportation (MJ/yr)	AFEX Processing (MJ/yr)	Biorefinery (MJ/yr)	Row Total (MJ/yr)
Ammonia Production	1.84E+08	-	3.43E+09	-	3.61E+09
Phosphorus Pentoxide	-2.92E+07	-	-	-	-2.92E+07
Potassium Chloride	6.67E+06	-	-	-	6.67E+06
Diesel	4.40E+08	3.18E+07	-	-	4.72E+08
Natural Gas	-	-	1.18E+10	-	1.18E+10
Electricity	-	-	2.30E+09	-7.34E+09	-5.05E+09
Ethanol	-	-	-	-4.06E+10	-4.06E+10
Enzyme Production	-	-	-	3.04E+08	3.04E+08
Column Total	6.02E+08	3.18E+07	1.76E+10	-4.77E+10	-2.95E+10

Table 22 RaBIT process energy balance (20,000 ton/day basis)

	Cultivation and Harvesting (MJ/yr)	Transportation (MJ/yr)	AFEX Processing (MJ/yr)	Biorefinery (MJ/yr)	Row Total (MJ/yr)
Ammonia Production	1.84E+08	-	3.43E+09	-	3.61E+09
Phosphorus Fertilizer	-2.92E+07	-	-	-	-2.92E+07
Potassium Fertilizer	6.67E+06	-	-	-	6.67E+06
Diesel	4.40E+08	3.18E+07	-	-	4.72E+08
Natural Gas	-	-	1.18E+10	-	1.18E+10
Electricity	-	-	2.30E+09	-4.55E+09	-2.26E+09
Ethanol	-	-	-	-3.75E+10	-3.75E+10
Enzyme Production	-	-	-	2.26E+08	2.26E+08
Column Total	6.02E+08	3.18E+07	1.76E+10	-4.18E+10	-2.36E+10

Global climate change potential reported in CO_2 equivalents is reported in Table 23. The RaBIT process was 7% more carbon negative compared to the SSCF process when based on the whole 20,000 ton/day process When comparing based on per gallon of ethanol, the RaBIT process (-18.0 kg CO_2 eq./gal) was 17% more carbon negative than the SSCF process (-15.4 kg CO_2 eq./gal). Solids combustion, ethanol combustion, and enzyme production are the main causes for the global climate change potential differences.

Table 23 Global climate change potential (20,000 ton/day basis)

	SSCF Process	RaBIT Process
	(kg CO2 eq./yr)	
Sequestration	-1.61E+10	-1.61E+10
Cult and Harvest	3.64E+07	3.64E+07
Fertilizer	2.14E+07	2.14E+07
Transportation	2.74E+07	2.74E+07
Depot	1.12E+09	1.12E+09
Biorefinery	5.15E+09	4.23E+09
Electricity Credit	-9.66E+08	-4.32E+08
Ethanol Use	2.92E+09	2.69E+09
Total	**-7.82E+09**	**-8.43E+09**

Acidification potentials are shown in Table 24. When based on the 20,000 ton/day plant, the SSCF process has 28% more acidification potential due to greater solids being sent to the furnace, enzyme production, and future ethanol combustion. When based on per gallon of ethanol, the SSCF process has only 19% more acidification potential.

Both processes share the same eutrophication potential when basing off the 20,000 ton/day plant (Table 25). The SSCF process (1.05E-03 kg PO_4 eq./gal) does show less eutrophication potential compared to the RaBIT process (1.15E-03 kg PO_4 eq./gal) when based on per gallon of ethanol.

Table 24 Acidification potentials (20,000 ton/day basis)

	SSCF Process	RaBIT Process
	SOx Acidification (kg H+/yr)	
Cultivation and Harvesting	1.36E+04	1.36E+04
Transport	1.02E+04	1.02E+04
Depot	1.40E+05	1.40E+05
Biorefinery	4.59E+08	1.24E+06
	NOx Acidification (kg H+/yr)	
Cultivation and Harvesting	1.24E+07	1.24E+07
Transport	2.05E+06	2.05E+06
Depot	1.84E+07	1.84E+07
Biorefinery	1.60E+10	1.28E+10
Ethanol Use	2.03E+08	1.87E+08
	NH3 Acidification (kg H+/yr)	
Cultivation and Harvesting	5.51E+07	5.51E+07
Total (kg H+/yr)	***1.67E+10***	***1.30E+10***
Total (kg H+/gal EtOH)	**32.9**	**27.7**

Table 25 Eutrophication potentials (20,000 ton/day basis)

	SSCF Process	RaBIT Process
	Eutrofication (kg PO4 eq./yr)	
Nitrogen	1.62E+05	1.62E+05
Phosphorus	3.76E+05	3.76E+05

Sensitivity analysis was also performed for global climate change potential by manipulating soil carbon sequestration. Global climate change potential for cellulosic ethanol has always been a controversial topic. The majority of studies find cellulosic ethanol as carbon negative, but studies by Liska et al. (2014) and Searchinger et al. (2008) have argued the opposite amid much controversy.

Soil organic carbon sequestration sensitivity results are shown in Figure 52. The original assumptions were based on data from Follett et al. (2012). The Follet data, combined with other

assumptions, resulted in a 0.74 kg C/kg corn stover harvested carbon sequestration value. This number included both the stover harvested and carbon in the roots allocated to the corn stover based on mass. The results showed that the carbon sequestration value needed to be reduced by approximately 50% before the system becomes carbon positive (more CO_2 released to the atmosphere than sequestered by the corn plant).

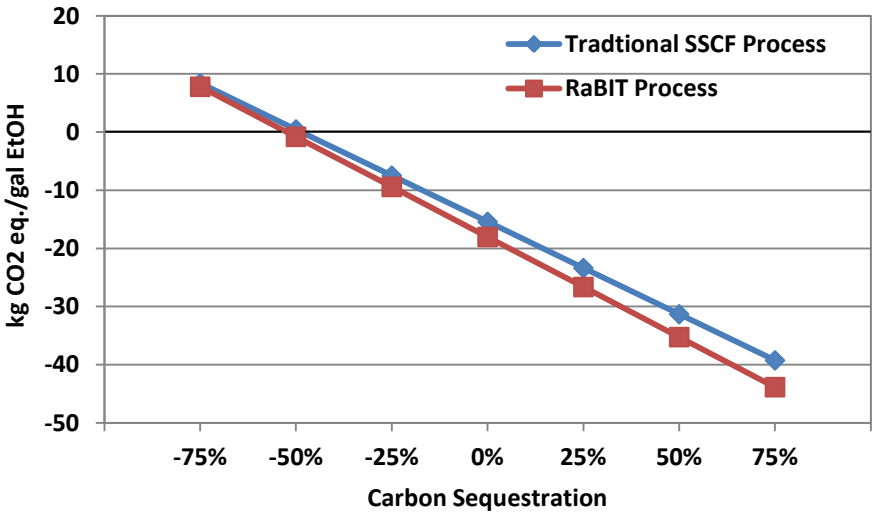

Figure 52 Effect of varying soil organic carbon sequestration on global climate change potential

7.5 Conclusion

Both economic and life cycle analysis were performed comparing a traditional SSCF cellulosic ethanol process to the RaBIT process. When based on original lab data, the RaBIT process was not economical with an MESP of $7.04/gal compared to $4.10/gal for the SSCF process. The RaBIT Process model was changed by replacing enzymatic hydrolysis centrifugation with filter pressing, reducing seed culture requirements backed by lab data, and doubling the number of fermentation cycles. The changes resulted in a lower MESP for the RaBIT process ($3.81/gal) compared to the SSCF process ($4.10/gal). Life cycle analysis showed the RaBIT process had lower climate change potential and acidification potential, while

the SSCF process had lower eutrophication potential and higher energy production. Both processes were carbon negative. In conclusion, the RaBIT has the potential to be an effective cellulosic ethanol process and should be further researched.

CHAPTER 8: PERSPECTIVES

8.1 Overview and Conclusion

This dissertation investigated and improved the RaBIT process fermentations. The RaBIT process was previously invented by the Biomass Conversion Research Laboratory in a large part by Dr. Mingjie Jin. At the start of this work, the RaBIT process had only been performed over 5 cycles and did not show fermentation sustainability as shown by decreases in fermentation performance upon cell recyle. The novelty of the RaBIT process, at that time, was reduced enzyme loading and near complete xylose consumption within 24 h. Economics showed that the process was superior to other processes using the same biomass, enzymes, and microbe (Jin 2012c).

This dissertation investigated the following: RaBIT fermentation compatibility with other microbes (Chapter 2), nutrient dependency (Chapter 4), accurate viable cell profile determination (Chapter 4), pretreatment degradation product effects (Chapter 5), process changes (Chapter 6), economic comparison (Chapter 7), and LCA comparison (Chapter 7). The economic and life cycle analysis compared the RaBIT process to a traditional SSCF process (Chapter 3). The main goals, at the beginning of the dissertation, were to determine why microbe performance decreased upon recycle and to eliminate the performance decrease.

In the end, the two main objectives were completed. Accumulation of degradation products within the cell was determined as the likely cause for the xylose consumption decrease upon cell recycle. Shortening the fermentation time and fed-batch addition of hydrolysate eliminated the xylose consumption decrease over 10 cycles of fermentation, the most tested case. The economic analysis showed that the RaBIT process can still be more economical when

compared to a traditional cellulosic ethanol process. However, the gap between the RaBIT process and a traditional process has been reduced due to advancements in AFEX pretreatment and biocatalyst technology.

8.2 Future

The future of the RaBIT process is questionable. Further biocatalyst improvements may further decrease the economic benefits of the RaBIT process. On the other hand, dramatic reductions in seed culture costs would make the RaBIT process more attractive. Substituting corn steep liquor ($0.18/kg) for yeast extract ($10/kg) reduces the RaBIT MESP to $3.20/gal and eliminates some of the risk associated with the 20 fermentation cycle requirements. This substitution was not included in Chapter 7 as there are doubts on the availability of corn steep liquor (personal dialogue with MBI). AFEX hydrolysate may be an alternative to corn steep liquor. Aeration during the seed culture train would be a potential method for reducing seed culture costs.

Further research on the RaBIT process is recommended. Performing the RaBIT process using *Z. mobilis* 8b as a microbe should be investigated due to the capability to use AFEX hydrolysate as a seed culture media (Chapter 3). Using AFEX hydrolysate as a seed culture medium for *S. cerevisiae* GLBRCY128 should also be investigated. However, doubts exist in the BCRL on the suitability AFEX hydrolysate as seed culture media for yeast due to previous attempts using *S. cerevisiae* 424A(LNH-ST) (data not shown). The RaBIT process should also be investigated using different pretreatments such as dilute acid or extractive ammonia. There are strong suggestions that extractive ammonia pretreatment combined with fed-batch hydrolysate addition within RaBIT process fermentations may yield a healthier cell population.

Extractive ammonia hydrolysate shows increased ODs when compared to AFEX hydrolysates (da Costa Sousa, 2014; Jin et al., 2012a).

In a broader sense, research into breaking down the more recalcitrant oligosaccharides will be critical in the future. As the mass balances in Chapter 6 and 7 show, large quantities of oligosaccharides are still present after fermentation. For the traditional SSCF, ethanol yields could be increased by 12.5% if the oligosaccharides were hydrolyzed and consumed. In the same line of thinking if the residual polysaccharides were consumed, ethanol yields could be increased by a further 8%. Enzyme research will be critical for accomplishing this goal.

APPENDICES

Appendix A: pH Effect

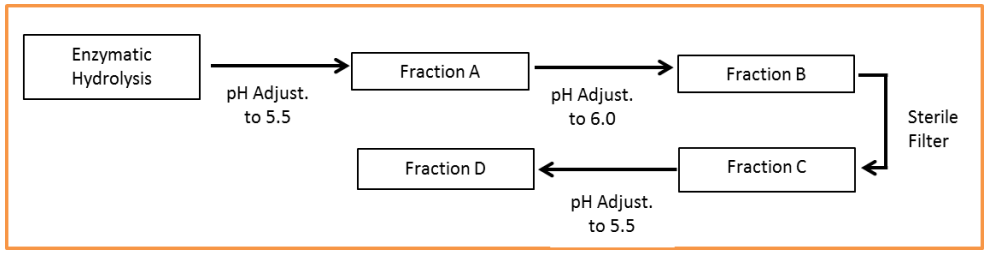

Figure 53 pH Adjustment Method/Hydrolysate Preparation.

Table 26 Results for pH adjustment effect

Hydrolysate Fraction	Glucose, g/L	Xylose, g/L	Ethanol, g/L	OD (600nm)
Fraction A	0.33 ± 0.00	13.21 ± 0.68	36.03 ± 0.16	13.9 ± 0.4
Fraction B	0.36 ± 0.04	8.80 ± 0.33	37.97 ± 0.22	14.2 ± 0.7
Fraction C	0.40 ± 0.03	8.22 ± 0.24	38.38 ± 0.06	13.8 ± 0.3
Fraction D	0.39 ± 0.01	14.46 ± 0.25	35.52 ± 0.02	13.6 ± 0.2

Original hydrolysate sugar concentration for glucose and xylose were 59.34±0.07 g/L and 29.49±0.03 g/L, respectively. Error values represent standard deviations

Appendix B: Synthetic Hydrolysate Recipe

Table 27 Synthetic Hydrolysate Base Recipe

Salts	***(mM)***
KH_2PO_4	6.81
K_2HPO_4	13.01
$(NH_4)_2SO_4$	35
KCl	42.93
NaCl	1.52
CaCl2·2H2O	6.42
MgCl2. 6H2O	14.58
Amino Acids	***(mM)***
L-Alanine	1.367
L-Arginine.HCl	0.168
L-Asparagine	0.266
DL-Aspartic acid.K	0.693
L-Cysteine.HCl	0.058
L-Glutamine	0.302
L-Glutamic acid.K	0.708
Glycine	0.441
L-Histidine	0.044
L-Isoleucine	0.306
L-Leucine	0.433
L-Lysine.HCl	0.204
L-Methionine	0.117
L-Phenylalanine	0.329
L-Proline	0.765
L-Serine	0.431
L-Threonine	0.362
L-Tryptophan	0.058
L-Valine	0.494667
L-Tyrosine	0.236
Nucleic Acids	***(mM)***
Adenine	0.06
Cytosine	0.06
Uracil	0.06
Guanine	0.06
Vitamins	***(μM)***
Thiamine HCl	0.47
Calcium Pantothenate	3.5
Biotin	0.12

Table 27 (cont'd)

Pyridoxine.HCl	2.5
Minerals	***(μM)***
$ZnCl_2$	23.33
$MnCl_2 \cdot 4H_2O$	106.17
$CuCl_2 \cdot 2H_2O$	2.22
$CoCl_2 \cdot 6H_2O$	0.04
H_3BO_4	26.95
$(NH_4)_6Mo_7O_{24} \bullet 4H_2O$	0.36
FeCl3·6H2O	23.33
Acids	***(mM)***
Sodium formate	3.27
Sodium nitrate	1.28
Sodium succinate	0.58
L-lactatic acid (90%)	4.67
Sodium acetate	37.33
Nicotinic Acid	0.03
Carbohydrates	(***mM)***
D-Mannose	1.4
L-Arabinose	23.33
D-Fructose	28
D-Galactose	3.38
D-Glucose	388.5
D(+)Xylose	233.33
Inositol	0.07
Ammonium Compounds	***(mM)***
Choline Chloride	0.35
Betaine.H2O	0.82
DL-Carnitine	0.35
Ammonium Compounds	***(mM)***
Glycerol	4.78
Acetamide	93.33

Table 28 Degradation Product Concentrations

Degradation Product Compounds	mg/L	Accumulating
Feruloyl amide	491.29	Yes
Coumaroyl amide	965.88	Yes*
HMF	0.09	No
p-Coumaric acid	263.67	Yes*
Ferulic acid	9.24	No
Benzoic acid	10.68	No
Syringic acid	1.53	No
Vanillic acid	5.54	No
Vanillin	30.27	No
Syringaldehyde	1	No
4-Hydroxybenzeldehyde	14.82	No
4-Hydroxyacetophenone	0.32	No
Benzamide	0.45	Yes
Vanillyl Alcohol	0.08	Yes
3-Hydroxybenzoic Acid	0.06	No
Acetovanillone	0.69	No
4-Hydroxybenzyl Alcohol	0.8	Yes
4-Hydroxybenzoic Acid	6.83	No
4-Hydroxybenamide	3.92	No
Vanillamide	21.62	Yes
Syringamide	6.86	Yes
GVL	0.13	No
Sinapic Acid	0.11	No

*para-Coumaric acid and coumaroyl amide were not included in the intracellular quantification experiment. Due to its concentration, it was still included in this study. In order to test the hypothesis, para-courmaric, while unknown whether it accumulates or not, was included in the accumulating catergory.

Appendix C: Traditional SSCF Process Procedure

Corn Stover

The corn stover was harvested from Hamilton County, Iowa, and baled by Iowa State University in October, 2011. Further details on the corn stover used can be found in Campbell et al. (2013). AFEX was performed in a pair of 450 L packed-bed reactors. The complete process can be found in Chapter 3. In brief, ammonia vapor was added at a 0.6 g/g biomass ratio. Initially at 100˚C, the biomass was allowed to sit for 30-150 minutes with no external heating before releasing the ammonia. Residual ammonia was removed by introducing low pressure steam at the top of the reactor allowing ammonia vapor to escape from the bottom. After pretreatment, the biomass was pelletized to increase bulk density. The pelleting process was performed as described in Bals et al. (2013) using a Buskirk Engineering PM810 flat die pellet mill. After pelleting, the biomass was dried in a convection oven at 50 °C. The composition was determined to be 34.8% glucan, 18.8% xylan, 3.2% arabinan, and 12.2% acid insoluble lignin. The pellets were stored at room temperature.

Seed Culture

Zymomonas mobilis 8b was used for the fermentations. The strain was provided by the National Renewable Energy Laboratory and was previously engineering to utilize xylose (Mohagheghi et al., 2004).

The seed culture preparation involved stages. For the first stage, a glycerol stock of the strain was used to inoculate a “rich media” composed of 100 g/L glucose, 20 g/L xylose, 10 g/L yeast extract, and 2 g/L potassium phosphate. This stage was performed in 15 mL centrifuge tubes with a 10 mL reaction volume under anaerobic conditions. The tubes were incubated at 30

°C and 100 RPM for 11 h. After 11 h, 5 mL of the first stage was transferred to new rich media 250 mL Erlenmeyer flasks using a reaction volume of 100 mL and incubated for another 11 h.

SSCF Process

The SSCF process was performed in 0.5 L Sartorius bioreactors. The biomass pellets were added at 20% solids loading using a total reaction mass of 400 grams (including biomass, enzymes, water, and inoculum). The biomass was previously autoclaved to eliminate contamination as was also done for the RaBIT process mass balance. The biomass was autoclaved in flasks covered with foil and an aluminum culture cap at 121 °C for 20 minutes with no added water. Half of the pellets were added to the biomass along with the required water. The pH was adjusted to 5.0 using 12.1 M hydrochloric acid. The commercial enzymes Cellic CTec3 and HTec3 (Novozymes, Franklinton, NC, USA) were added at a 10 mg protein/g glucan loading for each (20 mg/g total). The bioreactor was mixed at 50 °C and 100 RPM for 2 h. After 2 h, the second half of the biomass was added and the mixing reduced to 50 RPM. At 5 h, the mixing was increased to 300 RPM. Acid additions were made hourly for the first 5 h. Enzymatic hydrolysis was performed at 50 °C for 48 h.

After 48 h, the slurry was cooled to 32 °C and the pH was adjusted to 6.0 using 10 M potassium hydroxide. Corn steep liquor was added at a 0.25% final concentration. Next, 10% inoculum of *Z. mobilis* 8b was added. Fermentation continued for 72 h at 32 °C and 300 RPM. The pH was maintained at 6.0 using periodic additions of 10 M potassium hydroxide.

Composition and Oligomeric Sugar Analysis

Compositional analysis of biomass and unhydrolyzed solids was performed using the National Renewable Energy Laboratory's standard analytical method as described in Sluiter et al. (2010). The samples were milled before composition analysis using a Cyclotec^{TM} 1093 mill (Foss, Denmark) equipped with a 2 mm screen. Oligomeric and polymeric sugars were determined as also described in Sluiter et al. (2010).

HPLC Analysis

Samples taken during experiments were frozen at -20 °C for storage purposes until ready to be analyzed. Before analysis, the samples were centrifuged and the supernatant was diluted 10x before being run through the HPLC. Glucose, xylose, lactate and ethanol concentrations were analyzed through a Biorad Aminex HPX-87H column. Column temperature was maintained at 50^{o}C. The 5mM H_2SO_4 mobile phase flow rate was 0.6 mL/min.

Mass Balance

A mass balance was performed by first accounting for all sugars initially present in the biomass before enzymatic hydrolysis using the compositional analysis as mentioned above. After fermentation, the solids and liquids were separated by centrifugation at 5300 RPM for 30 min. The oligomeric sugars, monomeric sugars, and ethanol were analyzed for the liquid stream as described above. The mass and volume of the liquid stream was recorded. The water content of the wet solids was determined by addition of a known volume of water. Change is monomeric sugars and ethanol was used to determine the initial water content using the following equation: $Volume_{initial} * Concentration_{initial} = (Volume_{initial} + Volume_{addition}) * Concentration$. The solids were then washed with distilled water three times at a ratio of 2:1 by mass.

Appendix D: Cultivation and Harvesting Model

Table 29 Cultivation and Harvesting Inputs

Inputs	**kg/yr**
Biomass Input	5.96E+09
Nitrogen	5.77E+06
Phosphorous	2.22E+06
Potassium	2.79E+06
Cultivation/Harvesting	1.10E+07
Transport	7.98E+05
Total Diesel Input	1.18E+07
Fertilizer Energy for Production	**MJ/yr**
Nitrogen	1.84E+08
Phosphorous	-2.92E+07
Potassium	6.67E+06
Diesel Energy	**MJ/yr**
Cultivation/Harvesting	4.40E+08
Transport	3.18E+07
Total Diesel Input	4.72E+08

Table 30 Fertilizer Costs

0.55	$/kg = Ammonia
0.39	$/kg = Potash Cost
1.25	$/kg = Phosphorus pentoxide cost
0.65	$/MT biomass = Ammonia
0.34	$/MT biomass = Potash
1.07	$/MT biomass = Phosphorus Pentoxide
2.06	$/MT biomass = Total Fertilizer cost

Table 31 Farm machinery data from Vardas & Digman, 2013

	Initial investment	Useful life (yrs)	Annual use (hr)	Salvage	Repair factor 1	Repair factor 2	Annual investment (AAI)
Shredder	$37,000	10	200	30%	0.46	1.7	$2,590
Large round baler	$55,000	10	200	28%	0.43	1.8	$3,960
Large tractor	$124,000	12	500	27.50%	0.007	2	$7,492
Small tractor	$34,000	12	500	28%	0.007	2	$2,040
Bale wagon	$4,000	10	200	35%	0.19	1.3	$260

Table 32 Harvesting hourly cost and fuel usage

	Hourly fixed cost			Hourly operating cost			Hourly labor cost	Total		
	Depreciation	Interest (5%)	TIH (2%)	R&M cost	Fuel	Lube & Tire			Diesel (gal/hr)	HP
Shredder	$12.95	$0.65	$0.26	$27.65	$21.63	$3.24	$10.00	$76.38	7.725	150
Large round baler	$19.80	$0.99	$0.40	$41.18	-	-		$62.36	-	-
Large tractor	$14.98	$0.75	$0.30	$5.21	$32.45	$4.87	$10.00	$68.55	11.5875	225
Small tractor	$4.08	$0.20	$0.08	$1.43	$15.14	$2.27	$10.00	$33.21	5.4075	105
Bale wagon	$1.30	$0.07	$0.03	$0.94	-	-		$2.33	-	-

Appendix E: Transportation Modeling

3	mi = Average Transport distance within depot radius
40.2685	mi = Average Transport Distance from depots to biorefinery
60	kg/m^3 = loose density
400	kg/m^3 = pelleted density
3715	cu ft = short tractor trailer
4108	cu ft = long tractor trailer
6311.855	kg = per short distance load
36000	kg = per long distance load (limit based on law)
9.44E+05	= # of short distance loads
1.66E+05	= # of long distance loads
9.50E+06	= # of total miles
7	mpg = diesel average fuel efficiency
2.71E+06	gallons = diesel fuel required
2.8	$/gal = current diesel cost
7.60E+06	$ = total transport fuel cost
0.59	$/mile = Truck rental/costs
5.60E+06	$ = Total truck rental cost
3.72	$/MT = Hourly wage ($10/hr)
5.94	$/MT = Transportation Cost

Appendix F: AFEX Depot Modeling

Depot Requirements

For 450L Scale	
Biomass per run (kg)	45
Water loading	0.333333
Ammonia loading (w/w)	0.6
Water added (kg)	1.00E+01
Ammonia needed (kg)	8.10E-01
Ammonia recovery	9.70E-01
Steam required for stripping (kg)	18.9
Steam required for preheating (MJ)	2501472
Loose Biomass Density (kg/m^3)	60
Pelletized Biomass Density (kg/m^3)	400
Compressed NH3 (kg)	40.43698
Compressed NH3 (std m^3)	53.18566
Compressed NH3 (std m^3/s)	0.063316
Compression Work (kW)	14.80706
Compression Energy (MJ)	12.43793
Gamma	1.629889
Compressor Efficiency	0.8
Moisture After AFEX	0.444
Moisture Befor Pelleting	0.24
Final Moisture	0.02
Energy required for first drying (MJ)	49.19962
Energy required for second drying (MJ)	30.10253
Pellet Mill Rate (kg/hr)	9253
Power Consumption (kW)	280
Power consumption (MJ)	4.902194
Boiler Efficiency	0.9
Natural Gas Energy (BTU/cu ft)	1109
For 100MT/day Scale	
Biomass Needed (kg)	1.00E+05
Water needed (kg)	2.22E+04
Ammonia needed (kg)	1.80E+03
Steam Required for Heat (MJ)	2.45E+03
Compressor Electricity Required (MJ)	2.76E+04
Steam Required for Stripping (J)	5.73E+01
Energy Required for Drying (MJ)	1.76E+05
Pellet Mill Electricity (MJ)	1.09E+04
Total Boiler Energy Required (MJ)	1.99E+05

Total Natural Gas Required (cu ft)	1.70E+05

Purchased Costs

5.63E+05	$ = Reactors
6.07E+05	$ = Compressor
	$ = Steam
7.33E+05	Production
147000	$ = Pellet Mill

Variable Costs

0.14	$/kWh = Current Electricity Cost
10	$/1000ft^3 = Current Natural Gas Cost
550	$/MT = Current Ammonia Price
76.46	$/MT = Biomass Cost

Manufacturing Costs

546963.1	$/yr = Electricity
6.20E+05	$/yr = Natural Gas
3.61E+05	$/yr = Ammonia
2.79E+06	$/yr = Biomass
4.32E+06	$/yr = Total Cost

Appendix G: SSCF Biorefinery Modeling

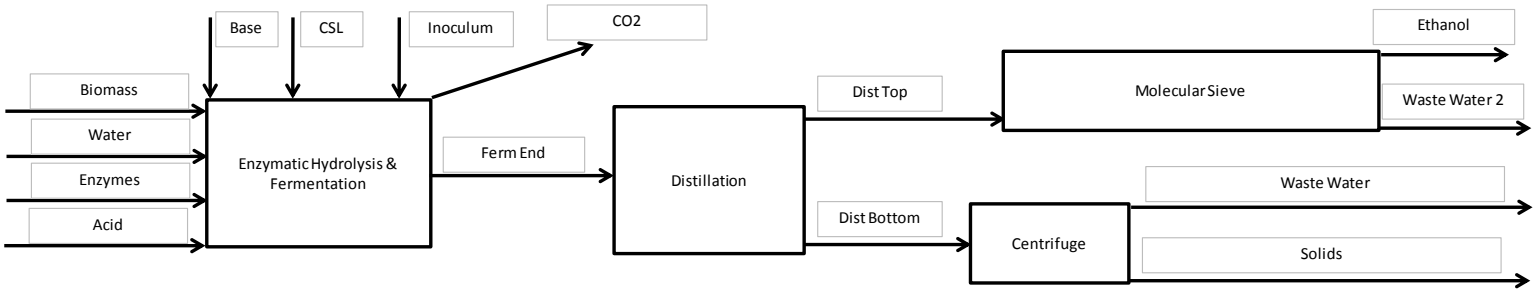

Stream ID	Total Mass (kg)	Mass Ethanol (kg)	Mass Water (kg)	Mass Mono Glucose (kg)	Mass Mono Xylose (kg)	Mass Olig Glucose (kg)	Mass Olig Xylose (kg)	Mass Poly Glucose (kg)	Mass Poly Xylose (kg)	Minor Sugars (kg)	Mass Lignin (kg)	Mass Ash (kg)	Mass Protein (kg)	Mass Acetate (kg)	Mass Bacteria (kg)	Mass Enzymes (kg)	Mass Acid (kg)	Mass Base (kg)	Mass CSL	Mass CO2 (kg)
Biomass	5.96E+09	0	0	0	0	0	0	2.18E+09	1.35E+09	3.33E+08	1.227E+09	4.51E+08	2.68E+08	1.55E+08	0	0	0	0	0	0
Water	2.14E+10	0	21445526881	0	0	0	0	0	0	0	0	0	0	0	0	0	0	0	0	0
Enzymes	43628770	0	0	0	0	0	0	0	0	0	0	0	0	0	0	43628770	0	0	0	0
Acid	51926659	0	0	0	0	0	0	0	0	0	0	0	0	0	0	0	51926659	0	0	0
Base	70446163	0	0	0	0	0	0	0	0	0	0	0	0	0	0	0	0	70446163	0	0
CSL	78468814	0	0	0	0	0	0	0	0	0	0	0	0	0	0	0	0	0	78468814	0
Inoculum	3.43E+09	121191317	3.14E+09	751731.2	50180179	0	0	0	0	0	0	0	0	0	4190281	0	0	0	0	115772300
Ferm End	2.98E+10	1.516E+09	24584279443	0	64975866	79950226.79	322609620	1.58E+08	8.32E+07	1.63E+07	1.172E+09	1.78E+08	0.00E+00	0.00E+00	1.03E+08	43628770	0	0	0	1448366602
Dist Bottom	2.9E+10	0	26794188062	0	64975866	79950226.79	322609620	1.58E+08	83213451	16273588	1.172E+09	1.78E+08	0	0	1.03E+08	43628770	0	0	0	0
Waste Water	2.39E+10	0	23536002042	0	57074770	70228241.17	283380137	0	0	0	0	0	0	0	0	0	0	0	0	0
Solids	5.07E+09	0	3258186020	0	7901096	9721985.626	39229483.3	1.58E+08	83213451	16273588	1.172E+09	1.78E+08	0	0	1.03E+08	43628770	0	0	0	0
Dist Top	1.53E+09	1.52E+09	16170057.51	0	0	0	0	0	0	0	0	0	0	0	0	0	0	0	0	0
Waste Water 2	1.59E+08	0	158662175.2	0	0	0	0	0	0	0	0	0	0	0	0	0	0	0	0	0
Anhydrous Ethanol	1.52E+09	1.52E+09	3038399.941	0	0	0	0	0	0	0	0	0	0	0	0	0	0	0	0	0

Figure 54 SSCF model process flow diagram and stream data.

Enzyme Data

43628770	kg = Total Enzyme Usage
1.8	MJ/kg = Steam Requirement (Dunn et al.)
4	MJ/kg = Electricity Requirement (Dunn et al.)
78531787	MJ = Steam Requirement
1.75E+08	MJ = Electricity Requirment

Overall Energy Data

3.259E+10	MJ = Heat Generated During Combustion
1.66E+09	MJ =Heat Required for Water Vaporization
0.85	= Turbogenerator efficiency
1.36E+10	MJ = Heat Required for Process
8.48E+09	MJ = Electricity Generated
9.51E+07	MJ = Electricity Required for Centrifuge
8.16E+07	MJ = Electricity Required for Mixing
9.82E+08	MJ = Electricity required for Cooling Water
8.36E+07	MJ = Electricity required for WWT
7.32E+09	MJ = Electricity Sold to Grid

Purchased Costs

2.68E+07	$ = Seed Train Bioreactors, Agitators, and Heat Exchangers
6.95E+07	$= Distillation
1.06E+06	$=Molecular Sieve Unit
3.08E+05	$ = Initial Molecular Sieve
1.56E+06	$ = Centrifuge
9.22E+06	$ = Cooling Water Tower
1.98E+08	$ = SSCF Tanks, agitators, and heat exchangers
1.10E+07	$ = Heat Exchangers
2.64E+07	$ = Steam and Electricity
1.27E+07	$ = WW Treatment Purchased

Material Prices

0.16953	$/kg = Biomass Cost

3.6	$/kg = Enzyme Cost
0.18	$/kg = Corn Steep Liquor Cost
1	$/kg = Base Cost (Solid cost)
0.25	$/kg = Acid Cost (98%)
0.5	$/kg = Dextrose monohydrate
2	$/kg = Xylose
10	$/kg = Yeast Extract
1.5	$/kg = Potassium Phosphate
0.14	$/kWh = Current Electricity Cost

Manufacturing Costs

1.01E+09	$ = Biomass
1.57E+08	$ = Enzyme
1.41E+07	$ = Corn Steep Liquor
7.04E+07	$ = Base Cost
1.30E+07	$ = Acid Cost
1.99E+08	$ = Glucose
1.44E+08	$ = Xylose
3.61E+08	$ = Yeast Extract
1.08E+07	$ = Potassium Phosphate
1.98E+09	$ = Total Costs

Appendix H: RaBIT Process E Biorefinery Modelling

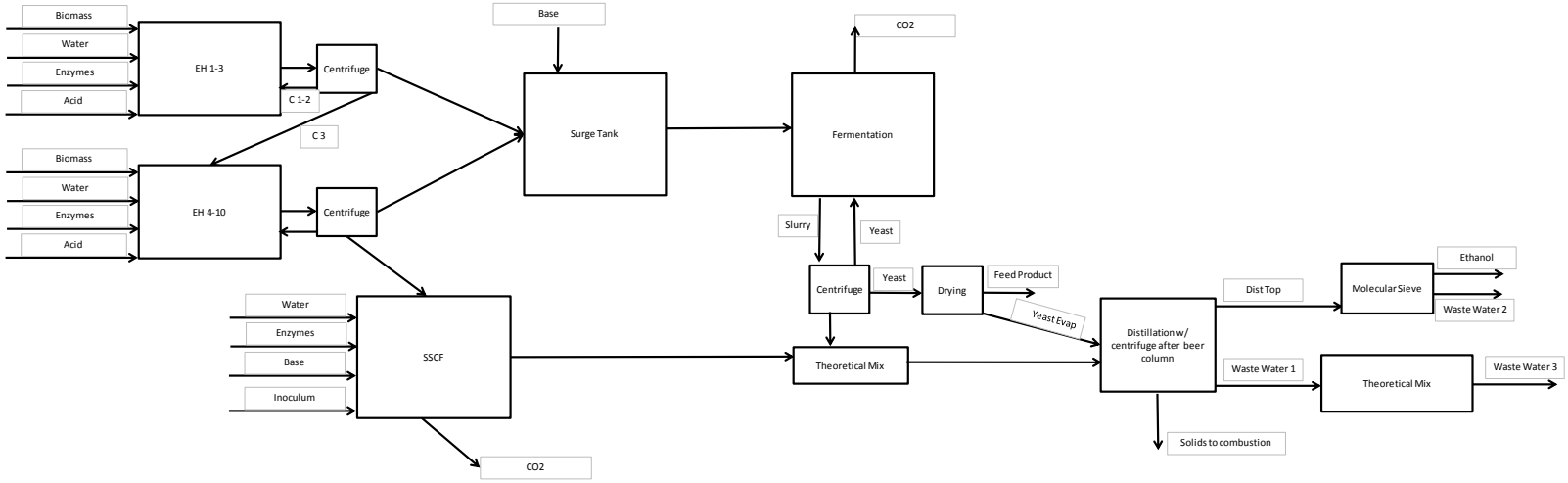

Figure 55 RaBIT model process flow diagram.

Stream ID	Total Mass (kg)	Mass Ethanol (kg)	Mass Water (kg)	Mass Mono Glucose (kg)	Mass Mono Xylose (kg)	Mass Olig Glucose (kg)	Mass Olig Xylose (kg)	Mass Poly Glucose (kg)	Mass Poly Xylose (kg)	Minor Sugars (kg)	Mass Lignin (kg)	Mass Ash (kg)	Mass Protein (kg)	Mass Acetate (kg)	Mass Yeast (kg)	Mass Enzymes (kg)	Mass Acid (kg)	Mass Base (kg)	Mass CO2 (kg)
Biomass	5.96E+09	0	0	0	0	0	0	2.18E+09	1.35E+09	3.33E+08	1226609160	4.51E+08	2.68E+08	1.55E+08	0	0	0	0	0
EH Water	24906109804	0	24906109804	0	0	0	0	0	0	0	0	0	0	0	0	0	0	0	0
EH Enzymes	30331934.96	0	0	0	0	0	0	0	0	0	0	0	0	0	0	3.03E+07	0	0	0
Acid	22908383.01	0	0	0	0	0	0	0	0	0	0	0	0	0	0	0	22908383	0	0
EH1	3.09E+09																		
EH2	3.89E+09																		
EH3	4.54E+09																		
EH4	5.14E+09																		
EH5	5.01E+09																		
EH6	5.08E+09																		
EH7	5.08E+09																		
EH8	5.08E+09																		
EH9	5.08E+09																		
EH10	5.08E+09																		
Hydrolysate Produced	2.25E+10	0	1.99E+10	1.39E+09	6.87E+08	1.91E+08	3.46E+08	0	0	0	0	0	0	0	0	1.52E+07	0	0	0
SSCF Water	2.14E+09	0	2.14E+09	0	0	0	0	0	0	0	0	0	0	0	0	0	0	0	0
SSCF Enzymes	2.34E+06	0	0.00E+00	0	0	0	0	0	0	0	0	0	0	0	0	2.34E+06	0	0	0
SSCF Base	5.28E+06	0	0.00E+00	0	0	0	0	0	0	0	0	0	0	0	0	0	0	5.28E+06	0
SSCF Inoculum Slurry	125550648	4639939.92	1.18E+08	0	1966557	0	0	0	0	0	0	0	0	0	599881	0	0	0.00E+00	0
SSCF Inoculum Pellet	5577713.09	0.00E+00	4.90E+06	0	78662.29	0	0	0	0	0	0	0	0	0	599881	0	0	0.00E+00	0
SSCF Inoculum Broth	1.20E+08	4.45E+06	1.13E+08	0	1887895	0	0	0	0	0	0	0	0	0	0	0	0	0.00E+00	0
SSCF Inoculum CO2	4432467.022	0	0.00E+00	0	0	0	0	0	0	0	0	0	0	0	0	0	0	0.00E+00	4432467
SSCF1	8.60E+08																		
SSCF2	8.60E+08																		
SSCF3	8.60E+08																		
SSCF4	8.60E+08																		
SSCF5	8.60E+08																		
SSCF6	8.60E+08																		
SSCF7	3.44E+09																		
SSCF Broth Slurry	7.67E+09	2.45E+08	5.81E+09	0.00E+00	2.12E+07	1.24E+07	4.84E+07	7.96E+07	5.38E+07	1.07E+07	1.08E+09	2.95E+08	0.00E+00	0.00E+00	0	1.75E+07	0	0.00E+00	0
SSCF CO2	234358001.6	0	0.00E+00	0	0	0	0	0	0	0	0	0	0	0	0	0	0	0.00E+00	2.34E+08
Ferm Base	16577208.98	0	0.00E+00	0	0	0	0	0	0	0	0	0	0	0	0	0	0	1.66E+07	0
Ferm Inoculum Slurry	2.77E+09	1.02E+08	2.61E+09	0	4.34E+07	0	0	0	0	0	0	0	0	0	1.32E+07	0	0	0.00E+00	0
Ferm Inoculum Pellet	1.23E+08	0.00E+00	1.08E+08	0	1.74E+06	0	0	0	0	0	0	0	0	0	1.32E+07	0	0	0.00E+00	0
Ferm Inoculum Broth	2.65E+09	1.02E+08	2.50E+09	0.00E+00	4.16E+07	0.00E+00	0.00E+00	0.00E+00	0.00E+00	0.00E+00	0.00E+00	0.00E+00	0.00E+00	0.00E+00	0.00E+00	0.00E+00	0.00E+00	0.00E+00	0.00E+00
Ferm Inoculum CO2	97783075.25	0	0.00E+00	0	0.00E+00	0	0.00E+00	0	0.00E+00	0	0.00E+00	0	0.00E+00	0	0.00E+00	0	0.00E+00	0.00E+00	9.78E+07
Ferm Slurry	2.23E+10	1.09E+09	2.07E+10	2.60E+07	1.20E+08	6.31E+07	2.58E+08	0	0	0	0	0	0	0	6.54E+07	0	0	0.00E+00	0.00E+00
Ferm1	2.23E+09																		
Ferm2	2.23E+08																		
Ferm3	2.23E+07																		
Ferm4	2.23E+06																		
Ferm5	2.23E+05																		
Ferm6	2.23E+04																		
Ferm7	2.23E+03																		
Ferm8	2.23E+02																		
Ferm9	2.23E+01																		
Ferm10	2.23E+00																		
Ferm Broth	2.17E+10	1.04E+09	2.02E+10	2.52E+07	1.17E+08	6.14E+07	2.51E+08	0.00E+00	0.00E+00	0.00E+00	0.00E+00	0.00E+00	0.00E+00	0.00E+00	0.00E+00	1.52E+07	0.00E+00	0.00E+00	0.00E+00
Ferm Pellet	6.08E+08	0.00E+00	5.30E+08	7.08E+05	3.30E+06	1.74E+06	7.11E+06	0	0	0	0	0	0	0	6.54E+07	0	0	0	0
Ferm CO2	1038481671	0	0.00E+00	0	0.00E+00	0	0	0	0	0	0	0	0	0	0	0	0	0	1.04E+09
Pre-Distillation	3.26E+10	1.40E+09	2.91E+10	2.52E+07	1.82E+08	7.38E+07	3.00E+08	7.96E+07	5.38E+07	1.07E+07	1.08E+09	2.95E+08	0.00E+00	0.00E+00	0.00E+00	3.27E+07	0.00E+00	0.00E+00	0.00E+00
Waste Water 1	26758299429	0	2.62E+10	2.28E+07	1.64E+08	6.65E+07	2.70E+08	0.00E+00	0.00E+00	0.00E+00	0.00E+00	0.00E+00	0.00E+00	0.00E+00	0.00E+00	0.00E+00	0.00E+00	0.00E+00	0.00E+00
Waste Water 2	2.80E+06	0.00E+00	2.80E+06	0	0.00E+00	0.00E+00	0.00E+00	0.00E+00	0.00E+00	0.00E+00	0.00E+00	0.00E+00	0.00E+00	0.00E+00	0.00E+00	0.00E+00	0.00E+00	0.00E+00	0.00E+00
Waste Water 3	26761096522	0	26237886962	22750819	1.64E+08	66493886.76	270202283	0	0	0	0	0	0	0	0	0	0	0	0
Solids	4477980792	0	2.87E+09	2.49E+06	1.79E+07	7.28E+06	2.96E+07	7.96E+07	5.38E+07	1.07E+07	1.08E+09	2.95E+08	0.00E+00	0.00E+00	0.00E+00	3.27E+07	0	0	0
Dry Feed Product	65389818.29	0	0.00E+00	0	0.00E+00	0	0	0	0	0	0	0	0	0	6.54E+07	0	0.00E+00	0.00E+00	0.00E+00
Dist Top	1470178634	1395749403	7.44E+07	0	0.00E+00	0	0.00E+00	0	0.00E+00	0	0.00E+00	0	0.00E+00	0	0.00E+00	0	0.00E+00	0.00E+00	0.00E+00
Anhydrous Ethanol	1.40E+09	1.40E+09	2.80E+06	0	0	0	0	0	0	0	0	0	0	0	0	0	0	0	0

Not to Be Included in Any Mass Balance Equations

Figure 56 RaBIT model stream data.

Enzyme Data

3.27E+07	kg = Total Enzyme Usage
1.8	MJ/kg = Steam Requirement (Dunn et al.)
4	MJ/kg = Electricity Requirement (Dunn et al.)
58800885	MJ = Steam Requirement
1.31E+08	MJ = Electricity Requirment

Overall Energy Data

2.818E+10	MJ = Heat Generated During Combustion
1.47E+09	MJ =Heat Required for Water Vaporization
0.85	= Turbogenerator efficiency
1.27E+10	MJ = Heat Required for Process
2.29E+07	MJ = Steam Energy Required for Filter Press
6.33E+09	MJ = Electricity Generated
5.54E+08	MJ = Electricity Required for Centrifuge and Mixing
1.20E+09	MJ = Electricity required for Cooling Water
9.87E+07	MJ = Electricity required for WWT
4.48E+09	MJ = Electricity Sold to Grid

Purchased Costs

2.49E+06	$ = Seed Train Bioreactors, Agitators, and Heat Exchangers
6.51E+07	$= Distillation
1.04E+06	$=Molecular Sieve Unit
2.83E+05	$ = Initial Molecular Sieve
8.00E+06	$ = Centrifuge
1.09E+07	$ = Cooling Water Tower
1.13E+08	$ = SSCF Tanks, agitators, and heat exchangers
8.46E+06	$ = Heat Exchangers
2.38E+07	$ = Steam and Electricity
1.36E+07	$ = WW Treatment Purchased
1.95E+06	$ = Filter Press

Material Prices

0.16953	$/kg = Biomass Cost
3.6	$/kg = Enzyme Cost
0.18	$/kg = Corn Steep Liquor Cost
1	$/kg = Base Cost (Solid cost)
0.25	$/kg = Acid Cost (98%)
0.5	$/kg = Dextrose monohydrate
2	$/kg = Xylose
10	$/kg = Yeast Extract
1.5	$/kg = Potassium Phosphate
0.14	$/kWh = Current Electricity Cost

Manufacturing Costs

1.01E+09	$ = Biomass
1.09E+08	$ = Enzyme
2.19E+07	$ = Base Cost
5.73E+06	$ = Acid Cost
1.21E+08	$ = Glucose
1.46E+08	$ = Xylose
2.92E+08	$ = Yeast Extract
8.77E+06	$ = Tryptone
1.72E+09	$ = Total Costs

REFERENCES

REFERENCES

Achyuthan, K. E., Achyuthan, A. M., Adams, P. D., Dirk, S. M., Harper, J. C., Simmons, B. A., & Singh, A. K. (2010). Supramolecular self-assembled chaos: polyphenolic lignin's barrier to cost-effective lignocellulosic biofuels. *Molecules*, *15*(12), 8641–88. doi:10.3390/molecules15118641

Aden, A., Ruth, M., Ibsen, K., Jechura, J., Neeves, K., Sheehan, J., Wallace, B., et al. (2002). Lignocellulosic Biomass to Ethanol Process Design and Economics Utilizing Co-Current Dilute Acid Prehydrolysis and Enzymatic Hydrolysis for Corn Stover. *NREL Technical Report*.

Ajanovic, A. (2011). Biofuels versus food production: Does biofuels production increase food prices? *Energy*, *36*(4), 2070–2076. doi:10.1016/j.energy.2010.05.019

Alaska Pellet Mill. (2010). Ring Die Pellet Mills. Retrieved March 12, 2015, from http://www.alaskapelletmill.com/ring_die_pellet_mills

Alvira, P., Tomás-Pejó, E., Ballesteros, M., & Negro, M. J. (2010). Pretreatment technologies for an efficient bioethanol production process based on enzymatic hydrolysis: A review. *Bioresource technology*, *101*(13), 4851–61. doi:10.1016/j.biortech.2009.11.093

Alonso, D. M., Bond, J. Q., & Dumesic, J. A. (2010). Catalytic conversion of biomass to biofuels. *Green Chemistry*, *12*(9), 1493. doi:10.1039/c004654j

Austin, G. D., Watson, R. W., & D'Amore, T. (1994). Studies of on-line viable yeast biomass with a capacitance biomass monitor. *Biotechnology and bioengineering*, *43*(4), 337–41. doi:10.1002/bit.260430411

Balan, V. (2014). Current Challenges in Commercially Producing Biofuels from Lignocellulosic Biomass, *2014*(i).

Balan, V., Bals, B., Chundawat, S. P. S., Marshall, D., & Dale, B. E. (2009). Lignocellulosic Biomass Pretreatment Using AFEX. In J. R. Mielenz (Ed.), *Biofuels: Methods and Protocols* (Vol. 581, pp. 61–77). Totowa, NJ: Humana Press. doi:10.1007/978-1-60761-214-8

Balan, V., da Costa Sousa, L., Chundawat, S. P. S., Marshall, D., Sharma, L. N., Chambliss, C. K., & Dale, B. E. (2009). Enzymatic digestibility and pretreatment degradation products of AFEX treated hardwoods (Populus nigra). *American Institute of Chemical Engineers*, *25*(2), 365–375. doi:10.1021/bp.160

Bals, B. D., & Dale, B. E. (2012). Developing a model for assessing biomass processing technologies within a local biomass processing depot. *Bioresource technology*, *106*, 161–9. doi:10.1016/j.biortech.2011.12.024

Bals, B. D., Gunawan, C., Moore, J., Teymouri, F., & Dale, B. E. (2013). Enzymatic hydrolysis of pelletized AFEX(TM) -treated corn stover at high solid loadings. *Biotechnology and Bioengineering*, *111*(2), 264–271. doi:10.1002/bit.25022

Bals, B., Murnen, H., Allen, M., & Dale, B. (2010). Ammonia fiber expansion (AFEX) treatment of eleven different forages: Improvements to fiber digestibility in vitro. *Animal Feed Science and Technology*, *155*(2-4), 147–155. doi:10.1016/j.anifeedsci.2009.11.004

Brochado, A. R., Matos, C., Møller, B. L., Hansen, J., Mortensen, U. H., & Patil, K. R. (2010). Improved vanillin production in baker's yeast through in silico design. *Microbial cell factories*, *9*(1), 84. doi:10.1186/1475-2859-9-84

Bryan, A. K., Goranov, A., Amon, A., & Manalis, S. R. (2009). Measurement of mass, density, and volume during the cell cycle of yeast. *Proceedings of the National Academy of Sciences*, *107*(3), 999–1004. doi:10.1073/pnas.0901851107

Campbell, T. J., Teymouri, F., Bals, B. D., Glassbrook, J., Nielson, C. D., & Videto, J. J. (2013). A packed bed Ammonia Fiber Expansion reactor system for pretreatment of agricultural residues at regional depots. *Biofuels*, *4*(1), 23–34. doi:10.4155/bfs.12.71

Carroll, A., & Somerville, C. (2009). Cellulosic biofuels. *Annual review of plant biology*, *60*, 165–82. doi:10.1146/annurev.arplant.043008.092125

Çaylak, B., & Vardar Sukan, F. (1998). Comparison of different production processes for bioethanol. *Turkish Journal of Chemistry*, *22*, 351–359. Retrieved from http://mistug.tubitak.gov.tr/bdyim/abs.php?dergi=kim&rak=96041

Cherubini, F., & Jungmeier, G. (2010). LCA of a biorefinery concept producing bioethanol , bioenergy , and chemicals from switchgrass. *The International Journal of Life Cycle Assessment*, 53–66. doi:10.1007/s11367-009-0124-2

Chundawat, S. P. S., Balan, V., & Dale, B. E. (2007). Effect of particle size based separation of milled corn stover on AFEX pretreatment and enzymatic digestibility. *Biotechnology and Bioengineering*, *96*(2), 219–231. doi:10.1002/bit

Chundawat, S. P. S., Donohoe, B. S., Da Costa Sousa, L., Elder, T., Agarwal, U. P., Lu, F., Ralph, J., et al. (2011). Multi-scale visualization and characterization of lignocellulosic plant cell wall deconstruction during thermochemical pretreatment. *Energy & Environmental Science*, *4*(3), 973. doi:10.1039/c0ee00574f

Chundawat, S. P. S., Vismeh, R., Sharma, L. N., Humpula, J. F., Da Costa Sousa, L., Chambliss, C. K., Jones, A. D., et al. (2010). Multifaceted characterization of cell wall decomposition

products formed during ammonia fiber expansion (AFEX) and dilute acid based pretreatments. *Bioresource …*, *101*(21), 8429–38. doi:10.1016/j.biortech.2010.06.027

Curran, M. A. (2006). Life Cycle Assessment: Principles and Practice. *National Risk Management Reserach Laboratory*.

da Costa Sousa, L. (2014). EXTRACTIVE AMMONIA (EA): A NOVEL AMMONIA-BASED PRETREATMENT TECHNOLOGY FOR LIGNOCELLULOSIC BIOMASS. *Michigan State University*.

da Silva-Filho, E. A., Brito dos Santos, S. K., Resende, A. D. M., De Morais, J. O. F., De Morais, M. A., & Ardaillon Simões, D. (2005). Yeast population dynamics of industrial fuel-ethanol fermentation process assessed by PCR-fingerprinting. *Antonie van Leeuwenhoek*, *88*(1), 13–23. doi:10.1007/s10482-004-7283-8

de Hoon MJL, Imoto S, Nolan J, Miyano S. (2004). Open source clustering software. *Bioinformatics, 20(9)*:1453-4.

de Vasconcelos, M. C. B. M., Bennett, R., Castro, C., Cardoso, P., Saavedra, M. J., & Rosa, E. A. (2013). Study of composition, stabilization and processing of wheat germ and maize industrial by-products. *Industrial Crops and Products*, *42*, 292–298. doi:10.1016/j.indcrop.2012.06.007

Dien, B. S., Cotta, M. A., & Jeffries, T. W. (2003). Bacteria engineered for fuel ethanol production: current status. *Applied Microbiology and Biotechnology*, *63*(3), 258–66. doi:10.1007/s00253-003-1444-y

Du, B., Sharma, L. N., Becker, C., Chen, S.-F., Mowery, R. a, Van Walsum, G. P., & Chambliss, C. K. (2010). Effect of varying feedstock-pretreatment chemistry combinations on the formation and accumulation of potentially inhibitory degradation products in biomass hydrolysates. *Biotechnology and bioengineering*, *107*(3), 430–40. doi:10.1002/bit.22829

Dunn, J. B., Mueller, S., Wang, M., & Han, J. (2012). Energy consumption and greenhouse gas emissions from enzyme and yeast manufacture for corn and cellulosic ethanol production. *Biotechnology letters*, *34*(12), 2259–63. doi:10.1007/s10529-012-1057-6

Eranki, P. L., Bals, B. D., & Dale, B. E. (2011). Advanced Regional Biomass Processing Depots : a key to the logistical challenges of the cellulosic biofuel industry. *Biofuels, Bioproducts and Biorefining*, 621–630. doi:10.1002/bbb

Ergudenler, A., Jennejohn, D., & Edwards, W. (n.d.). Heavy-Duty Diesel Vehicle Emissions in Greater Vancouver, 1–18.

Fan, C., Qi, K., Xia, X.-X., & Zhong, J.-J. (2013). Efficient ethanol production from corncob residues by repeated fermentation of an adapted yeast. *Bioresource technology*, *136*, 309–15. doi:10.1016/j.biortech.2013.03.028

Ferreira, A. P., Vieira, L. M., Cardoso, J. P., & Menezes, J. C. (2005). Evaluation of a new annular capacitance probe for biomass monitoring in industrial pilot-scale fermentations. *Journal of biotechnology*, *116*(4), 403–9. doi:10.1016/j.jbiotec.2004.12.006

Follett, R. F., Vogel, K. P., Varvel, G. E., Mitchell, R. B., & Kimble, J. (2012). Soil Carbon Sequestration by Switchgrass and No-Till Maize Grown for Bioenergy, 866–875. doi:10.1007/s12155-012-9198-y

Gan, Q., Allen, S. ., & Taylor, G. (2003). Kinetic dynamics in heterogeneous enzymatic hydrolysis of cellulose: an overview, an experimental study and mathematical modelling. *Process Biochemistry*, *38*(7), 1003–1018. doi:10.1016/S0032-9592(02)00220-0

Gao, D., Uppugundla, N., Chundawat, S. P., Yu, X., Hermanson, S., Gowda, K., Brumm, P., et al. (2011). Hemicellulases and auxiliary enzymes for improved conversion of lignocellulosic biomass to monosaccharides. *Biotechnology for biofuels*, *4*(1), 5. doi:10.1186/1754-6834-4-5

GHK. (2006). *A study to examine the benefits of the End of Life Vehicles Directive and the costs and benefits of a revision of the 2015 targets for recycling , re-use and recovery under the ELV Directive*.

Graham, R. L., Nelson, R., Sheehan, J., Perlack, R. D., & Wright, L. L. (2007). Current and Potential U.S. Corn Stover Supplies. *American Society of Agronomy*, 1–11. doi:10.2134/agronj2005.0222

Green, D. W., & Perry, R. H. (2007). *Perry's Chemical Engineers' Handbook* (8th ed.). McGraw-Hill.

GREET Life Cycle Model. (2014). Argonne National Laboratory.

Haines, A., Kovats, R. S., Campbell-Lendrum, D., & Corvalan, C. (2006). Climate change and human health: impacts, vulnerability and public health. *Public health*, *120*(7), 585–96. doi:10.1016/j.puhe.2006.01.002

Harris, C. M., Todd, R. W., Bungard, S. J., Lovitt, R. W., Morris, G., & Keli, D. B. (1986). Dielectric permittivity of microbial suspensions at radio frequencies : a novel method for the real-time estimation of microbial biomass, *9*, 181–186.

Hess, J. R., Wright, C. T., & Kenney, K. L. (2007). Cellulosic biomass feedstocks and logistics for ethanol production. *Biofuels, Bioproducts and Biorefining*, 181–190. doi:10.1002/bbb

Ho, N. W., Chen, Z., Brainard, A. P., & Sedlak, M. (1999). Successful design and development of genetically engineered Saccharomyces yeasts for effective cofermentation of glucose and xylose from cellulosic biomass to fuel ethanol. *Advances in biochemical engineering/biotechnology*, *65*, 163–92. Retrieved from http://www.ncbi.nlm.nih.gov/pubmed/10533435

Humbird, D., Davis, R., Tao, L., Kinchin, C., Hsu, D., Aden, A., Schoen, P., et al. (2011). Process Design and Economics for Biochemical Conversion of Lignocellulosic Biomass to Ethanol: Dilute-Acid Pretreatment and Enzymatic Hydrolysis of Corn Stover. *NREL Technical Report*.

Huuskonen, A., Markkula, T., Vidgren, V., Lima, L., Mulder, L., Geurts, W., Walsh, M., et al. (2010). Selection from industrial lager yeast strains of variants with improved fermentation performance in very-high-gravity worts. *Applied and environmental microbiology*, *76*(5), 1563–73. doi:10.1128/AEM.03153-09

IPCC (Intergovernmental Panel on Climate Change) (2007). Climate Change 2007 : Synthesis Report.

Irvine, G. M. (1985). The significance of the glass transition of lignin in thermomechanical pulping. *Wood Science and Technology*, *19*(2), 139–149. doi:10.1007/BF00353074

Ivanova, V., Petrova, P., & Hristov, J. (2011). Application in the Ethanol Fermentation of Immobilized Yeast Cells in Matrix of Alginate / Magnetic anoparticles , on Chitosan-Magnetite Microparticles and Cellulose-coated Magnetic anoparticles. *International Review of Chemical Engineering*, *3*(March), 289–299.

Jin, M. (2012c). INTEGRATED BIOLOGICAL PROCESSES FOR CONVERSION OF AFEXTM PRETREATED BIOMASS TO ETHANOL. *Michigan State University*.

Jin, M., Balan, V., Gunawan, C., & Dale, B. E. (2012b). Quantitatively understanding reduced xylose fermentation performance in AFEX^{TM} treated corn stover hydrolysate using Saccharomyces cerevisiae 424A (LNH-ST) and Escherichia coli KO11. *Bioresource technology*, *111*, 294–300. doi:10.1016/j.biortech.2012.01.154

Jin, M., Gunawan, C., Uppugundla, N., Balan, V., & Dale, B. E. (2012a). A novel integrated biological process for cellulosic ethanol production featuring high ethanol productivity, enzyme recycling and yeast cells reuse. *Energy & Environmental Science*, *5*(5), 7168. doi:10.1039/c2ee03058f

Jin, M., Sarks, C., Gunawan, C., Bice, B. D., Simonett, S. P., Avanasi Narasimhan, R., Willis, L. B., et al. (2013). Phenotypic selection of a wild Saccharomyces cerevisiae strain for simultaneous saccharification and co-fermentation of AFEXTM pretreated corn stover. *Biotechnology for biofuels*, *6*(1), 108. doi:10.1186/1754-6834-6-108

Jørgensen, H., Vibe-pedersen, J., Larsen, J., & Felby, C. (2007). Liquefaction of Lignocellulose at High-Solids Concentrations. *Biotechnology and Bioengineering*, *96*(5), 862–870. doi:10.1002/bit

Kaliyan, N., & Morey, R. V. (2009). Densification characteristics of corn stover and switchgrass. *Transactions of the ASABE*, *52*(3), 907–920. Retrieved from http://www.biomasschpethanol.umn.edu/August 2010

updates/Densification_Articles/Kaliyan and Morey_2009_Transactions of the ASABE_52(3)_907-920.pdf

Kazi, F. K., Fortman, J., Anex, R., Kothandaraman, G., Hsu, D., Aden, A., & Dutta, A. (2010). Techno-Economic Analysis of Biochemical Scenarios for Production of Cellulosic Ethanol. *NREL Technical Report.*

Keating, D. H., Zhang, Y., Ong, I. M., McIlwain, S., Morales, E. H., Grass, J. a, Tremaine, M., et al. (2014). Aromatic inhibitors derived from ammonia-pretreated lignocellulose hinder bacterial ethanologenesis by activating regulatory circuits controlling inhibitor efflux and detoxification. *Frontiers in microbiology*, *5*(August), 402. doi:10.3389/fmicb.2014.00402

Kim, S., & Dale, B. (2015). All biomass is local: The cost, volume produced, and global warming impact of cellulosic biofuels depend strongly on logistics and local conditions. *Biofuels, Bioproducts and Biorefining*, 1–13. doi:10.1002/bbb

Klein-Marcuschamer, D., Simmons, B. A., & Blanch, H. W. (2011). Techno-economic analysis of a lignocellulosic ethanol biorefinery with ionic liquid pre-treatment. *Biofuels, Bioproducts and Biorefining*, 562–569. doi:10.1002/bbb

Klinke, H. B., Thomsen, a B., & Ahring, B. K. (2004). Inhibition of ethanol-producing yeast and bacteria by degradation products produced during pre-treatment of biomass. *Applied microbiology and biotechnology*, *66*(1), 10–26. doi:10.1007/s00253-004-1642-2

Kotter, P. & Ciriacy, M. (1993). Xylose fermentation by Saccharomyces cerevisiae. *Applied microbiology and biotechnology* 38, 776–783.

Krishnan, C., Sousa, L. D. C., Jin, M., Chang, L., Dale, B. E., & Balan, V. (2010). Alkali-based AFEX pretreatment for the conversion of sugarcane bagasse and cane leaf residues to ethanol. *Biotechnology and Bioengineering*, *107*(3), 441–50. doi:10.1002/bit.22824

Kristensen, J. B., Felby, C., & Jørgensen, H. (2009). Yield-determining factors in high-solids enzymatic hydrolysis of lignocellulose. *Biotechnology for biofuels*, *2*(1), 11. doi:10.1186/1754-6834-2-11

Kuyper, M., Winkler, A. a, Van Dijken, J. P., & Pronk, J. T. (2004). Minimal metabolic engineering of Saccharomyces cerevisiae for efficient anaerobic xylose fermentation: a proof of principle. *FEMS yeast research*, *4*(6), 655–64. doi:10.1016/j.femsyr.2004.01.003

Kwiatkowski, J. R., McAloon, A. J., Taylor, F., & Johnston, D. B. (2006). Modeling the process and costs of fuel ethanol production by the corn dry-grind process. *Industrial Crops and Products*, *23*(3), 288–296. doi:10.1016/j.indcrop.2005.08.004

Laplace, J.M., Delgenes, J.P., Moletta, R., Navarro, J.M. (1991). Alcoholic fermentation of glucose and xylose by Pichia stipitis , Candida shehatae , Saccharomyces cerevisiae and

Zymomonas mobilis : oxygen requirement as a key factor. *Applied Microbiology and Biotechnology* 36, 158–162.

Lau, M. W., Dale, B. E., & Balan, V. (2008). Ethanolic fermentation of hydrolysates from ammonia fiber expansion (AFEX) treated corn stover and distillers grain without detoxification and external nutrient supplementation. *Biotechnology and bioengineering*, *99*(3), 529–39. doi:10.1002/bit.21609

Lau, M. W., Gunawan, C., & Dale, B. E. (2009). The impacts of pretreatment on the fermentability of pretreated lignocellulosic biomass: a comparative evaluation between ammonia fiber expansion and dilute acid pretreatment. *Biotechnology for biofuels*, *2*. doi:10.1186/1754-6834-2-30

Lawford, H. G., & Rousseau, J. D. (1997). Corn steep liquor as a cost-effective nutrition adjunct in high-performance Zymomonas ethanol fermentations. *Applied Biochemistry and Biotechnology*, *63-65*, 287–304. doi:10.1007/BF02920431

Lawford, H. G., & Rousseau, J. D. (2002). Performance testing of Zymomonas mobilis metabolically engineered for cofermentation of glucose, xylose, and arabinose. *Applied Biochemistry and Biotechnology*, *98-100*, 429–48. Retrieved from http://www.ncbi.nlm.nih.gov/pubmed/12018270

Li, C., Cheng, G., Balan, V., Kent, M. S., Ong, M., Chundawat, S. P. S., Sousa, L. daCosta, et al. (2011). Influence of physico-chemical changes on enzymatic digestibility of ionic liquid and AFEX pretreated corn stover. *Bioresource technology*, *102*(13), 6928–36. doi:10.1016/j.biortech.2011.04.005

Liggett, R. W., & Koffler, H. (1948). Corn Steep Liquor in Microbiology. *Bacteriological reviews*, *12*(4), 297–311. Retrieved from

Liska, A., Yang, H., & Milner, M. (2014). Biofuels from crop residue can reduce soil carbon and increase CO2 emissions. *Nature Climate …*, *4*(May), 398–401. doi:10.1038/NCLIMATE2187

LLNL (Lawarnce Livermore National Laboratory). (2013). Energy Flow. Retrieved July 23, 2014, from https://flowcharts.llnl.gov/

Luterbacher, J. S., Rand, J. M., Alonso, D. M., Jan, J., Youngquist, J. T., Maravelias, C. T., Pfleger, B. F., et al. (2014). Nonenzymatic sugar production from biomass using biomass-derived gamma-valerolactone. *Science*, *343*(January), 277–281.

Madson, P. W. (n.d.). Ethanol distillation : the fundamentals.

McCabe, W. L., Smith, J. C., & Harriott, P. (2005). *Unit Operations of Chemical Engineering* (7th ed.). McGraw-Hill.

McMillan, J. (1993). Xylose fermentation to ethanol: A review. *National Renewable Energy Laboratory Report*

Mohagheghi, A., Dowe, N., Schell, D., Chou, Y.-C., Eddy, C., & Zhang, M. (2004). Performance of a newly developed integrant of Zymomonas mobilis for ethanol production on corn stover hydrolysate. *Biotechnology Letters*, *26*(4), 321–325. doi:10.1023/B:BILE.0000015451.96737.96

Mohagheghi, A., Ruth, M., & Schell, D. J. (2006). Conditioning hemicellulose hydrolysates for fermentation: Effects of overliming pH on sugar and ethanol yields. *Process Biochemistry*, *41*(8), 1806–1811. doi:10.1016/j.procbio.2006.03.028

Moore, L. W. (2012). *Energy Use at Water and Waste Water Treatment Plants*.

Nichols, N. N., Sharma, L. N., Mowery, R. a., Chambliss, C. K., Van Walsum, G. P., Dien, B. S., & Iten, L. B. (2008). Fungal metabolism of fermentation inhibitors present in corn stover dilute acid hydrolysate. *Enzyme and Microbial Technology*, *42*(7), 624–630. doi:10.1016/j.enzmictec.2008.02.008

Nidetzky, B., Zachariae, W., Gercken, G., Hayn, M., & Steiner, W. (1994). Hydrolysis of ceilooligosaccharides by Trichoderma reesei cellobiohydrolases : Experimental data and kinetic modeling. *Enzyme Microbial Technology*, *16*, 43–52.

Nigam, P. S., & Singh, A. (2011). Production of liquid biofuels from renewable resources. *Progress in Energy and Combustion Science*, *37*(1), 52–68. doi:10.1016/j.pecs.2010.01.003

Novozymes. (2014a). Product benefits of Cellic® CTec3. Retrieved June 5, 2014, from http://www.bioenergy.novozymes.com/en/cellulosic-ethanol/CellicCTec3/product-description/Pages/default.aspx

Novozymes. (2014b). Product benefits of Cellic® HTec3. Retrieved June 5, 2014, from http://www.bioenergy.novozymes.com/en/cellulosic-ethanol/Cellic-HTec3/Product-description/Pages/default.aspx

Ohta, K., Beall, D. S., Mejia, J. P., Shanmugam, K. T., & Ingram, L. O. (1991). Genetic improvement of Escherichia coli for ethanol production: chromosomal integration of Zymomonas mobilis genes encoding pyruvate decarboxylase and alcohol dehydrogenase II. *Applied and Environmental Microbiology*, *57*(4), 893–900.

Page RD. (1996) TreeView: an application to display phylogenetic trees on personal computers. *Comput Appl Biosci., 12(4),* 357-8

Palmqvist, E., Hahn-Hägerdal, B., Galbe, M., & Zacchi, G. (1996). The effect of water-soluble inhibitors from steam-pretreated willow on enzymatic hydrolysis and ethanol fermentation. *Enzyme and Microbial Technology*, *0229*(95), 470-476.

Parreiras, L. S., Breuer, R. J., Avanasi Narasimhan, R., Higbee, A. J., La Reau, A., Tremaine, M., Qin, L., et al. (2014). Engineering and two-stage evolution of a lignocellulosic hydrolysate-tolerant Saccharomyces cerevisiae strain for anaerobic fermentation of xylose from AFEX pretreated corn stover. *PloS one*, *9*(9), e107499. doi:10.1371/journal.pone.0107499

Patil, N., & Patil, V. S. (2012). Molecular Sieve Dehydration Technology for Ethanol Dehydration. *Chemical Industry Digest*.

Pérez, J., Muñoz-Dorado, J., De La Rubia, T., & Martínez, J. (2002). Biodegradation and biological treatments of cellulose, hemicellulose and lignin: an overview. *International Microbiology*, *5*(2), 53–63. Retrieved from http://www.ncbi.nlm.nih.gov/pubmed/12180781

Pérez, S., & Samain, D. (2010). Structure and engineering of celluloses. *Advances in carbohydrate chemistry and biochemistry*, *64*(10), 25–116. doi:10.1016/S0065-2318(10)64003-6

Peters, M. S., Timmerhaus, K. D., & West, R. E. (2003). *Plant Design and Economics for Chemical Engineers* (5th ed.). McGraw-Hill.

Piotrowski JS, Okada H, Lu F, Li SC, Hinchman L, Ranjan A, et al. (2015a). Plant-derived antifungal agent poacic acid targets β-1,3-glucan. *Proceedings of the National Academy of Sciences. 112(12)*. E1490-E7.

Piotrowski JS, Simpkins SW, Li SC, Deshpande R, McIlwain SJ, Ong IM, et al. (2015b) Chemical Genomic Profiling via Barcode Sequencing to Predict Compound Mode of Action. *Chemical Biology. Methods and Protocols.* 299-318.

Piotrowski, J. S., Zhang, Y., Bates, D. M., Keating, D. H., Sato, T. K., Ong, I. M., & Landick, R. (2014). Death by a thousand cuts: the challenges and diverse landscape of lignocellulosic hydrolysate inhibitors. *Frontiers in microbiology*, *5*(March), 90. doi:10.3389/fmicb.2014.00090

Powell, C. D., Quain, D. E., & Smart, K. A. (2003a). Chitin scar breaks in aged Saccharomyces cerevisiae. *Microbiology*, *149*(11), 3129–3137. doi:10.1099/mic.0.25940-0

Powell, C., Quain, D., & Smart, K. (2003b). The impact of brewing yeast cell age on fermentation performance, attenuation and flocculation. *FEMS Yeast Research*, *3*(2), 149–157. doi:10.1016/S1567-1356(03)00002-3

Qi, B., Luo, J., Chen, G., Chen, X., & Wan, Y. (2012). Application of ultrafiltration and nanofiltration for recycling cellulase and concentrating glucose from enzymatic hydrolyzate of steam exploded wheat straw. *Bioresource technology*, *104*, 466–72. doi:10.1016/j.biortech.2011.10.049

Ren, C., Chen, T., Zhang, J., Liang, L., & Lin, Z. (2009). An evolved xylose transporter from Zymomonas mobilis enhances sugar transport in Escherichia coli. *Microbial cell factories* 8, 66. doi:10.1186/1475-2859-8-66

Rogers, P., Lee, K., & Tribe, D. (1979). Kinetics of alcohol production by Zymomonas mobilis at high sugar concentrations. *Biotechnology letters*. Retrieved from http://link.springer.com/article/10.1007/BF01388142

Saha, B. C. (2003). Hemicellulose bioconversion. *Journal of industrial microbiology & biotechnology*, *30*(5), 279–91. doi:10.1007/s10295-003-0049-x

Sarks, C., Jin, M., Sato, T. K., Balan, V., & Dale, B. E. (2014). Studying the rapid bioconversion of lignocellulosic sugars into ethanol using high cell density fermentations with cell recycle. *Biotechnology for biofuels*, *7*, 73. doi:10.1186/1754-6834-7-73

Sato, T. K., Liu, T., Parreiras, L. S., Williams, D. L., Wohlbach, D. J., Bice, B. D., Ong, I. S., et al. (2013). Harnessing Genetic Diversity in Saccharomyces cerevisiae for Improved Fermentation of Xylose in Hydrolysates of Alkaline Hydrogen Peroxide Pretreated Biomass. *Applied and Environmental Microbiology*, (November). doi:10.1128/AEM.01885-13

Searchinger, T., Heimlich, R., & Houghton, R. (2008). Use of US croplands for biofuels increases greenhouse gases through emissions from land-use change. *Science*, *319* (February), 1238–1240.

Sheehan, J., Aden, A., Paustian, K., Brenner, J., Walsh, M., & Nelson, R. (2004). Energy and Environmental Aspects of Using Corn Stover for Fuel Ethanol. *Journal of Industrial Ecology*, *7*(3), 117–146.

Slininger, P. J., Bothast, R. J., Okos, M. R., & Ladisch, M. R. (1985). Comparative evaluation of ethanol production by xylose-fermenting yeasts presented high xylose concentrations. *Biotechnology Letters*, *7*(6), 431–436. doi:10.1007/BF01166218

Sluiter, J. B., Ruiz, R. O., Scarlata, C. J., Sluiter, A. D., & Templeton, D. W. (2010). Compositional analysis of lignocellulosic feedstocks. 1. Review and description of methods. *Journal of agricultural and food chemistry*, *58*(16), 9043–53. doi:10.1021/jf1008023

Sreenath, H. K., & Jeffries, T. W. (1999). 2-Deoxyglucose as a Selective Agent for Derepressed Mutants of Pichia stipitis. *Applied Biochemistry and Biotechnology*, *77*(1-3), 211–222. doi:10.1385/ABAB:77:1-3:211

Stickel, J. J., Knutsen, J. S., Liberatore, M. W., Luu, W., Bousfield, D. W., Klingenberg, D. J., Scott, C. T., et al. (2009). Rheology measurements of a biomass slurry : an inter-laboratory study. *Rheologica Acta*, 1005–1015. doi:10.1007/s00397-009-0382-8

Stratford, M., & Keenan, M. (1988). Yeast flocculation: quantification. *Yeast*, *4*, 107–115. Retrieved from http://onlinelibrary.wiley.com/doi/10.1002/yea.320040204/abstract

Taherzadeh, M. J., & Karimi, K. (2007). Enzyme-based hydrolysis processes for ethanol from lignocellulosic materials: a review. *BioResources*, *2*(4), 707–738.

Tang, X., Da Costa Sousa, L., Jin, M., Chundawat, S. P., Chambliss, C. K., Lau, M. W., Xiao, Z., et al. (2015). Designer synthetic media for studying microbial-catalyzed biofuel production. *Biotechnology for biofuels*, *8*(1), 1. doi:10.1186/s13068-014-0179-6

Teixeira, J. A., & Mota, M. (1990). Experimental Assessment of Internal Diffusion Limitations in Yeast Flocs, *43*, 13–17.

Teymouri, F., Laureano-Perez, L., Alizadeh, H., & Dale, B. E. (2005). Optimization of the ammonia fiber explosion (AFEX) treatment parameters for enzymatic hydrolysis of corn stover. *Bioresource technology*, *96*(18), 2014–8. doi:10.1016/j.biortech.2005.01.016

Ueadaira, H., & Uedaira, H. (1969). Diffusion Coefficients of Xylose and Maltose in Aqueous Solution. *Bulletin of the Chemical Society of Japan*, *42*(8), 2140–2142.

UNICA (The Brazilian Sugarcane Industry Association). (2014). Sugarcane Industry in Brazil.

U. S. EPA (Environmental Protection Agency). Calculations and References. (2015). Retrieved June 9, 2015, from http://www.epa.gov/cleanenergy/energy-resources/refs.html

U. S. DOE (Department of Energy). U. S. Billion-Ton Update. (2011).

U. S. DOL (Department of Labor). Average Energy Prices for the U.S. and Selected Metropolitan Areas. (2015). Retrieved June 9, 2015, from http://www.bls.gov/regions/midwest/data/averageenergyprices_selectedareas_table.htm

U.S. EIA (Energy Information Administration). (2013). U.S. ethanol production and the Renewable Fuel Standard RIN bank. Retrieved July 23, 2014, from http://www.eia.gov/todayinenergy/detail.cfm?id=11551

U.S. EPA (Environmental Protection Agency). (2012). TRACI Version 2.1.

Vadas, P. A., & Digman, M. F. (2013). Production costs of potential corn stover harvest and storage systems, *4*, 1–7.

Varvel, G. E., Vogel, K. P., Mitchell, R. B., Follett, R. F., & Kimble, J. M. (2008). Comparison of corn and switchgrass on marginal soils for bioenergy. *Biomass and Bioenergy*, *32*(1), 18–21. doi:10.1016/j.biombioe.2007.07.003

Vidal, B. C., Dien, B. S., Ting, K. C., & Singh, V. (2011). Influence of feedstock particle size on lignocellulose conversion--a review. *Applied biochemistry and biotechnology*, *164*(8), 1405–21. doi:10.1007/s12010-011-9221-3

Wallace, R., Ibsen, K., McAloon, A., & Yee, W. (2005). Feasibility Study for Co-Locating and Integrating Ethanol Production Plants from Corn Starch and Lignocellulosic Feedstocks (Revised). Retrieved from http://www.osti.gov/scitech/biblio/15011708

Wheals, A. E., Basso, L. C., Alves, D. M., & Amorim, H. V. (1999). Fuel ethanol after 25 years. *Trends in biotechnology*, *17*(12), 482–7. Retrieved from http://www.ncbi.nlm.nih.gov/pubmed/10557161

Wood, S., & Cowie, A. (2004). A Review of Greenhouse Gas Emission Factors for Fertiliser Production, (June).

Wu, J., Lakshminarayan, P. G., & Babcock, B. A. (1996). Impacts of Agricultural Practices and Policies on Potential Nitrate Water Pollution in the Midwest and Northern Plains of the United States, *148*, 1–36.

Yang, B., Dai, Z., Ding, S.-Y., & Wyman, C. E. (2011). Enzymatic hydrolysis of cellulosic biomass. *Biofuels*, *2*(4), 421–450. doi:10.4155/bfs.11.116

Yerushalmi, L., & Volesky, B. (1985). Importance of agitation in acetone-butanol fermentation. *Biotechnology and bioengineering*, *XXVII*, 1297–1305. Retrieved from http://onlinelibrary.wiley.com/doi/10.1002/bit.260270905/pdf

Zhao, X. Q., & Bai, F. W. (2009). Yeast flocculation: New story in fuel ethanol production. *Biotechnology Advances*, *27*(6), 849–56. doi:10.1016/j.biotechadv.2009.06.006

Zhao, X.-Q., & Bai, F. (2012). Zinc and yeast stress tolerance: micronutrient plays a big role. *Journal of biotechnology*, *158*(4), 176–83. doi:10.1016/j.jbiotec.2011.06.038

Zhu, K.-X., Zhou, H.-M., & Qian, H.-F. (2006). Comparative study of chemical composition and physiochemical properties of defatted wheat germ flour and its protein isolate. *Journal of Food Biochemistry*, *30*(3), 329–341. doi:10.1111/j.1745-4514.2006.00067.x